INVESTIGATING THE ROLE OF THE EXTRACELLULAR CALCIUM-SENSING RECEPTOR (CaSR) IN VASCULAR PATHOPHYSIOLOGY USING A NOVEL MOUSE MODEL OF SELECTIVE ABLATION OF CaSR FROM MOUSE VASCULAR SMOOTH MUSCLE CELLS

DR. THOMAS DAVIES

PHD THESIS 2013

SUMMARY

The extracellular calcium-sensing receptor (CaSR) is a G-protein coupled receptor central to systemic Ca^{2+} homeostasis in mammals. We have previously shown that CaSR is expressed in primary bovine aortic vascular smooth muscle cells (VSMCs). Furthermore, dominant-negative adenoviral knockdown of this receptor in bovine VSMCs *in vitro* causes enhanced calcification in the presence of culture conditions which mimic vascular calcification *in vivo*. Using mineralising conditions *in vitro*, we have also previously demonstrated that positive pharmacological allosteric activation of CaSR using the calcimimetic, R-568, significantly reduces calcification of bovine VSMCs. These findings now implicate the CaSR, not just in systemic Ca^{2+} homeostasis, but also in potential protection against vascular calcification; a condition associated with increased blood pressure, left ventricular hypertrophy, chronic kidney disease and cardiovascular morbidity. Using a specific targeted deletion strategy, we have developed CaSR-specific knockout in VSMCs driven by the SM22α promoter. Using *in vitro, ex vivo* and *in vivo* approaches, here, I have characterised the cardiovascular phenotype of this novel transgenic mouse model. *In vivo* data demonstrate that ablation of CaSR from VSMCs causes hyperkalaemia at 3 months of age and hypercalcaemia throughout life. 3 month old CaSR-VSMC Knockout (KO) mice also exhibit reduced bone mineral integrity and increased heart weight at the age of 18 months. *Ex vivo* analysis implicates the VSMC-CaSR as a modulator of blood vessel tone. CaSR-VSMC KO mice exhibit reduced luminal diameters of the aorta and mesenteric arteries. CaSR-VSMC KO also reduces contractile tone in addition to evoking Ca^{2+}-dependent relaxation only, compared to CaSR-wild-type (WT) mice which exhibit both Ca^{2+}-dependent contraction and relaxation of the aorta. *In vitro* analyses confirm that CaSR expression and activation reduces Ca^{2+}-dependent proliferation and mineralisation. In conclusion, the VSMC CaSR is a modulator of vascular tone *ex vivo* and of VSMC proliferation and calcification *in vitro*.

ACKNOWLEDGMENTS

I would firstly like to take this opportunity to extend my gratitude to both Cardiff University, for allowing me to carry out my research at this institution, and to my funders; the Biotechnology and Biological Sciences Research Council (BBSRC) and Amgen Limited.

I would like to thank my supervisors Professor Daniela Riccardi and Professor Paul Kemp for their constant support and kindness during my study. I have deeply valued their input, comments and friendships over the past few years. I would also like to thank Martin Schepelmann, Dr. Sarah Brennan and Dr. Polina Iarova for their immense contributions to this project, and I am now extremely pleased to regard them as dear friends rather than colleagues. I also thank Dr. David Edwards for kindly providing me with the equipment necessary to carry out my research. I am also grateful to my friends within our group for the many enjoyable discussions and good memories during the last few years that I will not forget. I will always treasure your friendships, your laughs and endearing personalities: Aisha, Alex, Anna, Becky, Belinda, Bill, Birgitta, Brenda, Charlie, Cleo, Dave, Helen, Hsiu, Jess, João, Julia, Laurie, Leanne, Lydia, Mark, Marisol, Milica, Patrizio, Pawel, Rachel, Seva, Shuang and Stuart.

To my good friends, my siblings and family who were there for me, who made the time for me whether I had any or not, I thank you all. And lastly, I thank my partner Nik for his ongoing and unending support throughout this challenging endeavour.

ABBREVIATIONS

1,25-dihydroxyvitamin D_3	$1,25(OH)_2D_3$
1,25-dihydroxyvitamin D_3 24-hydroxylase	CYP24
25-hydroxyvitamin D_3	$25(OH)D_3$
Adenosine diphosphate	ADP
Adenosine triphosphate	ATP
Adenylyl cyclase	AC
Alkaline phosphatase	ALP
Aminoglycoside antibiotic	AGA
Annexin 5	Anx-5
Apolipoprotein B	apoB
Apolipoprotein E	apoE
Arachidonic acid	AA
Autoimmune hypoparathyroidism	AH
Autosomal dominant hypocalcaemia	ADH
Autosomal dominant hypophosphatemic rickets	ADHR
Bone morphogenetic proteins	BMPs
Bone morphogenetic protein 2	BMP-2
Bone morphogenetic protein 4	BMP-4
Bone morphogenetic protein 6	BMP-6
Bone morphogenetic protein 7	BMP-7
Breast arterial calcification	BAC
Calcific uremic arteriolopathy	CUA
Calcifying vascular cell	CVC
Calcium ion	Ca^{2+}
Calcium ion (free ionized)	Ca^{2+}_o
Calmodulin	CaM
Cardiovascular Disease	CVD
Chronic kidney disease	CKD
Collagen type I	Col1
Computerised tomography	CT
Concentration of calcium ion	$[Ca^{2+}]$
Connexin	Cx
Coronary arterial calcification	CAC
Cyclic 3'-5'adenosine monophosphate	cAMP
Cyclic 3'-5'guanosine monophosphate	cGMP
Diacylglycerol	DAG
Dulbecco's Modified Eagle Medium	DMEM
End-stage renal disease	ESRD
Endoplasmic reticulum	ER
Endothelial cells	EC

Endothelial nitric oxide synthase	eNOS
Endothelium-derived hyperpolarisation	EDH
Endothelium-derived hyperpolarising factor	EDHF
Endothelium-derived relaxation factor	EDRF
Epoxyeicosatrienoic acids	EET
Extracellular matrix	ECM
Extracellular regulated protein kinase	ERK
Extracellular calcium-sensing receptor	CaSR / CaS / CaR
Familial hypocalciuric hypercalcaemia	FHH
Fibroblast growth factor 23	FGF23
Fibroblast growth factor receptor	FGFR
Free ionized extracellular calcium concentration	$[Ca^{2+}]_o$
Fetal bovine serum	FBS
Generalized arterial calcification of infants	GACI
G protein-coupled receptor	GPCR
Guanosine diphosphate	GDP
Guanosine triphosphate	GTP
Guanylyl cyclase	GC
Heart disease	HD
Human embryonic kidney 293 cells	HEK293
Hydrochloric acid	HCl
Hydrochloride	HCl^-
Hydroxyapatite	HA
Inorganic phosphate	Pi
Inositol 1,4,5-trisphosphate	IP_3
Inositol 1,4,5-trisphosphate receptor	IP_3R
Interferon-γ	IFN-γ
Internal elastic lamina	IEL
Intracellular free ionised calcium concentration	$[Ca^{2+}]_i$
Jun amino-terminal kinase	Jun
Knockout	KO
Large conductance Ca^{2+}-activated K^+ channels	BK_{Ca}
L-type voltage-gated Ca^{2+} channel	L_{Ca}
Low-density lipoprotein	LDL
Low-density lipoprotein receptor	LDLR
Matrix gla protein	MGP
Matrix metalloproteinase	MMP
Matrix vesicle	MV
Metabotropic glutamate receptors	mGluRs
Microcomputerised tomography	μCT
Mitogen-activated protein kinase	MAPK
Myoendothelial junction	MEJ

Myoendothelial projection	MP
Myosin light chain	MLC
Myosin light chain kinase	MLCK
Myosin heavy chain phosphatase	MLCP
National Centre for Health Services	NCHS
National Health Interview Survey	NHIS
Neonatal severe hyperparathyroidism	NSHPT
Nitric oxide	NO
Nitric oxide synthase	NOS
Nucleotide pyrophosphatase/phosphodiesterase-1	NPP1
Osteocalcin	OC
Osteoprotegrin	OPG
Osterix	OSX
Parathyroid cell	PTC
Parathyroid gland	PTG
Parathyroid hormone	PTH
Parathyroid hormone-related peptide	PTHRP
Sodium Phosphate co-transporter	PiT-1
Phosphatidylinositol 3-kinase	PI_3-K
Phosphatidylinositol 4,5 bisphosphate	PIP_2
Phosphatidylinositol-4 kinase	PI4-K
Phosphatidylinositol 4-phosphate	PI4
Phospholipase A_2	PLA_2
Phospholipase B	PLB/Akt
Phospholipase C	PLC
Phospholipase D	PLD
Platelet-derived growth factor	PDGF
Polymerase chain reaction	PCR
Potassium chloride	KCl
Prostacyclin	PGI_2
Protein kinase A	PKA
Protein kinase C	PKC
Protein kinase G	PKG
Pyrophosphate	PPi
Receptor activator of nuclear factor kappa-B	RANK
Receptor activator of nuclear factor kappa-B ligand	RANKL
Renin-angiotensin-aldosterone system	RAAS
Reverse transcriptase PCR	RT-PCR
Reverse transcription	RT
Ryanodine Receptor	RyR
Sarcoplasmic reticulum	SR
Sarcoplasmic reticulum Ca^{2+}- ATPase	SERCA
Smooth muscle actin 22 α	SM22α

Standard error of mean	SEM
Store operated Ca^{2+} entry	SOCE
Stress-activated protein kinase ERK kinase 1	SEK1
Thiosulphate	$S_2O_3^-$
Tissue non-specific alkaline phosphatase	TNAP
Transforming growth factor β	TGF-β
Transglutaminase 2	TG2
Transmembrane domain	TMD
T-type voltage-gated Ca^{2+} channel	T_{Ca}
Tumour necrosis factor	TNF
University of California San Francisco	UCSF
Vascular calcification	VC
Vascular endothelial growth factor	VEGF
Vascular smooth muscle cells	VSMC
Venus flytrap domain	VFT
Vitamin D receptor	VDR
Vitamin D response elements	VDRE
Vitamin D_3	VD_3
Voltage-gated Ca^{2+} channels	VGCC
Wild-type	WT
α_1-adrenergic receptor	α_1-AR
α_2-Heremans Schmid glycoprotein	Fetuin A
α-Modified Eagle Medium	αMEM
β-glycerophosphate	βGP
γ-aminobutyric acid receptors	$GABA_BRs$

TABLE OF CONTENTS

LIST OF FIGURES

CHAPTER 2:

METHODS

CHAPTER 3:

IN VIVO CHARACTERISATION OF THE SM22α X fl CaSR MOUSE MODEL WITH SELECTIVE ABLATION OF CaSR IN VASCULAR SMOOTH MUSCLE CELLS:

CHAPTER 4:

EX-VIVO CHARACTERISATION OF THE SM22α x fl CaSR MOUSE MODEL:

MODULATION OF TONE IN RESPONSE TO VASOCONSTRICTORS AND VASORELAXANTS

CHAPTER 7:

THESIS DISCUSSION & FINAL CONCLUSIONS

LIST OF TABLES

CHAPTER 1:

GENERAL INTRODUCTION

1.1 The cardiovascular system: an anatomical perspective

The cardiovascular system comprises an intricate network of large vessels, small vessels and capillaries (Burton, 1954). This delicate network serves as a transport mechanism, delivering crucial O_2 throughout the body to cells and tissue. The familiar blood vessel observed in a myriad of higher organisms is easily distinguishable by its open luminal structure surrounded by a resilient and elastic wall (Conway *et al.*, 2001). Blood vessels comprise of three distinct cell layers; each of which demonstrate significant and unique roles in maintaining vascular function (Figure 1).
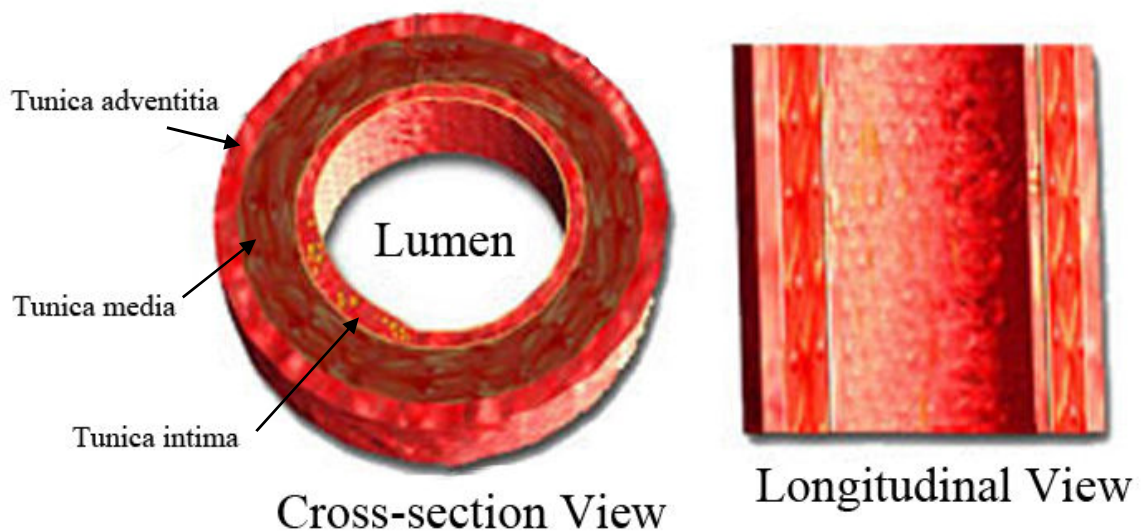
Figure 1. Blood vessel morphology. A typical arteriole consisting of a tunica intima, tunica media and tunica adventitia. Modified from CardioSmart.org (CardioSmart, 2012)**.**

1.1.1 Vascular endothelium

As a single layer of endothelial cells and the internal elastic lamina (IEL) membrane (Gutterman, 1999), the vascular endothelium is a minority cell population in the vasculature, however this does not subtract from the major physiological role that these cells elicit in the cardiovascular system. The role of endothelial cells (ECs) in the vasculature has been extensively investigated over the years since pioneers Robert Furchgott and John Zawadzki first observed the crucial role of endothelial cells in acetylcholine-dependent dilation (Furchgott, 1984, Furchgott *et al.*, 1984, Furchgott and Vanhoutte, 1989). Furchgott showed that dilation of the aorta through acetylcholine can only be achieved when an intact endothelium is present. Furthermore, enzymatic or physical removal of these endothelial cells consistently causes vessels to be devoid of an acetylcholine-dependent dilation (Furchgott, 1984, Furchgott *et al.*, 1984, Furchgott and Vanhoutte, 1989). In fact, in other aortic preparations lacking the endothelium, Furchgott and Zawadzki demonstrated the opposite; a contractile role of acetylcholine (Furchgott and Vanhoutte, 1989). Prior to this notion, it was commonly believed that contraction and dilation was co-ordinated chiefly by the vascular smooth muscle cells themselves (VSMCs). We now know that indirect endothelial-dependent dilation of VSMCs can occur by signalling through ECs by a number of agents including adenosine diphosphate (ADP), adenosine triphosphate (ATP), bradykinin, thrombin, serotonin, histamine, acetylcholine, epoxyeicosatrienoic acids (EETs), prostacyclin (PGI_2), a cyclooxygenase-dependent metabolite of arachadonic acid (AA) and nitric oxide (NO)- a product of L-arginine and the nitric oxide synthase (NOS) pathway (Cherry *et al.*, 1982, Vanhoutte *et al.*, 1986, Palmer *et al.*, 1987, Vanhoutte, 1987, Furchgott and Vanhoutte, 1989, Bukoski *et al.*, 1997, Wang and Bukoski, 1998, Edwards *et al.*, 2008, Luksha *et al.*, 2009).

From these initial studies by Furchgott and Zawadzki it was clear that the endothelium is profoundly important in co-ordinating vascular tone. In fact, the discovery of an endothelium-derived relaxation factor (EDRF) has been investigated thoroughly over the past decades. It is now accepted that EDRF and NO are indistinguishable, although multiple dilation and hyperpolarising factors still exist (Palmer *et al.*, 1987, Sandow *et al.*, 2009, Chadha *et al.*, 2011). Interestingly, this has posed questionable molecular

mechanisms by which the endothelium and tunica media signal to one another. Although NO diffuses easily to adjacent VSMCs, it was clear that in order for additional endothelium-derived hyperpolarizing factors (EDHFs) to evoke dilation in VSMCs, there must be a semi-permeable barrier at work to deliver these molecules (Lew *et al.*, 1989, Sandow *et al.*, 2009). It was first proposed that endothelial pockets that extend through the internal elastic lamina form connections with VSMCs allowing the transfer of diffusible molecules. This was first described in 1957 by Moore and Ruska who isolated small vessels from a dog heart and noted small invaginations and vesicles between ECs and VSMCs through the IEL (Moore and Ruska, 1957). Since then, they have been characterised as myoendothelial gap junctions (MEJs) and play a key role in transcellular and paracellular diffusion of small solutes and molecules (Moore and Ruska, 1957, Chaytor *et al.*, 1998, Edwards *et al.*, 2008, Heberlein *et al.*, 2009). These small 0.5µm diameter MEJs exhibit an inversely proportionate abundance in increasingly smaller vessels, although the type of vessel is a major predictor of MEJ presence (Haas and Duling, 1997). This arguably has important functional ramifications in smaller resistance vessels which require acute and localised signalling (Michel *et al.*, 1995). From a structural perspective, MEJs are composed of small connexin proteins, specifically, Connexin 37 and 40 (Cx37 and Cx40) in the vasculature and are typically found in larger vessels (Simon and McWhorter, 2002). Interestingly, Cx37 and Cx40 are the only connexin family members found in the mouse aorta where they function in a compensatory manner, although Cx43 has been reported in a heterogeneous manner in other vessels (Nicholson and Bruzzone, 1997). Knockout (KO) studies of these connexins specifically in mouse endothelial cells causes severe systemic cardiovascular abnormalities such as haematomas (Simon and McWhorter, 2002). There is also now evidence that endothelial cells extend through the IEL to make physical contact with vascular smooth muscle cells by myoendothelial projections (MPs) (Aaronson, 2012, Tran *et al.*, 2012). Furthermore, these projections are proposed to house endoplasmic/sarcoplasmic reticula (ER/SR) which extend from the main cytosolic body of the cell into this outward cellular appendage (Kerr *et al.*, 2012). In this way, Ca^{2+} is more readily and locally available for release from these internal stores through inositol triphosphate (IP_3) receptors present on their surfaces, signalling adjacent vascular smooth muscle cells to contract or dilate accordingly (Kerr *et al.*, 2012). This mechanism is described in Figure 2.
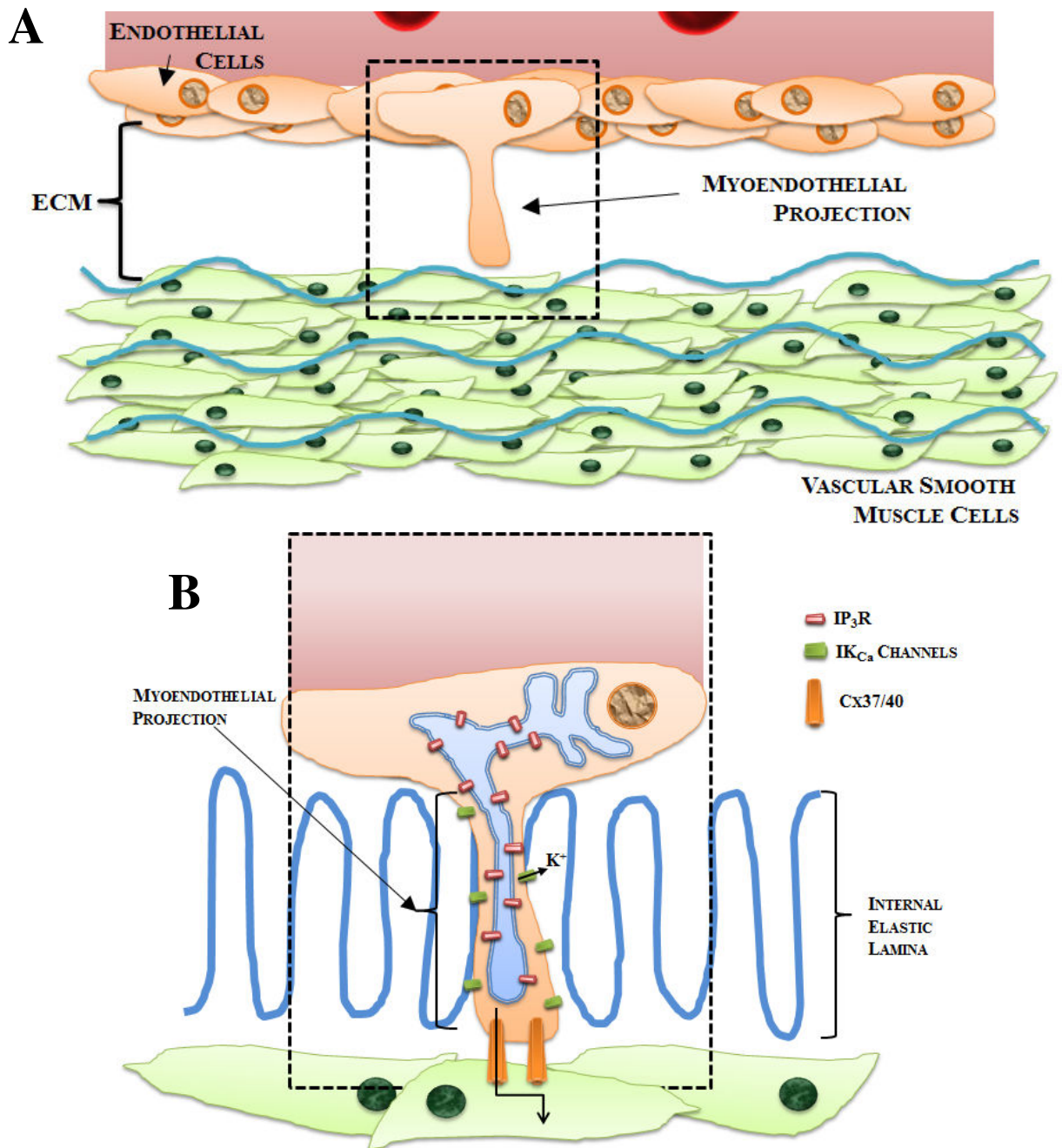
Figure 2. Myoendothelial gap junctions in arterial vessel walls. (A) Myoendothelial projections extend into the internal elastic lamina where they form connections by connexins to VSMCs. (B) The endothelial endo/sarcoplasmic reticulum (ER and SR respectively) is extended into the myoendothelial projection allowing for very localised Ca^{2+} signalling. Inositol trisphosphate receptors (IP_3Rs) are activated by inositol trisphosphate (IP_3) causing an increase in intracellular Ca^{2+}. This is accompanied by hyperpolarisation of the endothelial cell by removal of K^+ through intermediate conductance Ca^{2+}-activated potassium channels (IK_{Ca}) (Busse *et al.*, 2002). Ca^{2+}_i can stimulate the production of nitric oxide synthase and ultimately nitric oxide which translocates to adjacent VSMCs. This ultimately induces vasodilation of VSMCs. Figure adapted from Kerr *et al* and Tran *et al* (Kerr *et al.*, 2012, Tran *et al.*, 2012).

1.1.2 Vascular smooth muscle cells

The tunica media cell layer is enriched with an abundance of vascular smooth muscle cells (VSMCs) which exhibit a characteristically elastic phenotype (Chamley-Campbell and Campbell, 1981). The number of VSMCs that comprise the tunica media is indeed incredibly variable. Layers of VSMCs in smaller vessels decrease with decreases in luminal diameter. It has been reported that vessels of >300μm comprise around 6-8 layers of VSMCs. Comparatively, smaller resistance vessels and arterioles with diameters of 30-50μm can have just a single monolayer of VSMCs (Miller *et al.*, 1987, Wagenseil *et al.*, 2009, Wagenseil *et al.*, 2010). Contractility and support is typically provided through the enriched ECM laid down in the form of collagen. Although collagens I, II, III, IV, V and VI have been reported in abundance in the tunica media, there is evidence that collagens I and III are predominantly responsible for giving strength to the vessel wall, particularly in the descending aorta (Wagenseil and Mecham, 2009). In addition to collagen, strength is provided by fenestrated sheets of elastin which provide much structural support (O'Connell *et al.*, 2008). These ECM components are absolutely critical for a functional vessel and, interestingly, mice lacking the elastin (*Eln*) gene die soon after birth due to cardiovascular abnormalities including stiff arteries, high left ventricular pressure and low cardiac output (Wagenseil *et al.*, 2010). Intriguingly, during this study investigators found that mice heterozygous for the *Eln* gene displayed a significant increase in layers of elastic lamina. Heterozygote mice developed, on average, 11 elastic laminae compared to the normal 8 wild-type lamina sheets (Wagenseil *et al.*, 2010).

Functionally, VSMCs play a crucial role in maintaining vascular tone (Furchgott and Vanhoutte, 1989, Dora, 2010, Garland and Weston, 2011) however, to carry out contractile responses and act as an integral structural component of the vessel wall, VSMC must adopt multiple phenotypes (Chamley-Campbell and Campbell, 1981). The two major phenotypes that VSMCs adopt have been designated synthetic and contractile. In the synthetic phenotype, VSMCs are more actively engaged in the synthesis of extracellular matrix (ECM) components, contain few myofilaments and may undergo proliferation. This is, unsurprisingly accompanied by an upregulation in intracellular free

ribosomes, endoplasmic reticulum and mitochondria to aid these functions (Thyberg *et al.*, 1995, Yoshida *et al.*, 2005). In the contractile state, the cytoplasm is rich in myofilaments such as actin and smooth muscle actin 22 α (SM22α) (Han *et al.*, 2009). Interestingly, some researchers have demonstrated the ability of SM22α and actin to co-localise and bind to one another (Kobayashi *et al.*, 1994, Fu *et al.*, 2000). This phenotype switching is a principal determinant of healthy cardiovascular function.

1.1.3 Vascular adventitia

The outer tunica adventitia layer is composed of pavement endothelial cells and fibroblasts that act as a protective lining to the blood vessels (Burton, 1954). Furthermore, these outer cells house a plethora of fibrillar collagens, elastic fibres and elastic lamellae which are secreted by the VSMCs and heterogeneous myofibroblasts. These function to construct an elaborate ECM in the tunica adventitia (Gerrity and Cliff, 1972, Bendeck *et al.*, 1994). Interestingly, microarray analysis for matrix protein expression such as Col1 and elastin using specific gene oligonucleotides in neonatal mice has demonstrated that expression of these adventitial ECM proteins progressively increases from 7-14 days after birth, followed by a decrease in expression from approximately 2-3 months. These results are not only consistent in mice, but also in humans (Stenmark, 2006, Wagenseil and Mecham, 2009). In addition to these matrix proteins, numerous basement membrane constituents are also expressed including fibronectin and matrix metalloproteinases (MMPs) (Stenmark, 2006, Wagenseil and Mecham, 2009). These findings suggest that the vascular adventitia serves as an early structural scaffold of the vessel wall in which the endothelium and VSMCs will develop and mature within.

Together, the three cell layers function to allow the passage of blood through a vast network of arteries, veins and capillaries throughout the body to deliver O_2 to organs and tissues, as well as to remove CO_2 from these regions, preventing the development of an anaerobic environment (Burton, 1954, Wagenseil and Mecham, 2009).

1.2 Ca^{2+} signalling in VSMC and phenotype switching

As a secondary messenger within the cell, free ionised calcium (Ca^{2+}_o) can elicit numerous functional changes to vascular cells, more importantly, in ECs and VSMCs. In VSMCs, rises in intracellular Ca^{2+} (Ca^{2+}_i) causes contraction (Mulvany and Nyborg, 1980, Mulvany and Aalkjaer, 1990). Contraction ensues when the intracellular calcium ion concentration ($[Ca^{2+}]_i$) in the VSMC increases. This way, Ca^{2+} is a direct facilitator of vasoconstriction. Changes in $[Ca^{2+}]_i$ can come about in a variety of ways and are indeed co-ordinated through the actions of appropriate receptors sensitive to Ca^{2+}_o including the extracellular calcium-sensing receptor (CaSR) (Ward, 2004), Ca^{2+}-channels (Adams et $al.$, 1989), sarcoplasmic reticulum receptors, α_1-adrenergic receptors and muscarinic M3 receptors (Carafoli, 1987, Felder, 1995, Carafoli, 2002).

1.2.1 Vasoconstriction of vascular smooth muscle cells

Contraction of VSMCs is co-ordinated through the action of Ca^{2+}_i (Morgan and Morgan, 1984a, Wray et $al.$, 2005, Ledoux, 2006). The main source of Ca^{2+}_i is obtained from the extracellular environment. Ca^{2+} influx occurs when the plasma membrane is depolarised. Ca^{2+} influx can occur through voltage-gated Ca^{2+}-channels (VGCCs). Of the ten members of the VGCC family, two are found in the cardiovascular system; Ca_V 1.2 and Ca_V 1.3 (Mangoni et $al.$, 2003, Rhee et $al.$, 2009). The first type, large "L-type" voltage-gated Ca^{2+}-channel (L_{Ca}) requires a strong depolarisation for activation and subsequently causes an influx of Ca^{2+} (Catterall et $al.$, 2005). The second method of Ca^{2+} uptake is through T-type voltage-gated Ca^{2+}-channels (T_{Ca}). These channels are activated by weaker polarisations (Benham et $al.$, 1987, Smirnov and Aaronson, 1992, Catterall et $al.$, 2005). Together, these two channel types help maintain vascular tone through the actions of Ca^{2+} flowing in to VSMCs. During depolarisation, cations such as Ca^{2+} are transported into the cell through VGCCs, thus inducing a contractile response. During hyperpolarisation, as a consequence of an efflux of K^+, VGCCs are closed, Ca^{2+}_i is sequestered to internal stores resulting in dilation. (Jaggar et $al.$, 1998). The actions of Ca^{2+}_i as a vasoconstrictor, particularly within vascular smooth muscle, are well-documented. When Ca^{2+}_i is elevated, it binds to CaM and consequently, CaM-dependent activation of myosin light-chain kinase (MLCK) occurs (Dillon et $al.$, 1981). During

activation of myosin light chain (MLC) through MLCK, myosin ATPase is stimulated, causing the hydrolysis of ATP. Ultimately this leads to myosin chain bridging between actin and myosin filaments (Bárány, 1967, Hai and Murphy, 1989). Myosin chains can later be broken down to dilate VSMCs by the action of myosin light-chain phosphatase (MLCP) (Kitazawa *et al.*, 2009). In this way MLCK and MLCP have antagonistic roles.

Although Ca^{2+}-channels play a significant role in Ca^{2+} entry into the cell, other mechanisms exist, often in combination to allow $[Ca^{2+}]_i$ to increase and allow contraction (Morgan and Morgan, 1984b, Morgan and Morgan, 1984a). A rise in free cytosolic Ca^{2+} can be obtained from intracellular stores, often when G-protein coupled receptors (GPCRs) are activated (Minneman, 1988). A well-studied example of this is the α_1-adrenergic receptor (often termed adrenoceptors/α_1-ARs) which responds to catecholamines such as dopamine, norepinephrine and the selective agonist phenylephrine (Minneman, 1988). When agonists bind to α_1-ARs, G-protein signalling occurs through the $G_{q/11}\alpha$ subunit (Gosau *et al.*, 2002). Heterotrimeric G_q activates PLC which in turn hydrolyses phosphatidylinositol 4,5-bisphosphate (PIP_2) into IP_3 and diacylglycerol (DAG). Increased IP_3 induces IP_3 receptor activation and subsequentl release of Ca^{2+} from internal stores (Berridge, 1984, Berridge and Irvine, 1984, Minneman, 1988). The elevation in Ca^{2+}_i is then free to bind to CaM as previously described and elicit a MLC-mediated contraction of the VSMC (Itoh *et al.*, 1989, Wray *et al.*, 2005, House *et al.*, 2008). Mechanisms of Ca^{2+}-mediated vasodilation and vasoconstriction can be observed in Figure 3.

1.2.2 Vasodilation of vascular smooth muscle cells

In order for endothelial cells to elicit a dilatory response, an intracellular signalling pathway is initiated. In the case of the well-characterised endothelium vasodilator acetylcholine, this binds to the muscarinic acetylcholine M3 metabotropic, G-protein coupled receptor (GPCR) at the plasma membrane (Boulanger *et al.*, 1994, Andersson, 2002). Activation of M3 receptors then activates the G_q pathway (Kunkel and Peralta, 1993). This leads to activation of phospholipase C (PLC) and production of inositol

triphosphate (IP_3) which acts on IP_3 receptors on the endoplasmic reticulum (Berridge, 1993). Consequently, Ca^{2+} is liberated from internal stores into the cytosol thereby increasing $[Ca^{2+}]_i$. Additionally, store depletion initiates Ca^{2+} entry into the endothelial cell via the store operated Ca^{2+} entry channel (SOCE) (Edwards *et al.*, 2008). This Ca^{2+}_i binds to CaM which activates endothelial nitric oxide synthase (eNOS) (Morris and Billiar, 1994). Since eNOS is Ca^{2+} and calmodulin-dependent, it is largely active when $[Ca^{2+}]_i$ is high despite being constitutively expressed (Palmer *et al.*, 1988, Bredt and Snyder, 1990, Knowles and Moncada, 1994). In its active state, eNOS catalyses the conversion of L-arginine into L-citrulline and NO; the diffusible EDRF which is largely accepted to be translocated through MEJs to adjacent VSMCs (Walford and Loscalzo, 2003). In VSMCs, NO exerts its dilatory role by binding to the soluble heme-containing enzyme, guanylyl cyclase (GC). The activation of this leads to accumulation of cyclic guanosine monophosphate (cGMP). cGMP directly inhibits Ca^{2+} influx by inhibiting voltage-gated Ca^{2+}-channels (Bolotina *et al.*, 1994) and can also activate protein kinase G (PKG), specifically PKG-1. These actions of NO, cGMP and PKG collectively serve to activate the sarcoplasmic reticulum Ca^{2+}- ATPase (SERCA) and sequester $[Ca^{2+}]_i$ (Simmerman and Jones, 1998, Massberg *et al.*, 1999, Walford and Loscalzo, 2003, Kitazawa *et al.*, 2009). Interestingly, PKG-1 carries out two actions as a potent regulator of vasodilation. In addition to activating SERCA, PKG-1 also phosphorylates the large conductance Ca^{2+}-activated K^+ channels (BK_{Ca}). By phosphorylating BK_{Ca} channels, they become open and cause membrane hyperpolarization. Downstream of this, voltage-dependent Ca^{2+}-channels are closed preventing Ca^{2+} influx and further dilation (Kitazawa *et al.*, 2009).
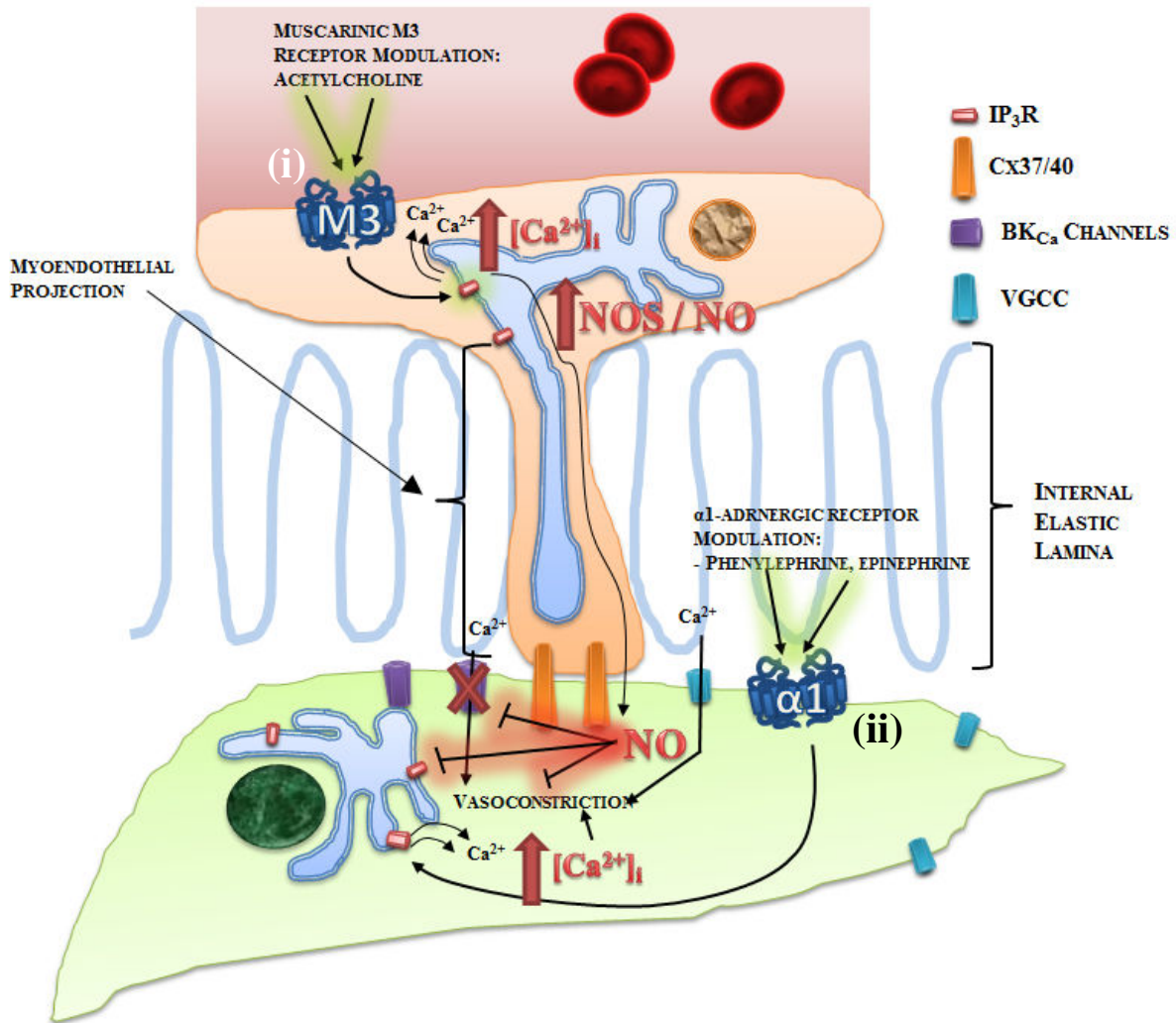
Figure 3. Mechanisms of Ca^{2+}-mediated vasodilation and vasoconstriction. (i) Vasodilators such as acetylcholine bind to muscarinic M3 GPCRs on endothelial cells. Binding induces signal transduction, resulting in activation of IP$_3$Rs on the ER/SR. Ca$^{2+}_i$ is increased as Ca^{2+} is released from internal stores causing endothelial Ca^{2+}-dependent activation of eNOS. NO generated from the enzymatic actions of eNOS is diffused in a paracellular manner. NO is small enough to diffuse in the absence of myoendothelial junctions. Here, NO inhibits Ca^{2+} influx from BK$_{Ca}$ channels, activation of IP$_3$Rs and lastly vasoconstriction. (ii) Activation of α$_1$-adrenergic receptors by agonists such as phenylephrine or epinephrine causes activation of VSMC IP$_3$Rs. Ca^{2+} is liberated from internal stores and results in myosin bridging in VSMCs and vasoconstriction.

1.3 Vascular calcification; an introduction to soft tissue mineralisation

Vascular calcification is often a consequence of an unhealthy lifestyle, and a pathophysiological state that will affect every adult as they progressively enter their senior years of life (Demer and Tintut, 2008). Statistical data from a study carried out in 2004 indicate that, by the age of approximately 60, most men and women have some Ca^{2+} deposits in the distal aorta (Allison, 2004). Vascular calcification promotes heart failure and hypertrophy by interfering with normal vessel compliance and elasticity (Demer and Tintut, 2008). Until the early 1990's VC was considered to be the passive and cell-independent mineralisation within blood vessels, driving elastic smooth-muscle cells in vessel walls towards something biologically more reminiscent of bone. It was widely believed that, over time, Ca^{2+}_o and inorganic phosphate (Pi) in extracellular fluids may coalesce into inorganic minerals such as hydroxyapatite (HA) and whitlockite; minerals which are insoluble under normal physiological conditions (O'Neill, 2008, O'Neill and Koba, 2010). In 1994, Linda Demer and colleagues challenged this theory declaring for the first time in a seminal study that calcification at atherosclerotic lesions may be co-ordinated through transdifferentiation of VSMCs in human and bovine aortae (Demer and Watson, 1994). This controversial claim indicated that the complexities of a metabolically active biological system may somehow interfere with fundamental physicochemical processes that one might observe in a simple chemical reaction *in vitro*. For the first time the group showed that osteogenic markers, such as bone morphogenetic protein 2 (BMP-2), were upregulated in calcified atherosclerotic lesions *in vivo*. The consequences of this finding ushered in a new theory of soft tissue mineralisation, which supersedes the previous notion that cells in the vascular wall have an unchanging phenotype. Since this pioneering research, the theory of vascular cell transdifferentiation has introduced a new niche for cardiovascular research (Boström *et al.*, 1993, Demer and Watson, 1994).

In recent years, numerous research groups have attempted to define where this transdifferentiation phenomenon may occur, and, if it is the sole determinant of atherosclerotic and vascular calcification. Vascular smooth muscle cells are present in the tunica media of blood vessels and have shown to be key players in this phenotype

switching (Luo *et al.*, 1997, Davies, 2003, Shao *et al.*, 2005, Shao, 2006, Shen *et al.*, 2011), most likely due to their overwhelming presence in the arterial wall (Burton, 1954). The tunica media is comparatively large in comparison with the intima, which consists of just one layer of endothelial cells, suggesting that VSMCs play a major role in determining the vessel phenotype overall. VSMCs are characteristically contractile, for example, by α_1-AR stimulation (Hoffman and Lefkowitz, 1982, Minneman, 1988, Heusch, 2011). Similarly, they can also elicit dilation indirectly through activation of muscarinic M3 receptors on endothelial cells (Felder, 1995, Andersson, 2002). In this regard, VSMCs are largely the major physical modulators of vascular tone and during calcification vascular tone is often significantly impaired. This evidence indicates that these VSMCs exhibit significant plasticity, and so may be susceptible to transdifferentiation.

It has been extensively documented that vascular calcification is associated with a loss of the ability of vascular smooth muscle cells to contract, indicating that a change occurs in this region of the vessel wall. Consequently, much research into VC in recent years has been investigated in VSMCs and, encouragingly, many research groups have demonstrated the ability of primary mouse VSMCs in culture to undergo transdifferentiation at the molecular level when pro-mineralising conditions are present (Luo *et al.*, 1997, Davies, 2003, Shao *et al.*, 2005, Shao, 2006, Shen *et al.*, 2011). This has been shown in isolated VSMCs from rats (Ciceri *et al.*, 2011, Ciceri *et al.*, 2012), cows (Shioi *et al.*, 1995, Shalhoub *et al.*, 2006, Alam *et al.*, 2008, Kircelli *et al.*, 2012) and humans (Proudfoot *et al.*, 2000, Reynolds, 2004, Reynolds, 2005, Olesen *et al.*, 2006, Shalhoub *et al.*, 2010). Typically, these researchers note the presence of visual nodules in *in vitro* cell cultures as well as the gain of expression of numerous osteogenic markers including the master osteoblastic transdifferentiation factor Runx2 (often termed cbfa1), osteocalcin (OC), alkaline phosphatase (ALP) and collagen type-I (Col1).

1.4 Classification of vascular calcification

Calcification is a condition that can affect many cell types and blood vessels. To date, numerous types have been classified including atherosclerotic calcification of the tunica intima, medial calcification of the tunica media, aortic valve calcification and calciphylaxis (Freeman and Otto, 2005, Thom *et al.*, 2006). It has been predicted that the often co-localisation of intimal and medial calcification indicates that these calcifications are one unified process. However, a study by Duhn *et al* has produced evidence suggesting that the two are distinctively separate processes. The group demonstrated this by examining breast arterial calcification (BAC) in patients with chronic kidney disease (CKD). A study of the breast tissue of 16 patients all showed signs of calcification exclusively in the tunica media. The group concluded that BAC could be an important indicator and marker of medial calcification (Drüeke and Massy, 2011, Duhn *et al.*, 2011). The key distinctions between intimal and medial calcification have been covered extensively in a number of review articles (London, 2003, Kapustin and Shanahan, 2009, London, 2011). Differences widely accepted across the field are that intimal calcification is a consequence of inflammation consistent with the development of plaques and occlusive lesions, whereas medial calcification is typically a condition of conductance vessels such as the femoral artery and aorta and is tightly-linked to Ca^{2+}_{o}/Pi dysregulation often present in CKD patients (London, 2003, Shroff and Shanahan, 2007, Kapustin and Shanahan, 2009, London, 2011).

1.4.1 Intimal atherosclerotic calcification

Atherosclerosis is an inflammatory disease of the cardiovascular system which is significantly accelerated by high serum cholesterol (Demer, 2001), smoking (Witteman *et al.*, 1993, Howard *et al.*, 1998), hypertension (Ross, 1993, Ross, 1999), lipoproteins (Ghiselli *et al.*, 1981, Williams *et al.*, 2010), high blood sugar (Jongstra-Bilen *et al.*, 2006), dead smooth muscle cells and macrophages (Jongstra-Bilen *et al.*, 2006). Atherosclerosis begins in younger years in humans and extends into adulthood where such conditions are present that exacerbate it (Allison, 2004). Typically, bifurcations of blood vessels are susceptible target areas for the development of atherosclerotic calcification where turbulent blood flow can cause shear stress to the vascular endothelium (Daugherty *et al.*, 1997, Fayad and Fuster, 2001). At these sites, lipoproteins can deposit and small plaques can begin to develop, extending outward into the lumen (Ivanovski *et al.*, 2009). Additionally, plaque growth is positively correlated with calcification of the intima where lipids, macrophages, lymphocytes, fibroblasts and dead VSMCs can coagulate with Ca^{2+}_o and Pi products such as HA (Amento *et al.*, 1991, Clarke *et al.*, 2006). Interestingly, the stability of plaques in calcified regions is determined chiefly by ECM components, specifically collagen. When the fibrous cap of the plaque is poor in ECM proteins this can be an indicator that rupture and subsequent thrombosis is likely to follow. Surprisingly, although thrombosis is a major consequence of plaque rupture, 90% of ruptures are asymptomatic and can be effectively repaired at the vessel wall (Budoff and Gul, 2008), however, repeated cycles of rupture and repair can occur as seen in Figure 4. Plaque rupture is a crucial event in cardiovascular morbidity. At rupture, plaque contents are released into the lumen of the affected artery inducing blood adhesion and coagulation (Williams *et al.*, 2010). Plaque instability can be induced by a number of factors including inflammatory cytokines such as interferon-γ (IFN-γ) present in the vasculature (Binder, 2004). These can act to potentiate instability by inhibiting the synthesis of the crucial structural collagens (type I and III) laid down by surrounding VSMCs. Ultimately, this reduces the robustness of the fibrous cap increasing the risk of rupture (Amento *et al.*, 1991). Plaque stability can be further increased when the lipid pool within the plaque is high, in addition to a significantly reduced amount of macrophages and lymphocytes which normally evoke mechanical stress on the fibrous cap in greater abundances (Libby, 2002). Additionally, lowered

blood pressure and oxidative stress can help maintain plaque stability (Libby and Aikawa, 2002).
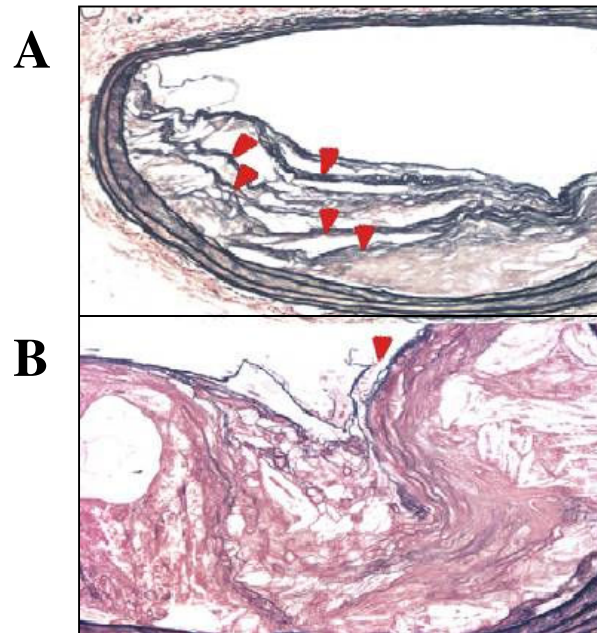
Figure 4. Recurrent atherosclerotic plaque rupture in the brachiocephalic artery of an apolipoprotein E deficient (apoE$^{-/-}$) / transglutaminase 2 deficient (TG2$^{-/-}$) double-knockout mouse. Red arrowheads indicate numerous previous fibrous caps. (A) Five successive plaque ruptures and repairs. (B) One fibrous cap with a dense lipid pool. Figure taken from Williams *et al* (Williams *et al.*, 2010).

1.4.2 Medial vascular calcification

The principal type of calcification in this investigation relates to the calcification of the tunica media. Accumulation of Ca^{2+}_o and Pi minerals, particularly HA ($Ca_{10}(PO_4)_6(OH)_2$) in the VSMC layer is a well-documented characteristic of medial vascular calcification (Nitta *et al.*, 2004, Johnson, 2005, Johnson *et al.*, 2006, Shroff and Shanahan, 2007, Nitta, 2011). Medial or "Mönckeberg" calcification was first described in 1903 by Johann Georg Mönckeberg (Mönckeberg, 1903) and is often detected in uremic and diabetic patients, suggesting that medial vascular calcification is at least in part a consequence of failure to excrete Pi (Giachelli, 1999). This is indeed observable in patients suffering with hyperphosphataemia, typically brought on by CKD (Jono *et al.*, 2000). Until recently, authors have disagreed that medial calcification is exclusively a condition of the tunica media and not just an addition to the internal elastic lamina (Micheletti *et al.*, 2008). Both *in vivo* and *in vitro* models have shown that VSMCs demonstrate significant plasticity enabling them to transdifferentiate (Olesen *et al.*, 2006, Hruska, 2009, Speer *et al.*, 2009). The current transdifferentiation hypothesis, which is supported by much experimental data, suggests that VSMCs may begin to calcify when exposed to a number of conditions including a reduction in protective factors, and an increase in pro-calcific factors (Johnson *et al.*, 2006). These factors cause VSMCs to excrete matrix vesicles (MVs); extracellular lipid bilayer-enclosed microstructures. It is likely that cells do this in order to off-load an excess of mineral components from internal stores, for example, from the ER (Anderson *et al.*, 2005, Kapustin *et al.*, 2011). Unfortunately, evidence suggests that these MVs which firstly act as a 'rescue mechanism' for the cells, actually provide an extracellular nidus for calcification and coagulation of factors including HA (Chen *et al.*, 2010a). In these conditions VSMCs adopt a more osteoblastic phenotype. They begin to express a number of osteoblast gene markers including ALP, osterix (OSX), osteoprotegrin (OPG), OC and the osteoblast transcriptional regulator, Runx2 (Shroff and Shanahan, 2007, Neven *et al.*, 2010). Calcification is often an asymptomatic consequence of this mineral accumulation in the tunica media (Abedin, 2004). Interference with elastic lamina and healthy extracellular matrix components can increase turgidity and stiffness of major vessels such as the aorta, femoral and brachiocephalic arteries (Guérin *et al.*, 2000). Consequently, individuals suffer from blood pressure increases and reductions in blood flow. This is often attributed to the

decreased contractility, vessel compliance and increased aortic stiffness. In excess, medial calcification can usher in a compensatory mechanism by the heart to normalise this effect, and so patients with medial calcification are prone to the development of left ventricular hypertrophy (Davies and Hruska, 2001, Nitta *et al.*, 2004, Nitta, 2011). A diseased human femoral vessel artery can be seen in Figure 5.
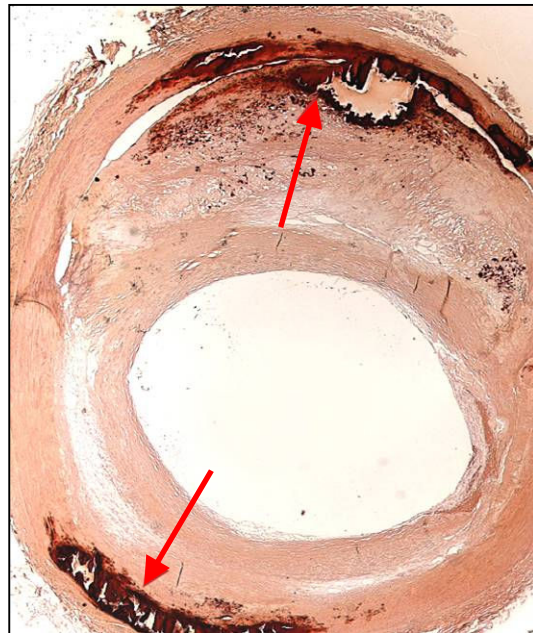
Figure 5. Medial arterial calcification in a human femoral artery. Mineralisation in the VSMC layer is confirmed with alizarin red staining (red arrowheads). Medial calcification can be observed in lesions indicated with red arrows. Tearing of the vessel wall can be seen in these heavily calcified regions. Image courtesy of Dr. Alexander at Manchester University.

1.4.3 Aortic valve calcification

Aortic valve calcification is the third most common cause of adult heart disease (Thom *et al.*, 2006). The condition becomes more severe in ageing individuals. This is best observed in individuals over the age of 80 where 1 in 25 will have some degree of aortic valve calcification (Lindroos *et al.*, 1993). The molecular mechanisms promoting this disease state are currently unknown, although research data support the idea that VSMCs transdifferentiate in the aortic valve into osteoblast-like cells (Nigam and Srivastava, 2009, Wen *et al.*, 2012). This has been demonstrated in mice where the Notch1 gene has been knocked out. Nigam and Srivastava showed that Notch1 has a repressive effect on osteogenic marker expression. The group showed this by looking at mRNA and protein levels of BMP-2 which was significantly upregulated in Notch1-KO mice fed high-fat diets (Figure 6). More importantly, Notch1-KO was associated with calcification of the aortic valve (Nigam and Srivastava, 2009).

WT Mice   **Notch1-KO Mice**
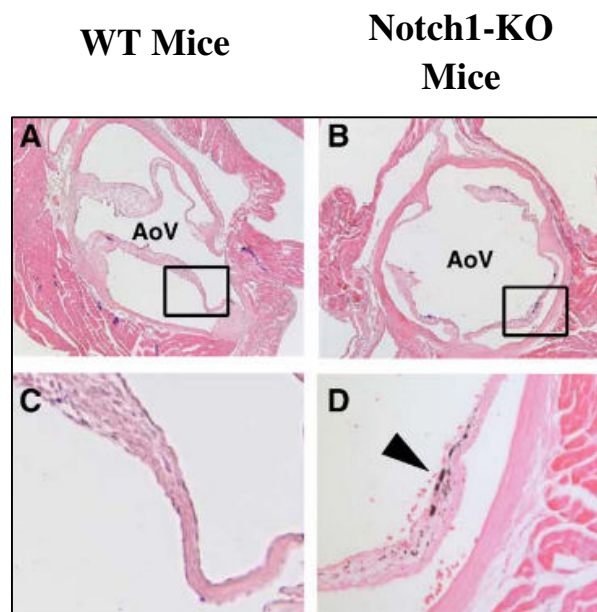
Figure 6. Aortic valve calcification in Notch1-knockout mice. (A and C) low- and high-powered magnification of von Kossa-stained aortic valves in WT mice fed on a normal diet. (B and D) low- and high-powered magnification of von Kossa-stained aortic valves in Notch1-KO mice fed on a high-fat diet (20% anhydrous milkfat / 1% corn oil / 0.2% cholesterol). In panel D mineral deposits can be seen as confirmed by the presence of black von Kossa nodules. Figure adapted from Nigam and Srivastava (Nigam and Srivastava, 2009).

1.4.4 Calciphylaxis / calciphic uremic arteriolopathy

Calciphylaxis, often termed calciphic uremic arteriolopathy (CUA), is a condition often associated with CKD and diabetes (Hayden and Goldsmith, 2010). CUA is a visible manifestation of dysregulated Ca^{2+}_o and Pi metabolism and often presents itself in patients with CKD or end-stage renal disease (ESRD). Patients suffer from small eschars on the skin on the lower body. Interestingly, such eschars are rarely seen on higher body extremities (Rogers *et al.*, 2007). Reports suggest that these darkened patches of skin contain subcutaneous Ca^{2+} deposits. Furthermore, these deposits are co-localised with adipose tissue suffering from hypoxia as a direct result of calcification (Wilmer and Magro, 2002). CUA is particularly dangerous since these small calcifications can result in larger-scale necrosis (Wilmer and Magro, 2002). Researchers have also reported an upregulation of osteogenic markers in smooth muscle cells in these calcified lesions (Ahmed *et al.*, 2001). CUA visible lesions can be observed in Figure 7.
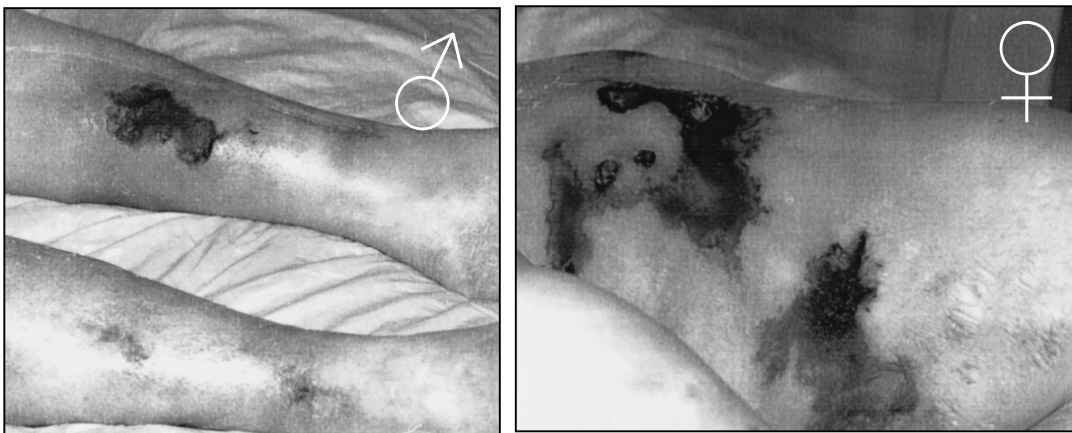
Figure 7. Skin lesions of calciphylaxis patients. (Left) Calcific ulcers present on a male Caucasian patient with diabetes on dialysis. (Right) Medial left thigh calcified lesions on an obese, diabetic caucasian female with diabetes on dialysis. Figure adapted from Wilmer and Magro (Wilmer and Magro, 2002).

1.5 Vascular calcification: epidemiology and associated diseases

Interestingly, despite well-documented health problems in western societies in recent years, VC is not a new pathological development. Unearthing of the mummified remains of a 5,300 year old "ice-man" discovered in the Tyrolean Alps in 1991 confirmed VC in ancient civilisations. Murphy *et al* conducted conventional radiography on the remains in 2003 and computed tomography (CT) revealed that the male of approximately 45 years old exhibited degenerative arthritis and vascular calcification of the aorta and carotid arteries (Murphy *et al.*, 2003). Vascular calcification is abundantly widespread, affecting humans of all ethnic groups with varying degrees of severity (Roger *et al.*, 2011). Calcification and related cardiovascular disease (CVD), including stroke and heart attacks, is most prevalent in white and black populations with lower incidence in Asian populations (Table 1). It often correlates with hypertension, type II diabetes and most exuberantly demonstrable in patients suffering with CKD (Johnson *et al.*, 2006, Prosdocimo *et al.*, 2010). Moreover, VC is at its most pathological (and effectively irreversible) manifestation in patients with ESRD. ESRD is reached after substantial, prolonged and severe CKD. The kidney function in ESRD patients is so drastically diminished that healthy Pi metabolism and $1,25(OH)_2D_3$ synthesis are severely compromised. Because of this, the likelihood and relative intensity of VC is inversely and proportionately exaggerated during ESRD, which is often a key predictor of cardiovascular mortality (Witteman *et al.*, 1986, Mizobuchi *et al.*, 2009).

Additional predictors of cardiovascular disease include high blood cholesterol and type II diabetes. In fact, the American Heart Association released stroke and CVD statistics based on a 2008 analysis and showed that 33.6 million Americans over the age of 20 have inappropriate serum cholesterol levels of over 240mg/dL. Furthermore, a staggering 18.3 million Americans (~8% of the population) suffer from diabetes mellitus. Updates to the statistics were also made in 2012, revealing that adults over the age of 20 who are overweight or suffer from obesity in America amount to 149.3 million; an alarming 67.3% of the total US population. In addition to these striking statistics, the study also showed that 1 in 3 deaths in 2008 were related to CVD complications in people below the age of 75. This was below the life expectancy of 77.9 in the US (Thom *et al.*, 2006,

Rosamond *et al.*, 2007, Rosamond *et al.*, 2008, Lloyd-Jones *et al.*, 2009, Lloyd-Jones *et al.*, 2010a, Lloyd-Jones *et al.*, 2010b, Roger *et al.*, 2011, Roger *et al.*, 2012). Taken together, these statistics (based on the 2008 analyses) reveal that 82.6 million Americans (36.2% of the population) suffer from CVDs, of which VC is also a predominant contributor. 811,900 of these individuals later died from CVD mortality (Thom *et al.*, 2006, Rosamond *et al.*, 2007, Rosamond *et al.*, 2008, Lloyd-Jones *et al.*, 2009, Lloyd-Jones *et al.*, 2010a, Lloyd-Jones *et al.*, 2010b, Roger *et al.*, 2011, Roger *et al.*, 2012). These concerning statistics are best visualised in Figure 8, detailing overall annual costs resulting from these CVD health complications.

It should also be noted that, in the UK, statistics released by the British Heart Foundation and European Heart Network state that the cost of prescription medication for hypertension, heart disease and heart failure therapies have actually dropped between 2010 and 2011 (Nichols *et al.*, 2012). Costs have dropped from approximately £400 million to £330 million per year. Although this appears to be in stark contrast to US statistics, it is reported that this is due to cheaper therapies put in place. However, estimates of the cost of CVD to the UK economy as a whole are approximately £19 billion per year, consuming some ~6% of the health care annual budget (Nichols *et al.*, 2012).

ETHNIC GROUP	% HD PREVALENCE
American Whites	11.9%
American Blacks	11.2%
Hispanic / Latinos	8.5%
American Indian/Alaskan Natives	8.0%
Asian	6.3%
Indian	9.0%
Korean	4.0%

Table 1. Heart disease prevalence within different ethnic groups. Statistics were derived from the American Heart Association compilation from the National Health Interview Survey (NHIS) and National Centre for Health Statistics (NCHS) in 2009. Data relate to different ethnic groups residing within the United States suffering from heart disease (HD) over the age of 18 (Roger *et al.*, 2011).

Direct and Indirect Costs of Cardiovascular Disease in the United States
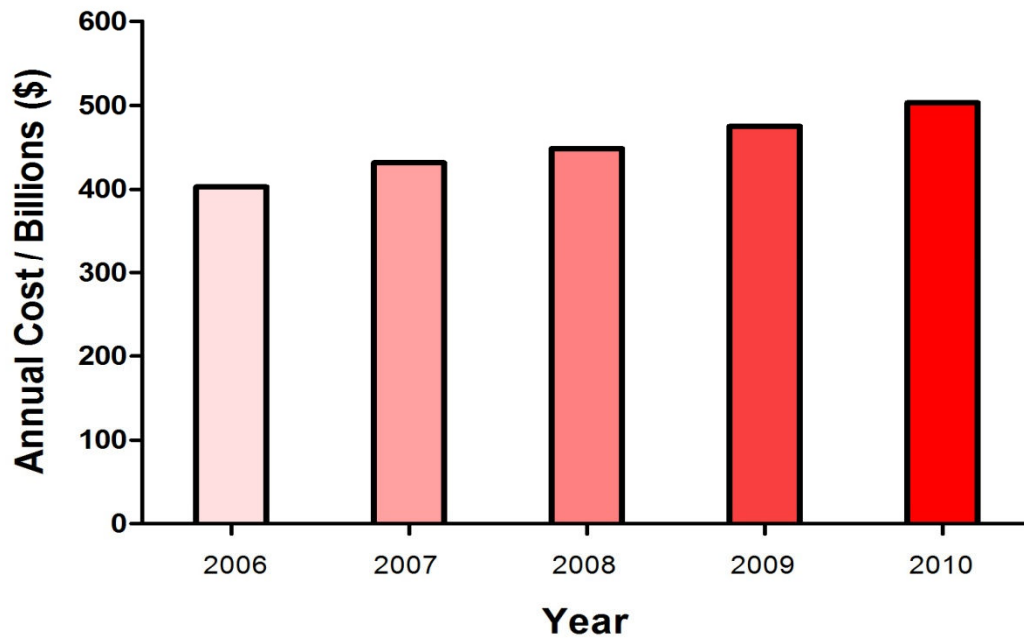
Figure 8. **Cardiovascular disease costs in the United States over 5 years**. Data released by the American Heart Association detail direct and indirect annual costs to the US through cardiovascular disease. Costs relate to health expenditures, cost of physicians and professionals, hospital services, home health care, and prescribed medications in addition to lost productivity resulting from CVD mortality. 2006, $403.1 billion; 2007, $431.8 billion; 2008, $448.5; 2009, $475.3 billion; 2010, $503.2 billion (Thom *et al.*, 2006, Rosamond *et al.*, 2007, Rosamond *et al.*, 2008, Lloyd-Jones *et al.*, 2009, Lloyd-Jones *et al.*, 2010b).

1.6 Factors which exacerbate vascular calcification

Despite vascular calcification being largely multi-factorial, there are some key features which persist in all cases in humans. Regardless of ethnic background (or even species), we consistently see these familiar contributors across all areas of research.

1.6.1 Chronic kidney disease and dysregulated Pi metabolism

As a key player in Pi metabolism, the kidney has crucial role in the onset of calcification. During CKD, kidney function is diminished and has severe repercussions on Pi metabolism. The progression of CKD is a key predictor of VC (Bellasi *et al.*, 2009). In many cases, early stages of CKD induce vascular calcification, but the most dangerous manifestations are most observable in patients which develop full blown ESRD (Mizobuchi *et al.*, 2009, Shanahan *et al.*, 2011). In fact, patients with ESRD have extensive aortic and coronary calcification and ~50% of these patients have valvular calcification (Hujairi *et al.*, 2004). This is attributable largely to the diminished Pi excretion consequential of kidney dysfunction. This accumulation of Pi is a key feature of uremic patients and is termed hyperphosphataemia. Hyperphosphataemia has proved to be helpful predictor of vascular calcification.

1.6.2 Associations between Ca^{2+}_o, Pi, Ca x Pi, PTH and CKD

This association between Ca^{2+}_o, Pi, PTH, CKD and cardiovascular disease has been described in detail by Geoff Block and colleagues (Block *et al.*, 1998). Over the past few decades an association between secondary hyperparathyroidism and a decline in renal function has been documented (Slatopolsky *et al.*, 1972, Slatopolsky *et al.*, 1984). In a 1998 study, Block compiled data from patients of two groups. The first group were from the Case Mix Adequacy Study (1990) and the second group were from the Dialysis Morbidity and Mortality Study Wave 1 (1993). After normalising CKD patients in each group to account for differences in sex, age of onset, diabetes and smoking, Block and colleagues were able to associate patients with high serum Pi (>6.5mg/dL), and patients with high serum Ca^{2+} x Pi product (>40mg/dL) with premature death (Block *et al.*, 1998).

The correlation was a clear indication that high Pi brought on by CKD and calcification were strongly intertwined in patients of all backgrounds. Work by Block *et al* has been particularly crucial in intimately linking actions of the parathyroid, the CaSR, Pi, Ca^{2+}_o homeostasis, CKD and heart disease. With large amounts of clinical data on patients with CKD, diabetes and heart disease, it has become easier to carry out epidemiological studies in these areas.

1.7 Mechanisms of vascular calcification

Vascular calcification is a multifaceted and multifactorial state which can be either symptomatic or asymptomatic (Abedin, 2004). As a result, attributing a specific pathway or single hypothesis which underlines how VC starts, progresses and develops is challenging. When looking at pathways for disease, one must consider the vast variety of genes, proteins and cell-types involved in regulating healthy and compliant vascular walls, albeit keeping in mind basic physicochemical processes which can coexist in biological systems. In 2004, Giachelli reviewed mechanisms that surround vascular calcification and attempted to envelop major aspects of pathogenesis in blood vessels and gather them into an intelligible and organised mechanism (Giachelli, 2004). Giachelli proposed that Ca^{2+}_o and Pi coalesce in the vasculature and precipitate to form crystals of hydroxyapatite and whitlockite. Indeed, this was found to be a good predictor of VC, particularly in CKD patients where serum Ca^{2+}_o and Pi levels are elevated (Goodman *et al.*, 2000). Since calcification is a consequence of build-up of these minerals, this is a good place to start in developing a complete hypothesis. Secondly proposed, is the balance between calcification inhibitors and promoters discussed in the next section.

1.8 Inhibitors of vascular calcification (genetic factors)

In order to determine whether a gene plays a role in disease it is often knocked out to generate a null-mouse, or a tissue-specific knockout mouse. These mice will either lack the gene in every cell type, or may have specific deletion of the gene driven by a tissue-specific promoter. Reviewed in this section will be genetic determinants of vascular calcification, as demonstrated from *in vivo* studies.

1.8.1 Fetuin A

Fetuin A (α2-Heremans-Schmid glycoprotein) is a circulating endogenous inhibitor of mineralisation which has been shown to be taken up by VSMCs (Chen *et al.*, 2010b). This glycoprotein has been shown to have a significant role in bone development and is highly correlated with CKD where progression of the disease is associated with decreased serum levels of fetuin A. It has also been shown that fetuin-A is a potent binder of apatite, and is therefore often considered an anti-mineralising factor (Jahnen-Dechent *et al.*, 2011). Typically, fetuin A is highly expressed in the developing fetus, where it might play a protective role against fetal ectopic mineralisation (Merx *et al.*, 2005). This may be because embryonic Ca^{2+}_o is approximately 1.7mM; hypercalcaemic compared to adult. This embryonic relative hypercalcaemia is speculated to be for the purpose of optimal developmental regulation during organogenesis (1.0-1.3mM $[Ca^{2+}]_o$) (Kovacs and Kronenberg, 1997, Finney *et al.*, 2008). Interestingly, CKD patients in dialysis with reduced fetuin A levels appear to have increased vascular calcification with greater CVD mortality rates (Reynolds, 2005). Fetuin A also acts as a protease inhibitor and *in vitro* studies have shown that it can regulate VSMC apoptosis and matrix vesicle calcification (Reynolds, 2005). The protective role of fetuin A is clearly observable in transgenic mice lacking the fetuin A gene. Merx *et al* demonstrate that, in fetuin A-deficient mice, ectopic and dystrophic calcification is extremely widespread. Paradoxically to our area of investigation, this knockout mouse demonstrates significant calcification in muscles, the heart, lungs, kidneys but, very surprisingly, not the aorta; a region which normally calcifies during CVD (Merx *et al.*, 2005). Calcifications of the heart and myocardium are observed in Figure 9 where von Kossa staining confirms the presence of mineral. Since

aortic calcification was not observed, it is likely that the aorta has multiple protective mechanisms to prevent calcification, even in the absence fetuin A.
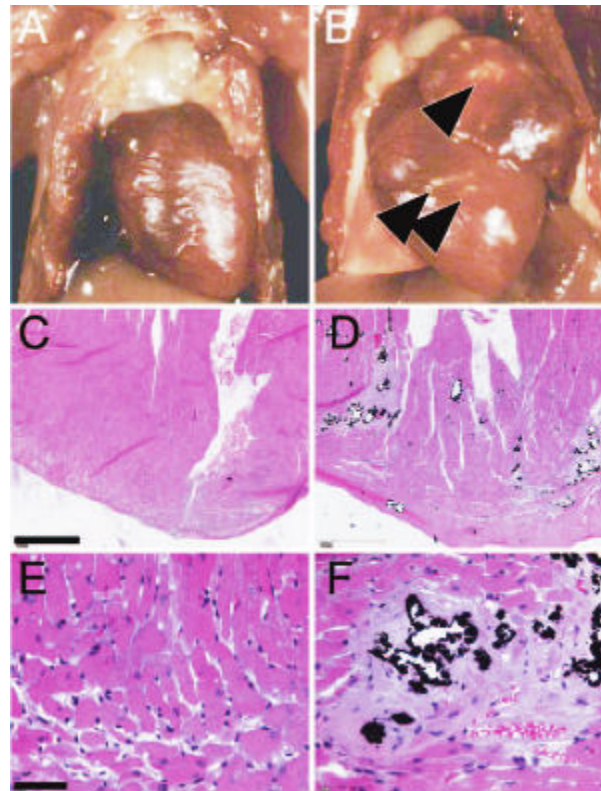
Figure 9. Fetuin A knockout mice show spontaneous ectopic calcification of the heart. (A) WT mouse heart viewed by light microscopy. (B) KO mouse heart viewed by light microscopy. Small white calcified lesions can be observed (black arrows). (C) low-powered light microscopy of WT mouse myocardium tissue sections stained with von Kossa. (D) low-powered light microscopy of KO mouse myocardium tissue sections. KO tissue is speckled with small black nodules of mineral (von Kossa positive). (E) High-powered light microscopy of WT mouse myocardium tissue sections stained with von Kossa. Tissue is devoid of ectopic mineral. (F) High-powered microscopy of KO myocardium tissue sections. Black mineral deposits are visible. Figure adapted from Merx *et al* (Merx *et al.*, 2005).

1.8.2 MGP

Initially discovered in bone, Matrix gla (γ-carboxyglutamic acid) protein (MGP), is a Ca^{2+}_o-binding protein abundant in serum (Price and Williamson, 1985). In addition to bone, MGP is normally expressed in cartilage, tooth, VSMCs, kidney, heart and the lung (Khoshniat *et al.*, 2011). Post-translational modification of MGP is crucially important for it to elicit its protective role. The endoplasmic reticulum-bound γ-carboxylase enzyme is essential in converting immature MGP to a mature form containing Ca^{2+}_o-binding γ-carboxyglutamic acid (Gla) residues, using vitamin K as a co-factor (Furie, 1990, Wallin *et al.*, 2001). Crucially, it has been shown that MGP in its mature form can bind Ca^{2+}_o in addition to BMP-2; a potent promoter of calcification. Interestingly, Zebboudj *et al* have shown that MGP/BMP-2 complexes can form *in vitro* (Zebboudj *et al.*, 2002). The group found that balance of these two proteins was crucial in determining the extent of calcification (Zebboudj *et al.*, 2003). MGP is likely to co-ordinate its protective role in VSMCs chiefly by its synthesis and secretion by these cells, therefore making MGP readily and locally available as a protective agent (Proudfoot *et al.*, 1998). MGP, however, can be tightly controlled by the actions of its inhibitor, warfarin. Studies have shown that in rat VSMCs *in vitro*, warfarin increases mineralisation in a dose-dependent manner (Beazley *et al.*, 2012).

Interestingly, in addition to fetuin A-KO mice demonstrating widespread ectopic calcification, MGP-deficient mice also develop a similar phenotype, reaffirming the protective roles of these factors. Luo *et al* developed a MGP$^{-/-}$ mouse, and in 1997 reported severe calcification of all blood vessels in these mice. Calcification continued a few weeks into life until mice died of aortic rupture before adulthood. This further illustrates the essential role of MGP in the regulation of vascular calcification (Luo *et al.*, 1997). An important distinction between fetuin-A and MGP-KO mice is that MGP-KO mice develop calcification of the aorta. Ectopic mineralisation of the cardiovascular system is seen in MGP-KO mice in Figure 10.
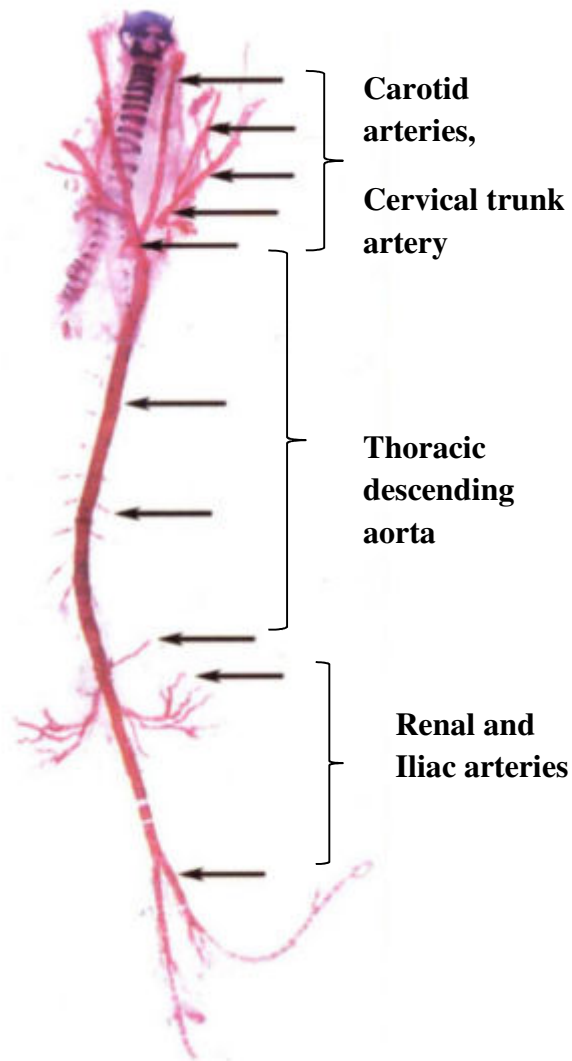
Figure 10. Ectopic mineralisation of blood vessels in MGP knockout mice. 4-week old mice lacking MGP show significant calcification of all major blood vessels by alizarin red staining. Calcification can be seen in separate arteries indicated by black arrows. Figure adapted from Luo *et al* (Luo *et al.*, 1997).

1.8.3 Pyrophosphate

Inorganic pyrophosphate (PPi) is a potent inhibitor of medial calcification found all over the body. PPi is extensively produced in all cells undergoing DNA synthesis where PPi is a bi-product of the action of deoxynucleoside triphosphatases in the nucleus (Herdewijn and Marlière, 2012). Its levels are also tightly controlled by the actions of tissue non-specific alkaline phosphatases (TNAPs) anchored into the plasma membrane that act extracellularly (Schoppet and Shanahan, 2008, Villa-Bellosta *et al.*, 2011). TNAPs play a crucial role in the catalytic hydrolysis of PPi into small Pi ions, therefore, can be considered as factors which exacerbate vascular calcification and hyperphosphataemia. PPi has been shown to be a direct inhibitor of hydroxyapatite formation, even at concentrations as low as 100nM (Francis *et al.*, 1969). Extracellular PPi is generated by the actions of nucleotide pyrophosphatase/phosphodiesterase-1 (NPP1) which hydrolyse ATP (Schoppet and Shanahan, 2008). Research by Villa-Bellosta has shown this to be a tightly localised process, taking part within blood vessels. This was found when mRNA transcripts for NPP1 and TNAPs were located in mouse and rat aortae. Furthermore, the group showed that in NPP1 knockout mice, aortae did not synthesize PPi (Villa-Bellosta *et al.*, 2011). The crucial role of PPi as a protector against vascular calcification is clear in children with generalized arterial calcification of infants (GACI). This disorder is caused by inactivating mutations in the NPP1 gene. Consequently, the sufferer cannot synthesize PPi and the result is large scale systemic calcification culminating in lethal aortic rupture (Rutsch *et al.*, 2001, Rutsch *et al.*, 2003, Prosdocimo *et al.*, 2010).

1.8.4 BMP-7

Bone morphogenetic proteins (BMPs) comprise a family of some 30 proteins typically involved in osteogenesis and organogenesis (Hruska, 2005). BMP-7 is a member of the transforming growth factor β (TGFβ) superfamily and acts as a crucial morphogen throughout development and adulthood (Hruska, 2005, Hruska, 2009). Normally, BMP-7 is expressed widely in the kidney and functions to maintain the differentiated phenotype of tubular cells through paracrine and autocrine signalling. Their role in osteogenic and renal development is best seen in mice deficient in BMP-7. These mice die postnatally due to skeletal patterning defects, hypomineralisation of the ribcage and skull (as seen in Figure 11) and renal dysplasia (Hofmann *et al.*, 1995). Interestingly, studies have shown that despite BMP-2 being so structurally similar to BMP-7, they both promote two very different mechanisms of actions in VSMCs. BMP-2 is typically an osteogenic marker and drives mineralisation- even in the vasculature (Lee *et al.*, 2003). Conversely, BMP-7 is a protective morphogen which maintains and promotes the VSMC phenotype (Dorai *et al.*, 2000). Furthermore, its expression is reportedly diminished during vascular calcification. Its potent role as a cardiovascular protective agent is seen in low density lipoprotein receptor (LDLR)-deficient mice; a mouse model used to initiate and accelerate atherosclerosis. Atherosclerosis induction with high-fat diets in LDLR$^{-/-}$ appears to be rescued with BMP-7 treatment. During treatment, skeletal remodelling is resumed to the normal and hyperphosphataemia is significantly reduced (Davies, 2003). Although interestingly, one study suggests that BMP-7 may be deleterious, inducing thrombogenicity of atherosclerotic plaques (Sovershaev *et al.*, 2010).
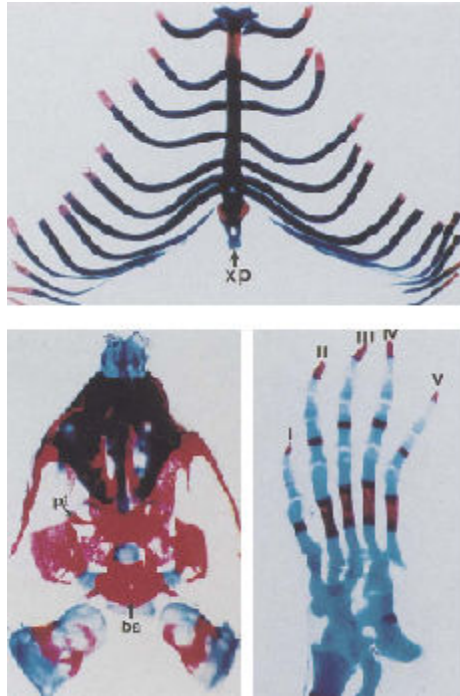
WT Control Mouse   **BMP-7 KO Mouse**
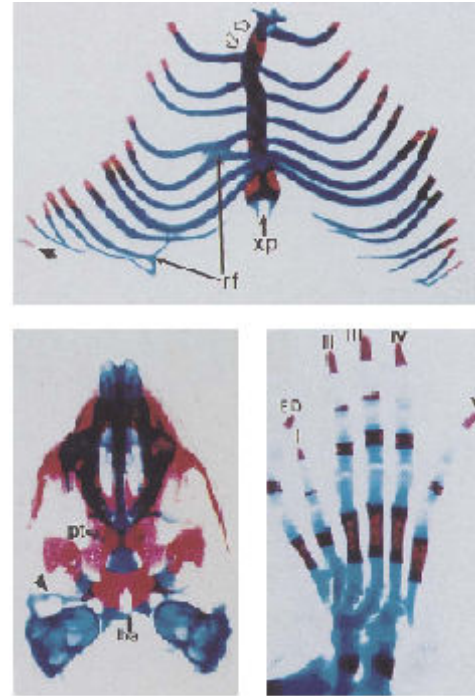
Figure 11. BMP-7 knockout mice demonstrate skeletal developmental defects of the skull, ribcage and right hindlimb. (Left panel) WT mice show normal skeletal growth of the ribcage (upper), skull (lower left) and right hundlimb (lower right). (Right panel) BMP-7 KO mice show abnormal ribcage development in size and shape (upper panel), presence of a cavity in the basosphenoid bone and fusion between the right alisphenoid bone and inner ear in the skull (lower left), and extra digits on right hindlimbs (lower right). Skeletons were stained with alcian blue (cartilage) and alizarin red (Ca^{2+} in bone). Figure adapted from Hofmann *et al* (Hofmann *et al.*, 1995).

1.8.5 FGF23

Fibroblast growth factor 23 (FGF23) is a major phosphaturic hormone produced in bone and upregulated during haemodialysis (Pai *et al.*, 2011). FGF23 binds to the FGF receptor (FGFR) in the presence of its obligatory coreceptor Klotho, and plays a critical role in Pi metabolism, vitamin D regulation and overall renal function. When serum Pi levels become elevated, osteoclasts and osteoblasts begin to secrete FGF23 (Yamazaki *et al.*, 2010). Circulating FGF23 then acts to reduce serum Pi. This is done primarily by reducing the expression of the sodium/phosphate transporters in the kidney such as NaPi-IIa and Pit-2 (Shimada *et al.*, 2004). This way, excess plasma Pi is eliminated from extracellular fluids and excreted (Sage *et al.*, 2009). Interestingly, two genetic disorders exist in humans which demonstrate substantial FGF23 dysregulation. These are autosomal dominant hypophosphataemic rickets (ADHR) and hyperphosphataemic familial tumoral calcinosis caused by activating and inactivating mutations of *FGF23* respectively. The latter can be recapitulated in mice where *FGF23* is knocked out (Figure 12). In these mice, severe ectopic calcification occurs with mineral deposition in the kidney and aorta. This has been confirmed experimentally by numerous groups including that of Stubbs *et al*, who showed calcification by alizarin red staining in mice at just 6 weeks of age (Stubbs *et al.*, 2007). Klotho-deficient mice also share many phenotypic characteristics of FGF23-deficient mice. In a 1997 publication detailing the phenotype of these mice, investigators noted premature arteriosclerosis, osteoporosis and medial calcification of the aorta (Figure 13) (Kuro-o *et al.*, 1997).
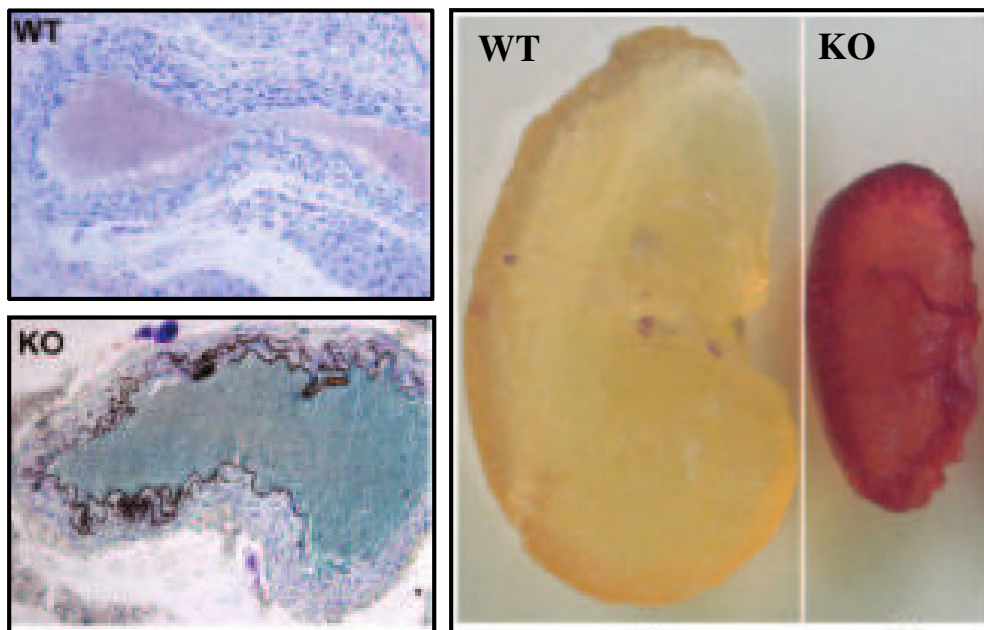
Figure 12. FGF23-knockout mice show ectopic calcification in the aorta and kidney. Upper left: WT mouse aortae stained with von Kossa. Lower left: KO mouse aortae stained with von Kossa show mineralisation in the tunica intima and media. Right panel: WT and KO mouse kidneys stained with alizarin red. KO kidneys appear significantly smaller than WT and are abundant in Ca^{2+} as confirmed by alizarin red staining. Figure adapted from Stubbs *et al* (Stubbs *et al.*, 2007).
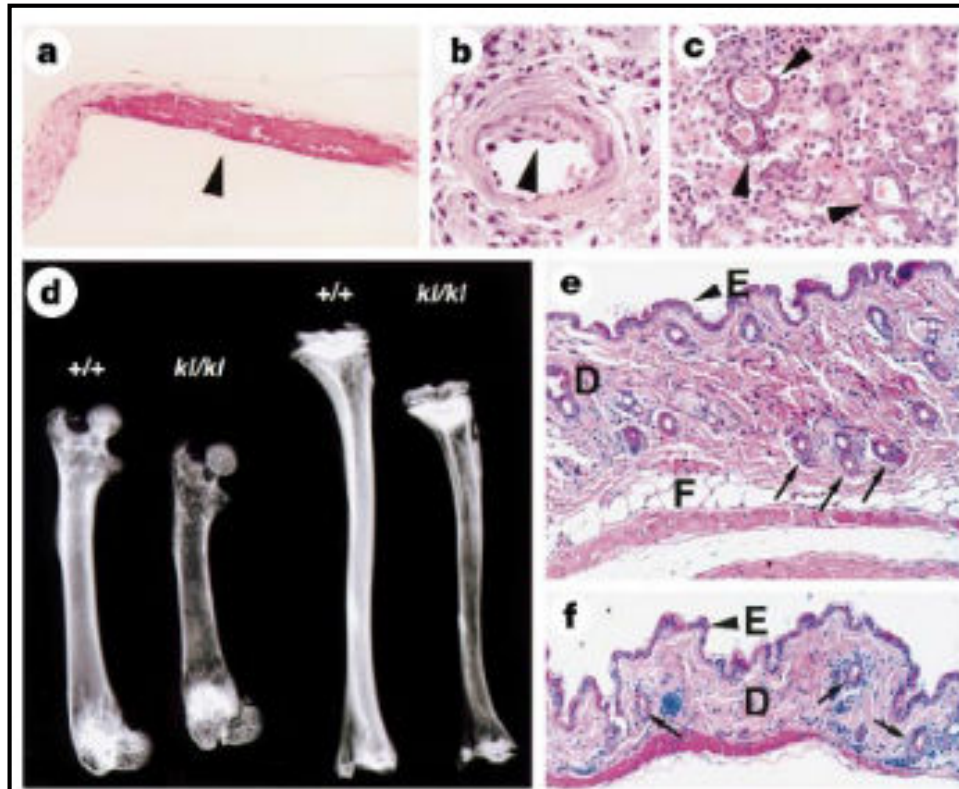
Figure 13. Klotho deficient mice exhibit aortic calcification, osteoporosis and skin atrophy. (a) Calcification of the aorta in Klotho$^{-/-}$ mice. (b) Intimal thickening in muscular artery. (c) Calcification in kidney arteries. (d) Bone radiographs of femurs (left two) and tibiae (right two). (e) Skin sections of control mice. (f) Skin sections of Klotho$^{-/-}$ mice (Kuro-o *et al.*, 1997).

1.8.6 Osteoprotegrin

Osteoprotegrin (OPG) is a member of the tumour necrosis factor (TNF) receptor gene superfamily and is a soluble circulating ligand of receptor activator of nuclear factor kappa-B ligand (RANKL); a major promoter of mineralisation of bone (Kendrick and Chonchol, 2011). OPG is also highly expressed in vascular cells such as VSMCs and endothelial cells (Kendrick and Chonchol, 2011). Normally, OPG plays an important role in bone metabolism and is secreted to inhibit osteoclast function. In OPG-deficient mice there is a significantly reduced bone density and mass, however, a group who overexpressed OPG in the liver showed that mice gain bone density and mass (Bucay *et al.*, 1998). Many studies including research by Dhore *et al* suggest a role for OPG as a protector against vascular calcification and atherosclerosis. Dhore *et al* showed that OPG is upregulated systemically during atherosclerosis (Dhore *et al.*, 2001). This once again suggests that OPG is tightly regulated to reduce ectopic calcification and mineralisation.

1.9 Inhibitors and treatments of vascular calcification (non-genetic factors)

In many cases it has been reported that non-genetic factors play significant roles in inhibiting vascular calcification. Such factors, which are not the direct products of genes, cannot be investigated by means of gene-knockout. For this reason, researchers have demonstrated the potential of these non-genetic factors as calcification inhibitors by treating animals predisposed to vascular calcification, or by performing *in vitro* analysis on vascular cells cultured in the presence of these factors. These factors will be reviewed here.

1.9.1 Thiosulphate

Since the 1980's, thiosulphate has been suggested as a treatment for kidney stones (Yatzidis and Agroyannis, 1987). More recently, several groups have demonstrated the benefit of sodium thiosulphate treatment in reducing the severity of CUA and the development of Ca^{2+} x Pi stone formation in hypercalciuric rats (Hackett *et al.*, 2009, Hayden and Goldsmith, 2010). In a study by Pasch *et al,* uremia was induced by feeding rats adenine for 4 weeks. Thiosulphate treatment completely inhibited aortic calcification, which was abundantly widespread in control mice (Pasch *et al.*, 2008). The action of thiosulphate is likely to be due to the ability of the $S_2O_3^-$ anion to chelate Ca^{2+}_o and inhibit HA formation. For this reason, $S_2O_3^-$ can be considered as a non-genetic inhibitor to HA formation- similar to MGP; a genetically controlled endogenous factor. However, there is evidence (particularly in this publication) that thiosulphate can reduce bone strength, possibly by interfering with healthy mineral metabolism in these areas (O'Neill, 2008, O'Neill and Koba, 2010). For this reason, the potential of thiosulphate as an anti-VC treatment remains controversial.

1.9.2 Calcimimetics

Calcimimetics such as R-568 are positive allosteric modulators at the CaSR and have been used extensively in vascular calcification studies (Alam *et al.*, 2008, Ivanovski *et al.*, 2009, Koleganova *et al.*, 2009, Caudrillier *et al.*, 2010, Chen *et al.*, 2011). Recently our group demonstrated that treating bovine VSMCs in mineralising conditions with R-568 reduced mineralisation of these cells (Alam *et al.*, 2008). Here, bovine VSMCs were mineralised in the presence of β-glycerophosphate (βGP) and 1.8mM Ca^{2+}_o. 1nM R-568 was shown to have a significant effect at reducing mineralisation of these VSMC cultures, although we have also shown (not published) that concentrations as low as 100pM can also reduce mineralisation in these cultures *in vitro*. Additionally, in human coronary artery SMC cultures which were also mineralised, R-568 also reduced calcification, measured as Ca^{2+} incorporation of mineralised cell cultures (Shalhoub *et al.*, 2010). Studies into vascular calcification are however not limited to *in vitro* studies. Numerous investigators have used *in vivo* models to observe this in animal models.

In a 2008 study, Piecha *et al* investigated the role of R-568 and the active form of vitamin D, calcitriol, in vascular calcification in uremic rats. Uremia was introduced using 5/6 nephrectomies since renal failure is often accompanied by vascular calcification in blood vessels such as the aorta and femoral arteries (London, 2003, Torres and De Broe, 2012). After the procedure, animals were fed on standard rodent diets supplemented with a control, R-568 (17mg/kg body weight per day) or calcitriol (3ng/kg body weight per day). The study reported that R-568 and calcitriol were effective at reducing PTH secretion, but R-568 only was effective in reducing serum Pi. Additionally, the group demonstrated that R-568 only was effective at increasing expression of CaSR at the mRNA and protein level (Piecha *et al.*, 2008).

In 2009, the same group attempted to tease out the role of CaSR in the rat cardiovascular system, with a specific interest in the role of CaSR in vascular calcification and vascular remodelling. Over a course of 12 weeks post-nephrectomy, the group firstly showed that, as a consequence of the nephrectomy, rats had significantly thicker aortic walls compared

to sham-operated rats. Additionally, calcitriol treatment (30ng/kg body weight) increased aortic calcification and VSMC proliferation in uremic rats compared to untreated uremic rats. The group also demonstrated that R-568 treatment (20mg/kg body weight per day), but not calcitriol, in both sham-operated and uremic rats led to a significant increase in CaSR expression in the intima when compared to untreated control animals in each group. The group concluded that calcitriol appeared to contribute to greater calcification and proliferation in the aortic wall using the concentration tested, whereas R-568 reduced both of these processes (Koleganova $et\ al.$, 2009). These findings suggest that modulation of CaSR by calcimimetics improves the overall cardiovascular function. One way this protective treatment might occur is through upregulation of the CaSR protein, as confirmed in this study by immunohistochemical analysis. Additionally using apoE knockout mice, which are genetically pre-disposed to vascular calcification, calcimimetics also demonstrated an effective role in reducing calcification of the aorta (Ivanovski $et\ al.$, 2009). ApoE$^{-/-}$ mice were fed regular rodent diets with R-568, calcitiol or a vehicle. It was shown that R-568 (1mg/kg body weight per day) and not calcitriol significantly reduced serum Ca^{2+}_{o}, Pi and calcification of the tunica media.

With the success of such studies in animal models, clinical trials have begun in humans investigating the role of the calcimimetics in vascular calcification. One such trial is the ADVANCE study: a randomized study to determine the role of calcimimetics and low-dose active vitamin D treatment in patients undergoing haemodialysis (Raggi $et\ al.$, 2011) for more than 3 months with serum PTH at 100-300pg/mL, $>50mg^2/dL^2\ Ca^{2+}$ x Pi product receiving active vitamin D and calcium-based phosphate-binders. Coronary arterial calcification (CAC) was assessed in these patients using computed tomography and patients who scored highly for CAC from tomography analysis were placed on low-dose vitamin D (2µg paricalcitol per dialysis session) and 30-180mg/day cinacalcet. After 52 weeks of treatment, patients were re-assessed for CAC scores. It was concluded that patients undergoing combinatory treatment of cinacalcet and vitamin D scored lower for CAC at the end-point in the aorta and mitral valve. These data suggest that calcimimetics (particularly cinacalcet) which are approved for the treatment of secondary hyperparathyroidism, appear to have an additional role in suppressing vascular calcification in human trials (Raggi $et\ al.$, 2011).

In addition to the ADVANCE study, an ongoing study also assesses the effectiveness of cinacalcet on cardiovascular outcome function. The "Evaluation of Cinacalcet HCl Therapy to Lower Cardiovascular Events" (EVOLVE) trial was set up to assess the cardiovascular outcome of cinacalcet-treated patients suffering with CKD. Patients are already receiving a background of current treatments including Ca^{2+}-based Pi-binders and vitamin D sterols. 3,883 patients on haemodialysis and sufferers of secondary hyperparathyroidism were recruited. Patients were randomized from 22 countries, and were found to have a significant burden of cardiovascular abnormalities and manifestations of CKD. This on-going study will determine whether cinacalcet treatment reduces cardiovascular disease severity compared to placebo-treated patients, however, as a global study with such a wide variety of patients on different background treatments, it will be difficult to make accurate comparisons between outcomes (Chertow *et al.*, 2012b).

1.9.3 Vitamin D

Vitamin D in its active form (termed calcitriol) is often prescribed to patients suffering from advanced CKD or renal failure to normalise the hypocalcemia which often accompanies this condition (Teng *et al.*, 2005, Mathew *et al.*, 2008). During the progression of CKD, serum levels of calcitriol steadily decline, facilitating the development of secondary hyperparathyroidism (Dusso *et al.*, 2011). This is particularly due to the reduction in renal mass which reduces overall renal 1α-hydroxylase activity (Hu *et al.*, 2012). Here, secondary hyperparathyroidism is an expected consequence, particularly since calcitriol has been shown to reduce expression of the PTH gene by increasing intestinal reabsorption of Ca^{2+}. However, with deficiencies in vitamin D activation from the kidney, PTH becomes ineffective at restoring normocalcaemia (Dusso *et al.*, 2011). As kidney disease becomes more severe, PTH becomes less effective and so regulating this with vitamin D analogs is often an intervention taken (Teng *et al.*, 2005, Mathew *et al.*, 2008, Bergwitz and Jüppner, 2010). However, vitamin D treatment can be

dangerous since this promotes vascular calcification by Pi retention and hyperphosphataemia, so treatment is often carefully monitored (Renkema *et al.*, 2008). Indeed, there are many reports, both in the clinic and in uremic animal models demonstrating beneficial effects of certain vitamin D receptor agonists such as calcitriol and paricalcitol on vascular calcification and CKD (Teng *et al.*, 2005, Mathew *et al.*, 2008, Piecha *et al.*, 2008, Takeda *et al.*, 2010, Olgaard *et al.*, 2011).

1.9.4 Mg^{2+}

Patients suffering with advanced CKD have reduced circulating Mg^{2+} levels, indicating a possible protective role of this cation against calcification (Tzanakis *et al.*, 1997, Ishimura *et al.*, 2007). It has been shown that Mg^{2+} -an agonist of CaSR- reduces mineralisation in bovine VSMC cultures induced by 10mM βGP over 14 days (Kircelli *et al.*, 2012). This was shown with a prominent reduction of 76% Ca^{2+} incorporation in VSMCs cultured in medium containing βGP in the presence of 2mM Mg^{2+}. Further shown in these studies was the ability of Mg^{2+} to reduce ALP activity in a concentration-dependent manner, in addition to upregulation of the expression of MGP. Mg^{2+} was also effective in reducing in the expression of Sox9 and Runx2, key regulators of chondrogenic and osteogenic differentiation, respectively. Kircelli *et al* propose that Mg^{2+} may in part promote this protective role through CaSR activation (Kircelli *et al.*, 2012). Kircelli *et al* did not investigate the use of Mg^{2+} because of its ability to act as a CaSR agonist, but because it has been observed clinically that patients suffering from vascular calcification have a significantly reduced serum Mg^{2+} concentration (Ishimura *et al.*, 2007, Turgut *et al.*, 2008). Interestingly, one should also note that Pi-binders, which are prescribed to patients suffering with CKD, often come in Mg^{2+}-form. From the mid-1980's, magnesium hydroxide was prescribed as a Pi binder, however, patients often suffered from a number of side-effects including diarrhoea and mild hyperkalaemia. Magnesium carbonate has since been favoured with its less severe side effects (O'Donovan *et al.*, 1986, Plagemann *et al.*, 2011). A clinical trial of patients treated with magnesium carbonate in 1996 showed the effectiveness of Mg^{2+} as a reducer of serum Pi (Delmez *et al.*, 1996).

1.9.5 La³⁺

In addition to the role of Mg^{2+}, other polyvalent cations have been investigated to test for a possible involvement in vascular calcification (Zhao *et al.*, 2011). In 2011 Zhao *et al* investigated the role of lanthanum (La^{3+}) in bovine VSMC cultures. The group isolated bovine VSMCs and cultured them in medium under mineralising conditions (10mM βGP for up to 12 days). The addition of lanthanum chloride was sufficient to significantly reduce Ca^{2+} incorporation and mineralisation when compared to cells incubated in the absence of La^{3+}. Interestingly, the effect of La^{3+} was biphasic, with lower concentrations evoking concentration-dependent reductions in mineralisation while concentrations greater than 0.1µM either had no effect or exacerbated calcification. The group also demonstrated upregulation of CaSR protein expression level when VSMC cells were incubated in the presence of 0.1µM La^{3+}. In addition to these findings, Zhao *et al* also demonstrated an increase in apoptosis in VSMCs incubated in the presence of La^{3+}, however, significance was only achieved in conditions where concentrations as high as 50-200µM $LaCl_3$ were used. In the presence of 0.1µM $LaCl_3$ apoptosis was not significantly increased when compared to control conditions (Zhao *et al.*, 2011). These data suggest a possible role of La^{3+} in the mineralisation of VSMCs through activation of the VSMC CaSR, particularly through ERK activation which was also demonstrated in this publication.

The role of La^{3+} in rat VSMC mineralisation was also investigated by Shi *et al* in 2009. The group induced mineralisation in rat VSMCs with 10mM βGP and found that calcification was also significantly reduced in the presence of La^{3+} up to concentrations of 10µM. ALP activity was also decreased as a consequence of La^{3+} addition in a concentration-dependent manner (Shi *et al.*, 2009). It should also be noted that lanthanum carbonate is often prescribed to patients with CKD to chelate serum Pi (Frazão and Adragão, 2012). A clinical trial using lanthanum carbonate as a phosphate binder found that serum Pi was significantly lowered in patients taking this drug (Al-Baaj *et al.*, 2005). CKD patients with hyperphosphataemia taking 375mg $LaCO_3$ a day for 4-weeks showed a 70% reduction in serum Pi to levels <1.8mM. Similar results were obtained from a more recent clinical trial with $LaCO_3$ treatment over 12 weeks (Hutchison *et al.*, 2008).

Since an increase in plasma Pi is linked to an increased risk of VC, these findings suggest that such a reduction in plasma Pi levels could also account for the reduced calcification as seen in mineralised VSMC cultures containing La^{3+}. Collectively, these data suggest that certain polyvalent cations such as Mg^{2+} and La^{3+} have a significant effect in reducing mineralisation of VSMCs *in vivo* and in *in vitro* models of VC.

1.10 Promoters of vascular calcification

In addition to the calcification inhibitors described, a number of calcification promoters exist which can drive mineral deposition or the transdifferentiation of vascular cells into osteoblast-like cells, and more recently, chondrocyte-like cells (Neven *et al.*, 2010). Many contributors include inorganic phosphate (Pi), steroid hormones, oxidized lipids, BMP-2 and BMP-4 (Vattikuti and Towler, 2004) and inflammatory cytokines such as interleukins (Jaffe *et al.*, 2007). Of particular interest are BMP-2 and BMP-4, which are produced by endothelial cells exposed to hypoxia, turbulent blood-flow and inflammation (Johnson *et al.*, 2006).

1.10.1 Cell plasticity

There are currently multiple theories targeting a number of cells of the vasculature for initiating and propagating mineralisation and providing a niche for calcification. Namely, several hypotheses refer to (i) the transdifferentiation of native VSMCs in the tunica media (Giachelli, 2004, Alam *et al.*, 2008, Panizo *et al.*, 2009, Sage *et al.*, 2011), (ii) calcification driven by calcifying vascular cells (CVCs); adventitial/subendothelial myofibroblasts with transdifferential plasticity (Radcliff, 2005, Abedin, 2006, Jaffe *et al.*, 2007), (iii) circulating osteoprogenitors derived from bone marrow (Shao *et al.*, 2005, Pal and Golledge, 2011), and lastly (iv) pericytes, or cells which play an integral role in the maintenance of the blood-brain barrier and angiogenesis (Collett and Canfield, 2005). It is currently believed that these highly plastic cell types exhibit great multilineage potential and are therefore susceptible to pro-mineralising factors, although sometimes distinction between them is not always clear.

Sage *et al* have demonstrated that VSMCs isolated from mouse aortae mineralise in the presence of high Pi (3mM). During this process, the group showed an upregulation of the key osteogenic markers; BMP-2 and osteopontin. These findings demonstrate the plasticity of VSMCs (Sage *et al.*, 2011). The notion that additional cells in the vascular wall could be responsible for calcification came from the fact that some VSMC preparations do not mineralise even in the presence of mineralising conditions (or at least

mineralise very poorly). For this reason, researchers have isolated subpopulations of the vessel wall which are prone to mineralising. Collett and Canfield report that CVC/subendothelial myofibroblasts undergo osteoblastic transdifferentiation more readily than VSMCs, often in the absence of mineralising conditions (Collett and Canfield, 2005, Abedin, 2006). These cells may be rich in Ca^{2+} and Pi, and may bud off vesicles into the ECM as matrix vesicles. Matrix vesicles are characteristic for being rich in phosphatidylserine. This phosphatidylserine has a high affinity for Ca^{2+}, and so can act as nucleation sites for calcification (Genge *et al.*, 2008). Circulating osteoprogenitors are also thought to play vital roles in initiating calcification. The presence of circulating bone marrow-derived osteoprogenitors has long been controversial. However, Long *et al* have successfully used antibody-based approaches to obtain cell populations expressing osteogenic markers from the blood (Eipers *et al.*, 2000). Interestingly, such osteoprogenitors also express VSMC markers such as α-smooth muscle actin (αSMA). Strikingly, in a mouse model in which osteoblasts were pharmacologically ablated, before 'osteoblast rescue' (where osteoblasts were reintroduced into the mouse) repopulation of bone surfaces was preceded by an expansion of αSMA-positive cells (Kalajzic *et al.*, 2008). These data would suggest that the osteogenic and vascular smooth muscle phenotypes exhibit great plasticity and some important crossover. Cottler-Fox *et al* report that the bone marrow releases these osteoprogenitor cells in response to stem-cell mobilising cytokines (Cottler-Fox *et al.*, 2003). These cells may then migrate in the vasculature to the sight of an unhealthy vessel. Within the vessel wall, these cells may then differentiate into osteoblasts and proliferate. Here, they undergo ectopic biomineralisation (Cottler-Fox *et al.*, 2003, Pal and Golledge, 2011). Vascular pericytes also have the potential to migrate about the vasculature. Canfield suggests that pericytes are recruited at the site of angiogenesis to proliferate and group near the tip of the sprouting vessel. Various factors regulate this process, including vascular endothelial growth factor (VEGF) and platelet-derived growth factor (PDGF). However, how these cells are recruited and how they contribute to angiogenesis is not entirely clear (Cho *et al.*, 2003, Jain, 2003, Collett and Canfield, 2005). Pericytes seem to share some features of adventitial myofibroblasts and since they exhibit such a great degree of plasticity, the distinction between the two cell types is not always clear (Collett and Canfield, 2005).

1.10.2 PiT-1 / matrix vesicles

Evidence in the field of vascular pathology suggests that a major contributor of VSMC mineralisation is the phosphate co-transporter (PiT-1), which is somehow involved in the transdifferentiation of VSMCs and matrix mineralization (Jono *et al.*, 2000). Increases in plasma Pi and Ca^{2+}_o levels are potent regulators of PiT-1 levels. Indeed, increases in $[Ca^{2+}]_o$ cause an increase in expression levels of PiT-1 in human VMSCs (Jono *et al.*, 2000). Furthermore, increased plasma Pi stimulates Pi uptake by PiT-1. This rapid influx of Pi into the cell upregulates a number of osteogenic-related genes, including Runx2 and osteopontin (Li *et al.*, 2006). Pi which is then increased intracellularly is often loaded into matrix vesicles as a possible rescue mechanism. These Ca^{2+} and Pi-rich matrix vesicles are later secreted by cells and promote nucleation of minerals in the ECM as described earlier (Giachelli, 2004, Genge *et al.*, 2008). Interestingly, matrix vesicles are bodies typically responsible for normal biomineralization in a variety of tissues, including bone and cartilage (Anderson, 2003). Normally, these vesicles contain lipid-dependent Ca^{2+}-binding proteins, notably annexin-5 (Anx-5), which has been demonstrated to enhance mineral formation (Genge *et al.*, 2008).

1.10.4 Alkaline phosphatase

Tissue non-specific alkaline phosphatases are enzymes typically expressed in osteoblasts (Liu *et al.*, 2012). ALPs function to liberate Pi from nucleotides and proteins. In patients with CVD, circulating levels of ALP are significantly higher than normal levels, suggesting that more Pi is available for the formation of mineral deposits in the vasculature (Abramowitz *et al.*, 2010). This is also seen in mineralised VSMCs of whole vessels of bovine and human respectively, where ALP activity is upregulated during mineralising conditions (Shroff *et al.*, 2010, Kircelli *et al.*, 2012). This is often contradictory though to reports seen in *in vitro* experiments in mice where ALP activity is not increased in mineralising conditions. It is therefore proposed that: (i) ALP activity in the mouse may be considerably lower compared to larger mammals such as cows and humans, (ii) mineralisation can occur still in the absence of ALP activity (Prosdocimo *et al.*, 2010, Sage *et al.*, 2011).

1.10.5 Vitamin D / Calcitriol

As discussed earlier, vitamin D in its active form, calcitriol, plays a crucial role in extracellular Ca^{2+}_o and Pi homeostasis. Interestingly, calcitriol appears to have a biphasic effect on cardiovascular function. Several investigators have reported that calcitriol suppresses VC and atherosclerosis (Teng *et al.*, 2005, Mathew *et al.*, 2008, Piecha *et al.*, 2008, Takeda *et al.*, 2010, Olgaard *et al.*, 2011), whereas others report that it can exacerbate VC and atherosclerosis (Lopez, 2006, Koleganova *et al.*, 2009). This apparent contradiction is generally ascribed to variations in the type of vitamin D analog, its dosage and route of administration (Hu *et al.*, 2012). In a study in India researchers showed that vitamin D treatment to restore normal levels (~30ng/mL) had no benefit in patients with established CKD and associated cardiovascular disease (Rajasree *et al.*, 2001). Furthermore, they report that high-dose vitamin D treatment (>89ng/mL) was associated with the progression of cardiovascular disease. This can also be seen in animal studies where uremic rats are either injected or fed vitamin D-rich diets and develop arterial calcifications (Lopez, 2006, Koleganova *et al.*, 2009). 30ng/kg (calcitriol/body weight) was injected every day in the Koleganova study while Lopez *et al* administered 80ng/kg (calcitriol/body weight) by injection every other day, making both studies comparable (Lopez, 2006, Koleganova *et al.*, 2009).

1.10.6 Phosphate / Ca^{2+}

Pi and Ca^{2+} are the two major contributors to vascular calcification. In patients suffering from CKD or ESRD, serum Pi and Ca^{2+}_o are typically elevated, when compared to those measured in normal subjects (>1.4mM and >1.2mM, respectively). These conditions allow for the deposition of mineral such as HA in the vasculature (Li *et al.*, 2006, O'Neill, 2008, Lau *et al.*, 2010). The deleterious effects of elevated plasma Pi levels are seen in uremic mice where high-Pi diets rapidly enhance mineral deposition in arteries (El-Abbadi *et al.*, 2009). Hyperphosphataemic patients are often prescribed Pi-binders to removes excess Pi (Frazão and Adragão, 2012, Shigematsu *et al.*, 2012). Preferentially, Pi binders which are not Ca^{2+}-based are favourable, since the burden of additional Ca^{2+} may exacerbate calcification and mineral formation as seen in these patients who develop hypercalcaemia (Block *et al.*, 1998, Renkema *et al.*, 2008, Frazão and Adragão, 2012).

Such binders include lanthanum carbonate, sevelamer hydrochloride and aluminium hydroxide. Oral administration allows for intestinal chelation of Pi, which can then be excreted in faeces (Albaaj and Hutchison, 2005, Shigematsu *et al.*, 2012). Hypercalcaemia also promotes the incidence of vascular calcification (Guérin *et al.*, 2000). In kidney disease, hyperparathyroidism-induced hypercalcaemia (>2.6mM) promotes significantly more calcification than that observed in normocalcaemic patients, however, in order for calcification to initiate, protective factors must be downregulated (Guérin *et al.*, 2000, Floege and Ketteler, 2004, Hagström *et al.*, 2009, Frazão and Adragão, 2012, Hu *et al.*, 2012, Shigematsu *et al.*, 2012).

1.10.7 BMP-2 / BMP-4

Many osteogenic markers upregulated during VC are often observed at the mRNA and protein level (Boström *et al.*, 1993). Bone morphogenetic proteins were firstly described in the vessel walls of mice with atherosclerosis (Boström *et al.*, 1993, Demer and Watson, 1994). Microarray analysis of senescent VSMCs shows that cells downregulate anti-calcifying factors such as MGP, whilst upregulating BMPs 2 and 4 (Burton *et al.*, 2009, Burton *et al.*, 2010). Upregulation of BMPs is also accompanied by a modest increase in the expression of other osteogenic markers, including osteoprotegrin, collagen type I and ALP (Burton *et al.*, 2009). In 2010 Yao *et al*, investigated the effects of MGP overexpression or knockout. Both mouse models were bred with the apoE$^{-/-}$ mouse model of atherosclerosis. The authors showed that MGP overexpression, even in the presence of apoE-deficiency and a high-fat diet significantly reduced ectopic calcification of arteries which was also correlated with significantly reduced BMP expression. Conversely, the group found that in MGP/apoE-double knockout mice, high-fat diet feeding induced a pathological and lethal phenotype which mice could not tolerate that was accompanied by an upregulation in BMP-4 expression (Yao *et al.*, 2010). In this way the pro-calcifying properties of BMPs have been effectively demonstrated.

1.10.3 VSMC Apoptosis

VSMC apoptosis has been shown to be a major contributor of vascular calcification *in vitro* and *in*-vivo (Proudfoot *et al.*, 2000, Reynolds, 2005, Shanahan *et al.*, 2011). Proudfoot *et al* demonstrated that *in vitro* human VSMCs started to die rapidly by apoptosis after 28 days in mineralising conditions. This was confirmed with nucleic acid fragmentation, and was significantly reduced in the presence of the caspase inhibitor ZVAD.fmk (Proudfoot *et al.*, 2000). Furthermore, the rate of calcification and mineral nodule development was significantly reduced in the presence of ZVAD.fmk. A similar result was achieved when Reynolds *et al*, who induced mineralisation of human VSMCs in the presence of high Pi or absence of the same caspase inhibitor (Reynolds, 2005). Importantly, these studies illustrate that apoptosis is a key event in initiating and promoting mineralisation. The collective involvement of all of these pro-calcifying factors can be observed in Figure 14.
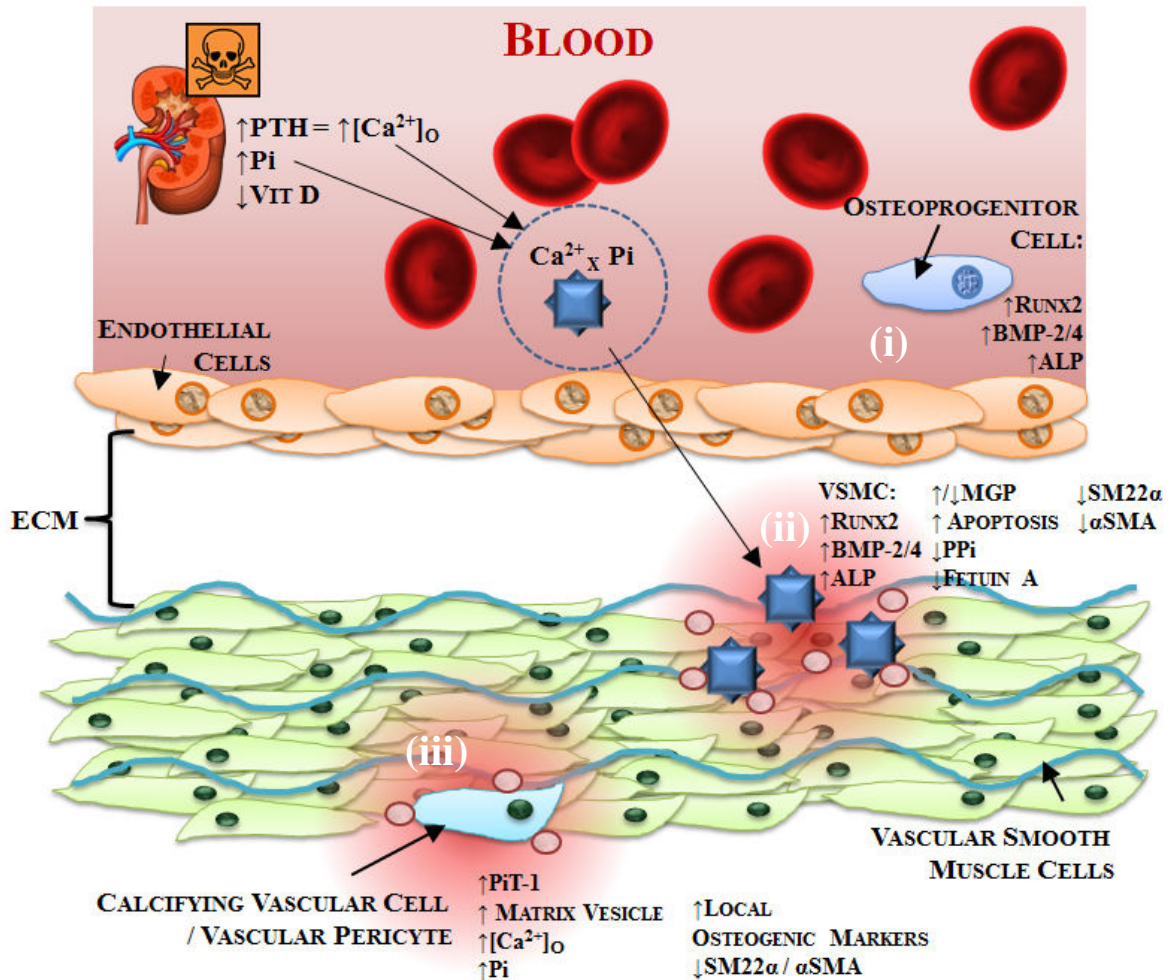
Figure 14. Mechanisms of vascular calcification. Increases in Ca^{2+}_o and Pi can be triggered by PTH and hyperphosphatemia respectively. Additionally, secondary hyperparathyroidism can occur from CKD. Ca^{2+} and Pi can accumulate in the intima forming a nidus for atherosclerosis and atherosclerotic calcification. (i) Bone marrow-derived osteoprogenitor cells may migrate to the vasculature and increase local levels of osteogenic markers, forming a site for further calcification propagation. (ii) Ca^{2+} x Pi products formed, such as hydroxyapatite, can signal medial VSMCs to transdifferentiate and upregulate osteogenic markers. MGP is often upregulated initially as a protective factor, but may also be downregulated in sites of advanced calcification. VSMC markers SM22α and αSMA are also downregulated during calcification. (iii) Calcifying vascular cells, or pericytes, susceptible to osteogenic differentiation upregulate osteogenic markers into the surrounding tunica media. Ca^{2+} and Pi may also be offloaded in the form of matrix vesicles (Collett and Canfield, 2005, Reynolds, 2005, Shobeiri *et al.*, 2010, Nitta, 2011, Shanahan *et al.*, 2011).

1.10.4 Vascular calcification inhibitors vs. promoters

We have seen the diversity of promoters and inhibitors of vascular calcification and how they can be utilised in scientific research and in life. There are clearly numerous types of vascular cells at work, utilising a vast number of promoting and inhibiting calcification factors. Table 2 details common inhibitors and common promoters of calcification.

CALCIFICATION INHIBITORS	CALCIFICATION PROMOTERS
Pyrophosphate	Collagen Type I
Mg^{2+}	Sox9
La^{3+}	Vitamin D
Thiosulphate	RANKL
Fetuin A	BMP-2
MGP	BMP-4
BMP-7	Ca^{2+} / Ca^{2+}_o
LDR	Osteocalcin
Apolipoproteins	Runx2
Osteoprotegrin	Alkaline Phosphatase
FGF23	Osterix
Calcimimetics (?)	Warfarin
Phosphate-binders	Phosphate
Vitamin D	Oxidative Stress
	LDL

Table 2. Inhibitors and promoters of vascular calcification. Osteogenic genes including BMP-2, BMP-4, Runx2, and alkaline phosphatase; known bone-related genes and promoters vascular calcification. Circulating inhibitors such as Mg^{2+}, BMP-7, PTH, fetuin A and pyrophosphate protect from calcification.

1.11 Models of vascular calcification

Vascular calcification has been extensively studied using *in vitro*, *ex vivo* and *in vivo* techniques. Interestingly, researchers often use bovine VSMCs as a model for VC, specifically due to high tissue availability and similar physiological activity with human VSMCs, however, mouse, rat and human VSMCs are often used as models for VC investigation *in vitro, ex vivo and in vivo*.

1.11.1 *In vitro* models of VC

Since vascular calcification occurs in the tunica media, which comprises of vascular smooth muscle cells, investigators often manipulate these cells in *in vitro* experiments. Primary VSMCs are typically isolated from the descending thoracic aorta of mice, rats, cows or taken from human biopsies. VSMCs are typically cultured in the presence of 1.2-1.8mM Ca^{2+}_o (Shioi *et al.*, 1995, Proudfoot *et al.*, 1998, Olesen *et al.*, 2006, Alam *et al.*, 2008, Prosdocimo *et al.*, 2010). Then, to mimic pathophysiological conditions normally present during vascular calcification, experimental conditions include an increase in Ca^{2+}_o and/or Pi in the culture medium in the presence of pro-mineralising factors such as ascorbic acid, βGP or Pi. Interestingly, despite researchers using different Ca^{2+}_o concentrations, phosphate delivery (βGP/Pi), as well as varying FBS concentrations (which contains protective factors such as MGP and fetuin A), data appear fairly reproducible and consistent (Shioi *et al.*, 1995, Proudfoot *et al.*, 1998, Olesen *et al.*, 2006, Alam *et al.*, 2008, Shi *et al.*, 2009, Prosdocimo *et al.*, 2010). These different experimental conditions are described in Table 3.

GROUP	HOST ORGANISM /CELL TYPE	CONDITIONS
(Alam *et al.*, 2008)	Bovine VSMC	- 5mM βGP - 1.2/1.8/2.5mM Ca^{2+}_o - 5% FBS **- 10 DAYS**
(Shioi *et al.*, 1995)	Bovine VSMC	- 10mM βGP + 50µg / mL Ascorbic Acid - 1.8mm Ca^{2+}_o - 15% FBS **- 14 DAYS**
(Chen *et al.*, 2010a, Kircelli *et al.*, 2012)	Bovine VSMC	- 10mM βGP + 50mg / mL Ascorbic Acid - 1.8mm Ca^{2+}_o - 15% FBS **- 7-14 DAYS**
(Olesen *et al.*, 2006)	Human VSMC	- 8mM βGP - 1.2mM Ca^{2+}_o - 10% FBS **- 36 DAYS**
(Proudfoot *et al.*, 1998)	Human Placental Pericyte/CVC	- 1.0mM Pi - 1.8mM Ca^{2+}_o - 20% FBS **- 8 WEEKS**
(Prosdocimo *et al.*, 2010)	Rat VSMC	- 3-5mM Pi - 1.8mM Ca^{2+}_o - 10% FBS **- 12 DAYS**
(Shi *et al.*, 2009)	Rat VSMC	- 10mM βGP - 1.2/1.8mM Ca^{2+}_o - 10% FBS **- 9-12 DAYS**
(Beazley *et al.*, 2012)	Rat VSMC	- 1.6mM Pi / 10µM Warfarin - 1.2 / 1.8mM Ca^{2+}_o (Not specified) - 1% FBS **- 6 DAYS**
(Sage *et al.*, 2011)	Mouse VSMC	- 3mM Pi - 1.2mM Ca^{2+}_o - 10% FBS **- 7-14 DAYS**
(Mikhaylova *et al.*, 2007, Faverman *et al.*, 2008)	Mouse VSMC	- 5mM βGP + 25µg/mL Ascorbic Acid - 0.5mM Ca^{2+}_o - 10% FBS **- 7 DAYS**

Table 3. Mineralisation conditions used for vascular calcification experiments *in vitro*. Ca^{2+}_o concentrations tested range from 0.5mM-2.5mM. Pi is provided in an inorganic form up to 3mM, whereas the organic form, β-glycerophosphate, is added at concentrations between 5-10mM. FBS is provided at concentrations between 5-20%. The duration of the experiments can vary significantly from 7 days to 8 weeks.

1.11.2 *In vivo* models of VC

As discussed previously, it has become clear that several targeted gene-knockout animal models have been generated in an attempt to recapture the phenotype seen in patients with CKD, and indeed in many cases the phenotype appears a lot more severe than in human patients. The MGP and OPG mouse models have shown large-scale ectopic calcification of blood vessels (Luo *et al.*, 1997, Bucay *et al.*, 1998). However, these models are not as informative as one would hope for since a severe phenotype develops quickly. For this reason, numerous research groups focus on mouse models with reduced morbidity and mortality, where calcification develops over time. In this manner, developmental regulation of the process of calcification and VSMC transdifferentiation can be monitored more accurately. Available *in vivo* models of vascular calcification are described overleaf in Table 4.

GROUP	HOST ORGANISM	MODIFICATION	PHENOTYPE	
(Price *et al.*, 2006, Tamagaki *et al.*, 2006, Shobeiri *et al.*, 2010)	Rat	Adenine feeding	Uremia, cardiovascular calcifications	
(Schurgers *et al.*, 2007, Beazley *et al.*, 2012)	Rat	Warfarin feeding	Uremia, cardiovascular calcifications	
(Lopez, 2006, Piecha *et al.*, 2008, Koleganova *et al.*, 2009)	Rat	5/6 Nephrectomy	CKD / Uremia	↑PTH ↑Pi ↑Creatinine
(Massy *et al.*, 2005, Pai *et al.*, 2011, Ting *et al.*, 2011)	Mouse	5/6 Nephrectomy	CKD / Uremia	↑PTH ↑Pi ↑Creatinine
(Delsing *et al.*, 2001, Massy *et al.*, 2005, Ivanovski *et al.*, 2009)	Mouse	ApoE-KO / High-fat diet	Atherosclerosis and vascular calcification	
(Davies, 2003, Shao *et al.*, 2005, Morony *et al.*, 2008, Malik *et al.*, 2010).	Mouse	LDLR-KO / High-fat diet	Atherosclerosis and vascular calcification	

Table 4. A summary of *in vivo* models of vascular calcification. Traditionally, rat and mouse models are used, where calcification is induced either genetically, by surgery or by diet modification.

1.11.2.1 5/6 Nephrectomised animals

Patients with advanced CKD develop cardiovascular calcifications often in the presence of inappropriately raised serum Pi level, in combination with increases in PTH levels (Schoppet and Shanahan, 2008, Lau *et al.*, 2010, Shanahan *et al.*, 2011). To reproduce this condition *in vivo*, a model of uremia is created by performing two-stage 5/6 nephrectomy. During this procedure, mice or rats have one kidney entirely removed in addition to removal of 2/3 of the remaining kidney. In this manner, the full complement of serum Pi is poorly-handled and leads to a pathological hyperphosphataemic state. Researchers have utilised this technique to induce vascular calcification *in vivo*, often in combination with either a high phosphate or high-fat diets (Lopez, 2006, Piecha *et al.*, 2008, Koleganova *et al.*, 2009). Koleganova *et al* showed that 5/6 nephrectomy in rats induced a significant increase in serum Pi (2.78mM operated vs. 2.28mM sham-operated, P<0.001) in addition to increases in PTH, but not overall $[Ca^{2+}]_o$. The group also suggested that the CKD-state these rats have after operation was confirmed by an upregulation in serum creatinine; a marker of late CKD and ESRD (Koleganova *et al.*, 2009). Using this method, other investigators have come to similar conclusions (Wada *et al.*, 1997b, Lopez, 2006, Kawata *et al.*, 2008, Piecha *et al.*, 2008). Rats are preferentially used for such studies, however mice are increasingly used due to the ease of genetic modification in addition to the induction of uremic conditions (Massy *et al.*, 2005, Pai *et al.*, 2011, Ting *et al.*, 2011).

1.11.2.2 Adenine feeding

Adenine feeding is a relatively simple and non-invasive technique and is typically carried out in rats to induce CKD and vascular calcification. Supplementing rat diets with 0.75% adenine for as little as 4 weeks induces the formation of medial calcifications (Price *et al.*, 2006, Shobeiri *et al.*, 2010). CKD follows nephrotoxicity induced by the metabolic breakdown of adenine into the nephrotoxic compound 2,8-dihydroxyadenine. Pathology occurs when this compound precipitates and forms crystals in the microvilli and proximal tubular epithelia (Akintonwa *et al.*, 1979, Price *et al.*, 2006, Tamagaki *et al.*, 2006). In a 2006 study, Tamagaki demonstrated that adenine feeding to Wistar rats over a period of 6 weeks caused a significant increase in serum Pi and creatinine, while serum Ca^{2+}_o and

calcitriol levels were markedly reduced. Furthermore, the parathyroid glands of these rats were enlarged and PTH levels were increased (Tamagaki *et al.*, 2006). Adenine feeding as part of CKD induction remains popular due to its simplicity and cost-effectiveness, however, 5/6 nephrectomies remain more consistent and reliable for kidney failure simulation.

1.11.2.3 Warfarin-feeding in rats

Warfarin feeding has also proved to be an effective way at inducing vascular calcification, specifically through its involvement in the vitamin K cycle (Price *et al.*, 1998, Price *et al.*, 2000). The vitamin K-dependent γ-carboxylation system is essential for converting glutamic acid (glu) residues into γ-carboxyglutamic acid (gla) residues (Wallin and Hutson, 2004, Schurgers *et al.*, 2007). The anti-calcifying agent MGP is secreted by VSMCs and binds Ca^{2+}_o to reduce mineralisation. In order to bind Ca^{2+}_o MGP requires this γ-carboxylation (Proudfoot and Shanahan, 2006). Warfarin acts as a direct inhibitor of carboxylase reductase enzymes in the vitamin K cycle, inhibiting the proper function of MGP and blood coagulation proteins. In fact, Shurgers *et al* demonstrated a 50% increase in arterial calcification in warfarin-treated rats compared to untreated controls (Schurgers *et al.*, 2007, Beazley *et al.*, 2012). Disruption of the vitamin K cycle in this way consequently leads to severe alterations in Ca^{2+}_o homeostasis in the vasculature and arterial calcifications, as seen in numerous studies in rats (Price *et al.*, 1998, Price *et al.*, 2000, Wallin and Hutson, 2004, Schurgers *et al.*, 2007). Limitations of this model are that warfarin is readily excreted and needs constant application by dietary supplementation.

1.11.2.4 ApoE-knockout mice / high-fat diet

Apolipoprotein E (apoE) is a component of all lipoproteins except low density lipoproteins (LDL). It is also a component of chylomicron particles which are synthesized in the liver (Zhang *et al.*, 1992, Bro *et al.*, 2003, Massy *et al.*, 2005, Ivanovski *et al.*, 2009). ApoE functions to mediate high-affinity binding of lipoproteins to apoE receptors which evoke cellular uptake of lipids and cholesterol in the liver. In the absence

of this, lipoproteins are free to disperse throughout the vasculature inducing a hypercholesterolaemic state. Elevations in plasma cholesterol induce VC, atherosclerosis and premature heart disease (Ghiselli *et al.*, 1981, Delsing *et al.*, 2001, Massy *et al.*, 2005, Ivanovski *et al.*, 2009). This model's limitation is that often the ensuing calcification is secondary to atherosclerotic plaque formation, which occurs in the tunica intima. Although some medial calcification can occur, this is not exclusively of the tunica media. Consequently, any arising phenotype will be due to both atherosclerosis, inflammation and vascular calcification (Massy *et al.*, 2005).

1.11.2.5 LDLR-knockout mice

The LRL receptor (LDLR) functions to remove cholesterol-rich low density lipoproteins (LDLs) and intermediate density lipoproteins (IDLs) from the circulation (Ishibashi *et al.*, 1993). LDLs and IDLs have a key role in the delivery of cholesterol to peripheral tissue (Glass and Witztum, 2001). LDLs are taken up by cells via the LDL receptor (LDLR) by recognising and binding an N-terminal domain of apolipoprotein B (apoB) on the lipoprotein. Consequently, cholesterol can be taken up by cells and utilised in cellular processes (Go and Mani, 2012). In a mouse model lacking the LDLR, cholesterol remains in the vasculature, resulting in hypercholesterolaemia (Ishibashi *et al.*, 1993, Binder, 2004, Demer and Tintut, 2008). As a result, atherosclerotic plaques and vascular calcifications occur, particularly when these mice are fed a high fat diet. The LDLR-deficient mouse model has been used extensively to recapitulate vascular disease (Davies, 2003, Shao *et al.*, 2005, Morony *et al.*, 2008, Malik *et al.*, 2010). However, in a similar manner to the apoE$^{-/-}$ mouse model, the LDLR-knockout mouse often recapitulates atherosclerosis, inflammation and vascular calcification which are not exclusively of the tunica media.

1.12 The extracellular calcium-sensing receptor (CaSR) and mammalian physiology

Since the discovery of the significant role of Ca^{2+} in physiology by Sydney Ringer in the late 19th century, the method by which cells homeostatically regulate levels of this cation within the cell and its extracellular fluid has become an attractive arena for scientific investigation (Ringer, 1882a, Ringer, 1882b, Ringer, 1883). By mass, this divalent cation is categorically the most abundant mineral in the body, and contributes to numerous life processes (Cheng *et al.*, 2007). The ability of free ionized Ca^{2+} (Ca^{2+}_o) to perform as a first messenger in biological processes has eluded the scientific community, that is, until work by Brown *et al* led to the discovery of a gene encoding a protein central to Ca^{2+}_o homeostasis (Brown *et al.*, 1993). In 1993 the group first identified a bovine gene encoding a GPCR in the parathyroid gland (Brown *et al.*, 1993). Crucially, the protein product of this gene was found to be abundantly expressed in parathyroid glands and served a role in regulating Ca^{2+}_o concentrations in extracellular fluids. This Ca^{2+}_o regulator is now known as the extracellular calcium-sensing receptor, with various polynomial acronyms including CaS, CaR and the more popular designation; CaSR (Brown *et al.*, 1993, Bai and Trivedi, 1998, Chang *et al.*, 2008).

The bovine parathyroid gland (PTG) clone generated by Brown *et al,* designated BoPCaR1 had a 3,255bp open reading frame encoding a protein of 1,085 amino acids (Brown *et al.*, 1993). It was found to contain three distinct domains. These are (i) a large hydrophilic N-terminal domain of 613 amino acids, which contained a 21 amino acid eukaryotic signalling peptide, (ii) a central region of 250 amino acids encoding seven transmembrane domains, and (iii) a hydrophilic 222 amino acid C-terminal domain (Brown *et al.*, 1993). In accordance with this highly specific arrangement of domains, CaSR is a member of the group C GPCR superfamily and its topology is described in Figure 15 (Bräuner-Osborne *et al.*, 2007). CaSR shares homology with metabotropic glutamate receptors (mGluRs 1-8) (Nakanishi, 1992, Kunishima *et al.*, 2000, Gama, 2001, Hermans and Challiss, 2001, Jingami *et al.*, 2003), γ-aminobutyric acid receptors (GABA$_B$Rs) (Galvez *et al.*, 2000, Bettler *et al.*, 2004), the bone Ca^{2+}_o-sensor GPRC6A (Pi *et al.*, 2005), taste, pheromone and orphan receptors (Herrada and Dulac, 1997, Matsunami and Buck, 1997, Cao *et al.*, 1998, Hoon *et al.*, 1999, Nelson *et al.*, 2002).

Furthermore, as with other members of this superfamily, the bovine CaSR shares high sequence homology (>90%) with other closely-related organisms including the rat, mouse and human CaSR which are 1,079aa (Riccardi *et al.*, 1995), and 1,079aa (Pi *et al.*, 2000) and 1,078aa (Aida *et al.*, 1995, Mei, 2004) respectively.

Intriguingly, this gene thought to have a predominant role exclusively in parathyroid cells is ever-more demonstrating localization and potentially significant roles in Ca^{2+}_o homeostasis and signalling throughout the whole body. CaSR is now known to be expressed at variable levels in most major systems of the body including the respiratory (Kovacs and Kronenberg, 1997, Finney *et al.*, 2008), cardiovascular (Weston, 2005, Smajilovic *et al.*, 2006, Smajilovic *et al.*, 2007, Alam *et al.*, 2008, Weston *et al.*, 2008), renal (Riccardi *et al.*, 1995, Kifor *et al.*, 1997, Bai and Trivedi, 1998, Riccardi *et al.*, 1998, Levin *et al.*, 2006, Mariano *et al.*, 2008, Riccardi and Brown, 2009, Caudrillier *et al.*, 2010), digestive (Gama *et al.*, 1997, Cheng *et al.*, 1999, Geibel *et al.*, 2001, Busque *et al.*, 2005, Dufner *et al.*, 2005), musculoskeletal (House *et al.*, 1997, Chang *et al.*, 2008, Aguirre *et al.*, 2010, Christian *et al.*, 2010) and nervous (Ruat and Molliver, 1995, Cao *et al.*, 1998, Gama, 2001, Shozo *et al.*, 2004, Vizard *et al.*, 2008) systems. In spite of this, there has previously been some controversy whether this widespread expression is indeed true, particularly in blood vessels. However, this has since been attributed to the inherent difficulty in detecting CaSR at both the mRNA and protein level (Farzaneh-Far *et al.*, 2000, Wang *et al.*, 2003, Weston, 2005, Peiris *et al.*, 2006, Shalhoub *et al.*, 2006, Smajilovic *et al.*, 2006, Molostvov *et al.*, 2007, Loretz, 2008, Pistilli *et al.*, 2012). There is now such overwhelming evidence that it is difficult to refute that CaSR is expressed in this diverse variety of systems.
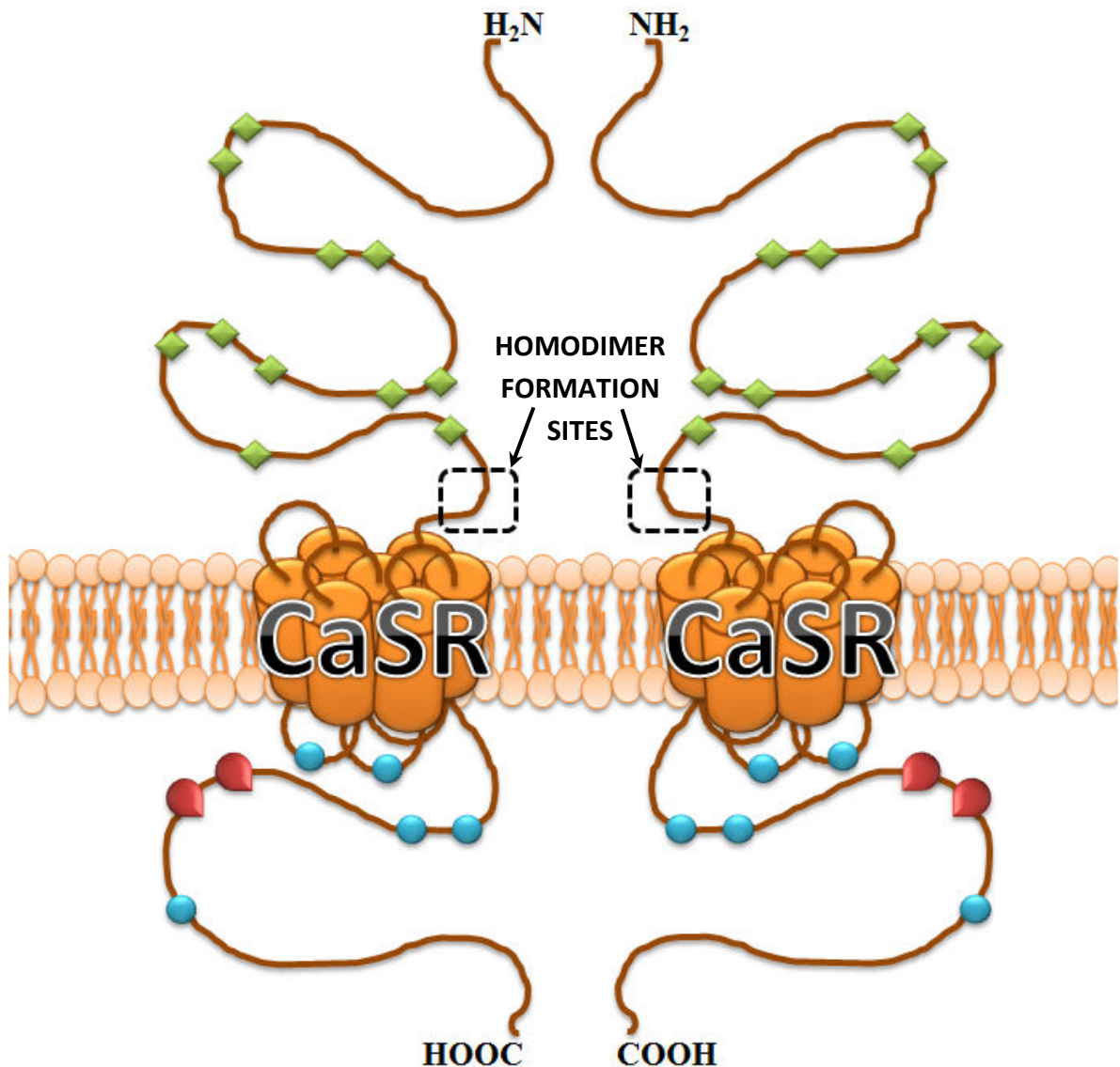
Figure 15. Topology of the human extracellular calcium-sensing receptor (CaSR). The seven-membrane-spanning GPCR exhibits an extracellular N-terminus and an intracellular C-terminus. The three domains can be seen; extracellular, transmembrane and intracellular. Active sites for enzymatic reactions are demonstrated diagrammatically. Human CaSR contains 11 N-linked putative glycosylation sites (green diamonds), 9 of which are highly conserved in rat, human, rabbit and bovine. Also present in mature human CaSR are 2 putative intracellular protein kinase A sites (red circles), and 5 protein kinase C sites (blue circles). Conserved cysteine regions are highlighted by black dotted lines. These cysteine sites are required for dimerization of the protein into a homodimer. Agonist binding is attributed to the venus flytrap (VFT) domain of the receptor which forms during dimerization, however, allosteric modulators (calcimimetics and calcilytics) bind to the transmembrane domain of the CaSR homodimer (Bai and Trivedi, 1998, Ray *et al.*, 1999, Hu and Spiegel, 2003, Chang and Shoback, 2004, Smajilovic and Tfelt-Hansen, 2007).

1.13 CaSR, Vitamin D and PTH in Ca^{2+}_o homeostasis

Since its discovery, CaSR has shown to have a crucial role in Ca^{2+}_o homeostasis (Brown *et al.*, 1993, Brown and MacLeod, 2001). Under physiological conditions, chief cells in the parathyroid constantly secrete parathyroid hormone (PTH) which subsequently acts on kidney and bone to resorb Ca^{2+}. Additionally PTH promotes the renal conversion of 25-hydroxyvitamin D_3 ($25(OH)D_3$) to 1,25-dihydroxyvitamin D_3 ($1,25(OH)_2D_3$) which in turn acts on the intestine to resorb Ca^{2+} and phosphate (Pi). These actions maintain levels of $[Ca^{2+}]_o$ to approximately 1.0-1.3mM (Brown, 1991, Brown *et al.*, 1993, Quinn *et al.*, 1998). When $[Ca^{2+}]_o$ is above ~1.0mM, it activates the CaSR which inhibits PTH secretion by the PTG. The whole system is stringently controlled by transcriptional regulation of PTH and a series of enzymes that activate endogenous vitamin D_3 (VD_3) precursors. In this section, the roles of CaSR, vitamin D and PTH will be discussed in Ca^{2+}_o homeostasis.

1.13.1 Vitamin D

Conversion of vitamin D precursors to active 1,25-dihydroxyvitamin D_3 (calcitriol) from its endogenously inactive forms is crucial to Ca^{2+}_o homeostasis. In the body, calcitriol synthesis begins in the skin by activation of the precursor steroid 7-dehydrocholesterol in response to photonic stimulation by sunlight, specifically, ultraviolet radiation (Borle, 1974, Brown, 1991, Lips, 2006). From this reaction, cholecalciferol (VD_3) is produced. This then translocates to the liver where it undergoes a first hydroxylation, producing a more active metabolite (Usui *et al.*, 1990, Nagpal *et al.*, 2005). Initially, 25-hydroxylase, a cytochrome P450 enzyme present in the liver, converts VD_3 to 25-hydroxyvitamin D_3 ($25(OH)D_3$). This is then translocated again to the kidney through the circulatory system and this metabolite is then further converted using 1α-hydroxylase, a PTH-regulated enzyme present on the inner mitochondrial membrane of proximal tubules in the kidney (Brenza *et al.*, 1998, Murayama *et al.*, 1999). This finally catalyses the formation of 1,25-dihydroxyvitamin D_3 ($1,25(OH)_2D_3$), also known as calcitriol (Armbrecht *et al.*, 1998, Brenza *et al.*, 1998, Murayama *et al.*, 1999). This active metabolite can now enter the cell where it binds to the vitamin D Receptor (VDR) (Sun *et al.*, 2010). VDR has been reported to have both genomic and non-genomic effects. Non-genomic effects have been

described, for example, when a calcitriol:VDR complex induces intracellular signalling pathways including Ras and extracellular-regulated kinase (ERK)-1/2/5 (Dwivedi *et al.*, 2002). The calcitriol:VDR complex then forms a more complex VDR signalling complex with the retinoid X receptor (Dwivedi *et al.*, 2002). This calcitrol:VDR:retinoid X receptor complex is then able to bind to vitamin D response elements (VDREs) which accordingly induce transcriptional changes in the nucleus, therefore, eliciting genomic effects on the cell (Chen *et al.*, 2000, Canaff, 2002, Lips, 2006). VDREs have been documented in the promoter regions of Ca^{2+}_o-binding genes including osteocalcin and calbindin (Lips, 2006, Shu *et al.*, 2010). Interestingly, research has also shown that the human CaSR gene also contains a VDRE in the promoter region of the gene which is sensitive to $1,25(OH)_2D_3$. In mutagenic studies where this region has been mutated in CaSR, transcriptional upregulation of CaSR mRNA by $1,25(OH)_2D_3$ is lost (Canaff, 2002).

1.13.2 PTH

The role of PTH in this vitamin D cycle is deeply intertwined and carefully orchestrated. Its role has been well-documented over recent decades (Rader *et al.*, 1979, Teitelbaum *et al.*, 1986, Sanders *et al.*, 2000, Castro *et al.*, 2002, Bergwitz and Jüppner, 2010). PTH is secreted from chief cells of the PTG and can play a direct and indirect role in Ca^{2+}_o homeostasis in the kidney, intestines and bone (Chang *et al.*, 2008). More specifically in the kidney and intestines, investigators have confirmed that PTH binds to its PTH/PTH-related peptide (PTHrP) receptor, a GPCR of family B (Castro *et al.*, 2002). PTH or PTHrP agonist binding induces one of many intracellular signalling pathways. Typically, it can activate $G_q/_{11}$-mediated PLCβ leading to IP_3 production, Ca^{2+}_i mobilization, protein kinase C (PKC) activation and activation of adenylyl cyclase (AC) through G_s which increases intracellular cyclic adenosine monophosphate (cAMP) (Castro *et al.*, 2002, Fujita *et al.*, 2002). In this way, PTH can regulate the transcription of crucial genes involved in Ca^{2+}_o homeostasis. Downstream effects of PTH signalling include changes in the expression of the *P450C1* gene encoding 1α-hydroxylase; an enzyme responsible for bioactivation of 25-hydroxyvitamin D_3 (Dwivedi *et al.*, 2002), and the *CYP24* gene encoding the 1,25-dihydroxyvitamin D_3 24-hydroxylase (CYP24). (Armbrecht *et al.*,

1998, Dwivedi *et al.*, 2002, Bergwitz and Jüppner, 2010). Since $[Ca^{2+}]_o$ is, as one would expect, regulated to tight constraints and limits, these two enzymes are synergistically upregulated in response to both $1,25(OH)_2D_3$ and PTH. Modulation is crucial as $1,25(OH)_2D_3$ is toxic at high levels and, in excess, can induce hypercalcaemia (Dwivedi *et al.*, 2002). For this reason, $1,25(OH)_2D_3$ is synchronously produced, bound to the VDR signalling complex and any excess is hastily degraded by the enzymatic actions of CYP24.

1.13.3 CaSR

As intricately controlled as the actions of PTH and vitamin D are, their actions and acute regulation would be largely unregulated were it not for CaSR. In the parathyroid glands, CaSR acts as a master controller of PTH secretion. CaSR and its role in Ca^{2+}_o metabolism is described diagrammatically below in Figure 16.
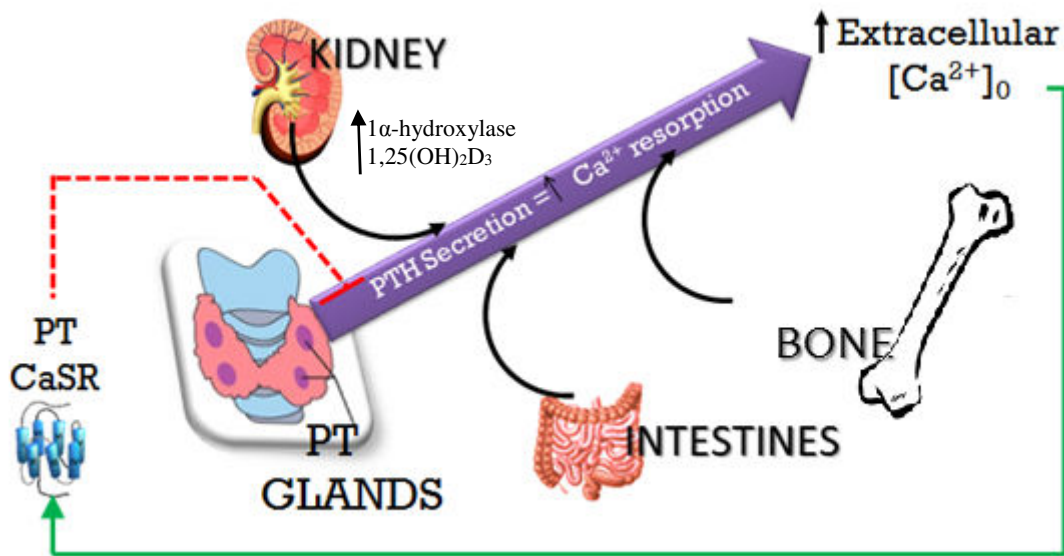
Figure 16. The role of CaSR in $[Ca^{2+}]_o$ homeostasis. Parathyroid glands secrete PTH into extracellular fluids. PTH acts on the kidney to increase Ca^{2+} absorption and on bone to release Ca^{2+} from bone mineral. Additionally, PTH in the kidney upregulates 1α-hydroxylase activity and therefore the presence of $1,25(OH)_2D_3$ which also increases Ca^{2+} resorption here and in the intestines. Once $[Ca^{2+}]_o$ has returned to normal physiological concentrations (~1.2mM), PTH secretion is controlled and inhibited by Ca^{2+}_o acting at the CaSR. Figure adapted from (Brown, 1991, Brown *et al.*, 1993, Chang and Shoback, 2004).

The principal agonist of CaSR is Ca^{2+}_o (however, other cations can activate CaSR). The wide variety of extracellular agonists that activate CaSR can be categorised into two distinct groups. These include firstly type I orthosteric CaSR agonists, which activate CaSR in the absence of Ca^{2+}_o. These are positively charged agonists such as polyvalent cations (Brown *et al.*, 1993, Ohanian *et al.*, 2005, Guang-wei *et al.*, 2011, Kircelli *et al.*, 2012), highly charged polyamines (Quinn *et al.*, 1997, Wang *et al.*, 2003, Thomsen *et al.*, 2012) and positively charged aminoglycoside antibiotics (Thomsen *et al.*, 2012). In addition, type II CaSR agonists, or allosteric modulators, require Ca^{2+}_o to activate the CaSR (Hebert, 2006). These agonists include certain L-amino acids (Conigrave *et al.*, 2002) and positive and negative pharmacological allosteric modulators of CaSR such as calcimimetics (Nemeth *et al.*, 1998, Hebert, 2006, Francis *et al.*, 2008) and calcilytics (Nemeth *et al.*, 2001, Nemeth, 2002, Rybczyńska *et al.*, 2010) respectively. Furthermore, CaSR function and sensitivity is also affected by changes in extracellular pH and ionic strength (Quinn *et al.*, 2004, Riccardi and Brown, 2009).

1.14 CaSR: Orthosteric agonists of the receptor

The CaSR exists at the plasma membrane as a homodimer. During synthesis of CaSR, the protein product is translocated to the endoplasmic reticulum (ER). This intracellular transportation is co-ordinated by the CaSR signal peptide. At the ER, CaSR forms a homodimer through two intermolecular disulphide cysteine bonds between cys129 and cys132 (Ray *et al.*, 1999, Zhang *et al.*, 2001). Further post-translational modifications are then performed in the Golgi, more specifically, glycosylations to form the mature protein (Grant *et al.*, 2011). After this, the fully modified homodimer is trafficked to the plasma membrane where CaSR activation can occur. Recently, the classification of ortho- and allosteric modulators has been unclear since exact binding sites of CaSR agonists are not fully known (Bräuner-Osborne *et al.*, 1999, Zhang *et al.*, 2002). However, it is generally believed that agonist binding occurs in the venus flytrap (VFT) binding pocket of CaSR (Hu and Spiegel, 2003, Chang and Shoback, 2004).

1.14.1 Polyvalent cations

As the name suggests, the primary agonist of CaSR is Ca^{2+}_o however, numerous other polyvalent cations can stimulate the receptor including Mg^{2+}, Sr^{2+}, Gd^{3+} and La^{3+} (Riccardi *et al.*, 1995, Brown and MacLeod, 2001). However, in this case, Mg^{2+} is the most physiologically relevant since it is naturally present in extracellular fluids *in vivo* (Brown, 1999). Although not physiologically relevant, heavier metals such as Sr^{2+}, Gd^{3+} and La^{3+} have proved to be significant CaSR activators in *in vitro* studies and further illustrate the affinity of CaSR for positively charged ions. Chang *et al* investigated human embryonic kidney (HEK293) cells stably expressing a WT CaSR (HEK293-CaSR) and demonstrated that the addition of 5.5mM Mg^{2+} and 10µM Gd^{3+} to these cells significantly increases intracellular Ca^{2+} ($[Ca^{2+}]_i$) through CaSR signalling (Brown *et al.*, 1993, Chang *et al.*, 1998).

1.14.2 Polyamines

CaSR has an inherent affinity for positively charged molecules, including charged polyamines such as spermine, spermidine and putrescine. These polyamines have been shown to increase $[Ca^{2+}]_i$ in HEK293-CaSR cells (Quinn *et al.*, 1997). This paper showed the affinity of CaSR for polyamines follow the order: spermine > spermidine > putrescine. Furthermore, changes in Ca^{2+}_o can change the sensitivity of the receptor for these polyamines, and so these polyamines are often recognised as both ortho- and allosteric modulators of CaSR (Quinn *et al.*, 1997).

1.14.3 Aminoglycoside antibiotics

In addition to the aforementioned CaSR modulators, aminoglycoside antibiotics (AGAs) are CaSR orthosteric activators (Thomsen *et al.*, 2012). A study by McLarnon *et al* showed that human recombinant CaSR is responsive to AGAs including gentamicin, tobramycin, and neomycin in a concentration-dependent manner. These AGAs were effective with EC_{50} values of 258, 177, and 43 µM respectively (McLarnon *et al.*, 2002). These antibiotics are nephrotoxic and the group also showed that AGAs are more

effective when pH is lowered to mimic that of CaSR-expressing tissue such as the proximal tubules of the kidney (from pH7.4 to pH6.9). These findings suggest that the kidney CaSR is much more sensitive to AGAs than CaSRs in other tissues, and that CaSR may play a role in nephrotoxicity of the kidney (McLarnon *et al.*, 2002).

1.15 CaSR: Allosteric agonists of the receptor

The first presented evidence that modulators of CaSR act allosterically came from research into amino acid binding sites on additional GPCRs. The metabotropic glutamate receptor shares significant homology with CaSR, particularly at the putative binding site of amino acids such as L-Phe (Miedlich *et al.*, 2004). The binding site of L-PhE macromolecules to mGluRs has been localised at a triple serine motif (Ser-169-171). Mutagenesis experiments by this group in HEK293-CaSR cells revealed that these amino acid residues are crucial for L-Phe activation of CaSR in the presence of Ca^{2+}_o. These studies indicated that amino acids are crucial for allosterically modulating sensitivity of CaSR to Ca^{2+}_o (Zhang *et al.*, 2002).

1.15.1 Amino acids

CaSR is stimulated by amino acids with L-type stereoselectivity with specific affinities for L-Tyr, L-Trp, L-His and L-Phe (Conigrave and Quinn, 2000, Mun *et al.*, 2004, Mun *et al.*, 2005). In human parathyroid cells, CaSR is activated by L-type amino acids in the order L-Trp > L-Phe > L-His > L-Ala all demonstrating receptor activation in the millimolar range (Conigrave *et al.*, 2007). Using HEK293-CaSR cells, it was shown that L-Phe (normally effective at activating CaSR in the 0.3-30mM range in the presence of 1.0-1.5mM Ca^{2+}_o) was ineffective at activating CaSR in the absence of Ca^{2+}_o. This study was important in illustrating L-Phe as a type II agonist, which activates CaSR only in the presence of Ca^{2+}_o. Furthermore, when CaSR is maximally activated by 5mM Ca^{2+}_o in HEK293-CaSR cells, L-Phe cannot further activate CaSR (Conigrave *et al.*, 2000, Kobilka, 2000, Conigrave and Brown, 2006). CaSR is widely expressed in the gastrointestinal tract in gastrin cells in the stomach and basally on small intestine villous and crypt epithelial cells. These findings collectively suggest that CaSR may play a role in taste and digestion (Chattopadhyay *et al.*, 1998, Buchan *et al.*, 2001).

1.15.2 Calcimimetics

Calcimimetics are compounds which bind allosterically to CaSR and they demonstrate their effects only in the presence of Ca^{2+}_o. In 1998, Nemeth *et al* first classified the role of allosteric modulators in CaSR activity and investigated the effects of two compounds, NPS R-467 and NPS R-568, as potent selective inhibitors of PTH secretion in bovine parathyroid cells (Nemeth *et al.*, 1998). The group demonstrated firstly that NPS R-568 is a more potent activator of CaSR than NPS R-467. Secondly, that the compounds have enantiomeric selectivity, where NPS R-568 is significantly more potent than NPS S-568. This is depicted in Figure 17 where a concentration response for these two agents is shown in bovine parathyroid cells.
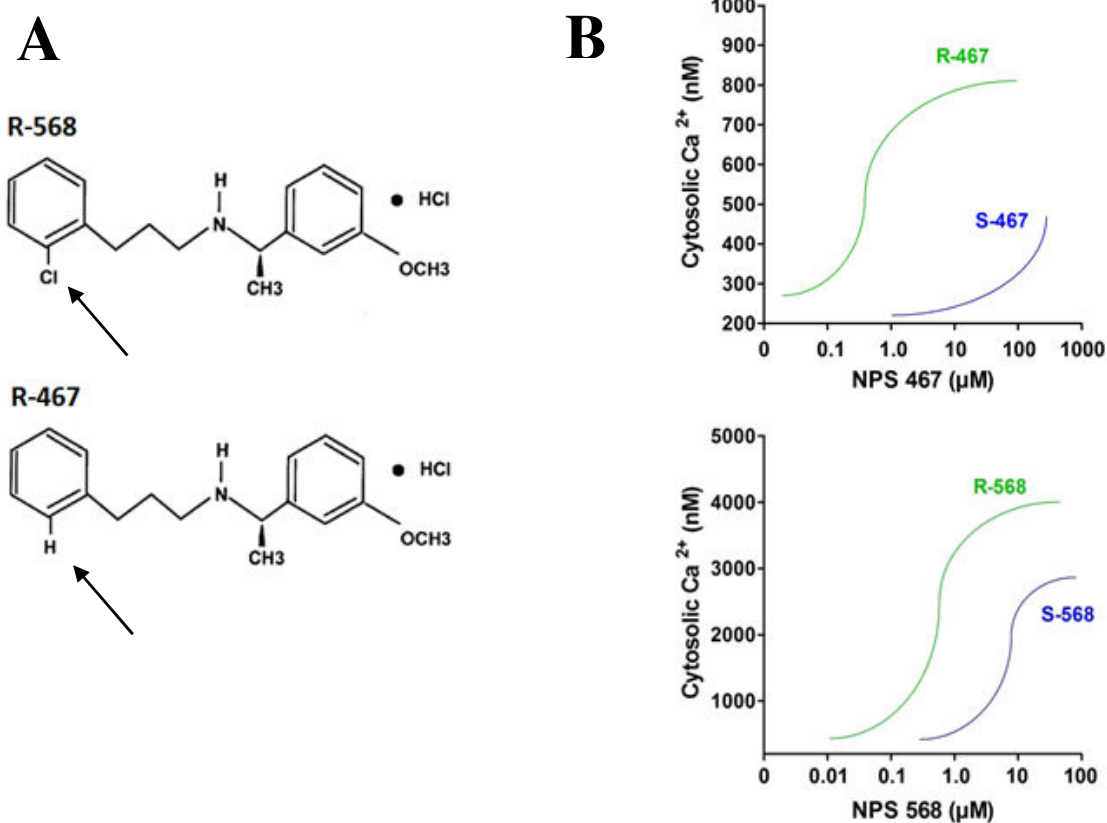
Figure 17. Calcimimetics increase intracellular Ca²⁺ through CaSR activation in bovine parathyroid cells. (A) The calcimimetic R-568 and R-467 are identical with the exception of the R-group indicated by black arrows. (B) Concentration-response curves of NPS 568 demonstrate more potent activity compared to NPS 467. R-type enantiomers shown greater potency in the case of both R-467 and R-568 when compared to S-type enantiomers. Experiments were conducted using bovine parathyroid cells loaded with the Ca²⁺-sensitive fluorescence dye fura-2 for Ca²⁺-imaging experiments. Figure adapted from Nemeth *et al* 1998 (Nemeth *et al.*, 1998).

The binding site of these calcimimetics to CaSR has been investigated and evidence suggests that binding sites are localised to the region of amino acids 668-837 (Miedlich *et al.*, 2004). This evidence comes from mutagenesis studies in HEK293-CaSR cells. Mutations in the receptor at the residues Phe-668, Phe-684, or Glu-837 show an enhanced potency of calcimimetics (Miedlich *et al.*, 2004). Calcimimetics have proved useful tools from a clinical perspective. Currently, commercially available calcimimetics such as Cinacalcet have been approved for the treatment of secondary hyperparathyroidism; a condition where the parathyroid glands produce inappropriately high levels of PTH. Here, calcimimetics activate the PTG CaSR and suppress further PTH secretion (Sprague *et al.*, 2003, Francis *et al.*, 2008, Piecha *et al.*, 2008, Serra *et al.*, 2008, Rothe *et al.*, 2011).

1.15.3 Calcilytics

The discovery of positive allosteric agonists of CaSR suggested that CaSR may be pharmacologically modulated with antagonists. Indeed, such compounds have been discovered and these named calcilytics have been shown to be effective at diminishing CaSR activity. In 2001, Nemeth *et al* demonstrated the effectiveness of a CaSR antagonist; NPS 2143, once again in bovine parathyroid cells with an IC_{50} of 41nM (Nemeth *et al.*, 2001). Encouragingly, this compound had an opposing effect on CaSR compared to calcimimetics, inducing rapid PTH secretion in bovine parathyroid cells as demonstrated in Figure 18. Calhex 231, another commercially available calcilytic, has been investigated in research to ascertain its pharmacological profile on CaSR in various cell types. It has been reported that acting on HEK293-CaSR, the IC_{50} values of both these calcilytics is in the region of 0.34-0.40μM, indicating similar inhibitory profiles on CaSR. However, the IC_{50} of NPS 2143 in HEK293-CaSR cells was approximately 10-fold less than that in bovine parathyroid cells, indicating higher sensitivity of the CaSR in the native parathyroid gland (Nemeth *et al.*, 2001). Comparable IC_{50} values were somewhat expected since both NPS 2143 and Calhex 231 share overlapping binding sites on the transmembrane domain of CaSR (Petrel *et al.*, 2004). This has been shown extensively in mutagenesis experiments where modification of particular amino acid residues such as Phe-668, Arg-680, or Phe-684 and Glu-837 significantly reduce the inhibitory effect of NPS-2143 (Miedlich *et al.*, 2004). Similarly, mutations in the aforementioned Phe-684 and Glu-837 residues significantly reduce the ability of Calhex 231 to inhibit the accumulation of inositol phosphates (Petrel *et al.*, 2003). In this regard it is hypothesized that both calcimimetics and calcilytics have overlapping binding sites on CaSR.
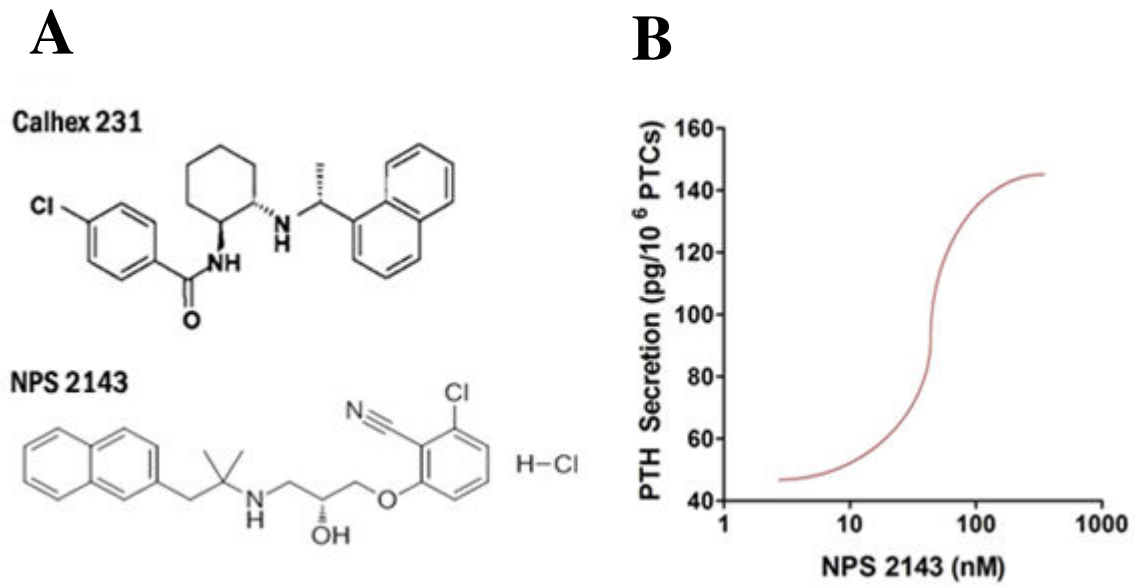
Figure 18. **Calcilytics act on CaSR to increase PTH secretion in bovine parathyroid cells**. (A) Two commercially available calcilytics, Calhex 231 and NPS 2143, act specifically on CaSR. (B) NPS 2143 acts on bovine parathyroid CaSR to selectively stimulate PTH secretion. IC_{50} for NPS 2143= ~43nM. Figure adapted from Petrel *et al* 2004 and Nemeth *et al* 2001 (Nemeth *et al.*, 2001, Petrel *et al.*, 2004).

1.16 CaSR signalling: Ca^{2+}_o as a first and second messenger

The CaSR is activated by polyvalent cations, polyamines, calcimimetics, calcilytics, antibiotics and amino acids (Brown and MacLeod, 2001, Hebert, 2006, Ward, 2011). As a GPCR, CaSR couples to various heterotrimeric G-proteins including the α-subunits $G_{q/11}$, G_i and $G_{12/13}$. Heterotrimeric complexes ($G_{\alpha\beta\gamma}$) are activated upon CaSR activation where the α-subunit (q11, i or 12/13) may dissociate from βγ-subunits and carry out signalling via secondary intracellular messengers. Interestingly, although the q11, i and 12/13 G-protein α-subunit pathways are well established, recent evidence suggests that there is a CaSR-G_s pathway which may be stimulated upon receptor activation. It has been proposed that this G_s pathway may have directly opposing effects to the G_i pathway, and is activated in prostate and breast cancer cells (Mamillapalli *et al.*, 2008, Mamillapalli and Wysolmerski, 2010). CaSR signalling pathways are diagrammatically represented in Figure 19.

Recent research has shown that CaSR signalling falls into 3 major categories (Kifor *et al.*, 2001, Huang *et al.*, 2002, Ward, 2011, Thomsen *et al.*, 2012). (i) The G_i inhibitory pathway may be activated, where the action of AC is inhibited, reducing the amount of intracellular cAMP and therefore the activation of protein kinase A (PKA). (ii) The $G_{12/13}$ pathway may also be activated where the actions of Rho and phospholipase D (PLD) activate phosphotidylinositol-4 kinase (PI4-K), subsequently cleaving phosphatidylinositol-4 phosphate (PI4) into PIP_2. PIP_2 within the cell is then utilised in further signalling cascades. (iii) Activation of the G_{q11} pathway causes an activation of PLC. PLC catalyses the formation of diacylglycerol (DAG) and IP_3 from PIP_2. IP_3 can then act on IP_3Rs on the ER to liberate Ca^{2+} from internal stores and increase $[Ca^{2+}]_i$. When the G_{q11} pathway is activated, phospholipase A2 (PLA_2) is also activated. This membrane-bound enzyme, also stimulated by ERK1/2, catalyses the formation of AA which can regulate the action of PKC. DAG formed from PIP_2 acts together with AA to activate PKC, which can initiate a mitogen-activated protein kinase (MAPK) signalling pathway. In this process, MAPK kinase and stress-activated protein kinase ERK kinase 1 (SEK1) can activate ERK 1/2, jun amino terminal kinase (JNK) and p38 MAPK. These downstream signals can then either feed-back into the G_{q11} pathway, or enter the nucleus

where they may carry out transcriptional regulation of genes (Kifor *et al.*, 2001, Huang *et al.*, 2002, Ward, 2011, Thomsen *et al.*, 2012).
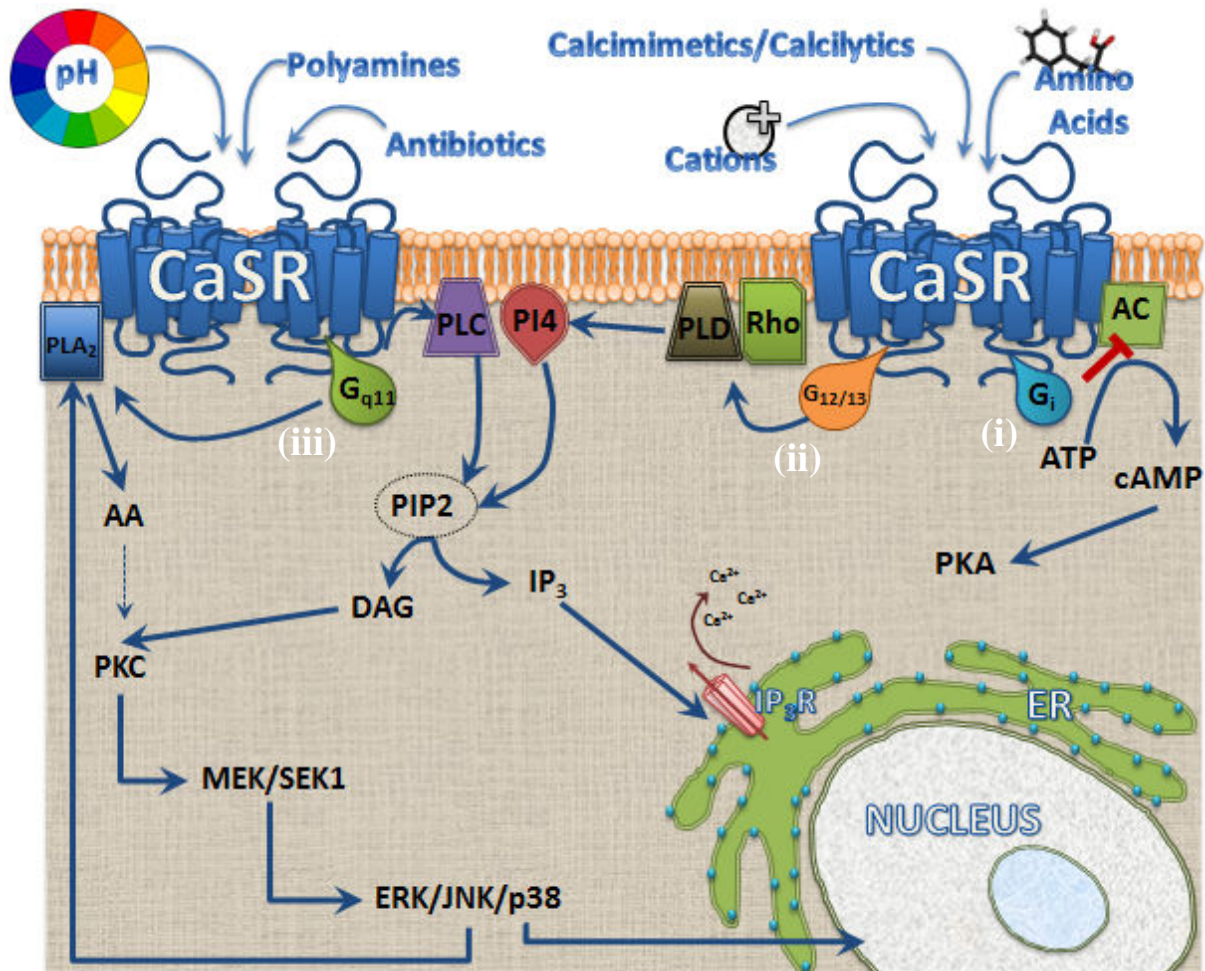
Figure 19. Signalling pathways activated by the CaSR. The CaSR is activated by polyvalent cations, polyamines, calcimimetics, calcilytics, antibiotics and certain amino acids. The three pathways (i), (ii) and (iii) illustrated are the best characterised CaSR pathways. There is evidence that a G_s pathway may also be activated by CaSR during malignancy, having opposite effects to the G_i pathway. Blue arrows indicate activation, red flat-ended arrows indicate inhibition. Abbreviations: adenylyl cyclase (AC), adenosine monophosphate (cAMP), protein kinase A (PKA), phospholipase D (PLD), phosphotidylinositol-4 kinase (PI4K), phosphatidylinositol-4 phosphate (PI4), phosphatidylinositol 4,5-bisphosphate (PIP2), phospholipase C (PLC), diacylglycerol (DAG), inositol triphosphate (IP3), IP3 receptor (IP3R), endoplasmic reticulum (ER), phospholipase A2 (PLA2), extracellular-regulated kinase (ERK 1/2), arachidonic acid (AA), protein kinase C (PKC), mitogen-activated protein kinase (MAPK), MAPK kinase (MEK), stress-activated protein kinase ERK kinase 1 (SEK1), jun amino terminal kinase (JNK). (Kifor *et al.*, 2001, Huang *et al.*, 2002, Ward, 2011, Thomsen *et al.*, 2012).

1.17 CaSR in disease

Natural mutations or polymorphisms in the human CaSR gene have been widely described (Hendy *et al.*, 2000, Rodrigues *et al.*, 2011, Eldeiry *et al.*, 2012). These alterations in gene sequence can predispose in affected individual to disorders of Ca^{2+} metabolism. Mutations can occur in the intracellular, transmembrane or extracellular domains and are more often missense mutations (Tfelt-Hansen *et al.*, 2003, Breitwieser, 2012). In addition to genetic determinants of CaSR function, humans may also acquire CaSR dysfunction through the action of autoantibodies. Here, recurring CaSR mutations that have been described in human patients will be described.

1.17.1 Genetic disorders of CaSR

In 2011, over 200 mutations in the CaSR gene were identified (D'Souza-Li, 2006, Rodrigues *et al.*, 2011). Now it is speculated that there are significantly more. Typical phenotypes resulting from these genetic abnormalities include familial hypocalciuric hypercalcaemia (FHH) and neonatal severe hyperparathyroidism (NSHPT). FHH is the result of a heterozygote inactivating mutation of CaSR. In 1972, Foley *et al* first documented asymptomatic hypercalcaemia (Foley *et al.*, 1972). These patients have small but significant increases (~10%) in serum calcium brought about by a mutation which can partially or completely remove CaSR function on one allele (Tfelt-Hansen *et al.*, 2003). Often, a single mutant allele can exert a dominant negative effect on the gene as a whole. As a result, the inverse sigmoidal relationship between serum PTH and blood Ca^{2+}_o is right-shifted in FHH patients. This can be recapitulated in normal patients on calcilytic treatment (Bai *et al.*, 1999, Tfelt-Hansen *et al.*, 2003). Similarly, NSHPT is an autosomal recessive disease and a consequence of an inactivating mutation in CaSR. In the vast majority of cases, NSHPT only surfaces when heterozygous and homozygous mutation of CaSR alleles occurs (Tfelt-Hansen *et al.*, 2003). Consequently, the sufferer has inappropriately elevated serum levels of PTH. This is due to the fact that CaSR cannot be activated by Ca^{2+}_o to inhibit PTH secretion. Infants younger than 6 months of age suffering from NSHPT often must undergo parathyroidectomy to prevent hyperparathyroidism. If surgery is not conducted, consequences can be fatal (Hendy *et al.*, 2000, D'Souza-Li, 2006, Rodrigues *et al.*, 2011).

In stark contrast to the severity of inactivating CaSR mutations lies autosomal dominant hypocalcaemia (ADH); a consequence of gain-of-function mutation of the CaSR gene. In this way, PTH secretion is suppressed in the face of physiological Ca^{2+}_o concentrations, thereby resulting in sustained hypocalcaemia. Surprisingly, serum PTH levels are almost normal in these individuals, however Ca^{2+} excretion in urine is significantly heightened (Hendy *et al.*, 2000, Tfelt-Hansen *et al.*, 2003). For this reason, patients may suffer from renal complications including nephrocalcinosis and renal stones (Raue *et al.*, 2011). Patients with ADH are often asymptomatic, however, younger patients may suffer from seizures as a consequence of hypocalcaemia (Tan *et al.*, 2003). ADH is associated with a shift in the relationship between serum PTH and blood Ca^{2+}_o. During ADH, the Ca^{2+}_o/PTH sigmoidal relationship is shifted leftwards, simulating normal patients on calcimimetic treatment (Hendy *et al.*, 2000, Tfelt-Hansen *et al.*, 2003). Bartter's Syndrome type V has also been documented in many patients (Watanabe *et al.*, 2002). This syndrome is a rare heterogeneous consequence of abnormalities in Na^+ and Cl^- absorption. Patients suffering with this syndrome often exhibit hypocalcaemia and hypercalciuria, renal salt wasting, metabolic alkalosis and activation of the renin-angiotensin-aldosterone system (RAAS) (Watanabe *et al.*, 2002). Studies have shown that missense mutations in 3 amino acids (L125P, C131W and A843E) of CaSR cause Bartter's Syndrome type V (Vargas-Poussou *et al.*, 2002, D'Souza-Li, 2006).

1.17.2 Acquired disorders of CaSR

A number of cases have arisen where patients have suffered from dysregulation in Ca^{2+}_o metabolism when genetic mutations in the CaSR gene have not been found. Autoimmune hypoparathyroidism (AH) occurs as a consequence of the presence of CaSR auto-antibodies resulting in hypocalcaemia and hyperphosphataemia. One study showed that 56% of 25 sufferers of AH exhibited a specific CaSR epitope essential for PTH binding (Li *et al.*, 1996c). These data suggest that CaSR acts as an antigen to direct an immune response against the parathyroid gland. PTH deficiency in these patients is a result of destruction of the parathyroid gland as an autoimmune inflammatory reaction (D'Souza-Li, 2006). This extracellular domain of CaSR has also been shown to be an antigen not

only for parathyroid destruction, but for interfering with normal activation of the receptor. As a result, patients suffer from hypercalcaemia through a significant increase in PTH secretion. In this manner, CaSR-directed antibodies themselves can be considered as partial agonists of the CaSR (Pallais *et al.*, 2004, D'Souza-Li, 2006).

1.18 CaSR in the cardiovascular system: a role in vascular tone

Traditional anatomy shows that blood vessels, particularly different arteries, are anatomically very similar. In recent years however, functional studies on an array of vessel types including pulmonary vessels, aortae, mesenteric arteries, the brachiocephalic, carotid and femoral arteries have demonstrated significantly unique characteristics in not only their ability to maintain vascular tone (Ohanian *et al.*, 2005, Smajilovic *et al.*, 2007, Harno *et al.*, 2008), but the genes which they express as a whole. In terms of arteriolar tone, smaller resistance vessels with diameters typically less than $500\mu m$ play crucial roles in maintaining vascular resistance by responding to endogenous hormones including bradykinin, endothelin, angiotensin II and prostacyclin (Weiss and Putney, 1978, Adams *et al.*, 1989, Furchgott and Vanhoutte, 1989, Masaki, 1995). In addition to this, arteries carry out Ca^{2+}-dependent contraction in a concentration-dependent manner as shown by various investigators (Wonneberger *et al.*, 2000, Smajilovic *et al.*, 2007). Interestingly, other investigators have reported Ca^{2+}-dependent dilation (Wu and Bohr, 1991). Regardless of the role Ca^{2+} plays in vascular tone in these vessels, it is clear that a mechanism for Ca^{2+}_o-sensing is at work which can modulate vessel tone.

1.18.1 CaSR and vascular tone (*ex vivo* studies)

It has become relatively clear how CaSR function controls systemic Ca^{2+}_o homeostasis from the parathyroid gland, however, less well-defined is the role of CaSR in the cardiovascular system. To characterise the role of CaSR here, researchers have adopted a variety of experimental approaches *in vivo*, *ex vivo* and *in vitro* to determine the role of CaSR in endothelial and vascular smooth muscle cells in a variety of different vessel types. Since Ca^{2+} is a player in setting the cardiovascular tone (Bukoski *et al.*, 1997), the idea of CaSR, a sensor of Ca^{2+}_o, playing a role in overall cardiovascular function seems extremely plausible. For this reason, the roles of CaSR in the cardiovascular system has been investigated over the past 15 years.

1.18.1.1 Small arteriole myography

The very first indication that CaSR may play a role in vascular tone modulation was suggested by Bukoski *et al* (Bukoski *et al.*, 1997). This group investigated the role of CaSR in rat mesenteric arteries. Initially, immunohistochemical analysis revealed that CaSR was only expressed in the perivascular nerves localised in the adventitia of these arteries. Additionally, western blotting and RT-PCR confirmed CaSR expression in the adventitia, where dorsal root ganglia are situated (Bukoski *et al.*, 1997). Wire myography experiments showed that whole mount mesenteric vessels with an intact adventitia achieved Ca^{2+}-dependent relaxation in a concentration-dependent manner with an EC_{50} of 2.47mM $\pm$ 0.17. Bukoski *et al* reported that this relaxation was endothelium-independent, chiefly due to relaxation persisting in the presence of the nitric oxide synthase inhibitors (Bukoski *et al.*, 1997). The group concluded that these responses were due to a CaSR present in the perivascular nerve network. This study was crucially important in initiating cardiovascular research into CaSR.

In 2005, Ohanian *et al* investigated the presence and possible role of CaSR in rat subcutaneous vessels (Ohanian *et al.*, 2005). Evidence that Ca^{2+} is a major player in

vasodilation is well-established (Lopez-Jaramillo *et al.*, 1990, Bukoski *et al.*, 1997) and so the group set out to investigate whether these observed effects were CaSR-mediated. Subcutaneous vessels of <250μm diameter were isolated from rats and biphasic dilation and contraction was measured using pressure myography where luminal pressure was set to 70mmHg to recapitulate *in vivo* conditions. It was shown that Ca^{2+}_o used at concentrations up to 10mM, induced concentration-dependent contraction followed by dilation indicated by an increasing luminal diameter. Mg^{2+} was also shown to induce dilation in these vessels. Furthermore, the role of additional CaSR agonists in vascular tone were investigated. Using the aminoglycoside antibiotics neomycin and kanamycin as alternative activators of CaSR, vasodilation could be detected using up to 10mM of these antibiotics in rat subcutaneous vessels (Ohanian *et al.*, 2005). In support of the idea that these effects could be mediated through CaSR, CaSR protein was detected in subcutaneous vessels. What is perhaps the most fundamental difference between these two studies by Ohanian and Bukoski, is that Ohanian *et al* did not pre-contract their vessels with phenylephrine. Instead, subcutaneous vessels were maintained at physiological luminal pressure (70mmHg) until the myogenic tone was stable. At this point, concentration-response curves using CaSR agonists were performed (Ohanian *et al.*, 2005).

Since the studies by Bukoski *et al* and Ohanian *et al*, additional *ex vivo* functional studies have been performed on rat vessels. Weston *et al* in 2005 experimented on rat mesenteric arteries of the second and third order (sizes between 150-250μm) and demonstrated that a functional CaSR was at work more specifically in endothelial cells. The group showed this by RT-PCR using CaSR-specific primers, immunohistochemical staining of CaSR immunoreactivity in blood vessels and through functional *ex vivo* electrophysiological experiments (Weston, 2005). The group used CaSR activators such as Ca^{2+}_o and calindol at concentrations of 3.0mM and 100nM respectively. In electrophysiology experiments, the authors measured hyperpolarisation in response to these CaSR agonists, which is commonly known to be associated with subsequent dilation or relaxation of vascular smooth muscle cells. However, despite measureable hyperpolarisation, calindol was unable to relax mesenteric vessels when placed on a wire myograph. The Weston group largely attribute this paradoxical finding to theory of K^+ clouds. For example, during α_1-

adrenergic activation by phenylephrine, or muscarinic M3 receptor activation by acetylcholine, K^+ channels are activated and cause K^+ efflux from the VSMCs or ECs respectively. Consequently, vasodilation by VSMC hyperpolarisation is theoretically inhibited due to local extracellular K^+ clouds generated by VSMCs. Using calindol, Weston *et al* showed that, in the presence of the α_1-adrenergic receptor agonist phenylephrine, the ability of calindol to hyperpolarise VSMCs was reduced. The group theorised that K^+ clouds generated by phenylephrine would prevent sustained hyperpolarisation of ECs and therefore prevent dilation by calindol. To investigate this, the group then used iberiotoxin in combination with phenylephrine to inhibit BK_{Ca} channels present on VSMCs. The group reported that the hyperpolarising effect of calindol in the presence of iberiotoxin was significantly enhanced suggesting that this was indeed the case. The group further investigated whether these effects were mediated through the EC-CaSR by denuding the endothelium in these vessels. EC removal removed the hyperpolarising effects of calindol suggesting that an EC-CaSR is at work in mesenteric arteries. Interestingly, the group also investigated the role of the calcilytic calhex 231. Results showed that addition of calhex 231 reduce hyperpolarisations induced by calindol, indicating the existence of possible competitive binding between these two pharmacological agents (Weston, 2005).

When considering the role of vascular CaSRs, vessel type and experimental conditions are crucially important. Large conductance vessels and small resistance vessels are not only morphologically different, but also contain different numbers of cells, specifically, the ratios of endothelial to vascular smooth muscle cells. Conductance vessels such as the aorta contain VSMCs which far outnumber endothelial cells. Conversely, endothelial cells and VSMCs in small resistance vessels are present in near equal numbers in two separate monolayers (Wagenseil and Mecham, 2009, Wagenseil *et al.*, 2009, Wagenseil *et al.*, 2010). For this reason, in order to be able to draw conclusions from different studies, comparable experimental protocols must be applied in like-for-like vessels. In this regard, the Ohanian *et al.* and Weston *et al*. studies are largely dissimilar since (i) different vessel types were used, and (ii) both studies used different starting conditions before the addition of CaSR agonists. Research from Weston *et al* clearly states that large conductance K^+ channels play a role in maintaining membrane potential, which has

significant implications on the intrinsic ability of vascular cells to undergo hyper- or depolarisation. If this is true, then pre-constricted vessels vs. unconstricted vessels will have significantly different basal resting membrane potentials. It is therefore highly likely that these factors, in combination with any CaSR-mediated effects, produce the differential results seen between these studies.

1.18.1.2 Aortic myography

In a 2007 paper, Smajilovic *et al* demonstrated CaSR-evoked relaxation of rat aortae using traditional wire myography. The group showed that the calcimimetic AMG 073 acted directly on CaSR present in both the endothelium and vascular smooth muscle cells. Experiments were conducted using a buffer containing 1.5mM Ca^{2+}_o. Crucially, this concentration was selected as it lies within the mid-range of activation of CaSR. The group selected this concentration from a Ca^{2+}_o concentration response curve in the rat aortae where Ca^{2+}_o induced concentration-dependent contraction in the presence of phenylephrine. Although this Ca^{2+}_o concentration response curve started from 10μM (no contraction) to ~3mM (maximum contraction), previous data points below 0.5mM were excluded since this is below the threshold of CaSR activation. The group firstly showed that this Ca^{2+}-dependent contraction of rat aortae was diminished in the presence of 3μM AMG 073, suggesting that calcimimetics may have a role in vasodilation and relaxation. Secondly, using rat aortae pharmacologically pre-contracted with 3×10^{-6} M phenylephrine, the group demonstrated that AMG 073 induced a concentration-dependent relaxation up to 45.8 ± 2.9% relative to phenylephrine pre-constriction. This was observed from a concentration of 1μM to ~20μM (exact maximum concentration not stated in the publication). Also reported was the inability of this calcimimetic to relax vessels which were not phenylephrine pre-constricted, although data were not shown. Interestingly, this ability of calcimimetics to relax rat aortae was partially endothelium dependent as suggested by the fact that endothelium-induced relaxation was reduced when using L-NAME and indomethacin which block NOS and prostaglandins, respectively. These data suggest that relaxation could be mediated synergistically via endothelial and vascular smooth muscle CaSRs. However, Smajilovic *et al* further

suggested that CaSR activation, and subsequent relaxation, could be endothelium-derived hyperpolarising factor-dependent. This idea comes from similar experiments where aortae were pre-contracted with 125mM KCl. Under these supraphysiological conditions, AMG 073 relaxation responses were absent, suggesting that this effect was dependent on endothelium-derived hyperpolarising factors (EDHFs) which were inhibited in the presence of this high K^+. Together, these data suggest that in the rat aorta calcimimetics have both endothelium-dependent and -independent effect on relaxation (Smajilovic *et al.*, 2007). However, the group maintain that these effects may be by CaSR-specific, or CaSR- non-specific mechanism since higher concentrations of AMG 073 were used ($>1\mu M$). The group speculate that there may be some non-specific Ca^{2+}-channel mediated effects present. Further evidence supporting the role of Ca^{2+} as a vasoconstrictor in the aorta is presented in other publications. For example, Ito *et al* used guinea pig aortae to demonstrate Ca^{2+} as a vasoconstrictor when used at concentrations from 0.1-2.5mM Ca^{2+}_o. Of note, the group started from a base-line buffer containing no Ca^{2+}_o (Ito *et al.*, 1991).

1.18.2 CaSR and vascular tone (*in vivo* studies)

A study by Fryer *et al* in 2007 looked extensively at the role of CaSR in hypertension (Fryer *et al.*, 2007). In this study, the group showed that the calcimimetic cinacalcet (1, 3 and 10mg/kg with 30 min of each concentration) acutely increased mean arterial blood pressure in both 5/6 nephrectomised rats and control animals. Animals were infused intravenously over 90 min with cinacalcet and demonstrated significant increases in carotid and mesenteric vascular resistance. Data from this study would therefore suggest that CaSR activation by calcimimetics appears to have a pro-hypertensive role. The authors suggested that this may be due to inhibition of synthesis of nitric oxide. This is thought to be the case since cinacalcet infusion decreases $[Ca^{2+}]_o$ in a dose-dependent manner through PTH inhibition in the PTGs (Fryer *et al.*, 2007). Interestingly, nephrectomised rats also attained a reduction in PTH secretion in response to $[Ca^{2+}]_o$ in the presence of increasing concentrations of cinacalcet. For this reason, the effects of cinacalcet on vascular tone and blood pressure in this study are thought to be secondary to parathyroid gland CaSR stimulation, and not by vascular CaSR stimulation directly (Fryer *et al.*, 2007).

Nakagawa *et al* also investigated the role of calcimimetics in blood pressure modulation, looking specifically at R-568 and S-568. The group investigated mean arterial pressure and heart rate from the femoral artery. Infusion of 0.7mg/kg R-568 over 10 minutes into the femoral vein was not sufficient to effect either mean arterial blood pressure and heart rate, although infusion of either R-568 or S-568 (2.1mg/kg over 3 minutes) was sufficient to reduce blood pressure and heart rate with R-568 having greater effects (Nakagawa *et al.*, 2009). Comparatively, this group observed short-term (over the course of 3 minutes) hypotensive effects of calcimimetics whereas Fryer *et al* observed hypertensive effects of calcimimetics in a more long-term treatment (over 90 minutes). Similarly, a study by Rybzynska *et al* showed that intravenous injection of 1mg/kg R-568 in normal wild-type rats was sufficient to reduce serum $[Ca^{2+}]_o$ and urinary phosphate excretion and mean arterial blood pressure (Rybczyńska *et al.*, 2006). These findings were also shown by the same group in spontaneously hypertensive rats, which became hypotensive in response to R-568 administration of 1mg/kg intravenously (Rybczyńska *et al.*, 2005). From these

studies it is clear that many factors effect vascular tone, including the calcimimetic compound itself, the dose used and the duration of treatment. Furthermore, since CaSR is so widely expressed, especially in such abundance in the PTGs, it is extremely difficult to identify whether or not vascular CaSR are playing a role in this process.

The role of calcilytics has also been investigated in blood pressure modulation. Rybczynska *et al* had previously seen that, in spontaneously hypertensive rats, R-568 decreased mean arterial pressure (Rybczyńska *et al.*, 2005), however, the group believe this to be a consequence of activation of the parathyroid CaSR and not relating to vascular CaSRs. Using normal wild-type rats, the group perfused animals intravenously with calcilytic NPS 2143 (1mg/kg). The group concluded that 2 hours post-perfusion, there was a significant increase in serum $[Ca^{2+}]_o$. This was also associated with a significant increase in serum PTH and mean arterial pressure. Interestingly, the group believe this results to be due to secretion of hypertensive factors from the parathyroid glands (Rybczynska *et al.*, 2006). Collectively, these *in vivo* studies illustrate the importance of CaSR activation by allosteric modulators. However, it still remains unclear whether changes in blood pressure arise from vascular CaSR activation, parathyroid CaSR activation or a combination of these.

1.19 CaSR: a role in the cardiovascular system?

We have seen how CaSR modulation plays a significant role in blood vessels tone modulation and calcification through a variety of different models. Previously discussed has been the extensive role of CaSR in the body and in the vasculature. Currently, there is no clear and discernable role for the CaSR in the cardiovascular system, or a role of the receptor in vascular diseases such as calcification *in vivo* although several studies suggest that the vascular CaSR might play an important role in preventing cardiovascular pathology (Bukoski *et al.*, 1997, Weston, 2005, Smajilovic *et al.*, 2006, Smajilovic *et al.*, 2007, Alam *et al.*, 2008, Weston *et al.*, 2008). A current hypothetical overview of CaSR function in the cardiovascular system is demonstrated in Figure 20.
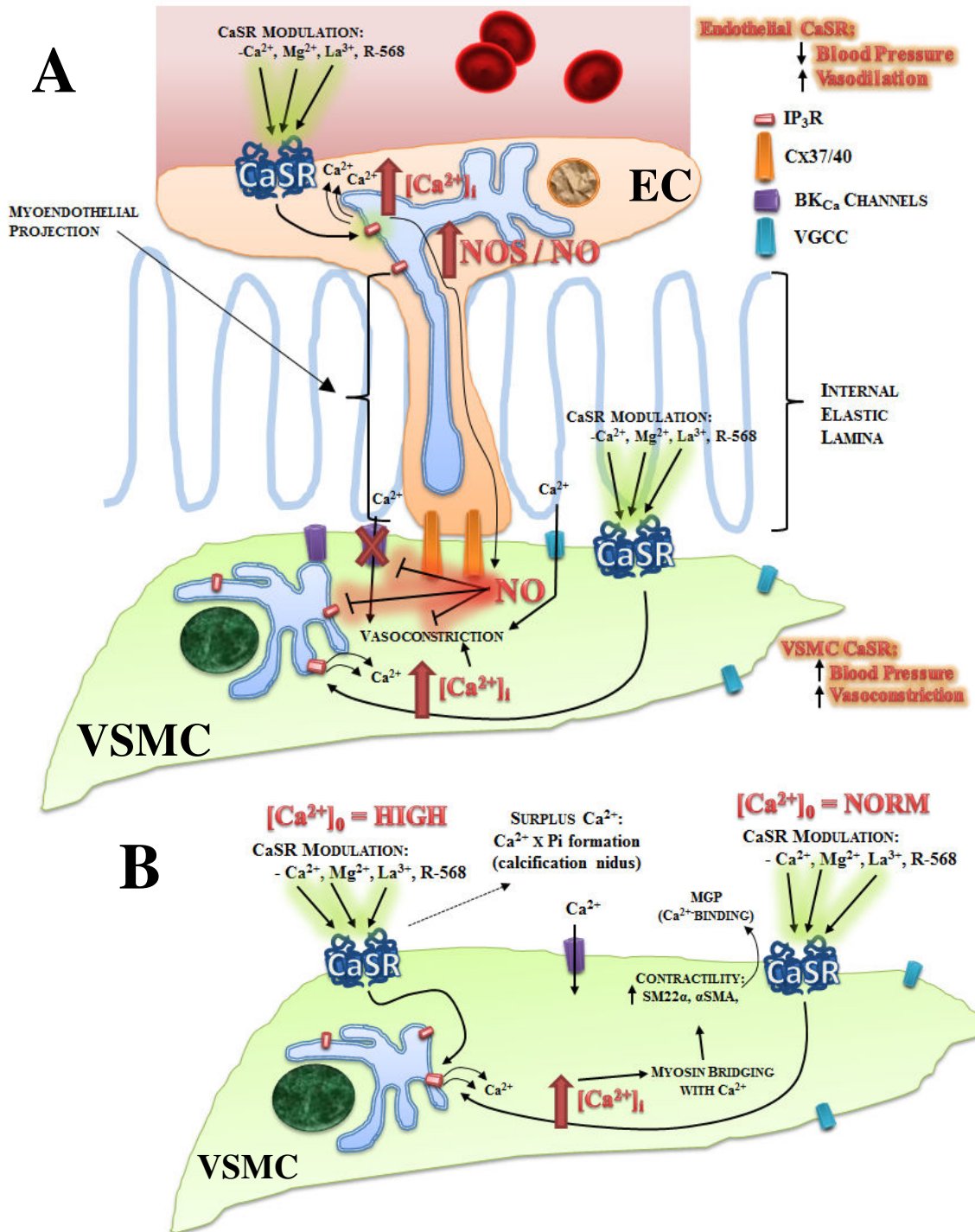
Figure 20. Potential roles of the CaSR in the cardiovascular system. (A) CaSR might play a role in maintaining vascular tone. Activation of CaSR in endothelial cells causes release of Ca^{2+} from internal stores (Weston, 2005). Consequently, the NOS/NO pathway is activated, causing inhibition of constriction and promotion of vasodilation through gap junctions. Endothelial CaSR is therefore likely to play a role in reducing blood pressure. Similarly, CaSR activation on VSMCs can lead to increases in VSMC $[Ca^{2+}]_i$ leading to Ca^{2+}_i-dependent myosin bridging and vasoconstriction. It is therefore likely that VSMC CaSR plays a role in blood pressure modulation too (Smajilovic *et al.*, 2011). (B) In the presence of physiological $[Ca^{2+}]_o$, CaSR agonists may cause increases in $[Ca^{2+}]_i$ and bridging of myosin. It is likely that this action

maintains the VSMC contractile phenotype and upregulation of actin products. Additionally, Ca^{2+} influx may occur to facilitate this contractile phenotype progression by the actions of BK_{Ca} and VGCCs (Weston *et al.*, 2008). Where high $[Ca^{2+}]_o$ is present, this may activate CaSR for more myosin bridging. Excess Ca^{2+}_o may be poorly handle by MGP. Consequently, surplus Ca^{2+} may bind phosphate over time and create small calcification nucleation sites.

1.19.1 Project scope and overview

In this introduction I have presented evidence for the role of the CaSR in the vasculature, specifically in vascular smooth muscle cells. Additionally, I have described how studies in the field have been conducted illustrating the importance of CaSR in blood pressure modulation and in vascular calcification. Vascular calcification is associated with numerous deleterious cardiovascular health complications including atherosclerosis, ventricular hypertrophy, high blood pressure and, of course, CKD. Furthermore, we have seen how CaSR modulation with pharmacological agents such as calcimimetics have demonstrated potential protective roles against both calcification and hypertension. Current findings reviewed in this thesis suggest that the extracellular calcium-sensing receptor, CaSR, is an attractive area of research in the area of cardiovascular physiology and disease which has been explored fairly little. It would appear that CaSR modulation *in vivo*, *ex vivo* and *in vitro* has significant implications on the anatomy and physiology of blood vessels and cells that impart them.

1.19.2 Aims

The overall aims of this PhD are:

(i) To determine the physiological role of the CaSR in the cardiovascular system, and its involvement in cardiovascular pathology.

(ii) To determine whether allosteric modulators of the CaSR, the calcimimetics, affect the vascular CaSR.

These will be tested adopting a number of *in vitro*, *ex vivo* and *in vivo* approaches using our newly developed mouse model of targeted CaSR ablation from VSMCs.

1.19.2.1 CaSR ablation in vascular smooth muscle cells

The major aim of this PhD research is to determine whether CaSR plays a role in vascular physiology and VC by characterising a new transgenic mouse model with selective ablation of CaSR in VSMCs. CaSR comprises 7 exons however, only exons 2-6 are transcribed and translated to make the mature CaSR protein (Rodrigues *et al.*, 2011). Exon 7 encodes the entire transmembrane domain of the receptor which allows (i) the receptor to be membrane-bound, and (ii) allows binding of agonists such as calcimimetics. Using a transgenic mouse model developed and provided by Dr. Wenhan Chang *et al* at UCSF (Chang *et al.*, 2008), floxed 'loxP' sites are incorporated either side of exon 7 of CaSR, as described in Figure 21. In this way, cre recombinase, an exogenous bacterial-derived enzyme, can be driven by tissue-specific promoters. When switched on by a tissue-specific promoter, the cre recombinase enzyme is produced specifically in that cell type. For this particular mouse model, the cre enzyme is driven by the modified SM22α promoter, produced by Li *et al* (Li *et al.*, 1996b). Li *et al* found that the SM22α promoter (a promoter expressed in multiple smooth muscle cell lineages) could be modified in such a way that selecting just a 445bp 5' region of this promoter could drive specific vascular smooth muscle cell, cardiac and early skeletal muscle expression of any genes flanking this promoter. Importantly, the group reported that, although this promoter was sufficient to have minor activity in early embryonic skeletal muscle (E9.5 and E12.5), expression of this promoter in development thereafter to adulthood is restricted to vascular smooth muscle cells (Li *et al.*, 1996a). The publication from 1996 showed this visually using a reporter mouse for lacZ under the control of this modified SM22α promoter (ΔSM22α). Currently, this method of VSMC-knockout of floxed genes using endogenously expressed cre recombinase under the control of this ΔSM22α promoter is the most specific *in vivo* knockout strategy available. In combination with the floxed CaSR mouse which was provided by Dr. Wenhan Chang *et al* (Chang *et al.*, 2008), ΔSM22α-driven cre allows specific knockout of CaSR in vascular smooth muscle cells, as illustrated in Figures 22 and 23.
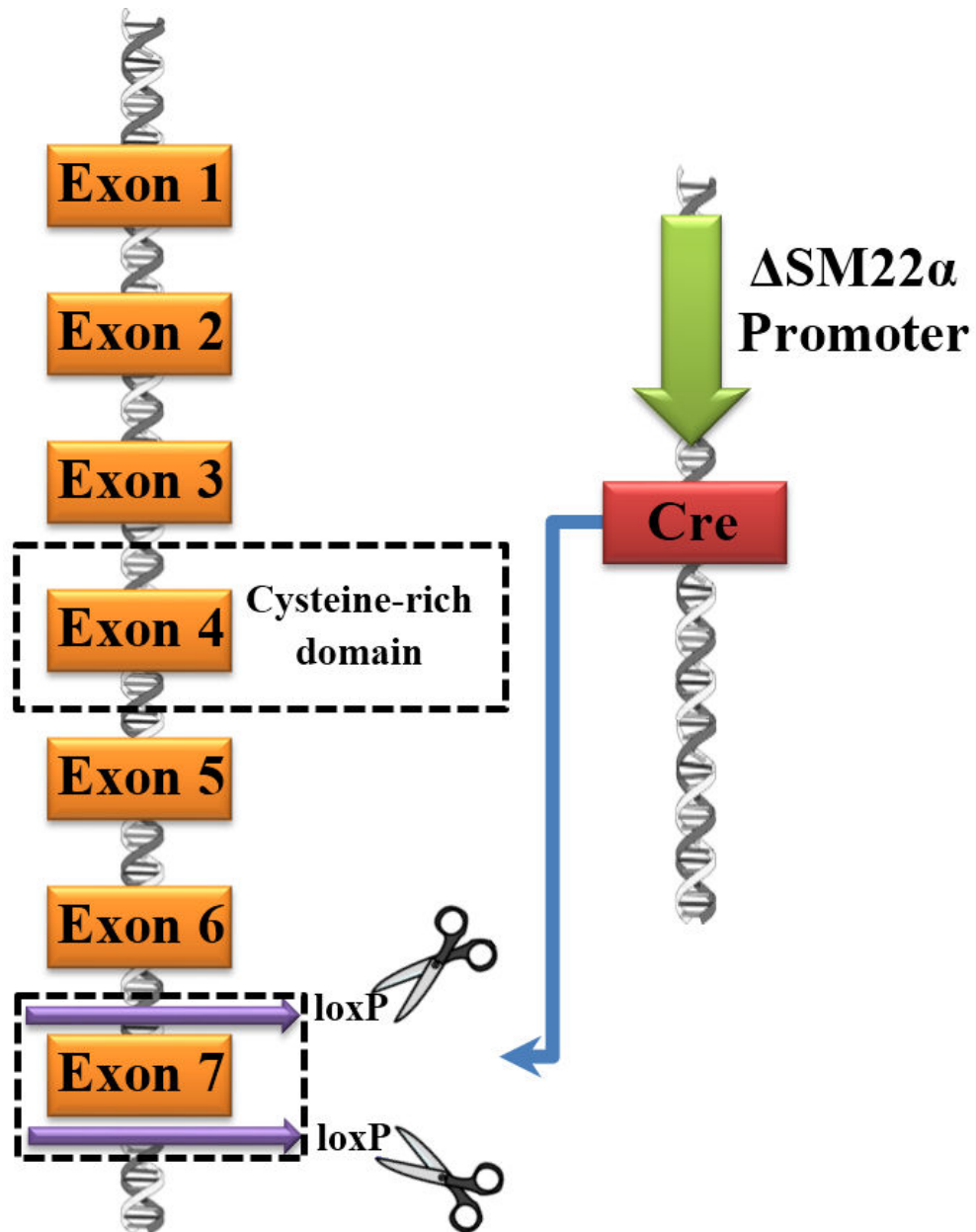
Figure 21. CaSR gene topology and ΔSM22α-driven CaSR knockout. The CaSR gene comprises 7 exons and 6 introns. Exons 2-4 encode the Venus flytrap (VFT) domain as described in Figure 15 (residues 36-513aa) which has a significant role in CaSR activation. Exon 4 also encodes the cysteine-rich domain (542-598aa) which helps maintain the structure and subsequent function of the receptor. Exon 7 contains agonist binding domains encoded within the transmembrane domain (TMD) and is flanked by loxP sites (purple arrows). Li *et al* ΔSM22α promoter drives the cre recombinase transgene in VSMCs to knock out this exon 7 (Li *et al.*, 1996a, Chang *et al.*, 2008).
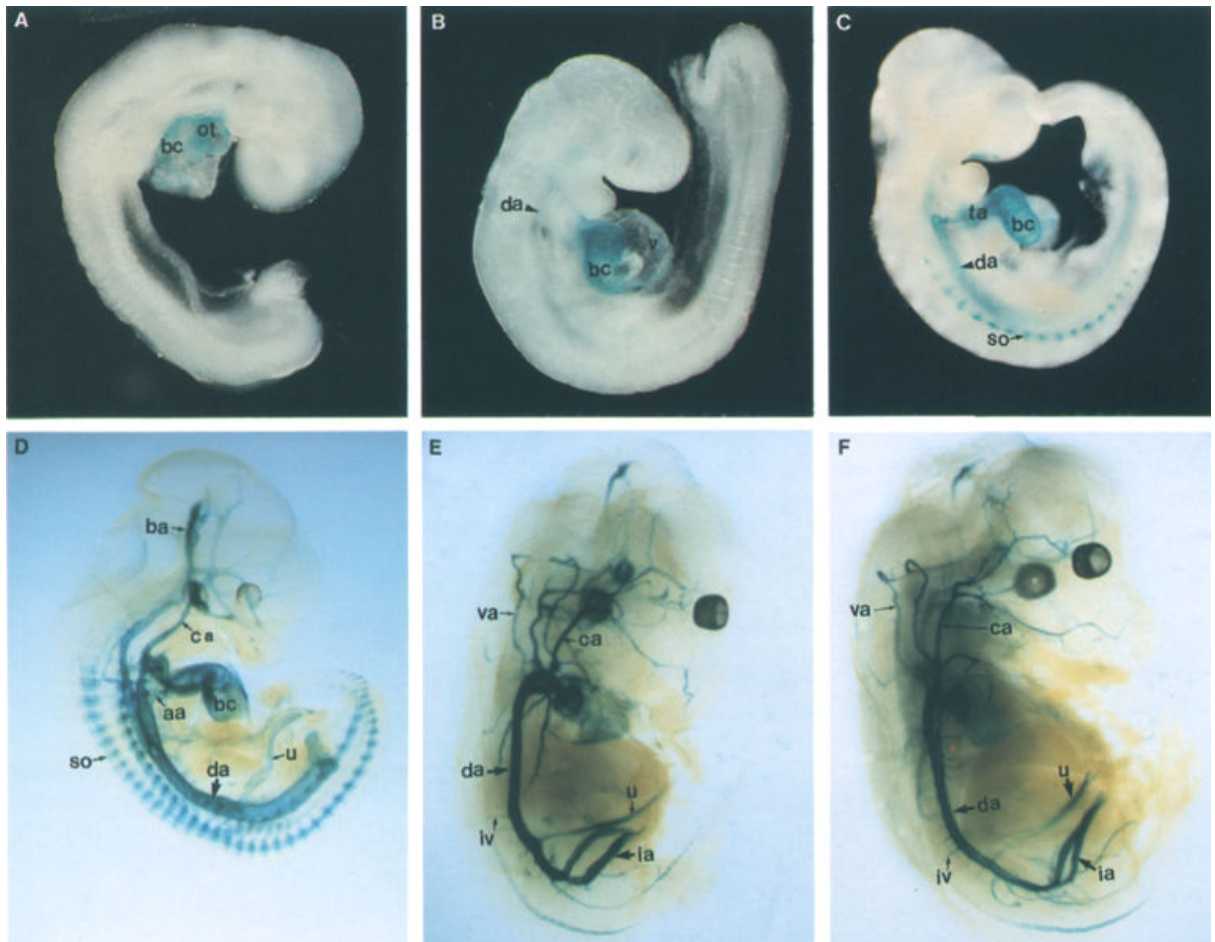
Figure 22. ΔSM22α-lacZ reporter mouse demonstrates cardiovascular specific expression of ΔSM22α. Transgenic mice harbouring the pSM2735/1093-1acZ sequence were stained for ΔSM22α expression. (A) LacZ activity detected in the outflow tract of the heart (ot) and bulbus cordis (bc) at E8.75. (B) By E9.0 LacZ staining was visible in the descending aorta (da). (C) lacZ staining was apparent in somites (so) by E10.0. (D, E, F) LacZ was visible at E11.5, 13.5 and E14.5 respectively in the following locations: aa, aortic arches; ba, basilar artery; bc, bulbus cordis; ca, carotid artery; da, dorsal aorta; ia, iliac artery; iv, intercostal vessel; ot, outflow tract; so, somite; ta, truncus arteriosus; u, umbilical vessel; v, ventricle; va, vertebral artery. Adapted from Li *et al* (Li *et al.*, 1996b).
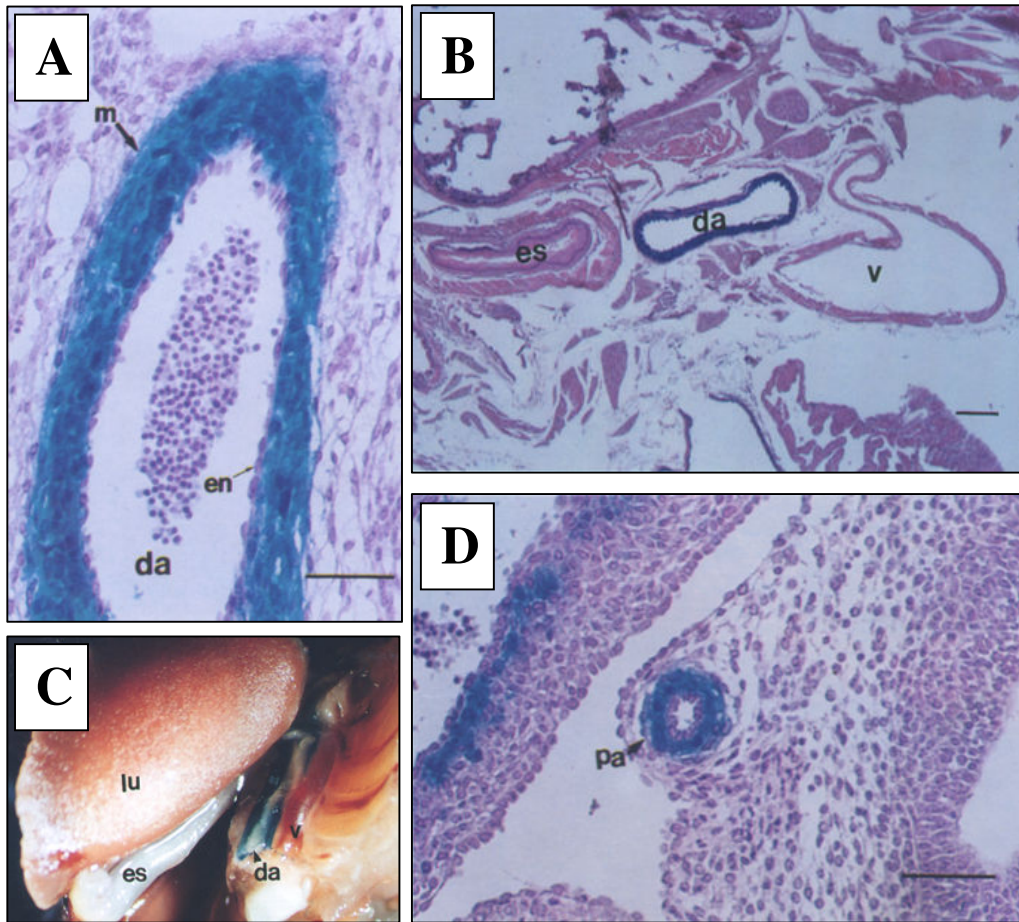
Figure 23. ΔSM22α-lacZ reporter mouse shows lacZ expression specifically in the tunica media of the descending aorta and pulmonary artery. (A, B, C) lacZ is visibly expressed specifically in vascular smooth muscle cells in the aorta. (D) lacZ expression is also visible in the pulmonary artery. LacZ expression was not seen in visceral of venous smooth muscle (v). m, smooth muscle; en, endothelium; da, dorsal aorta; lu, lung; es, oesophagus, v, vena cava; pa, pulmonary artery. Scale bar (A and D) 100µm, (B) 200µm. Mice age: E13.5. Adapted from Li *et al* (Li *et al.*, 1996b).

1.19.3 Part I

In order to determine whether CaSR ablation in VSMCs has an effect on reproduction, survivability and normal development of organs and tissues, *in vivo* characterisation of this novel mouse model is required. In the first part of this research, the SM22α x fl CaSR transgenic mouse model will be used for this *in vivo* characterisation.

In vivo analysis aims to:

(i)   Carry out initial characterisation of the SM22α x fl CaSR mouse model by observing general size, weight, appearance and viability.

(ii)   Determine whether Mendelian transmission is maintained during breeding of VSMC-CaSR WT and VSMC-CaSR KO mice by genotyping the offspring.

(iii)   Determine whether genotype affects genders of offspring and litter size.

(iv)   Determine whether CaSR protein is knocked out in VSMC-CaSR KO mice compared to VSMC-CaSR WT mice.

(v)   Carry out biochemical analysis of the serum of mice over time.

(vi)   Carry out measurements of bone mineral density in VSMC-CaSR WT and VSMC-CaSR KO mice.

1.19.4 Part II

It has previously been demonstrated that activation of CaSR by allosteric agonists in rat subcutaneous vessels causes hyperpolarisation (Weston *et al.*, 2008). For the second part of the project, my aim is to determine the physiological role of CaSR in the vasculature, and its potential role in maintaining myogenic tone. The hypothesis is that (i) CaSR in VSMCs may play an important role in vasoconstriction and relaxation, and that (ii) CaSR ablation from VSMCs may have repercussions on the effects of CaSR agonists to induce either contraction or relaxation. These hypotheses will be tested using the following techniques:

Ex vivo **analysis aims to:**

(i)   Determine the effects of CaSR ablation from VSMCs on aortae and mesenteric arteries isolated from VSMC-CaSR WT and VSMC-CaSR KO mice.

(ii)   Determine whether CaSR ablation affects the contractile tone in acutely isolated aortae and mesenteric arteries.

(iii) To determine the effects of CaSR ablation from VSMCs on the responses of orthosteric and allosteric modulators of CaSR on vascular tone of aortae and mesenteric arteries acutely isolated from VSMC-CaSR WT and VSMC-CaSR KO animals.

1.19.6 Part III

Using the SM22α x fl CaSR mouse as an experimental model, WT-CaSR and KO-CaSR VSMCs will be isolated and cultured *in vitro*. Proliferation, apoptosis, mineralisation, gene expression and transdifferentiation will be investigated in these cells, which will be cultured in a variety of conditions *in vitro*. Specifically, primary WT-CaSR and KO-CaSR VSMCs will be cultured in the presence of physiological and pathophysiological concentrations of Ca^{2+}_o with the addition of a variety of Pi concentrations, also, designed to recapitulate Ca^{2+}_o and Pi dysregulation *in vivo*. These conditions are similar to *in vitro* models described by other groups which recapitulate vascular calcification *in vitro*.

In vitro analysis aims to:

(i)   Establish an *in vitro* culture system of mouse VSMCs.

(ii)   Isolate VSMCs from VSMC-CaSR WT and VSMC-CaSR KO mice.

(iii)   Confirm that CaSR is deleted in cultured VSMCs from VSMC-CaSR KO mice by PCR and immunofluorescence.

(iv)   Determine the effects of targeted CaSR ablation from VSMC on cell proliferation by cell counting and cell apoptosis using immunofluorescence techniques.

(v)   Determine the effects of CaSR ablation on the role of Ca^{2+}_o and calcimimetics on cell proliferation and apoptosis.

(vi)   Determine the effects of CaSR ablation on mineralisation and Ca^{2+} incorporation using different concentrations of Ca^{2+}_o, Pi and the calcimimetic R-568 in VSMC-CaSR WT and VSMC-CaSR KO VSMCs.

(vii)   Determine whether mineralisation is associated with transdifferentiation of VSMCs by up-regulation of osteoblast-specific genes by VSMC-CaSR WT and VSMC-CaSR KO VSMCs in mineralised cultures.

CHAPTER 2:

METHODS

2.1 Breeding of SM22α x fl CaSR transgenic mice.

SM22α x fl CaSR mice, provided by Dr. Chang and colleagues, were of a mixed inbred background. Floxed and Cre mice were bred together to maintain genetic consistency of the C57BL/6J and 129S1/SvImJ background across all mice of the colony. WT SM22α x fl CaSR mice carry two WT CaSR alleles. Floxed mice contain two floxed CaSR alleles flanking Exon 7 (ΔExon 7). The cre transgene is required to knock out Exon 7 of genomic CaSR DNA. To obtain VSMC-CaSR WT mice, VSMC-CaSR floxed Cre$^{-/-}$ WT mice are bred with one another. In this way, cre is not available for inheritance in offspring, but control mice still contain the floxed alleles. Table 24 shows expected Mendelian ratios of offspring from WTxWT, WTxKO and KOxKO matings. Since heterozygote floxed/WT CaSR mice were not investigated in this study, this breeding strategy was adopted to prevent production of heterozygote mice. Hereafter, VSMC-CaSR WT mice and VSMC-CaSR KO mice will be referred to as WT and KO mice respectively.

A

	Flox/Cre-	Flox/Cre-	Flox/Cre-	Flox/Cre-
Flox/Cre-	Flox/Flox Cre-/-	Flox/Flox Cre-/-	Flox/Flox Cre-/-	Flox/Flox Cre-/-
Flox/Cre-	Flox/Flox Cre-/-	Flox/Flox Cre-/-	Flox/Flox Cre-/-	Flox/Flox Cre-/-
Flox/Cre-	Flox/Flox Cre/-	Flox/Flox Cre-/-	Flox/Flox Cre-/-	Flox/Flox Cre-/-
Flox/Cre-	Flox/Flox Cre-/-	Flox/Flox Cre-/-	Flox/Flox Cre-/-	Flox/Flox Cre-/-

B

	Flox/Cre+	Flox/Cre+	Flox/Cre-	Flox/Cre-
Flox/Cre-	Flox/Flox Cre+/-	Flox/Flox Cre+/-	Flox/Flox Cre-/-	Flox/Flox Cre-/-
Flox/Cre-	Flox/Flox Cre+/-	Flox/Flox Cre+/-	Flox/Flox Cre-/-	Flox/Flox Cre-/-
Flox/Cre-	Flox/Flox Cre+/-	Flox/Flox Cre+/-	Flox/Flox Cre-/-	Flox/Flox Cre-/-
Flox/Cre-	Flox/Flox Cre+/-	Flox/Flox Cre+/-	Flox/Flox Cre-/-	Flox/Flox Cre-/-

C

	Flox/Cre+	Flox/Cre+	Flox/Cre-	Flox/Cre-
Flox/Cre+	Flox/Flox Cre+/+	Flox/Flox Cre+/+	Flox/Flox Cre+/-	Flox/Flox Cre+/-
Flox/Cre+	Flox/Flox Cre+/+	Flox/Flox Cre+/+	Flox/Flox Cre+/-	Flox/Flox Cre+/-
Flox/Cre-	Flox/Flox Cre+/-	Flox/Flox Cre+/-	Flox/Flox Cre-/-	Flox/Flox Cre-/-
Flox/Cre-	Flox/Flox Cre+/-	Flox/Flox Cre+/-	Flox/Flox Cre-/-	Flox/Flox Cre-/-

Figure 24. Mendelian inheritance of floxed and cre alleles in the SM22α x fl CaSR mouse model. Punnet square diagrams demonstrate the ratios VSMC-CaSR WT (green) to VSMC-CaSR KO (red) offspring from 3 matings carried out during this project. (A) WTxWT breeding. (B) WTxKO breeding. (C) KOxKO breeding. Red: VSMC-CaSR KO mice. Green: VSMC-CaSR WT mice.

2.2 Determination of mouse whole body weight.

Mice were weighted from birth onwards at monthly intervals in a large plastic tub on a scale. Mice were left for approximately 5 minutes (min) to rest before body weight measurements were tabulated. After this time, five consecutive weight measurements were taken over the course of 2 minutes when mice were still. Body weight was determined by taking an average of these weights.

2.3 Genomic DNA (gDNA) isolation from SM22α x fl CaSR mice.

As part of the routine mouse identification, SM22α x fl CaSR mice were humanely scruffed and ear biopsies were obtained by an ear clip. Ear biopsies placed in 0.5 mL eppendorf tubes with 200 µL Ear Digest (Viagen) and 8 µL proteinase K (10mg/mL) (Bioline). Samples were incubated at 55ºC overnight. Reactions were terminated the next day by incubating at 85ºC for 45 min. The resulting solution containing gDNA was used as a template for genotyping PCRs.

2.4 Genotyping SM22α x fl CaSR transgenic mice.

PCRs were optimised for $MgCl_2$ concentration, annealing temperature and number of PCR cycles. All PCR reagents for mouse genotyping were provided in the Bioline BIOtaq DNA Polymerase kit. Each PCR reaction comprised of; 1.5 µL ear biopsy gDNA (obtained previously), 0.2 mM dNTPs, 1U BIOtaq DNA Polymerase, 4mM $MgCl_2$, 2.5 µL 10X PCR Buffer ($MgCl_2$-free), 100nM Forward Primer, 100nM Reverse Primer, 17.0 µL RNase/DNase- free dH_2O (total 25µL reactions). Genotyping primers for floxed CaSR allele detection were: *Forward fl CaSR* 5'-GTGACGGAAAACATACTGC-3', and *Reverse fl CaSR* 5'-CGAGTACAGGCTTTGATGC-3'. Genotyping primers for cre transgene detection were: *Forward Cre* 5'-CAGACACCGAAGCTACTCTCCTTCC-3', and *Reverse Cre* 5'-CGCATAACCAGTGAAACAGCATTGC-3'. The PCR conditions were: an initial denaturation at 95ºC for 5 min, thermal cycling parameters were:

denature; 95ºC x 5 min, anneal 50ºC/Cre and 46ºC/fl CaSR x 30 seconds, extend 72ºC x 2 min for 40 cycles. Final extension was carried out at 72ºC for 10 min then reactions were kept at 4ºC. Expected products were: Cre transgene amplicon; 500bp, WT CaSR amplicon; 133bp, fl CaSR amplicon; 167bp.

2.5 Detection of gDNA/cDNA amplicons by gel electrophoresis.

To each 25 µL PCR reaction, 6 µL of 5X gel loading dye was added. A gel electrophoresis tank was filled with 1X Tris Borate EDTA (TBE). Agarose was added to 100 mL 1X TBE in a conical flask to make a 100mL agarose gel. Throughout the project, different percentage gels were used for the optimal spread of different amplicons. Amplicons <200bp were run on 2.5% agarose gels, whereas products >500bp were run on 1% agarose gels. The agarose mixture was microwaved until it had dissolved. After cooling to ~55ºC, 5µL SafeView (NGS Biologicals) was added to the melted agarose and mixed until homogeneous. The mixture was then poured into a gel cast and allowed to polymerize for 30 min. The polymerized gel was immersed in 1X TBE within the electrophoresis tank. Previously prepared samples were loaded in each well, with an appropriate sized DNA ladder as a standard (DNA HyperLadders I, II, III, IV and V, Bioline). Gels were run at 10V/cm until the gel loading dye was visible approximately 80% towards the positive electrode. Gels were visualised and photographed using an ultraviolet transilluminator (Chemi-doc, BIORAD).

2.6 Determination of mouse organ weights.

Mice were culled at the age of 6 or 18 months. Organs, including the heart, liver, stomach, kidneys and spleen, were briefly washed in dH_2O then dried before recording the wet weight of the organ. Since male and female organ weights were not statistically different (not shown), they were grouped together for analysis.

2.7 Serum biochemical analysis of SM22α x fl CaSR mice.

Mice were culled at the age of 3 months and 18 months. Hearts were then exsanguinated for blood collection (performed by Martin Schepelmann at Cardiff University). Blood samples were allowed to coagulate for 30 min at room temperature before centrifugation for 5 min at 5,000g. Serum was extracted from the supernatant and snap frozen in liquid nitrogen for future use. Samples were sent to collaborators at AstraZeneca for biochemical analysis using photometric or ELISA-based systems. Analyses carried out were for Na^+, Cl^-, Mg^{2+}, K^+, Ca^{2+} and FGF23.

2.8 Calculation of bone density by microcomputerised tomography (μCT).

A cohort of mice at the age of 3 months were kept at UCSF by Dr Wenhan Chang. Male mice were culled at this age and bones were collected. The distal femur (a site rich in trabecular bone) and the tibia-fibula junction (TFJ) (rich in cortical bones) were analysed. Prior to scanning, the bones were fixed in 10% phosphate-buffered formalin for 24 hours then transferred to 70% ethanol. The bones were then scanned in tubes containing 70% ethanol using a Scanco vivaCT scanner (Scanco Medical, Basserdorf, Switzerland). For trabecular scans, 100 serial cross-sectional scans were performed from the end of the growth plate. 100 serial cross-sectional scans were also performed in cortical bone. For μCT analysis, thresholds in the manufacturers' software were applied to remove mineralised bone, focusing only on soft tissue. Experiments were conducted by Dr Wenhan Chang group, as described previously (Chang *et al.*, 2008).

2.9 Wire myography on acutely isolated mouse aortae and mesenteric arteries.

Aortae and mesenteric arteries of third order were isolated from VSMC-CaSR WT and VSMC-CaSR KO mice which were humanely killed by the Schedule one method of CO_2 inhalation in accordance with Home Office regulations. Aortae were placed in ice cold Krebs buffer (NaCl; 118mM, KCl; 3.4mM, $CaCl_2$; 1.0mM, KH_2PO_4; 1.2mM, $MgSO_4$; 1.2mM, $NaHCO_3$; 25mM, Glucose; 11mM) and continuously oxygenated by $O_2:CO_2$ 95% $O_2:5\%$ CO_2) gas bubbling on the side of the myography bath. Adventitia and fat were carefully removed and aortae were cut into 2mm rings. Rings were loaded onto a 4-channel wire myograph (DMT) with 40μm stainless steel wire. In the myograph well, aortic rings were incubated with Krebs buffer at 37°C, once again with constant $O_2:CO_2$ gas bubbling for the whole experiment. Wires were adjusted to stretch rings 100μm every ~20 seconds until a tone of 4 milliNewtons (mN) was achieved. Rings were then exposed to drugs and chemicals such as KCl, phenylephrine (PhE), acetylcholine (Ach), Ca^{2+}_o, R-568, spermine and L-NAME. Drugs were prepared in Krebs buffer and either applied in a concentration-dependent manner, or at specific concentrations. Data were recorded as changes in tone in units of mN.

2.10 Immunofluorescence of primary mouse VSMCs and fixed mouse aortae.

Primary VSMCs cultured in standard conditions (DMEM containing 1.2mM Ca^{2+}_o and 10% FBS) were trypsinised through 0.05% Trypsin EDTA / PBS (pH 7.4) treatment and plated onto 13mm glass coverslips in 4-well plates (Nunc) at a maximum of 15,000 cells per well. Cells were allowed to adhere and were routinely maintained in standard 1.2mM Ca^{2+}_o DMEM with 10% FBS. After a few days, when the cells had reached 75-100% confluency, they were fixed in 4% paraformaldehyde in 1X PBS (pH 7.4) for 10 min at 4°C. Cells were permeabilised using 0.5% Triton-X in 1 X PBS. Cells were then washed in 1X PBS three times for 5 min for each wash. A blocking buffer (1% BSA/1 X PBS/0.5% Triton-X) was subsequently applied for 60 min. Primary and secondary antibody incubations were carried out for 60 min with three 1 X PBS washes of 5 min each in between. Antibodies were diluted in the same blocking buffer and were used in 1:100-1:250 dilutions (according to the manufacturer's instructions). Antibodies used

were: rabbit anti-CaSR (Anaspec, Cat #53286), goat anti-SM22α (Abcam, Cat #ab14106), and either Alexa488 or Alexa594 (Molecular Probes) secondary antibodies which were raised in the appropriate species according to the primary antibody selected. For tissue fixation, organs were removed after the animal was culled. Excised tissues were washed in 1 x PBS, then fixed for 60 min in 4% PFA. Organs were embedded in OCT mounting medium, then frozen at -80ºC. Once frozen, a Leica CM1950 cryostat was used to generate 6µm cross-sectional slices. Sections were allowed to adhere to microscope slides and hydrophobic pens were used to seal off the tissue area. Immuno-staining was then performed following the same protocol as the VSMC staining described above.

2.11 Isolation of mouse primary vascular smooth muscle cells (VSMCs).

3 month old male mice were terminated by Schedule one in accordance with Home Office regulations. Each mouse carcass was splayed out and pinned down on a wax disc using 25-gauge needles. Aortae were dissected as shown in Figure 25. After removal of the fibrotic adventita, 2mm rings were prepared and allowed to adhere to the base of a T25 flask (Corning/BD Falcon) in the absence of medium for 10 min at 37ºC. While still moist, explants were carefully covered in Ca^{2+}_o-free DMEM (Invitrogen Cat#21068-028) containing 1.2mM Ca^{2+}_o (supplemented by $CaCl_2$), 10% Fetal bovine serum, (FBS) (Thermo-Fisher), 50U/mL Penicillin/Streptomycin, 2.5µg/mL Fungizone®, 2mM L-glutamine and 1mM sodium pyruvate. FBS was always heat-inactivated at 56ºC for 30 min before adding to medium. All cell culture reagents, excluding FBS, were provided by Invitrogen. Explants kept at 37ºC in a humidified incubator with 5% CO_2/95% O_2.

Explants were then left in the incubator for up to 2 weeks in order for the primary VSMCs to migrate out onto the plastic base of the flask (Figure 26). To split cells, cells were washed in 1X PBS and explants were removed gently using a sterile 25-guage needle. Cells were incubated with 0.05% Trypsin EDTA (Invitrogen) in 1X PBS for 3-5 min. After incubation with trypsin, equal volumes of fresh medium were added. This medium was the same as previously described however, after the first initial passage Fungizone®

was always removed thereafter. This medium is hereafter referred to as standard (i.e., 1.2mM Ca^{2+}_o) DMEM with 10% FBS. The trypsin-medium suspension was then centrifuged at 1,500g for 4 min to collect cells. The supernatant was then removed and cells were resuspended in the same medium and plated onto a single well of a 6-well plate. Cells had medium routinely changed every 3-4 days and were split to larger flasks when appropriate cell density was reached.
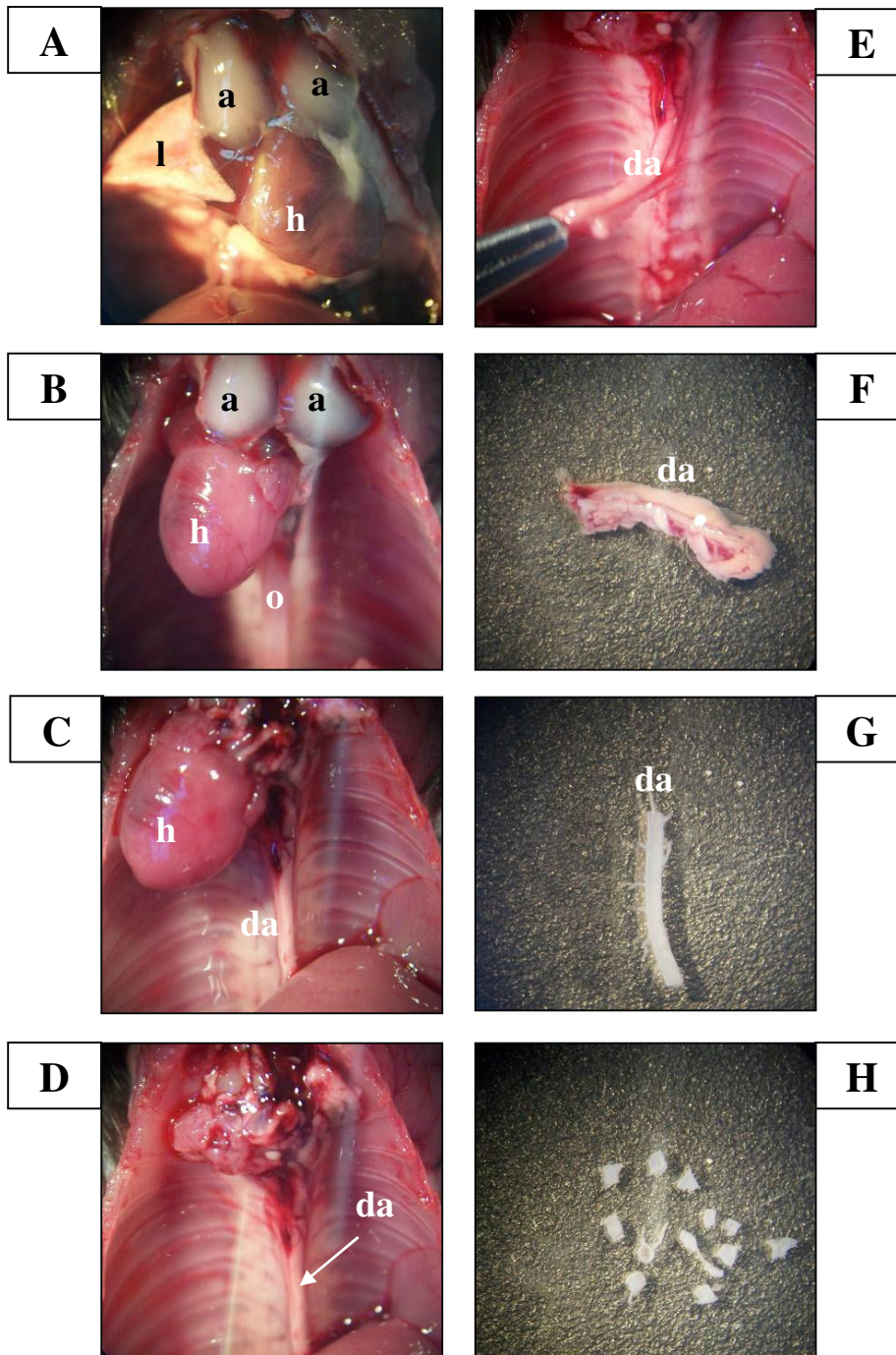
Figure 25. Explant isolation of primary mouse VSMCs. Mice were killed by a Schedule One procedure (i.e., cervical dislocation) in accordance with Home Office regulations. Organs were removed as shown (**A-D**) to allow access to the thoracic descending aorta. (**A**) The thoracic abdomen was cut open to reveal the heart (h), auricles (a) and lungs (l). (**B**) Lungs were removed and discarded, leaving the oesophagus (o) in view. (**C**) Auricles and oesophagus were removed to reveal the thoracic descending aorta (da). (**D**) The heart was removed at the base of all outward-extending vessels (vena cava, pulmonary vein, pulmonary artery and ascending aorta). (**E**) The descending aorta was dissected by cutting away from the spine in posterior-to-anterior direction. (**F**) Aorta in 1X PBS in a 100mm Petri dish. (**G**) Care was taken to remove the adventitia and fibrotic tissue from the vessel. The vessel was also squeezed from one end to another to disrupt the endothelial cell layer. (**H**) The aorta was cut into sagittal sections of approximately 2mm in length.

Mouse primary VSMCs
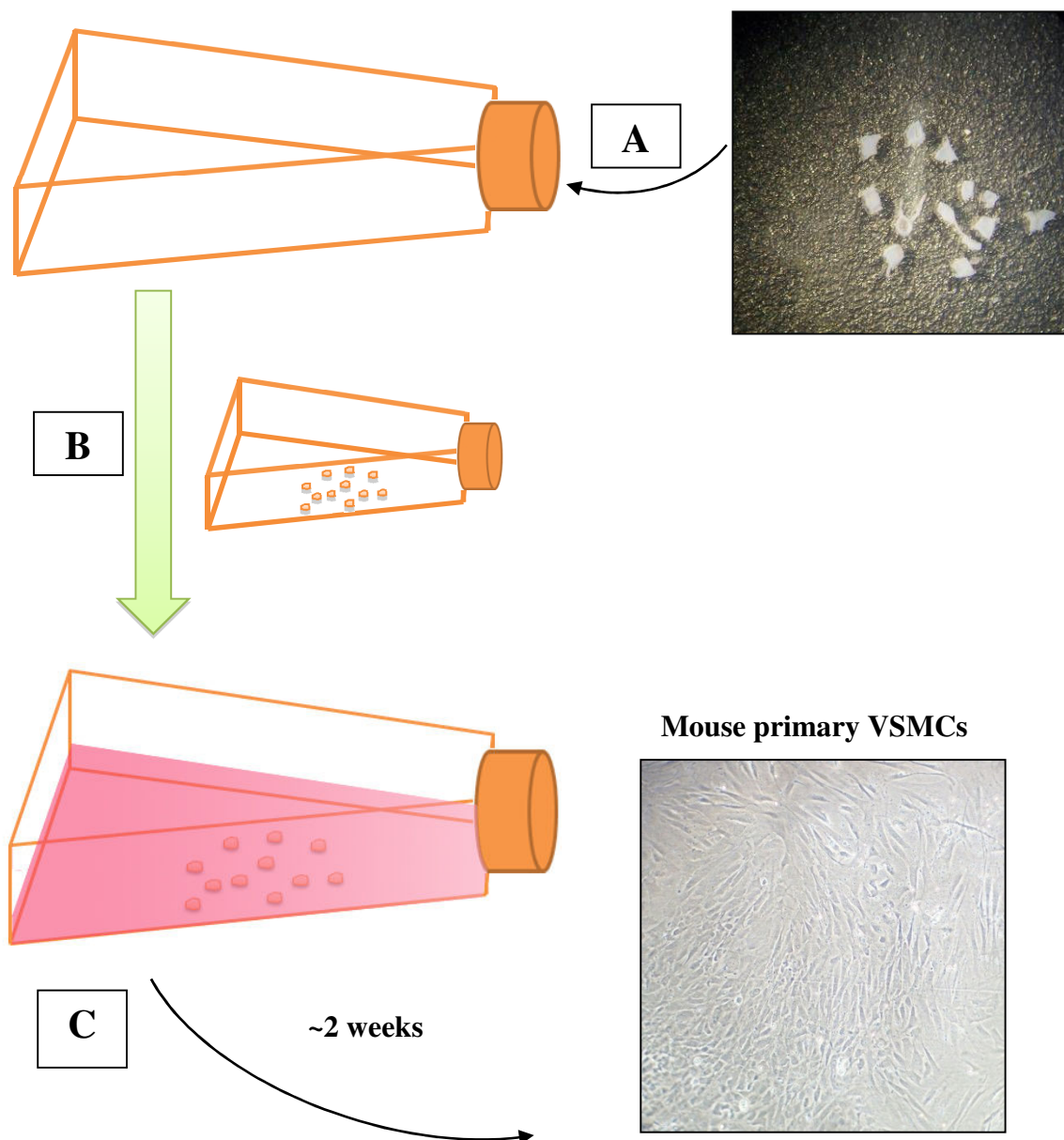
Figure 26. Explant culture of primary mouse VSMCs *in vitro*. Explants similar to those illustrated in Figure 25 are placed in the standard (1.2mm Ca^{2+}_o) DMEM with 10% FBS with 2.5U/mL Fungizone®. (A) Explants were lifted using a 25-guage needle and placed onto the base of a Corning/BD Falcon vented T25 cell- flask approximately 5mm apart. (B) Moist explants are sealed in the flask placed in an incubator with controlled humidity conditions and temperature of 37ºC (5% CO_2/95% O_2) for 10-20 min to adhere to the plastic whilst ensuring that they did not dry out completely. After adherence, ~5mL of fresh, pre-warmed DMEM was added slowly and gently to explants until they were immersed. (C) Explants were cultured for approximately 2 weeks to allow VSMCs to migrate out from the explant with careful medium changing every 4-5 days. While at "passage 0", cells were routinely maintained at in this medium containing Fungizone®. However, from passage 1 onwards, Fungizone® was removed from the culture medium

2.12 Quantification of total SM22a in WT and KO VSMCs by western blot.

Confluent WT and KO VSMCs cultured in standard DMEM containing 10% FBS and 1.2mM Ca^{2+}_o were lysed in 1X RIPA lysis buffer at 4ºC for 10 minutes. Cell lysates were spun down for 5 minutes at 12,000g, and supernatants were removed. Protein was quantified using a BCA assay kit according to manufacturers' instructions (Pierce). 5µg of protein was loaded onto a 10% SDS-PAGE gel (10% acrylamine, 0.5% bis-acrylamide, 0.1% SDS, 0.3% ammonium persulfate in Tris-HCl pH8.8). 25µL of TEMED was added to the mix to polymerise. Proteins were run by western blot at 200V for up to 45 minutes. Proteins were then transferred onto a PVDF membrane at 40V for 90 minutes in transfer buffer (3g tris, 15g glycine and 150mL methanol in 850mL dH_2O). PVDF membranes were blocked with 3% BSA in TBS-Tween (8.8g NaCl, 0.2g KCl, 2g tris and 500µL tween-20 in 1L dH_2O) for one hour before performing antibody immunostaining. SM22α protein was detected using a goat anti-SM22α antibody (abcam, 1:1000) in the blocking buffer described for 1 hour incubation. Membranes were washed in TBS-Tween three times for 5 min in between antibody incubation. A β-actin antibody was also run on duplicate samples as a positive control. A secondary anti-goat HRP-conjugated antibody was used (1:10,000) for 10 hour before washing membranes again in TBS-Tween. Signal was then produced by incubating membranes in an ECL western blotting substrate. Chemiluminescence was detected using BIORAD chemidoc system. Images were scanned and analysed in ImageJ software where densitometry was carried out on bands.

2.13 gDNA isolation of primary mouse vascular smooth muscle cells (VSMCs) for cellular genotyping.

VSMC-CaSR WT and VSMC-CaSR KO primary mouse VSMCs were cultured until they reached confluency in 24-well plates. Upon confluence, a mix of cell lysis buffer and proteinase K was prepared. For each well, 75µL "DirectPCR Lysis Reagent [Cell]" (Viagen) was added with 0.5mg/mL Proteinase K (Bioline). The cell lysis suspension was incubated at 55ºC overnight then the reaction was terminated by incubating the mixture at 85ºC for 45 min. The resulting gDNA was used as a template for PCR for the

detection of specific CaSR products. *Forward primer P4 5'-CCTCGAACATGAACAACTTAATTCGG-3'* and *Reverse primer P3L 5'-CGAGTACAGGCTTTGATGC-3'*. PCR followed the same PCR cycle method mentioned earlier, however, 4mM $MgCl_2$ was used with an annealing temperature of 55°C. β-actin primers were also run on the same samples in a PCR reaction as positive controls. The same conditions were used, except an annealing temperature of 54°C was used. *Forward primer β-actin 5'- TCCTAGCACCATGAAGATC -'3*, and *reverse primer β –actin 5'- AAACGCAGCTCAGTAACAG-3'*.

2.14 Cell viability detection of primary mouse VSMCs.

VSMCs were plated at 2,000 cells per well in a 96-well plate and allowed to adhere for 24 hours. After 24 hours, cells were quiesced by maintaining them in 1.2mM Ca^{2+}_o DMEM with 1% FBS. 48 hours after original plating, medium was switched to medium medium containing different concentrations of the CaSR agonists; (A) Ca^{2+}_o or (B) Ca^{2+}_o with R-568, both in standard DMEM with 10% FBS. In some cases, phosphate was also added at the final concentration of 1.4, 2.0 or 3.0mM to assess cell viability in mineralising conditions. When medium was added, this was considered day 0. Cells were incubated for 7 days in these medium at which point 0.5mg/mL Thiazolyl Blue Tetrazolium Bromide (MTT) was added for a further 2 hours. After 2 hours, media were removed and cells were washed gently in PBS. MTT crystals were then solubilised in 50µL DMSO per well and plates were quantified for absorbance at 570nm on a 96-well plate reader (Optima).

2.15 Cell-counting of primary mouse VSMCs.

Primary mouse VSMCs were plated into 24-well plates at 15,000 cells per well. Cells were allowed to adhere for 24 hours in standard DMEM containing 1.2mM Ca^{2+}_o and 10% FBS, then cells were qiesced by switching them into a medium containing medium 1% FBS. After a further 24 hours, medium was switched to media containing 10% FBS in the presence of different concentrations of Ca^{2+}_o (1.2mM, 1.8mM and 2.5mM Ca^{2+}_o).

Ca^{2+}_o manipulations in the culture medium were achieved by the addition of suitable volumes of 1M $CaCl_2$ stock solution (or equivalent volumes of water as the vehicle control).

2.16 Apoptosis detection in primary mouse VSMCs by DNA fragmentation (TUNEL).

WT and KO primary mouse VSMCs at passage 6 were trypsinised as described and plated on glass coverslips in 24-wel plates. 25,000 cells were plated per condition which was near confluent. This way proliferation would be kept to a minimum and would prevent interference of proliferation with apoptotic readout. Cells were allowed to adhere for 24h before placing in standard DMEM with 1.2mM Ca^{2+}_o, however containing just 1% FBS. After a further 24h, medium was changed to contain either 1.2, 1.8 or 2.5mM Ca^{2+}_o in the presence of 1mM Pi or 3mM Pi. VSMCs were also either treated with 10nM R-568 or a 0.001% DMSO vehicle. VSMCs were left in medium for 48h before fixation in 4% PFA. After fixation, cells were washed three times in 1X PBS. To permeabilise VSMCs, 0.2% Triton-X in PBS-Tween (0.05%) was added for 30 minutes. Cells were washed three times in 1x PBS-Tween. Cells were then acclimatised to the TUNEL reaction buffer for 10 minutes. Buffer contained 25mM tris-HCl, 200mM sodium cacodylate, 0.25mg/dL BSA and 1mM cobalt chloride). After this time, 640U/reaction terminal transferase (TdT, Roche Diagnostics) and 180pM Biotin-16-dUTP (Roche Diagnostics). Negative reactions contained the same reaction mix, but no TdT enzyme. After 2 hours incubation of cells with the reaction mix at 37ºC, reactions were terminated using a stop solution containing 300mM NaCl and 30mM sodium citrate. Cells were then washed three times in PBS-Tween for 5 min. Labelling was then performed by adding 1:500 FITC-Avidin (abcam) in PBS for 30 minutes. Cells were washed again with PBS-Tween before staining nuclei with 1mg/mL Hoescht (diluted 1:10,000) in PBS-Tween and fixed in prolong gold mounting medium (Invitrogen). Slides were sent to Vienna for Martin Schepelmann to quantify dead nuclei by a TissueFAX automated fluorescence cell counting system.

2.17 Mineralisation of primary mouse VSMCs.

VSMCs were plated at 40,000 cells per well in a 24-well plate in standard 1.2mM Ca^{2+}_o DMEM with 10% FBS, as previously described, and were allowed to reach confluency. When confluent, medium was removed and cells were washed with 1 X PBS. Mineralisation medium was then added, which contained 1.4mM, 2.0mM or 3.0mM inorganic phosphate (Stock 1M NaPi: 30.96mL 1M Na_2HPO_4 and 9.04mL 1M NaH_2PO_4.). Multiple conditions were set up where in addition to phosphate, medium also contained 1.2mM or 1.8mM in the presence or absence of the calcimimetic R-568 (10nM), or 2.5mM Ca^{2+}_o. Ca^{2+}_o was manipulated by the addition of suitable volumes of a 1M $CaCl_2$ stock solution. Cells were cultured for 10 days with medium changing taking place every 3-4 days. After 10 days incubation in the different experimental conditions, cells either underwent quantification of mineralisation (by alizarin red staining), immunostaining, or processed for RNA or protein isolation, as described previously.

2.18 Quantification of mineralisation of primary mouse vascular smooth muscle cells (VSMCs) using the O-Cresolphthalein complexone Ca^{2+} method.

VSMCs were cultured as described in mineralising conditions for 10 days in 24-well plates. After 10 days, cells were washed twice in 1 X PBS then decalcified at 37ºC for 3-5 hours in 0.6N HCl (500µL/well). After wells were decalcified, HCl was removed and stored at -20ºC. The remaining cell monolayer in each well was solubilised in 1% SDS in 0.1M NaOH. Solubilised samples were quantified using a BCA assay quantification kit and protein content was expressed in µg/mL. For calcium quantification, HCl samples were thawed and 5µL of each sample was mixed with 100µL AMP Buffer and 100µL Colour reagent in a 96-well plate. Standards for Ca^{2+}_o quantification were prepared using 7.5, 10.0, 12.5, 25.0 and 50.0mg/dL of $CaCO_3$ and mixed in the same way as samples. Once buffer and colour reagent were added, samples were incubated at room temperature for 15 minutes. After this time, sample absorbance on a 96-well plate reader (Optima) at 570nm wavelength was carried out.

For the purpose of analysing gene expression of VSMC and osteoblast markers in these mineralisation conditions, cDNA was prepared from osteoblasts and VSMCs and primer sets for smooth muscle cells, osteoblasts and chondrocytes were optimised for qPCR quantification of transdifferentiation. Due to time constraints, the only gene that was analysed for gene expression experiments in mineralising conditions was the master osteoblast transcription factor Runx2 (Chapter 6).

2.19 RNA isolation from primary VSMCs.

Cells were cultured for the purpose of experiments, I.e. for general RNA detection in confluent VSMC cultures, or for the detection of transdifferentiation at the transcriptional level in mineralised primary mouse VSMC cultures. When RNA was required at the end-point of these experiments, cells were removed from incubators and medium was removed. Cells were washed twice briefly in 1X PBS and TRIzol® reagent was added. To each sample 1mL TRIzol® Reagent, 0.2mL chloroform was added and the solution was shaken vigorously for 15 seconds, then left at room temperature for 5 min. RNA was then centrifuged at 12,000g for 15 min at 4ºC. Following centrifugation, aqueous and phenol phases were separated and RNA was carefully removed from the upper clear supernatant phase. To this, 0.5mL propan-2-ol was added and RNA was left to precipitate for 1 hour at -80ºC. Samples were then centrifuged at 12,000g for 30 min at 4ºC. The supernatant was removed and RNA pellets were allowed to dry at 55ºC. RNA was then resuspended in 20µL RNase/DNase- free dH_2O.

2.20 DNase digestion of RNA.

A recombinant DNase kit was used (Ambion) for DNase digestion. RNA previously prepared was quantified using a Nanodrop. DNase digestion was carried out by adding up to 10µg RNA to 5µL DNase I Buffer and 1µl DNase enzyme in a final volume of 50µL with RNase/DNase- free dH_2O. Reactions were incubated for 30 min at 37ºC. After this time, 50µL of Phenol:Chloroform:Isoamyl alcohol was then added to terminate the reaction. RNA was pelleted at 12,000g for 5 min at 4ºC. The upper aqueous supernatant

was transferred to a fresh eppendorf tube. 0.1 volumes of 3M sodium acetate (pH 5.2) were added with 3.0 volumes of 100 % ice cold EtOH. This was mixed and precipitated overnight at -20 ℃. The pellet was spun down the next day at 12,000g for 30 min at 4℃. The supernatant was removed and the pellet was allowed to dry at 55℃. This pellet was resuspended in 20 µL RNase/DNase- free H_2O.

2.21 cDNA synthesis of isolated RNA.

DNase-digested RNA was quantified using a Nanodrop. RNA was converted to cDNA using a "cDNA Synthesis Kit" (Bioline). Up to 1µg of RNA was used for each reaction, however, when samples were grouped, (e.g. RNA samples from mineralised VSMCs in different conditions) the same maximal amount of RNA was used for each reaction. RNA was obtained by the TRIzol® method described and was DNase-digested to remove genomic DNA contaminants. Using the kit, up to 1µg RNA was mixed with 50ng random hexamers and 10mM dNTPs. Reactions were made up to 10µL in RNase/DNase- free H_2O. RNA was incubated at 72℃ for 10 minutes. After incubation, the 10µL primed-RNA samples were placed at 4℃ for 2 minutes. Then, to each reaction 10U Ribosafe RNase inhibitor, 4µL of 5X RT buffer and 50U reverse transcriptase enzyme was added. Negative control samples were also prepared where RNA was added but no reverse transcriptase enzyme was added to the reaction mix. Reactions were then placed at 42℃ for 30 min. Reactions were terminated at 85℃ for 5 min before storing at 4℃. cDNA was stored at -20 ℃ for long term storage or used immediately for PCR.

2.22 Gel extraction of PCR amplicons for plasmid preparation.

After PCR amplification and amplicon separation using gel electrophoresis, bands were visualised on an ultraviolet transilluminator and excised using a sharp scalpel. Gel fragments (<1g) were placed in 1.5mL Eppendorf tubes and amplicons were extracted using the QIAquick Gel Extraction Kit (Qiagen). Gel pieces were incubated with 3 volumes per weight Buffer QG. The mixture was incubated at 50℃ for 10 min or until the gel had solubilised. To this mix, 1 volume of propan-2-ol was added and the solution

was loaded into a 2mL spin column. The reaction was spun at 12,000g for 1 min and the flow-through was discarded. The column was then washed with 0.75mL ethanol-containing Buffer PE and also spun for 1 min. After discarding the flow-through the column was spun again to remove residual ethanol. 50µL of elution buffer was then applied to the column containing 10mM Tris-HCl pH8.5 and amplicons were collected by centrifuging for 1 min at 12,000g. Amplicons were stored at -20ºC long-term or used immediately for ligation in a pGEM-T plasmid vector.

2.23 Preparation of qPCR recombinant plasmid standards using pGEM-T vector ligation.

Previously purified DNA amplicons were used for vector ligation in a pGEM-T transformation kit (Promega). Ligation reactions were prepared by taking 1µL of PCR product, with 5µL 2 X Rapid Ligation Buffer, 1U T4 DNA Ligase, 1µL pGEM®-T vector, and 3U T4 DNA Ligase made up to 10µL in dH$_2$O. Reactions were left for 1 hour at room temperature. After this time, JM109 *E. coli* competent cells were thawed on ice, then 50µL of cells were added to the ligation mix. These cells were heat-shocked at 42ºC for 45 seconds in a water bath, then returned to ice where the mix was made up to 1mL using 950µL SOC medium (Promega). Reactions were then placed in a shaking incubator at 37ºC for 90 min. The resulting transformed bacteria were then plated onto Luria-Bertani (LB) plates with 100µg/mL ampicillin. LB plates also had 50µL 100µM (isopropyl thiogalactoside) IPTG and 20µL 50mg/mL X-gal dried into the surface of them before bacteria were spread. This was to ensure that induction of the *lacz* operon could occur and that colour selection could also occur. Plates were incubated at 37ºC overnight. Successfully cloned white colonies were selected and inoculated into LB broth with 100µg/mL ampicillin overnight. The resulting *E. coli* culture was used for plasmid mini-prep purification.

2.24 Plasmid mini-prep purification.

Transformed plasmids from overnight cultures were pelleted at 4,000g for 5 min. The LB supernatant was removed and discarded in Virkon disinfectant solution. Using a Plasmid Mini Kit (Qiagen), the pellet of transformed cells was lysed and genetically modified plasmids were purified using the manufacturers' instructions exactly. Plasmids were eluted in elution buffer containing 10mM Tris-HCl pH8.5 and were quantified using a Nanodrop. Plasmids were sent to Cardiff DNA Sequencing Core for DNA sequencing and only plasmids with 100% sequence homology to known cDNA sequences were used for further quantitative analysis.

2.25 Confirmation of vector ligation and transfection into chemically competent *E. coli* cells using colony PCR for amplification.

Previously optimised conditions for each primer set were used in a standard PCR reaction to confirm the presence of the specific amplicon in each plasmid. A 20µL pipette tip was dipped into the overnight transformed *E.* coli culture and placed into 10µ dH_2O. The sample was boiled at 95ºC for 10 minutes. This was then used as a DNA template for amplification using the primer conditions in Table 5.

2.26 Quantification of transcriptional regulation by qPCR.

Control plasmids previously prepared had been quantified and the weights of recombinant plasmids were calculated using the following formula:

(Number of base pairs of plasmid vector + Number of base pairs of insert)

$$x\ (1.096\ x\ 10^{-21})$$

From this equation, the number of grams of plasmid in each mini-prep stock was calculated. Serial dilutions (1:10) were prepared from a stock containing 1×10^9 plasmid copies per µL (from 1×10^8 - 1×10^1 copies per µL). The diluted plasmids were used in a qPCR reaction to generate a standard curve: 12.5µL SYBR Green Mix with no MgCl$_2$ (Sigma Aldrich), 50nM forward primer, 50nM reverse primer, 2µL 25mM MgCl$_2$, 1µL plasmid, RNase/DNase- free dH$_2$O to 25µL. Data were used for statistical analysis when the R^2 efficiency of the plasmid standard curve for that primer set was >0.98. Primer sets to be used in qPCR amplification are listed in Table 5.

GENE	FORWARD PRIMER (5'→3')	REVERSE PRIMER (5'→3')	SOURCE
αSMA	CAGGCATGGATGGCATCAATCAC	ACTCTAGCTGTGAAGTCAGTGTCG	(Lee and Kim, 2007)
SM22α	ACCAAGCCTTCTCTGCCTCAAC	GCCACACTGCACTACAATCCAC	(Lee and Kim, 2007)
MGP	TGCGCTGGCCGTGGCAACCCT	CCTCTCTGTTGATCTCGTAGGCA	(Boström *et al.*, 2001)
CaSR 4-5	GAGGCCTGGCAGGTCCTGAA	TGATGGAGTAGTTCCCCACC	Tom Davies
CaSR 6-7	GTGGTGAGACAGATGCGAGT	GCCAGGAACTCAATCTCCTT	Tom Davies
Osterix	GATGACGGGTCAGGTAGAGTGAGCTG	CTTGAGGTTTCACAGCTTCTGGCTGG	(Nakano-Kurimoto *et al.*, 2009)
Runx2	GACGAGGCAAGAGTTTCACC	GTCTGTGCCTTCTTGGTTCC	Debbie Mason
Osteoprotegrin	GAGTGTGAGGAAGGGCGTTAC	GCAAACTGTGTTTCGCTCTG	Debbie Mason
Osteocalcin	CAGACAAGTCCCACACAGCA	CTTGGCATCTGTGAGGTCAC	Debbie Mason
ALP	GCTGGCCCTTGACCCCTCCA	ATCCGGAGGGCCACCTCCAC	Marisol Vazquez
Collagen II-α1	GGCCTCGCGGTGAGCCATG	GCCTCCTGGGCATCCTGGCC	Tom Davies
18S rRNA	GCAATTATTCCCCATGAACG	GGCCTCACTAAACCATCCAA	Marisol Vazquez
GAPDH	GACGGCCGCATCTTCTTGTGCA	TGCAAATGGCAGCCCTGGTGAC	Marisol Vazquez

Table 5. Primer sets for qPCR amplification of gene-specific products from RT-PCR. Amplicons are ligated into pGEM-T plasmid vectors. All primers were designed to span exon-exon junctions. Green= VSMC genes. Blue= Osteoblastic genes. Purple= Chondrogenic genes. Pink= Housekeeping genes.

2.27 Statistical analysis.

Statistical analyses were carried out using GraphPad Prism 5. Data are all expressed as the mean ± the standard error of mean (SEM). When data were normally distributed, comparisons between two sets of data were performed using a two-tailed t-test. When the comparisons were performed between the means of two or more samples, one way ANOVA was performed. Two way ANOVA was performed when there were more than one independent variable for analysis. Additionally, numerous repeats were conducted which allowed for the chance of a rare event to occur which would reject the null hypothesis. In this incidence Bonferroni's post-test was used where stated, particularly in analyses with multiple conditions or more than one independent variables. Significance levels were assigned using the standard scientific nomenclature: $P<0.05=*$, $P<0.01=**$ and $P<0.001=***$.

CHAPTER 3:

IN VIVO CHARACTERISATION OF THE SM22α X fl CaSR MOUSE MODEL WITH SELECTIVE ABLATION OF CaSR IN VASCULAR SMOOTH MUSCLE CELLS

CHAPTER 3: GENERAL INTRODUCTION

CaSR is an important GPCR involved in systemic $[Ca^{2+}]_o$ homeostasis (Brown *et al.*, 1993). To ascertain the function of the VSMC-CaSR, our collaborators at UCSF (Chang *et al.*, 2008) generated for us a new transgenic mouse model with selective ablation of the CaSR in VSMCs. To determine the role of the CaSR in the cardiovascular system, the first part of my studies involved an initial characterisation of the *in vivo* phenotype of these mice, specifically, of body weights, organ weights, bone densities and serum biochemistries.

CHAPTER 3: RESULTS

A Male SM22α x fl CaSR Mice

B Female SM22α x fl CaSR Mice
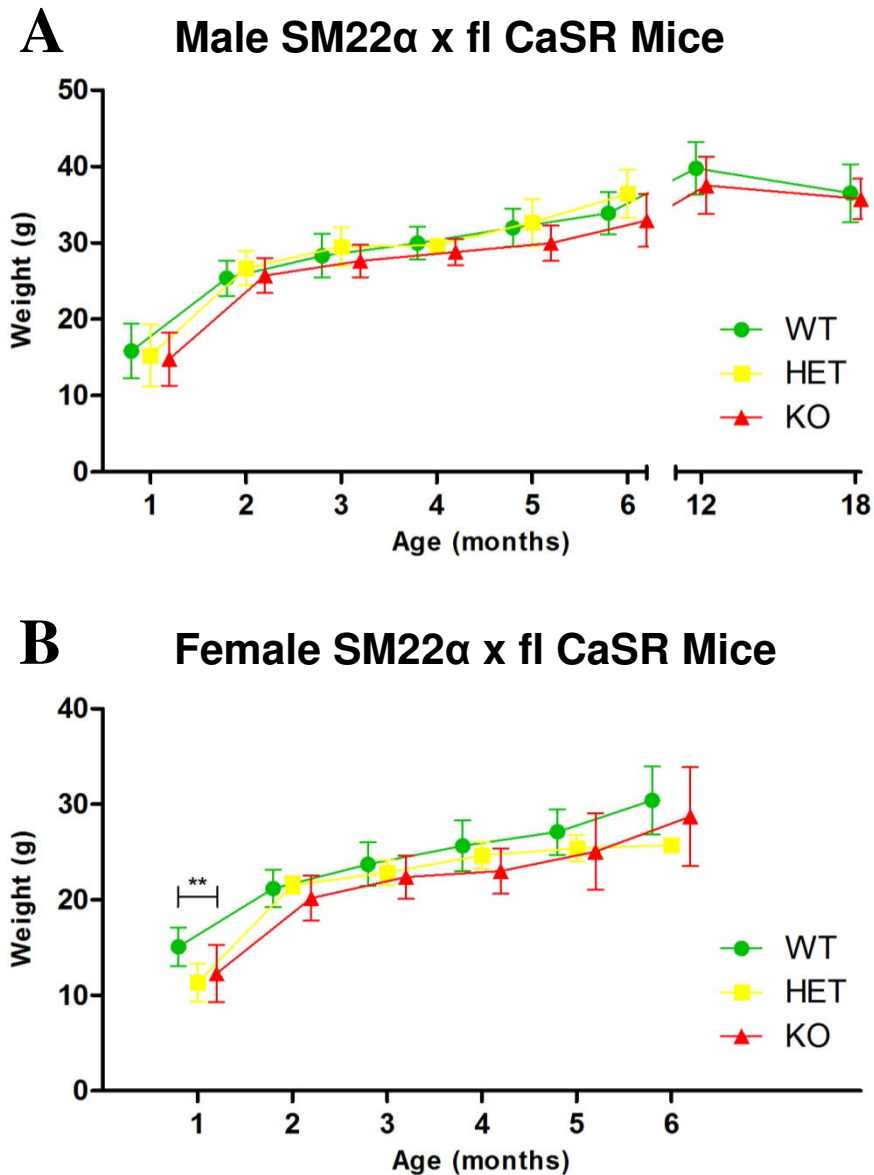
Figure 27. SM22α x fl CaSR mouse weights over time. Male and female mouse weights were taken at monthly intervals up to 6 months. 18 Months weights were also recorded for long-term characterisation of male mice. Female weights at 18 months were not tabulated as these mice were not kept for experiments. Mice were weighed on scales 5 times at each time point and average weights were calculated to correct for mouse movement. The number of animals used were as follows. 1 month: WT ♂N=49, ♀N=35; HET ♂N=9, ♀N=4; KO ♂N=21, ♀N=21. 2 month: WT ♂N=37, ♀N=33; HET ♂N=10, ♀N=5; KO ♂N=21, ♀N=19. 3 month: WT ♂N=65, ♀N=36; HET ♂N=17, ♀N=7; KO ♂N=27, ♀N=17. 4 month: WT ♂N=27, ♀N=19; HET ♂N=7, ♀N=4; KO ♂N=21, ♀N=13. 5 month: WT ♂N=42, ♀N=25; HET ♂N=10, ♀N=7; KO ♂N=19, ♀N=15. 6 month: WT ♂N=25, ♀N=8; HET ♂N=6, ♀N=3; KO ♂N=8, ♀N=6. 18 month: WT ♂N=3; KO ♂N=3. Data are expressed as mean ± SEM. Statistical analysis: two-way ANOVA with Bonferroni's post-test. P<0.01=**.

Figure 28. SM22α x fl CaSR wild-type, heterozygote and knockout mice are not observably different. Mouse bodies are not observably different in terms of external morphology in terms of colour, shape or size. All mice had comparative digit numbers with no apparent developmental abnormalities. They also showed equal signs of alertness, mobility, feeding and drinking habits.

SM22α x fl CaSR WT and KO mice have no observable phenotype and demonstrate normal body weights throughout their lifespan.

To determine whether the VSMC-CaSR KO had more widespread effects on the body of SM22α x fl CaSR and to determine whether this had any significant effect on body weights, male and female mice were weighed at monthly intervals. Male mice were heavier than female mice at all intervals, however no significant difference in body weights or observable trends were seen between any genotypes except for female mice at 1 month of age. In this group, comparisons reveal that 1 month old female KO mice are significantly lighter compared to WT mice (Figure 27, P<0.01).
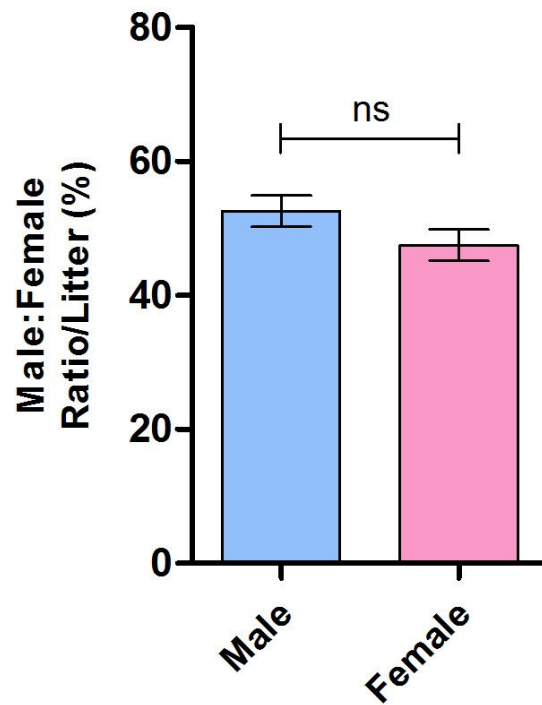
Figure 29. Male and female SM22α x fl CaSR mouse ratios in litters. Mouse litters were counted and the ratio of male:female mice was calculated. Data were tabulated from 48 different breedings between WTxWT, WTxKO, KOxKO mice. Litter number: N=48, mouse number: n=391. Data are expressed as mean ± SEM. Statistical analysis: unpaired two-tailed t-test. ns= not significant.
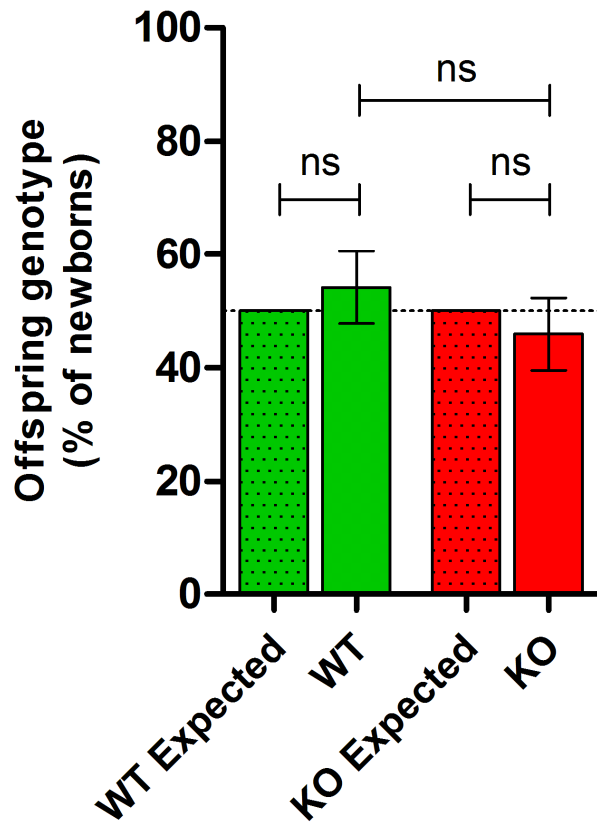
Figure 30. Genotype ratios in offspring from a WTxKO SM22α x fl CaSR mouse breeding. WT and KO mice were bred and offspring WT and KO ratios of each litter were calculated. Litter numbers for WT and KO was N=7. Data are expressed as mean ± SEM. Statistical analysis: one-way ANOVA. ns= not significant.
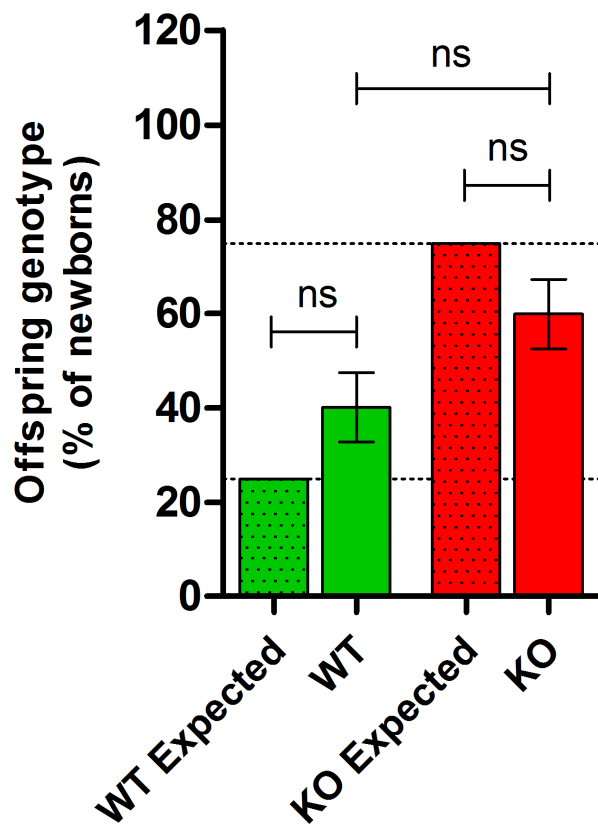
Figure 31. Genotype ratios in offspring from a KOxKO SM22α x fl CaSR mouse breeding. KO and KO mice were bred and offspring WT and KO ratios of each litter were calculated. Litter number: N=8. Data are expressed as mean ± SEM. Statistical analysis: one-way ANOVA. ns= not significant.
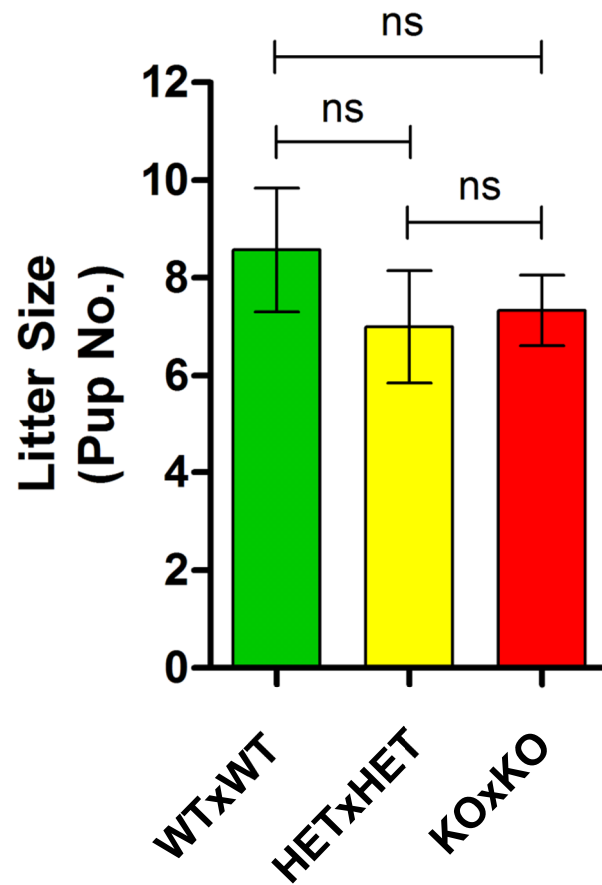
Figure 32. Litter sizes of SM22α x fl CaSR mouse breedings. Male and female mice were bred with partners of matching genotypes. From these breedings litter numbers were plotted to determine possible influence of the genotypes on litter size. Litter number: WT: N=7, HET: N=8, KO: N=9. Data are expressed as mean ± SEM. Statistical analysis: one-way ANOVA. ns= not significant.
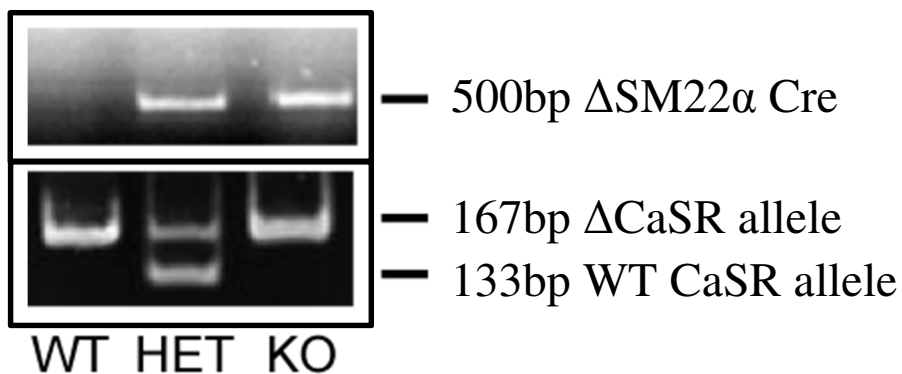
Figure 33. Confirmation of targeted-deletion of VSMC-CaSR in SM22α x fl CaSR mice by PCR. Mouse ear biopsies were lysed overnight for the isolation of genomic DNA Upper panel: PCR amplification of the exogenous cre transgene (500bp) detected in heterozygote (HET) and knockout (KO) mouse tissue only. Lower panel: PCR amplification of a portion of CaSR (untranslated genomic DNA downstream of exon 7) shows the presence of small WT amplicon with no loxP site, and a larger loxP-containing amplicon flanking exon 7 of CaSR. LoxP sites are present in wild-type, heterozygote and knockout mice. Heterozygotes show both WT and floxed amplicons.

SM22α x fl CaSR WT and KO mouse breeding show expected Mendelian inheritance for gender number of offspring.

If no selective gender preference during development is present we would typically expect all pups born to be 50:50, male:female. This was shown to be the case with no significant differences overall. Data were 52.53% Males ± 2.35 vs. 47.47% Females ± 2.35 (N=48 litters, n=391 mice, Figure 29). When WT and KO mice were bred, expected Mendelian inheritance would predict the ratio between WT and KO offspring to be 50:50. Indeed, this was found to be the case and all offspring followed this trend, with 54.10% ± 2.41 WT vs. 45.90% ± 2.41 KO (Figure 30). However, in the case of KOxKO breedings, the expected Mendelian inheritance for the ratio of WT:KO should be 25:75. This was however rarely seen, and statistical analysis by one-way ANOVA revealed these genotypes to be no different from one another; 40.13% ± 2.60 vs. 59.87% ± 2.68 (Figure 31). There was a very visible trend (albeit not significant) for KO mice to be more prevalent in these litters than WT mice.

In addition to measuring the ratios of genotypes of all offsprings, it was also important to measure the litter sizes of breedings from parents of different genotypes. This way, we could observe whether CaSR-ablation in VSMCs affects embryonic development and/or uterine function. Analysis of litter sizes showed there to be no significant difference between pups from WTxWT, HETxHET and KOxKO. Average litter sizes were 8.57 ± 0.48, 7.00 ± 0.41, 7.33 ± 0.24. These differences were not significantly different (Figure 32). Of course, it was also important to confirm whether mice had CaSR knocked out in VSMCs. For this reason, biopsies of each mouse were obtained and DNA was digested for PCR amplification of either the cre transgene or floxed alleles. Figure 33 demonstrates the effective detection of the cre transgene in HET and KO mice only.
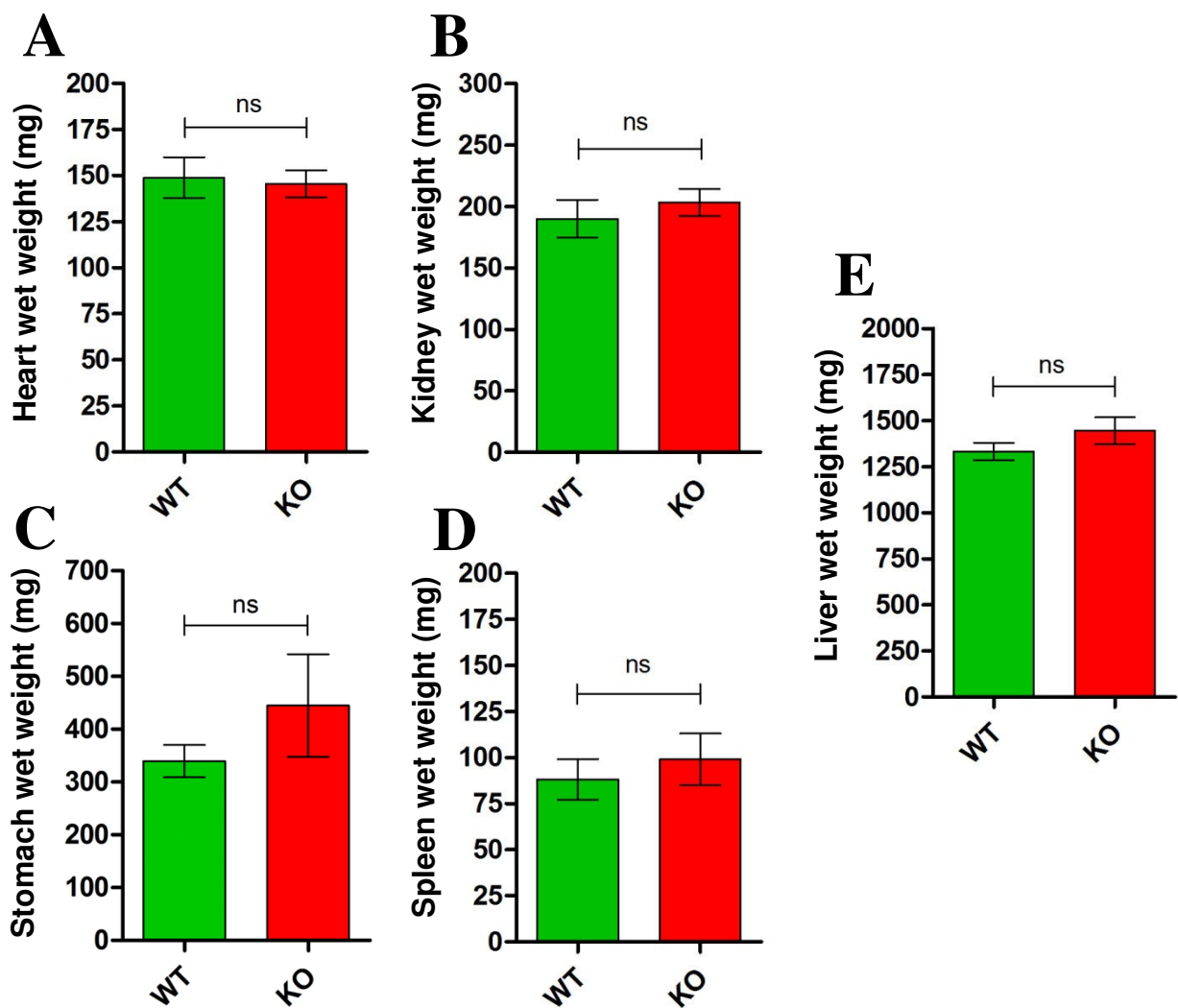
Figure 34. SM22α x fl CaSR WT and KO mouse organ weights at 6 months of age. Mice were humanely culled by Schedule one in accordance with Home Office regulations. Organs were dissected, washed briefly in Krebs buffer (described in methods) then dried before weighing. (A) Heart, WT N=8, KO N=6; (B) Kidney, WT N=8, KO N=7; (C) Stomach, WT N=8, KO N=7; (D) Spleen, WT N=8, KO N=6; (E) Liver, WT N=8, KO N=7. Data are expressed as mean ± SEM. Statistical analysis: unpaired two-tailed t-test ANOVA. ns= not significant.
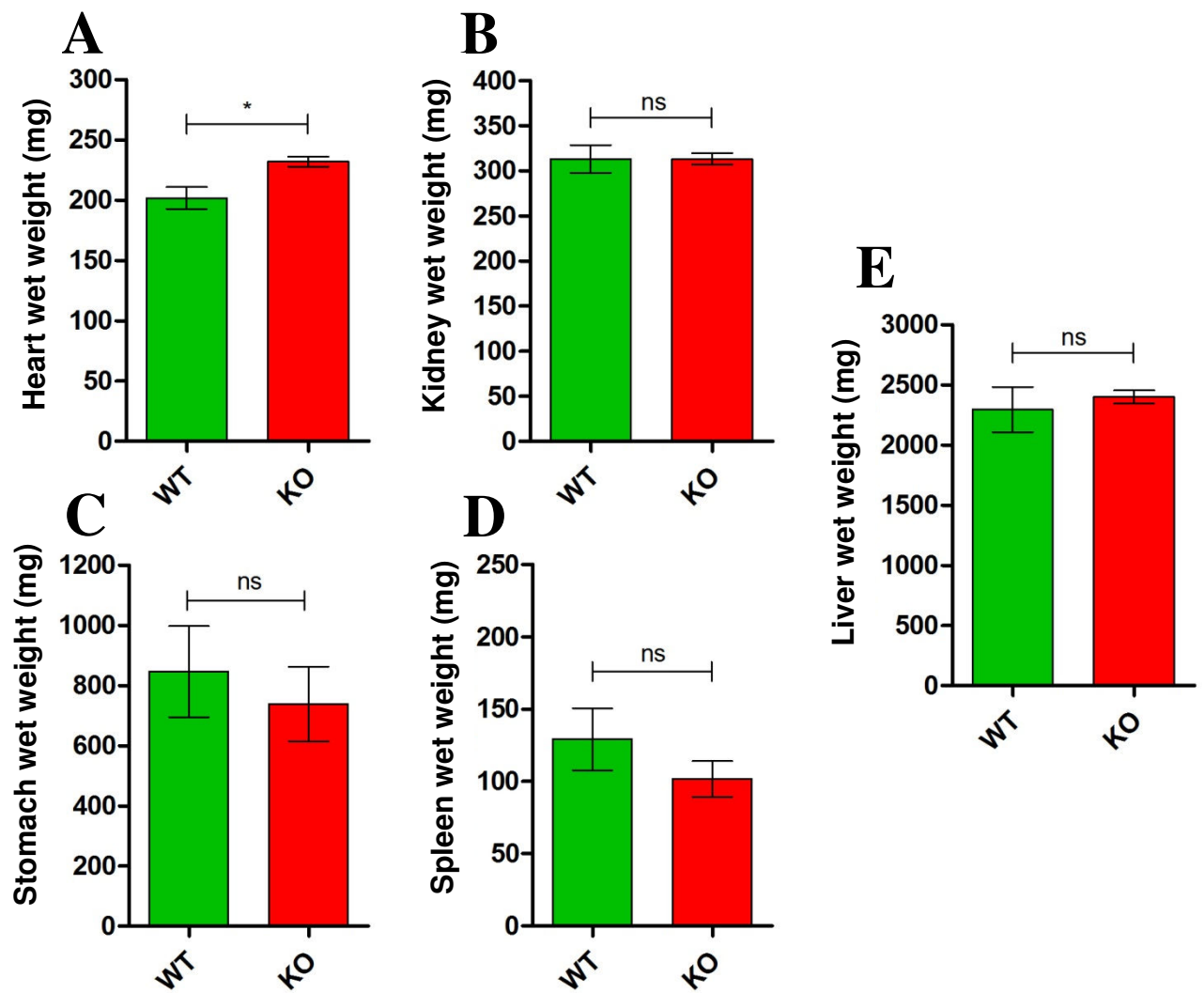
Figure 35. SM22α x fl CaSR WT and KO mouse organ weights at 18 months of age. Mice were humanely culled by schedule 1 in accordance with Home Office regulations. Organs were dissected, washed briefly in Krebs buffer (descriebd in methods) then dried before weighing. (A) Heart, WT N=5, KO N=4; (B) Kidney, WT N=6, KO N=4; (C) Stomach, WT N=6, KO N=4; (D) Spleen, WT N=6, KO N=4; (E) Liver, WT N=6, KO N=4. Data are expressed as mean ± SEM. Statistical analysis: unpaired two-tailed t-test. $P < 0.05$. ns= not significant.

Ageing SM22α x fl CaSR KO mice have heavier hearts compared to WT mice.

Hypertrophy of the heart is a key indicator of cardiovascular disease, kidney disease and vascular calcification (Nitta *et al.*, 2004, Nitta, 2011). Therefore, we weighed mouse hearts to determine whether any hypertrophy or hyperplasia of heart tissue had occurred in SM22α x fl CaSR WT or KO mice over time. Data retrieved from wet weights of all organs at 6 months of age revealed no significant difference between the hearts of WT and KO mice, nor any of the other organs investigated (Figure 34). Wet weights of WT and KO mouse hearts at 18 months showed a significant increase in heart weight in KO mice compared to WT mice (P<0.05, Figure 35). Conversely, other organ weights were recorded and showed no significant differences in wet weight at 3 and 18 months of age.
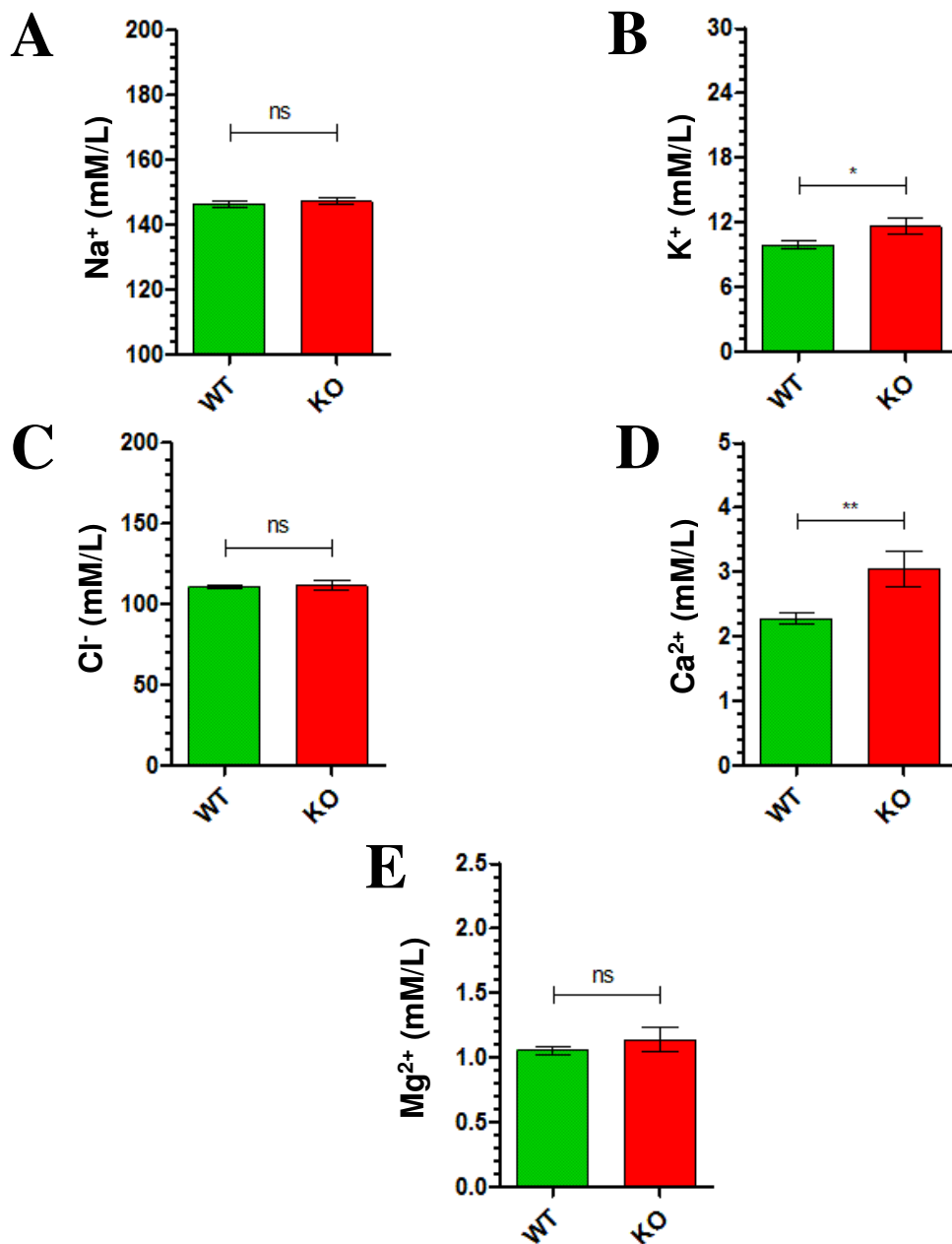
Figure 36. Biochemical analysis of WT and KO SM22α x fl CaSR male mouse serum at 3 months of age. (A) Serum Na^+ levels; 146.40mM ± 0.85 WT (N=11) vs. 147.30mM ± 1.11 KO (N=4). (B) Serum K^+ levels; 9.88mM ± 0.38 WT (N=11) vs. 11.60mM ± 0.75 KO (N=6), P<0.05=*. (C) Serum Cl^- levels; 110.6mM ± 0.97 WT (N=11) vs. 111.50mM ± 3.23 KO (N=4). (D) Serum Ca^{2+} levels; 2.28mM ± 0.10 WT (N=11) vs. 3.05mM ± 0.27 KO (N=6), P<0.01=**. (E) Serum Mg^{2+} levels; 1.06mM ± 0.03 WT (N=11) vs. 1.14mM ± 0.09 KO (N=6). Data are expressed as mean ± SEM. Statistical analysis: unpaired two-tailed t-test. P<0.05=*. P<0.01=**. ns= not significant.
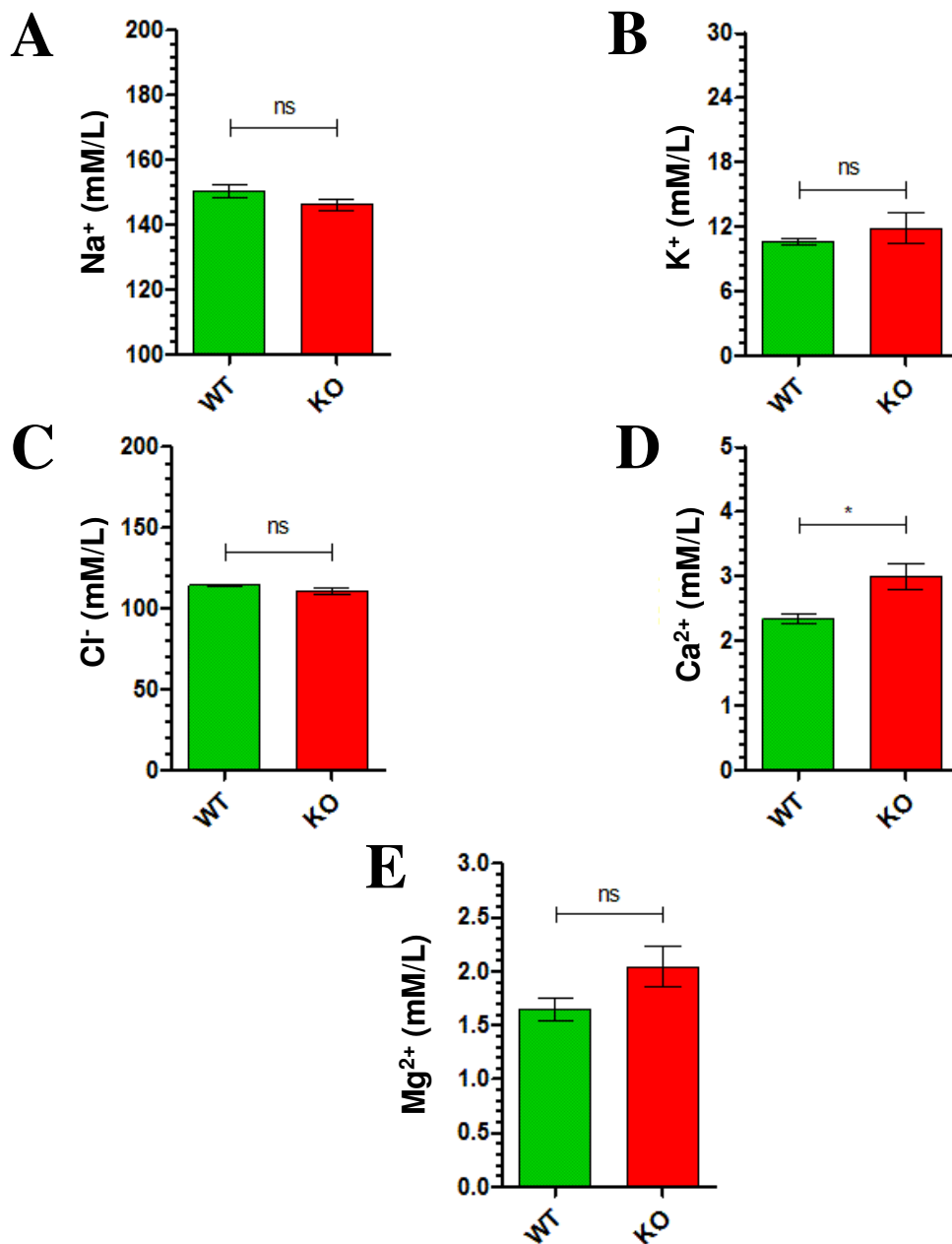
Figure 37. Biochemical analysis of WT and KO SM22α x fl CaSR male mouse serum at 18 months of age. (A) Serum Na^+ levels; 149.00mM ± 2.08 WT (N=3) vs. 146.30mM ± 1.76 KO (N=3). (B) Serum K^+ levels; 10.64mM ± 0.35 WT (N=3) vs. 11.88mM ± 1.45 KO (N=3). (C) Serum Cl^- levels; 114.30mM ± 0.67 WT (N=3) vs. 111.00mM ± 2.08 KO (N=3). (D) Serum Ca^{2+} levels; 2.34mM ± 0.08 WT (N=3) vs. 2.99mM ± 0.20 KO (N=3), P<0.05=*. (E) Serum Mg^{2+} levels; 1.65mM ± 0.10 WT (N=3) vs. 2.04mM ± 0.19 KO (N=3). Data are expressed as mean ± SEM. Statistical analysis: un-paired two-tailed t-test. P<0.05=*.. ns= not significant.
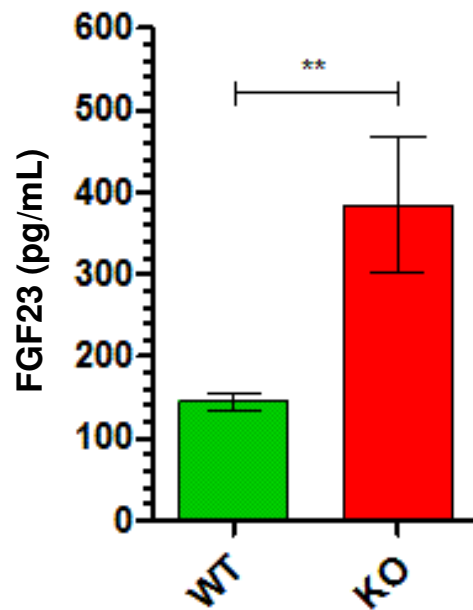
Figure 38. SM22α x fl CaSR KO male mice have increased FGF23 serum levels at the age of 3 months compared to WT mice. Mouse sera retrieved from WT and KO mice at 3 months of age were collected by centrifugation and quantified off-site at AstraZeneca with our collaborators João Graça and Dr. Sally Price. WT FGF23: 145.00pg/mL ± 10.99 (N=11). KO FGF23: 384.40pg/mL ± 83.49 (N=6). Data are expressed as mean ± SEM. Statistical analysis: unpaired two-tailed t-test. P<0.01=**.
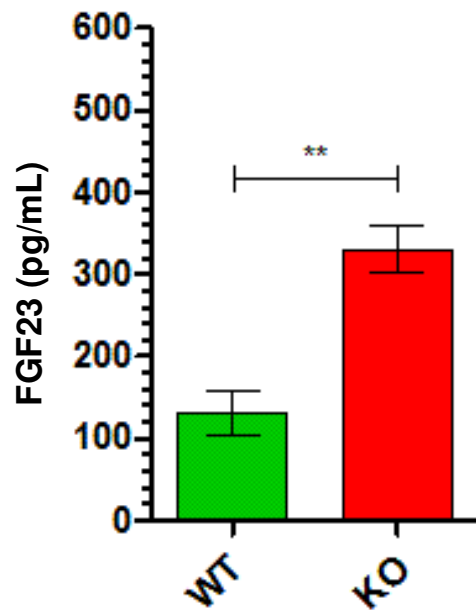
Figure 39. SM22α x fl CaSR KO male mice have increased FGF23 serum levels at the age of 18 months compared to WT mice. Mouse serum retrieved from WT and KO mice at 18 months of age were collected by centrifugation and quantified using an FGF23 kit. WT FGF23: 131.10pg/mL ± 26.27 (N=3). KO FGF23: 330.00pg/mL ± 28.68. Data expressed as mean ± SEM. Statistical analysis: un-paired two-tailed t-test. (N=3). P<0.01=**.

SM22α x fl CaSR KO mice exhibit mild hypercalcaemia and elevated levels of FGF23 compared to WT mice.

Biochemical analyses (performed by collaborators at AstraZeneca) revealed that KO mice exhibited hypercalcaemia at both age-points. At 3 months of age, WT mice have serum $[Ca^{2+}]$ of 2.28mM ± 0.10 compared with serum $[Ca^{2+}]$ levels of KO mice, which were 3.05mM ± 0.27 (Figure 36, P<0.01). This hypercalcemia in KO mice was maintained at 18 month, where serum $[Ca^{2+}]$ was 2.34mM ± 0.08 in WT mice compared with serum $[Ca^{2+}]$ of 2.99mM ± 0.20 in KO mice (Figure 37, P<0.05). Also observed was mild hyperkalemia in 3 month old mice 9.88mM ± 0.38 in WT compared with 11.61mM ± 0.74 in KO mice (Figure 36, P<0.05). This however, was not apparent in 18 month old mice.

Whether hypercalcaemia was modulated by components of the Ca^{2+}_{o}/Pi/Vitamin D/PTH axis also required investigation. FGF23 levels were shown to be significantly increased in KO mice compared with WT mice. In 3 month mice, WT serum concentrations were 145.00pg/mL ± 10.99 vs. 384.40pg/mL ± 83.49 in KO mouse serum (Figure 38, P<0.01). These differences were also maintained in 18 month mice where WT serum FGF23 concentrations were 131.10pg/mL ± 26.27 vs. 330.00pg/mL ± 28.68 (Figure 39, P<0.01).
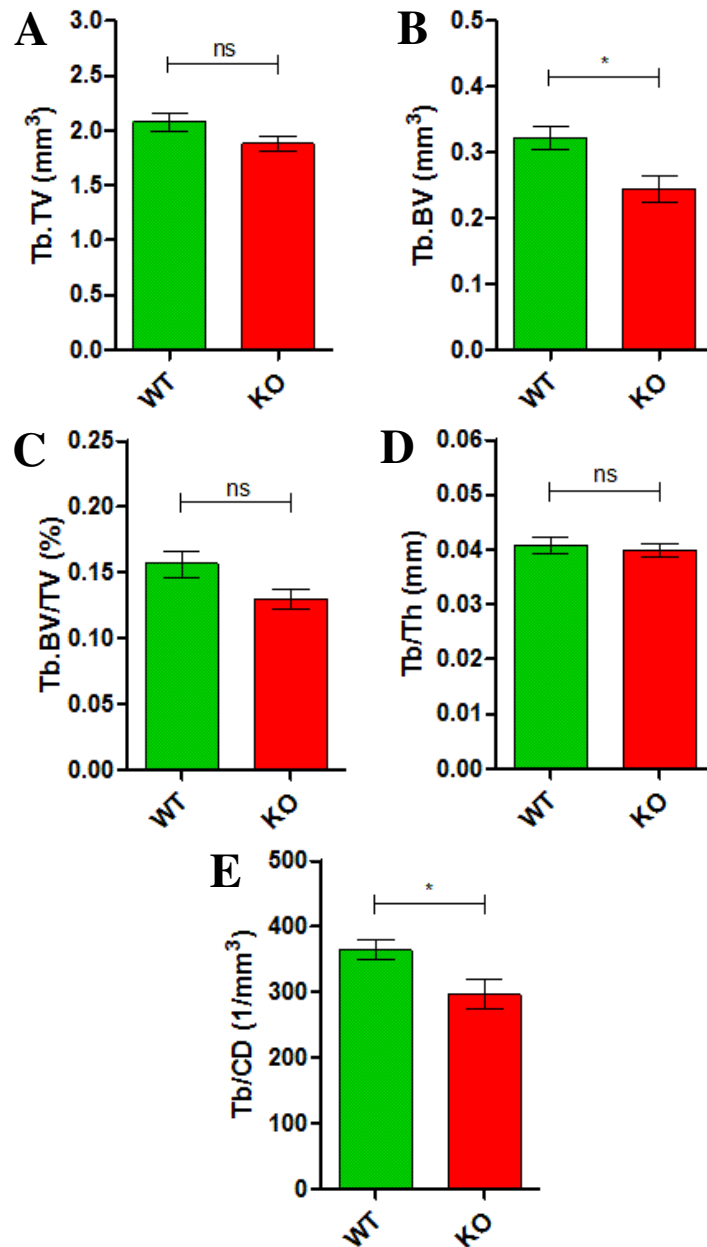
Figure 40. μCT analysis of 3 month old SM22a x fl CaSR mice distal femurs reveals reduced trabecular bone in KO mice compared to WT mice. Distal femurs were scanned in 70% ethanol using a Scanco vivaCT system. Trabecular bone was calculated by removing hard bone mineral from 3D-reconstructed images. (A) Trabecular bone length x Tissue volume. (B) Trabecular bone length x Bone volume. (C) Trabecular bone length x (Bone volume / Tissue volume). (D) Trabecular bone length / Trabecular bone thickness. (E) Trabecular bone length / Trabecular connectivity density. Abbreviations: Trabecular bone length (Tb); Tissue volume (TV); Bone volume (BV); Trabecular bone thickness (Th); Trabecular bone spacing (Sp); Trabecular connectivity density (CD) (N=7 WT, N=6 KO). Data are expressed as mean ± SEM. Statistical analysis: unpaired two-tailed t-test. P<0.05=*. ns= not significant. These experiments were performed by Dr. Wenhan Chang, UCSF.
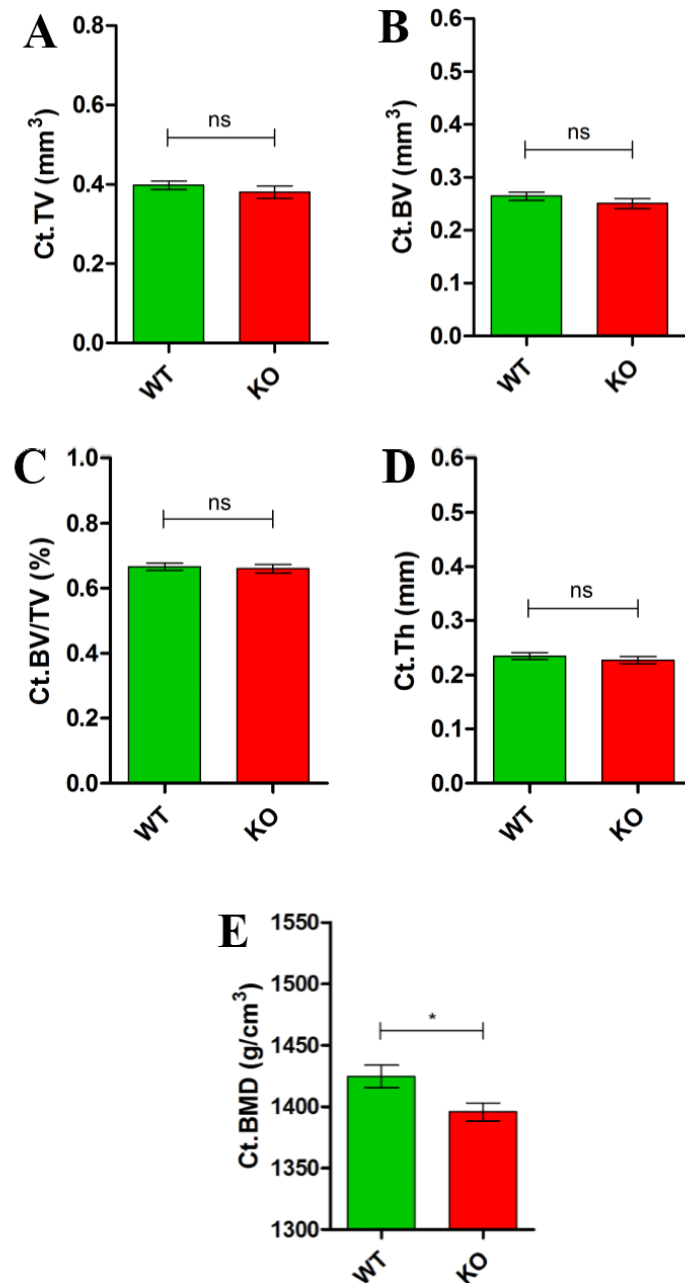
Figure 41. µCT analysis of 3 month old SM22a x fl CaSR mice tibia-fibula junctions reveals reduced cortical bone in KO mice compared to WT mice. Distal femurs were scanned in 70% ethanol using a Scanco vivaCT system. Cortical bone was calculated by removing hard bone mineral from 3D-reconstructed images. (A) Cortical bone length x Tissue volume. (B) Cortical bone length x Bone volume. (C) Cortical bone length x (Bone volume / Tissue volume). (D) Cortical bone length x Cortical bone thickness. (E) Cortical bone length x Bone mineral density. Abbreviations: Cortical bone length (Ct); Tissue volume (TV); Bone volume (BV); Cortical bone thickness (Th); Bone mineral density (BMD) (N=7 WT, N=6 KO). Data are expressed as mean ± SEM. Statistical analysis: unpaired, two-tailed t-test. P<0.05=*. ns= not significant. These experiments were performed by Dr. Wenhan Chang, UCSF.

SM22α x fl CaSR KO mice exhibit significant reductions in bone tissue compared with WT mice.

Data show that SM22α x fl CaSR mice exhibit hypercalcaemia. To investigate whether the source of this Ca^{2+} was from the bone, μCT was performed in collaboration with Dr. Wenhan Chang to determine bone densities on the transgenic SM22α x fl CaSR mouse model. Three month old WT and KO mice were culled and both distal femurs and tibia-fibula junctions were scanned using μCT. The results for the distal femur are illustrated in Figure 40. The Tb.TV was not significantly reduced in KO femurs compared to that of WT femurs from $2.08mm^3 \pm 0.09$ (N=7) WT vs. $1.88mm^3 \pm 0.07$ (N=6) KO. Tb.BV was significantly reduced in KO femurs compared to WT femurs; $0.32mm^3 \pm 0.02$ (N=7) WT vs. $0.25mm^3 \pm 0.02$ (N=6) KO, P<0.05. Tb.BV/TV was not significantly decreased in KO compared with WT; $0.16\% \pm 0.01$ (N=7) WT vs. $0.130\% \pm 0.008$ (N=6) KO. Tb/Th was not significantly different between WT and KO; $0.040mm \pm 0.001$ (N=7) WT vs. $0.040mm \pm 0.001$ (N=6) KO. In contrast, Tb/CD was significantly reduced in KO femurs compared to WT femurs; $1425.00g/cm^3 \pm 9.03$ (N=7) WT vs. $1396.00g/cm^3 \pm 7.29$ (N=6) KO.

The tibia-fibula junction bone density data are reported in Figure 41 and show some minor differences between WT and KO mice. Ct.TV was not different in WT mice compared with KO mice; $0.34mm^3 \pm 0.01$ (N=7) WT vs. $0.38mm \pm 0.02$ (N=6) KO. Ct.BV was not different in WT mice compared with KO mice; $0.26mm^3 \pm 0.01$ (N=7) WT vs. $0.250mm^3 \pm 0.01$ (N=6) KO. Ct.BV/TV was not different in WT mice compared to KO mice; $0.67\% \pm 0.01$ (N=7) WT vs. $0.66\% \pm 0.01$ (N=6) KO. Ct/Th was also not different in WT mice compared with KO mice; $0.24mm \pm 0.01$ (N=7) WT vs. $0.23mm \pm 0.01$ (N=6) KO. However, Ct.BMD (g/cm^3) was significantly reduced in KO mice compared with WT mice; $1425.00g/cm^3 \pm 9.03$ (N=7) WT vs. $1,396.00g/cm^3 \pm 7.29$ (N=6) KO, P<0.05.

CHAPTER 3: DISCUSSION

SM22α x fl CaSR ablation in VSMCs does not significantly affect genders of offspring in offspring or expected Mendelian inheritance.

My experiments show that VSMC-CaSR knockout does not significantly affect the reproductive ability and survival rates of mice (Figure 27, 28). Data show that male:female ratios are not different from one another in all breedings (Figure 29). In addition to this, litter sizes between WT, HET and KO mice were shown to not be different (Figure 32). Mendelian inheritance of the cre recombinase and floxed alleles was also shown to not be affected in WT and KO matings (Figure 30). Analysis of WTxKO matings shows that the percentage WT and KO offspring are not significantly different from the expected inherited ratio. Conversely, KOxKO matings seem to differ from the expected Mendelian inheritance ratio (Figure 31). One would at least expect the ratios of WT to KO pups to be significantly different which was not seen. The fact that the WT:KO ratio was nearer 40%:60% than the expected 25%/75% suggests that there is some selectivity in WT pups over KO pups. However, the spread of the data was quite broad across the breedings tabulated. In some cases it was seen that 83.33% of offspring in KOxKO breedings were actually KO, while other times there were only as few as 13.33%. The total number of KOxKO breedings used for this analysis was 8. Further breeding will increase the number of observations and conclusively determine Mendelian transmission for gender and offspring numbers. Whether there is some embryonic lethality or not has not yet been investigated. However, embryonic lethality might not be so surprising since during pregnancy, the cardiovascular system of the mother and child become intertwined for efficient delivery of nutrients and oxygen. A vascular phenotype would therefore affect embryonic development *in utero*. To clarify this, it would be both beneficial to carry out more breedings and also investigate embryonic lethality in the future.

SM22α x fl CaSR ablation in VSMCs does not affect organ or body weights.

Using the cre-lox system, we aimed to specifically knock out the CaSR in vascular smooth muscle cells. Although this deletion is shown to be specific to the cardiovascular system postnatally, according to the full characterisation by Li *et al (Li et al., 1996b),* it is possible that a cardiovascular phenotype resulting from this deletion could affect other

organs, particularly since blood vessels penetrate all organs for blood delivery. Indeed, if the blood delivery mechanism is altered, one could expect loss of functions or changes in size or morphology of organs. Gathering mouse weights over time and weighing organs has demonstrated that CaSR deletion from VSMC produces a phenotype. Despite there being no significant differences in body weight between WT, HET and KO mice, it was seen that body weights of just female mice at 1 month of age showed a significant reduction in body weight (in KO mice compared to WT mice, Figure 27). This finding suggests a possible developmental regulation by the VSMC-CaSR in female mice only. Further research is required into the embryonic development of these mice. Conversely, from 2 months onwards body weights are not different between any genotypes or sexes suggesting that, if any abnormalities were present early on in life, these are corrected or compensated for towards adulthood (Figure 27). At 3 months of age onwards, there were no differences between mouse body weights. Consistent with these findings, Martin Schepelmann in our research group has reported that mice of 3 months of age show that there is no significant difference in food and water consumption in KO mice compared to WT mice. In contrast, faecal excretion is significantly increased in KO mice compared with WT mice (p<0.05, data not shown). These data could reflect changes in water retention by the colon of KO animals, thereby mildly affecting body weights in young female mice.

SM22α x fl CaSR ablation in VSMCs produces heavier hearts in ageing mice.

My data show that VSMC-CaSR KO mouse hearts are heavier compared to VSMC-CaSR WT mouse hearts at 18 month of age (Figure 35). It is well-documented that one of the major manifestations of cardiovascular disease is left ventricular hypertrophy (Davies and Hruska, 2001, Nitta, 2011). During vessel calcification, VSMCs become rigid and lose the characteristic elastic phenotype. Consequently, systolic blood pressure is elevated and systemic blood-flow around the body is impeded. This can lead to cardiac remodelling to compensate for this deleterious state (Brunet *et al.*, 2011, London, 2011). From *in vitro* and *in vivo* studies where CaSR has shown to have a protective role against calcification in healthy blood vessels (Alam *et al.*, 2008), we would hypothesize that CaSR ablation in KO mice plays a role in early calcification of arteries. One can assume

that, if the vessels were to mineralise in a similar manner to what is observed during heart disease, expected outcomes such as increased blood pressure and hypertrophy may also develop. It is therefore likely that heavier hearts may be an indicator of cardiac remodelling and hypertrophy of the left ventricle. This observation is particularly interesting for two reasons; (i) pressure and force exerted by cardiac myocytes in the left ventricle must be significant enough to pump all blood leaving the heart around the whole body, in stark contrast to the right ventricle which delivers blood more locally to the pulmonary system (Stewart *et al.*, 2012); (ii) these data suggest that the VSMC-CaSR might play a role in the regulation of blood vessel tone and/or vascular calcification. If the left ventricle does indeed remodel to a hypertrophic state later in life, one might speculate that we will also detect differences in blood pressure in VSMC-CaSR KO animals compared to VSMC CaSR-WT animals. However, to further elucidate a role of the VSMC-CaSR in blood pressure modulation and cardiac remodelling further studies need to be conducted. Specifically, blood pressure measurement of young and ageing mice should be performed in addition to magnetic resonance imaging (MRI) to confirm ejection fractions from the left ventricle.

SM22α x fl CaSR mice exhibit hypercalcaemia, reduced bone integrity and elevated serum FGF23 levels.

Cardiovascular complications occur with poor diet, ageing, abnormal Ca^{2+}_o homeostasis and genetic predisposition (Lloyd-Jones *et al.*, 2008, Lloyd-Jones *et al.*, 2009, Lloyd-Jones *et al.*, 2010b, Roger *et al.*, 2011, Roger *et al.*, 2012). During advanced CKD, secondary hyperparathyroidism can occur which is often the leading cause of hypercalcaemia (Moe, 2004). It has been well-documented that CaSR knockout in the parathyroid gland causes hypercalcaemia (Chang *et al.*, 2008). During CaSR-ablation in the parathyroid gland, PTH suppression through CaSR activation does not occur, resulting in overall hypercalcaemia by hyperparathyroidism (Chang *et al.*, 2008). The ΔSM22α cre mouse model shows expression in VSMC through development and post-natally (Li *et al.*, 1996b), therefore, in our mouse model we should only achieve CaSR-KO in VSMCs, however, one should not assume that there is no leakage of this promoter. Hyprcalcaemia we observe in VSMC-CaSR KO mice should be a consequence of the

vascular phenotype itself and not related to the parathyroid glands. It should be noted that Chang *et al* have reported reductions in CaSR expression in other tissues in the PTG-CaSR knockout. This is possibly due to hypercalcaemia downregulating CaSR expression in these organs (Chang *et al.*, 2008) which has also been shown *in vitro* in primary bovine VSMCs (Alam *et al.*, 2008). Furthermore, the parathyroid-specific cre-lox CaSR knockout developed by Dr. Chang and colleagues shows marked reductions in osteoblast CaSR expression. These unexpected findings suggest that there may be more complicated signalling mechanisms at work and that PTG-CaSR activation may somehow be linked to the regulation of CaSR at both the mRNA and protein level in more unrelated tissues and cell types (Chang *et al.*, 2008). Importantly, this should be considered in regard to the SM22α x fl CaSR mouse model where similar alterations in expression of other CaSRs in other tissues may also occur.

Another important finding in these studies was that KO mice have significantly reduced bone mineral density. Figure 40 shows that the distal femurs of KO mice have lower trabecular bone volume, thickness and spacing. When considering that KO mice have hypercalcaemia this is perhaps not so unexpected, and one could suggest that the observed elevated $[Ca^{2+}]$ levels could be a consequence of Ca^{2+} resorption from bone. It is also interesting to note that trabecular bone is highly vascularised, and so the VSMC-CaSR may play a crucial role in the co-ordination of Ca^{2+} deposition from the blood to bones and vice versa (Chang *et al.*, 2008). For example, the VSMC-CaSR may play a role in mediating Ca^{2+} resorption from bone in areas rich in vascularised bone. In this instance it is not surprising that FGF23 levels are also elevated (Figures 38 and 39) since Pi is liberated during this bone resorption. Considering the presence of high $[Ca^{2+}]$, FGF23 and low bone density, it seems most likely that hypercalcaemia of KO mice is derived from bone demineralisation. Alternatively or in addition, CaSR ablation from VSMC could also lead to an impaired renal function, with decreases in $1,25(OH)_2D_3$ synthesis associated with hypercalcaemia. This latter hypothesis will need to be tested in greater detail by measuring $1,25(OH)_2D_3$ levels and characterising the renal phenotype of the SM22α x fl CaSR mouse.

It has been reported that CaSR is linked to Ca^{2+} exchangers and transporters including the Na^+/Ca^{2+} exchanger and plasma membrane Ca^{2+} ATPase (PMCA) (Blankenship *et al.*, 2001, Ba and Friedman, 2004). Studies have demonstrated that, in kidney cells, CaSR activation by agonists causes a reduction in the influx of Ca^{2+}_o into the cell (Blankenship *et al.*, 2001, Kip and Strehler, 2003). It may therefore be possible that in the absence of a CaSR, this signalling does not occur or this process is disturbed. At the VSMC level, this would be crucial if the CaSR is indeed, as previous studies have shown, protective against vascular calcification (Alam *et al.*, 2008). It may be the case that CaSR exerts its effects locally on Ca^{2+}-channels expressed in VSMCs. Voltage-gated Ca^{2+}-channels and Ca^{2+}-activated channels play a significant role in the transport of Ca^{2+} in and out of the cell. It has recently been shown that CaSR, which is expressed in human VSMCs, mediates increases in cytosolic Ca^{2+} when Ca^{2+}_o is applied in extracellular solutions in a concentration-dependent manner (Chow *et al.*, 2011). The same group showed that when a dominant-negative CaSR was transfected into these VSMCs, Ca^{2+} entry and increases in cytosolic Ca^{2+} were significantly reduced. Furthermore, the use of PLC inhibitors in WT VSMCs simulated this effect (Chow *et al.*, 2011). If this is also true in our SM22α x fl CaSR mouse model, it may be likely that KO VSMCs have less Ca^{2+}_i or a reduced uptake of Ca^{2+}_o from extracellular environments in response to CaSR ablation when compared to WT VSMCs. In this instance, it could be speculated that KO VSMCs would have less contractile tone compared to WT VSMCs which will be investigated in Chapter 4 and Chapter 5.

Consequences of hyperkalaemia in SM22α x fl CaSR KO mice.

Additionally observed in KO mice at 3 months of age was slight hyperkalaemia compared to WT mice. Although this was not seen in older mice, it may be an indication that renal function is disturbed in younger mice. Often, increases in serum K^+ indicate kidney dysfunction, possibly due to an alteration in the renin-angiotensin-aldosterone system (RAAS). Typically, renin promotes the conversion of angiotensinogen from the liver to angiotensin I. Angiotensin I then undergoes a conversion by angiotensin converting enzyme (ACE) to angiotensin II. Ultimately angiotensin II has effects on increasing K^+ excretion and water retention. Additionally, aldosterone secreted by the

adrenal glands in response to angiotensin II promotes these actions. Problems with renin and angiotensin activation would cause such increases in K^+ retention (Schmieder *et al.*, 2007, Sevá Pessôa *et al.*, 2012). Indeed, if K^+ is elevated, this would suggest that aldosterone is either downregulated or dysfunctional. To confirm whether this is true and if RAAS is dysfunctional, renin, ACE and aldosterone levels should be investigated in the future.

The role of the VSMC-CaSR on FGF23 secretion.

In addition to hypercalcaemia, FGF23 was significantly and consistently upregulated at 3 and 18 months of age. In order to understand how FGF23 can affect cardiovascular physiology, one must consider its role in the bone-parathyroid-kidney axis. FGF23 is typically produced by osteocytes and osteoblasts in response to high Pi or in the presence of $1,25(OH)_2D_3$ where it enters the circulatory system (Bergwitz and Jüppner, 2010). In terms of parathyroid interactions, the co-receptor of FGF23, Klotho, has been shown to be localised in the parathyroid where it binds FGF23 (Iddo *et al.*, 2007). FGF23 acts directly on the parathyroid gland to decrease PTH secretion through the inhibition of PTH mRNA, having downstream consequences of reducing serum Ca^{2+}_o, $1,25(OH)_2D_3$ and increasing Pi excretion (Iddo *et al.*, 2007). In regards to the SM22α x fl CaSR mouse model this seems somewhat contradictory since both Ca^{2+} and FGF23 levels are synchronously and inappropriately elevated. Since Ca^{2+}_o is up- or down-regulated in response to many regulating factors including Pi, PTH, FGF23 and $1,25(OH)_2D_3$, it is clear that one mechanism in this system dominates such that hypercalcaemia and high FGF23 levels can both be present and sustained. This once again suggests a possibility of high serum Pi possibly resorbed from bone, or retained in the kidney. It is possible that Pi may be the driver of both FGF23 secretion and hypercalcaemia by driving PTH secretion from the PTG. It was also shown that KO mice of 18 months of age have significantly heavier hearts compared to WT mice. FGF23 has been shown to promote left ventricular hypertrophy and cardiac remodelling in CKD patients (Gutiérrez *et al.*, 2009). If there is indeed a kidney phenotype in KO mice, this could also explain heavier hearts as a consequence of elevated FGF23 levels through adulthood. These possible hypotheses will be addressed in Chapter 7.

CHAPTER 3: CONCLUSION

In vivo phenotypic characterisation of the SM22a x fl CaSR mouse model.

Together my observations thus far include:

VASCULAR CALCIFICATION FEATURE	SM22α x fl CaSR
Hypercalcaemia (>2.5mM)	√
Elevated FGF23 levels (>200pg/mL)	√
Increased heart mass	√
High Ca^{2+} / High FGF23 together	√

Table 6. The relevance of the SM22α x fl CaSR mouse as a model of vascular calcification. Key features of vascular calcification are listed in the left column. Ticks indicate the presence of the abnormality detected in the *in vivo* analysis. Further research remains to fully elucidate the effectiveness of this model and confirmation of CaSR playing a role in VC, CKD and blood pressure modulation.

These observations point towards a role for CaSR in vascular physiology, maintenance of vascular tone and modulation of vascular calcification. These will be tested in the following experiments in Chapters 4-6.

It is clear that the SM22α x fl CaSR meets a significant proportion of the criteria essential for the development of vascular calcification. Although more extensive research remains to be conducted, it appears from this initial *in vivo* study that the VSMC-CaSR does play a significant role in the development, or events leading to vascular calcification.

Chapter Acknowledgments

CHAPTER 3: FUTURE WORK

Future work required to ascertain the role of the VSMC-CaSR in this *in vivo* system would be to analyse serum PTH, Pi and $1,25(OH)_2D_3$. Additionally, it would be beneficial to look for ectopic mineralisation in isolated blood vessels using specific mineral stains such as alizarin red. However, our collaborators have looked for calcification in KO mice at the age of 12 months and saw no calcification by µCT (data not shown). It is therefore likely that (i) µCT is not a sensitive enough method to detect small calcifications in blood vessels, or (ii) there is an upregulation of protective factors in response to VSMC-CaSR ablation preventing ectopic calcification. These issues can be addressed by analysing mouse serum for protective factors such as MGP and fetuin-A. Finally, since blood pressure is often a key indicator of altered cardiovascular function, it would make sense to analyse this in WT and KO mice. Tail cuff apparatus should be used to determine any differences between WT and KO blood pressures. In addition to this, myogenic tone should be investigated in both WT and KO mouse arteries. This will be performed in Chapter 4.

CHAPTER 4:

EX-VIVO CHARACTERISATION OF THE SM22α X fl CaSR MOUSE MODEL: MODULATION OF TONE IN RESPONSE TO VASOCONSTRICTORS AND VASORELAXANTS

CHAPTER 4: GENERAL INTRODUCTION

To further characterise the effects of CaSR ablation in vascular smooth muscle cells, *ex vivo* myography experiments were performed. This approach offers a unique experimental advantage of observing the effects and consequences of this gene knockout on vascular tone modulation. In this chapter, the effects of vasoconstrictors and vasorelaxants in isolated aortae and mesenteric arteries will be investigated. Blood vessels from both WT and KO mice will be assessed for their contractile responses to these vasoconstrictors and vasorelaxants. Wire myography (See Methods: 2.9 Wire myography on acutely isolated mouse aortae and mesenteric arteries) will be used to determine relaxation but not dilation since the apparatus does not measure this.

CHAPTER 4: RESULTS
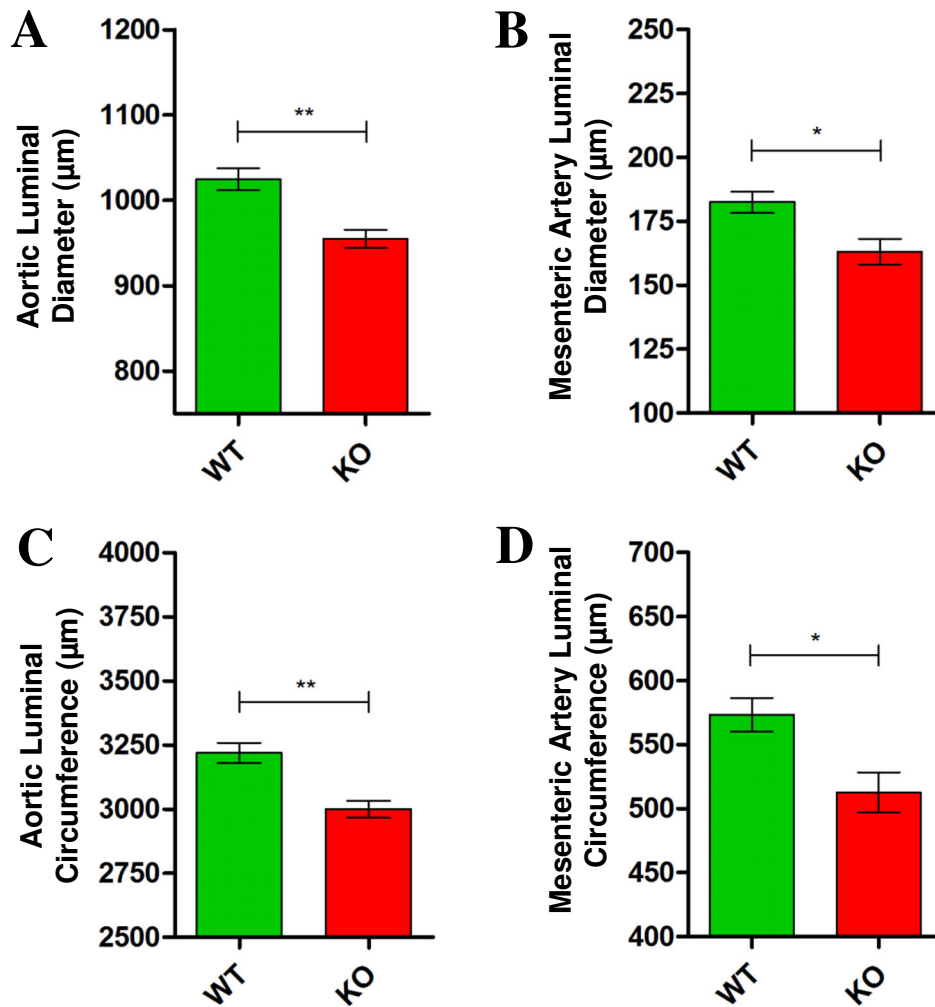
Figure 42. CaSR ablation in mouse VSMCs decreases the luminal diameter of thoracic descending aortae and mesenteric arteries. WT and KO mouse aortic rings and mesenteric artery rings were obtained from 5-6 month old animals. Vessels were pre-warmed to 37ºC in Krebs buffer containing 1.0mM Ca^{2+}_o as described in methods and mounted onto a wire myograph with either 40µm or 25µm diameter steel wire or gold wire (for aortae and mesenteric arteries respectively). Aortic rings were stretched by 100µm every 30 seconds, and mesenteric arteries by 20µm until a plateau was reached. For vessel acclimatisation to the myograph and buffer, the internal diameter of the vessel was set to a resting tension equivalent to that generated at 0.9 times the diameter of the vessel which was 40 mmHg for mesenteric arteries and 100 mmHg for aortae. This initial normalisation was performed in all myography experiments hereafter. Tension was recorded in milliNewtons (mN) and diameters were calculated using "Basic Normalisation" software (DMT, Denmark). (A) Luminal diameters of WT and KO aortae. (B) Luminal diameters of WT and KO mesenteric arteries. (C) Circumferences of WT and KO aortae. (D) Circumferences of WT and KO mesenteric arteries. Data expressed as average ± SEM. Statistical analysis: unpaired two-tailed t-test. P<0.05=*. P<0.01=**.

KO SM22α x fl CaSR mice have narrower aortae and mesenteric arteries compared to WT SM22α x fl CaSR mice.

In order to assess whether the VSMC-CaSR plays a role in vascular wall thickness, I used normalisation software provided by DMT for the analysis of luminal diameters and circumferences of rodent arteries. This software includes LaPlace's equation for the normalisation of tension in blood vessels. The assumption of this equation is that the tension (T) of the wall of the blood vessel is directly proportional to its radius (r) and pressure (p). This tension can be calculated as follows:

$$\text{T}_{(kg/s^2)} = \text{p}_{(kPa)} \text{ X } \text{r}_{(mm)}$$

In order to use LaPlace's equation to calculate the tension and diameter in a specific blood vessel, the micrometer dial is twisted to stretch wires apart by defined amounts. Using the wire myography mounted with, e.g. an aortic segment, I achieved the normalised internal circumference. This is the circumference one would expect to achieve in the resting vessel tension in the body. In the mouse, this is at 100mmHg and 40mmHg in aortae and mesenteric arteries respectively. Using LaPlace's equation, which plots tension and vessel radius, I defined this normalised internal circumference (IC_{100}) as the point at which the experimental data from the vessel ring meet with this on LaPlace's line. This value is taken as the resting vessel radius or circumference, and from this one can record vessel diameters or circumferences in WT and KO blood vessels. This can be demonstrated below:
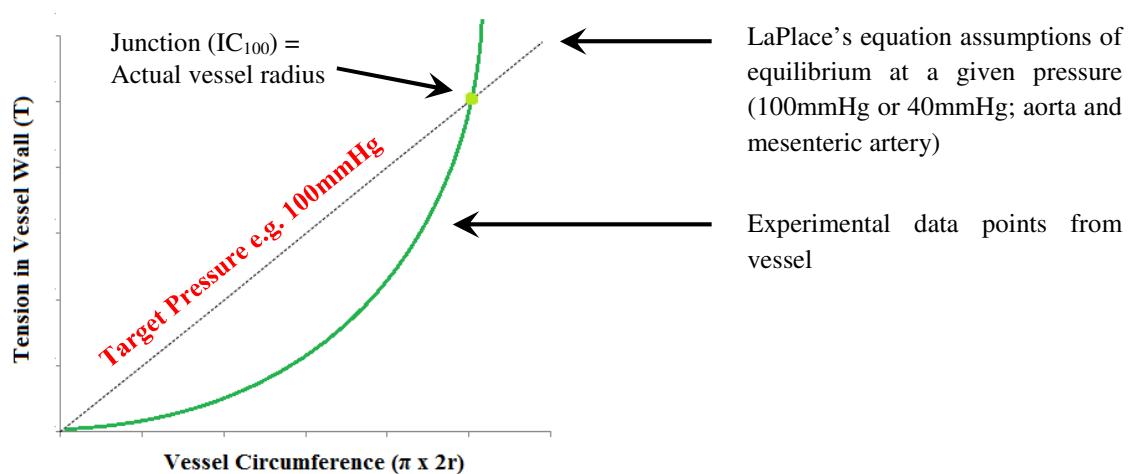
One should note that since this is not a closed *in vivo* circulatory system and only a small ring segment, this needs to be considered in the mathematics. For this reason, it is suggested that the internal circumference is set at 0.9 times the circumference one would expect under this pressure *in vivo*. Furthermore, since the tension required for each vessel is different, LaPlace's linear line will vary accordingly and is calculated using the following equation:

$$\text{Tension}_{\text{("X" mmHg)}} = \text{"X"} \times \left(\frac{IC}{2\pi}\right)$$

For the aorta, this would be "$40 \times \left(\frac{IC}{2\pi}\right)$" using the experimental data to generate the linear line to which the IC_{100} is calculated. Using this initial normalisation, one can calculate the normalised internal circumference specifically for each vessel ring, however for all experiments resting tension for the aorta was provided at 4mN and 2mN for mesenteric arteries since this is widely regarded as acceptable. Although the normalisation process was carried out, this was specifically to calculate the dimensions of the vessels and to elude any differences between WT and KO blood vessels.

In all experiments it was found that body organ weights and vessel diameters in male and females were not significantly different (data not shown), so male and female mouse data were pooled per genotype. Aortae and mesenteric vessels from mice were stretched ~100μm or ~20μm respectively every 30 seconds or when needed to reach the plateau. After each stretch, vessel tone was allowed to plateau and values of tension were tabulated against the distance the wires were apart. These values were entered into the DMT software where LaPlace's equation generated a graph as shown on the previous page for each ring segment. This procedure generated internal diameters and circumferences for all rings used. All aortic rings were considered for analysis, however, due to the selection process involved in dissecting mesenteric arteries and the inherent variance in vessel size and number in the gut, only mesenteric arteries of 2nd and 3rd order (between 100 and 200μm diameter) were considered and were selected for statistical analysis. For the aorta, diameters were 1025.00μm ± 12.72 (WT; N=8) vs. 955.00μm ± 10.51 (KO; N=6), while the average circumferential diameters were calculated by

multiplying these values by π. These were 3219.00µm ± 39.96 (WT; N=8) vs. 3000.00µm ± 33.02 (KO; N=6). Both parameters were significantly different at P<0.01 (Figure 42). For mesenteric arteries diameter (between 100-200µm) were 182.50µm ± 4.20 (WT; N=8) vs. 163.10µm ± 5.03 (KO; N=5) with circumferential diameters of 573.20µm ± 13.20 (WT; N=8) vs. 512.50µM ± 15.79 (KO; N=5). Both parameters were significant at P<0.05.
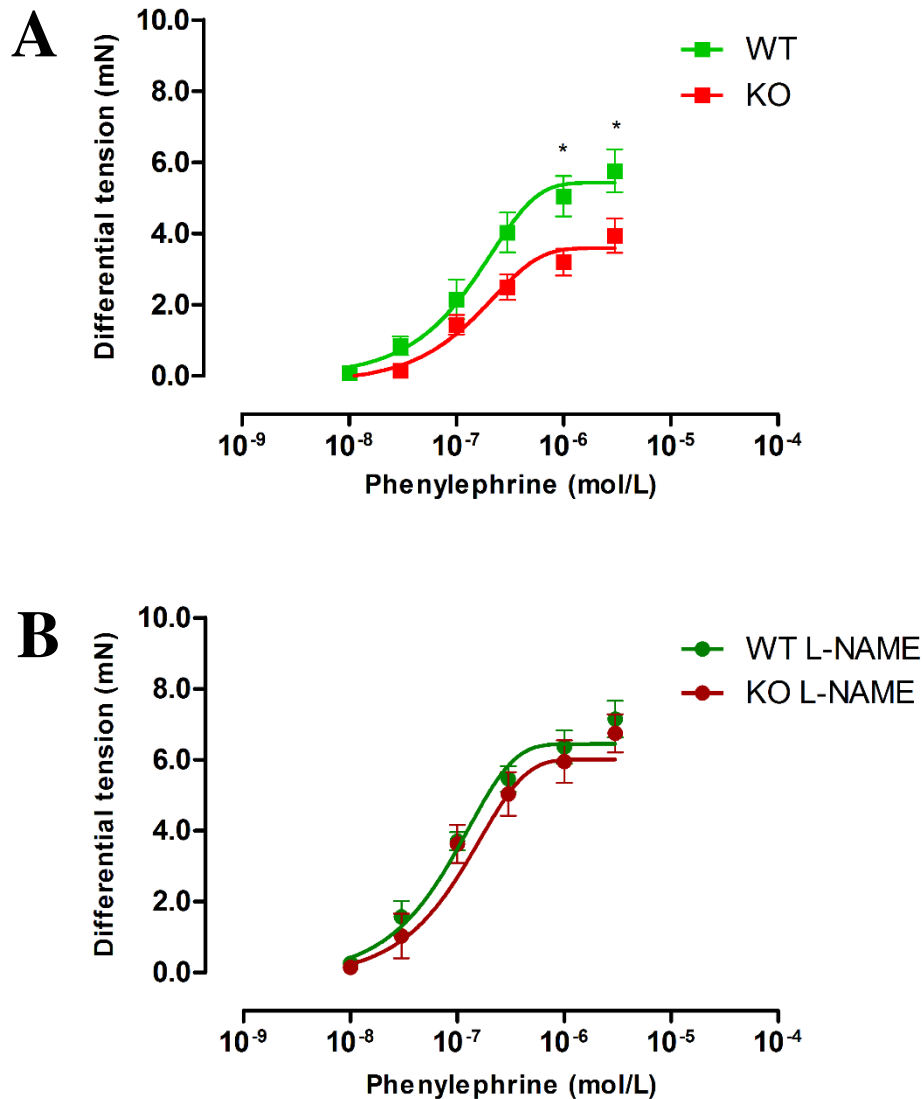
Figure 43. Selective CaSR ablation from mouse VSMCs decreases the vascular tone of mouse aortae in response to phenylephrine but not in the presence of L-NAME. WT and KO mouse aortic rings from 5-6 month old mice were mounted onto a wire myography as described in methods. Once vessels were manually stretched to 4mN, phenylephrine was applied to the bath in the myography chamber. Concentrations used ranged from 1×10^{-8}M to 3×10^{-6}M. After each application, vessel tone was allowed to stabilise by leaving tone to plateau before applying the next concentration. Experiments were either conducted in the absence (A) or presence (B) of 100μM of the eNOS inhibitor L-NAME. (A): N=5 WT (EC_{50}= 1.82×10^{-7}M); N=5 KO (EC_{50}= 1.98×10^{-7}M). (B) N=4 WT L-NAME (EC_{50}= 9.56×10^{-8}M); N=5 KO L-NAME (EC_{50}= 9.32×10^{-8}M. Sigmoidal lines of best fit are applied to data and data are expressed as mean ± SEM. Statistical analysis: two-way ANOVA. P<0.05=*. ns= not significant.
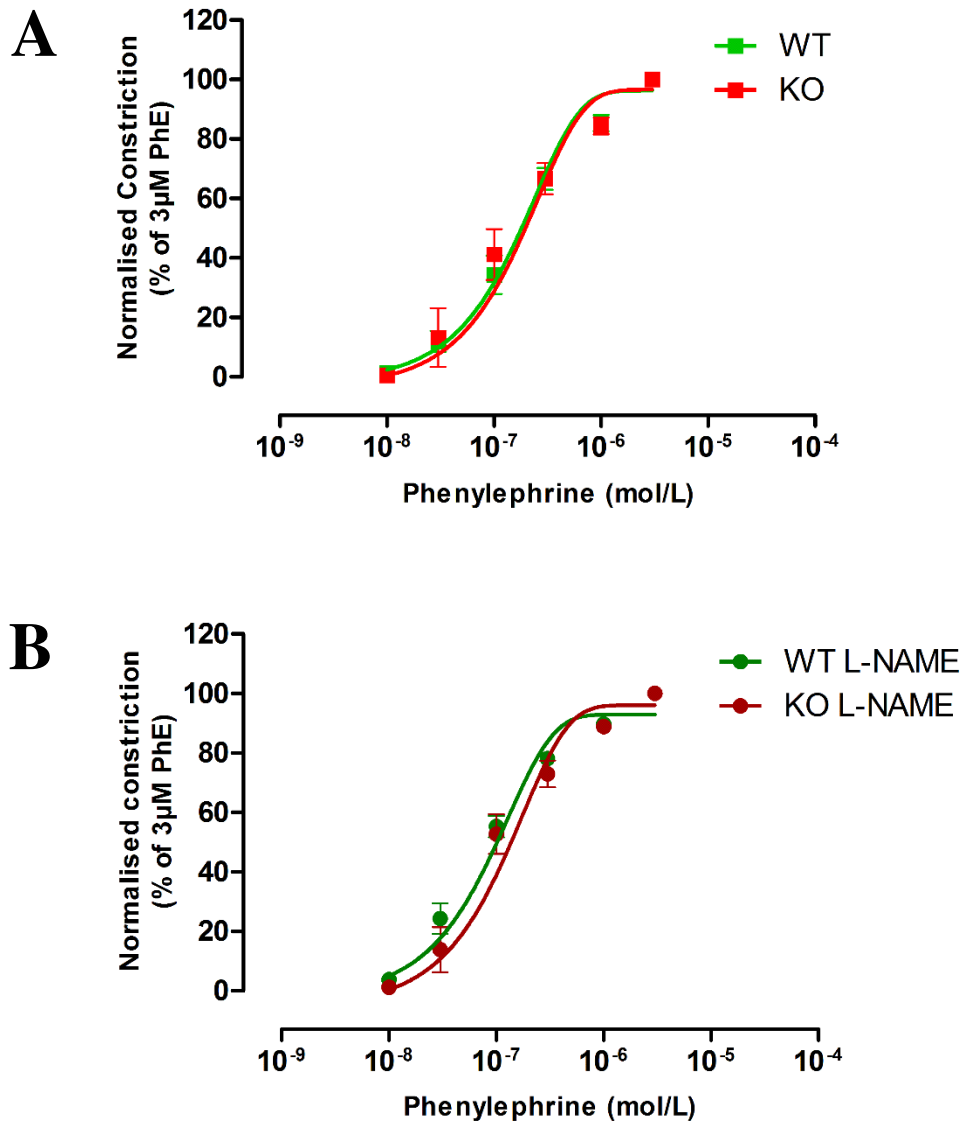
Figure 44. Selective CaSR ablation from mouse VSMCs does not affect concentration-response sensitivity to phenylephrine in mouse aortae in the presence or absence of L-NAME. Data presented are from aortic rings from the previous figure and have been normalised to the maximum concentration of phenylephrine used 3×10^{-6}M (3µM). For each vessel, the highest tone achieved was considered 100% with an application of 3×10^{-6}M phenylephrine. All lower concentrations of phenylephrine are expressed as percentages of this total maximum value from the starting point of 4mN (0%). Experiments were either conducted in the absence (A) or presence (B) of 100µM L-NAME. (A): N=6 WT ($EC_{50}= 2.01 \times 10^{-7}$M); N=5 KO ($EC_{50}= 1.71 \times 10^{-7}$M). (B) N=5 WT L-NAME ($EC_{50}= 9.24 \times 10^{-8}$M); N=5 KO L-NAME ($EC_{50}= 9.61 \times 10^{-8}$M). Sigmoidal lines of best fit are applied to data and data are expressed as mean ± SEM. Statistical analysis: two-way ANOVA. ns= not significant.
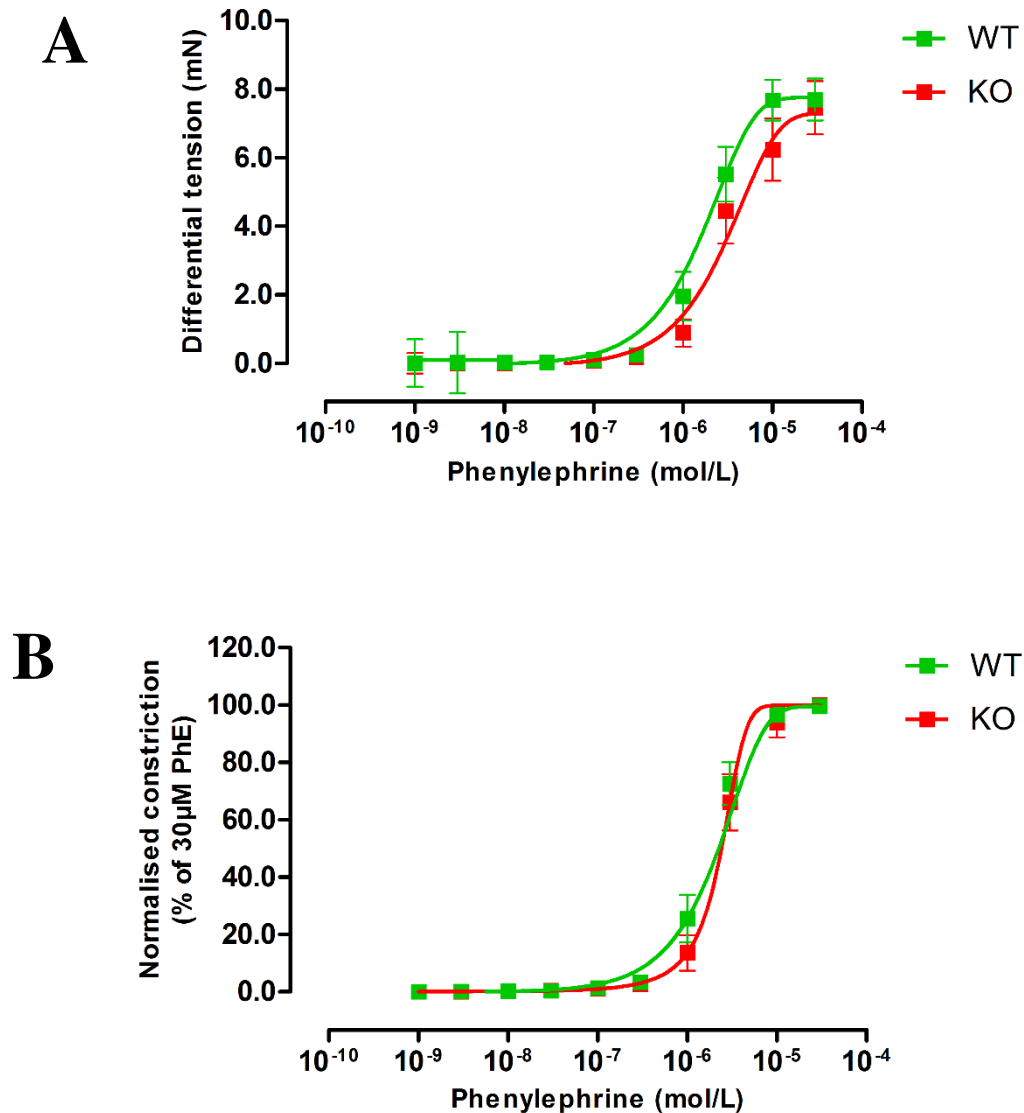
Figure 45. Selective CaSR ablation from mouse VSMCs does not affect phenylephrine concentration-responses in mesenteric arteries. WT and KO mouse mesenteric arteries from 5-6 month old mice were mounted onto a wire myograph as described in methods. Once vessels were manually pre-constricted to a force of 2mN, phenylephrine (PhE) was then applied: (A) in a concentration-dependent manner from 1 x 10^{-9}M to 3 x 10^{-5}M. For each vessel, the highest tone achieved was considered 100% with an application of 3 x 10^{-5}M (30μM) phenylephrine. All lower concentrations of phenylephrine are expressed as percentages of this total maximum value from the starting point of 2mN (0%). (A): N=8 WT (EC$_{50}$= 2.07 x 10^{-6}M); N=7 KO (EC$_{50}$= 2.60 x 10^{-6}M). (B): N=8 WT (EC$_{50}$= 2.03 x 10^{-6}M); N=7 KO (EC$_{50}$= 2.39 x 10^{-6}M). Sigmoidal lines of best fit are applied to data and data are expressed as mean ± SEM. Statistical analysis: two-way ANOVA. ns= not significant.
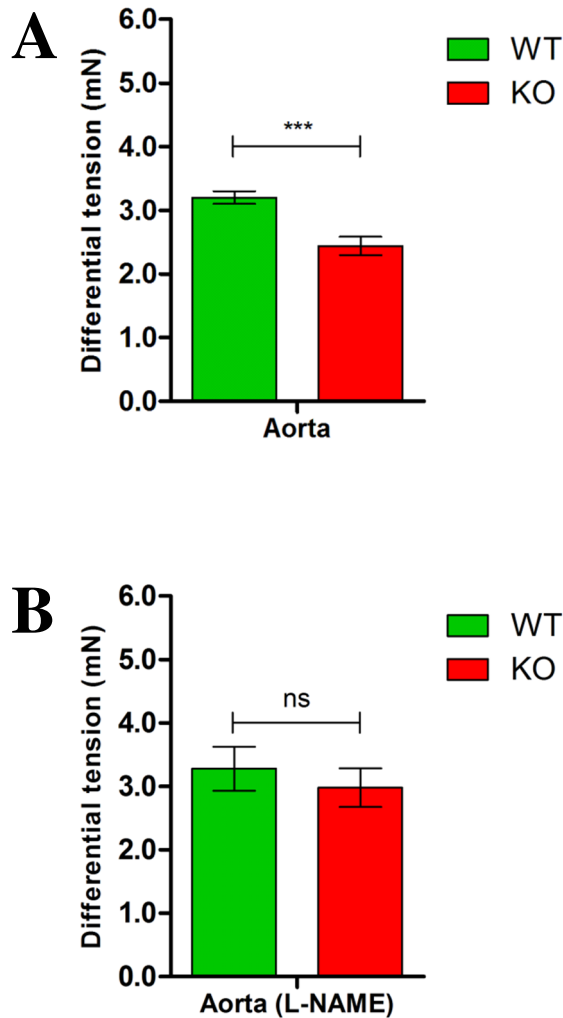
Figure 46. Selective CaSR ablation from mouse VSMCs significantly reduces KCl-induced vasoconstriction in the aorta in the absence, but not the presence of L-NAME. WT and KO mouse aortic rings from 5-6 month old mice were mounted onto a wire myograph as described in methods. Once vessels were manually normalised to 4mN, 40mM KCl was applied for 3 minutes until tone reached plateau. Tone from the 4mN starting point was calculated. (A) KCl-induced constriction in WT and KO aortic rings. (B) KCl-induced constriction in WT and KO aortic rings in the presence of 100μM L-NAME. (A): N=8 WT; N=5 KO. (B): N=5 WT L-NAME; N=6 KO L-NAME. Data are expressed as mean ± SEM. Statistical analysis: unpaired two-tailed t-test. P<0.001=***. ns= not significant.
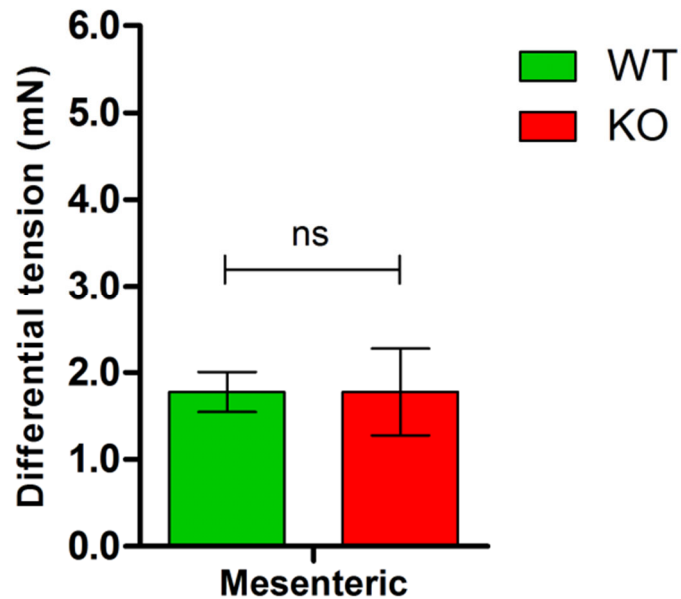
Figure 47. Selective CaSR ablation from mouse VSMCs does not reduce KCl-induced vasoconstriction in mesenteric arteries. WT and KO mouse mesenteric arteries from 5-6 month old mice were mounted onto a wire myograph as described in methods. Once vessels were manually pre-constricted to a force of 2mN, 40mM KCl was applied for 3 minutes until tone reached plateau. Differential tone from the 2mN starting point (0mN) was calculated. N=8 WT; N=5 KO. Data are expressed as mean ± SEM. Statistical analysis: unpaired two-tailed t-test. ns= not significant.

KO SM22α x fl CaSR mouse aortae have less contractile tone in response to phenylephrine and KCl when compared to WT SM22α x fl CaSR mouse aortae.

To determine whether a cardiovascular phenotype was present in KO mice, I assessed contractility of both WT and KO aortae and mesenteric arteries in response to vasoconstrictors phenylephrine and KCl. For the aorta, rings were manually stretched in Krebs buffer with 1.0mM Ca^{2+}_o, tensioned to 4mN and allowed to plateau. Typically, 2 aortic rings were used in every experiment per animal per condition. This meant that for an experiment with N=5 there were n=10 separate aortic rings. Data from all aortic rings from one mouse were averaged to get a representation of the whole aorta. However, in experiments using L-NAME, only one aortic ring was used per animal.

In mouse aortae, there was an observable trend for KO aortic rings to contract less than WT aortic rings in the presence of both phenylephrine and KCl (Figure 43 and 46). Phenylephrine was applied at concentrations ranging from 1×10^{-8}M to 3×10^{-6}M with each concentration added approximately every 2 minutes when the vascular tone reached plateau. Only in the presence of 1×10^{-6}M and 3×10^{-6}M phenylephrine were these differences significant (P<0.05; Figure 43A). These were: (i) for 1×10^{-6}M phenylephrine 5.05mN ± 0.57 (WT: N=5) vs. 3.20mN ± 0.38 (KO: N=5); (ii) for 3×10^{-6}M phenylephrine 5.76mN ± 0.61 (WT: N=5) vs. 3.94mN ± 0.48 (KO: N=5). These differences were not observed in the presence of L-NAME where both WT and KO aortic rings reached maximum tension at 7.14mN ± 0.51 (WT: N=4) vs. 6.74mN ± 0.53 (KO: N=5; not significant; Figure 43B). Data from these experiments were also normalised to determine whether WT and KO aortae were responding differently to these vasoconstrictors. Tone between the 4mN baseline and tone achieved from the maximal 3µM phenylephrine concentration represented a range of 0-100% contraction respectively. Tone achieved by each concentration of phenylephrine in both WT and KO aortic rings was therefore a % value within this range. In this way, it was shown that although KO aortae had reduced contractile tone, both WT and KO aortae responded to phenylephrine the same way (Figure 44), suggesting that the number of α_1-adrenergic receptors and their signal transduction machinery downstream of receptor activation was not affected by CaSR ablation from VSMCs.

In addition to the receptor-dependent vasoconstrictor phenylephrine, KCl was applied to determine any differences in vascular tone in WT and KO aortae through cell depolarisation through ion channels. As previously shown, phenylephrine was less effective at contracting KO aortic rings, with less contraction compared to WT aortic rings. In these experiments, it also was shown that KCl contracted KO aortic rings less than WT aortic rings. In the absence of L-NAME, maximal tone from 40mM KCl was 3.20mN ± 0.10 (WT: N=8) vs. 2.44mN ± 0.14 (KO: N=5), which was significant (P<0.001, Figure 46). In the presence of L-NAME this was not significantly different. In the presence of L-NAME, tone achieved by 40mM KCl addition was 3.28mN ± 0.35 (WT: N=5) vs. 2.98mN ± 0.30 (KO: N=6, Figure 46).

There is no significant difference in the contractile tone between WT and KO SM22α x fl CaSR mouse mesenteric arteries in response to phenylephrine or KCl.

Mesenteric arteries from WT and KO mice were also assessed for differences in phenylephrine and KCl responses. The same protocol was carried out for this experiment, except mesenteric arteries were manually tensioned to 2mN (vs. 4mN in the aorta). Concentration response curves to phenylephrine ranging from 1×10^{-9}M 3×10^{-5}M were performed in the presence of 1.0mM Ca^{2+}_{o}. At a maximal concentration of 3×10^{-5}M phenylephrine, tone achieved was 7.70mN ± 0.22 (WT: N=8) vs. 7.46mN ± 0.29 (KO: N=7) which was not significant (Figure 45). Similarly, when assessing the normalised % tone achieved for each concentration of phenylephrine compared to the maximum concentration of 30µM, there were no significant differences in these responses between WT and KO mesenteric arteries (Figure 45). Additionally, 40mM KCl did not evoke any significant differences between contractile tone in WT and KO mesenteric arteries. For 40mM KCl addition, vascular tone in mesenteric arteries was 1.78mN ± 0.23 (WT: N=8) vs. 1.78mN ± 0.50 (KO: N=5, Figure 47).
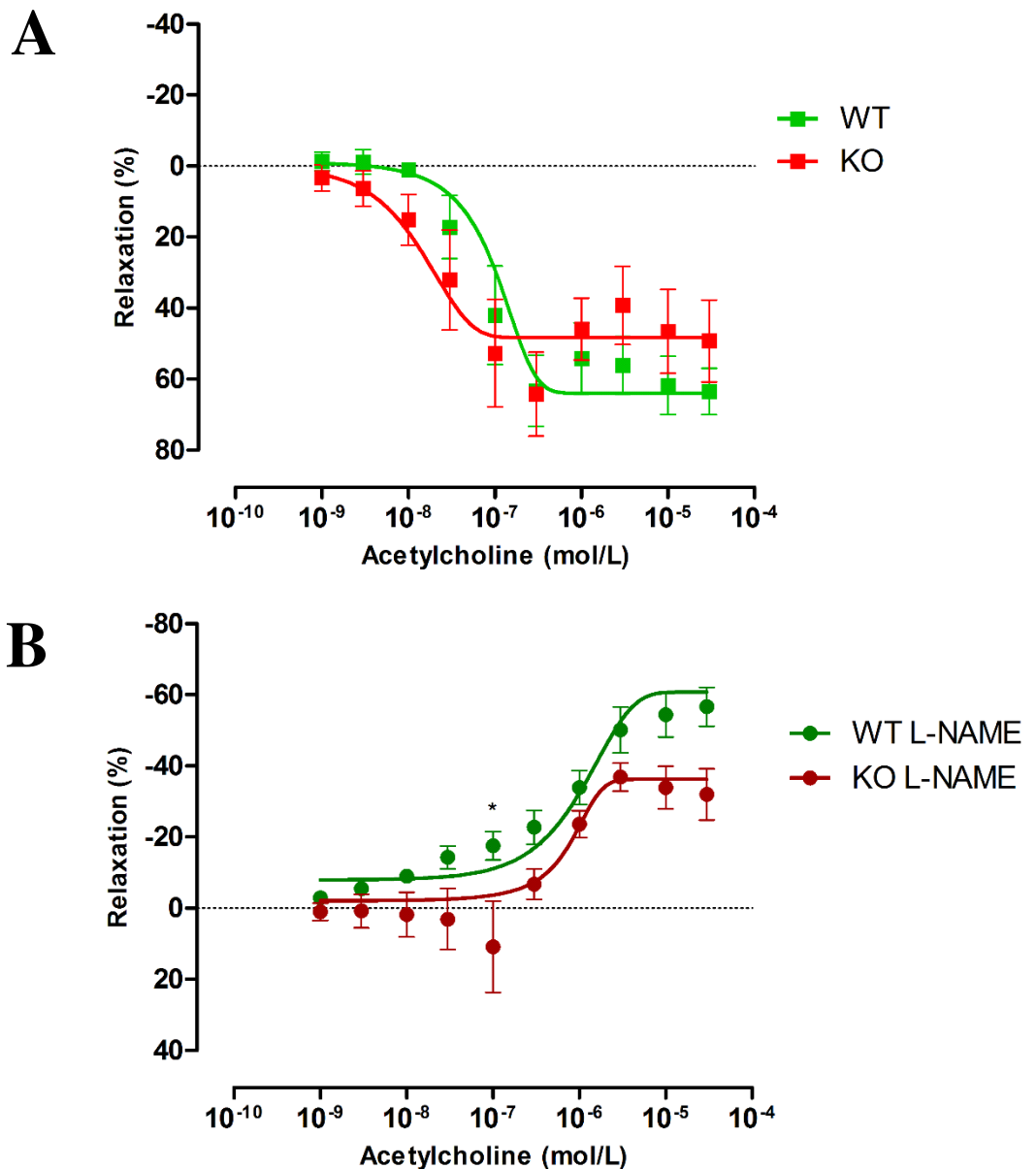
Figure 48. Selective CaSR ablation from mouse VSMCs does not significantly affect acetylcholine-induced relaxation in mouse aortae, but may reduce contraction in the presence of L-NAME. WT and KO mouse aortic rings from 5-6 month old mice were mounted onto a wire myograph as described in methods. Once vessels were manually tensioned to 4mN, 70% of the maximum tone was applied. In all cases, this was 300nM phenylephrine and once the tone had reached plateau, a concentration response of acetylcholine was performed of concentrations 1 x 10^{-9}M to 3 x 10^{-5}M. Percentage relaxation to acetylcholine of the phenylephrine pre-constricted aortic rings was calculated. (A): N=5 WT (EC_{50}= 6.93 x 10^{-8}M); N=5 KO (EC_{50}= 5.55 x 10^{-7}M). (B): N=4 WT L-NAME (EC_{50}= 7.41 x 10^{-7}M); N=5 L-NAME (EC_{50}= 5.72 x 10^{-7}M). Trends in the absence of L-NAME were not significant (A), however, trends in the presence of L-NAME were significant (B; P<0.001). Sigmoidal lines of best fit are applied to data and data are expressed as mean ± SEM. Statistical analysis: two-way ANOVA with Bonferroni's post-test. P<0.05=*, ns= not significant.

Acetylcholine is equally effective at relaxing both WT and KO SM22α x fl CaSR mouse aortae.

In order to assess changes in tone of the aorta in response to vasorlaxants and to determine whether any pathological conditions such as vessel stiffening or CaSR-knockout could interfere with tone, acetylcholine concentration-response curves were carried out on WT and KO aortic rings. To assess the role of vasorelaxants, acetylcholine was used for these experiments. Aortic rings were mounted in a wire myograph in the presence of 1.0mM Ca^{2+}_o as described, manually stretched to reach passive tension of 4mN before applying phenylephrine to obtain ~70% of the maximal vascular tone. This was determined previously by the phenylephrine concentration response curve, in all cases the concentration of phenylephrine required to achieve 70% of tone was 300nM. After the tone had stabilised and reached a plateau, an acetylcholine concentration-response was carried out as described using concentrations of the drug ($1 \times 10^{-9}M – 3 \times 10^{-6}M$). For aortic rings in the absence of L-NAME, there was no significant difference between WT and KO at any concentration ($P > 0.05$). There was, however, a difference between the EC_{50} values of WT ($6.93 \times 10^{-8}M$) and KO ($5.55 \times 10^{-7}M$) aortic rings. It was also observed that, after a concentration of approximately $3 \times 10^{-7}M$ acetylcholine, which has often been shown to contract vessels (Lüscher and Vanhoutte, 1986, Vanhoutte *et al.*, 2005), KO aortic rings appeared to contract more than WT aortic rings. It was however interesting to see that the maximal percentage relaxation achieved on average in both WT and KO aortic rings were very similar. This was seen at the concentration of $3 \times 10^{-7}M$ acetylcholine with 63.39% ± 10.01 (WT; N=5) vs. 64.29% ± 11.81 (KO; N=5). These values were not significantly different to one another (Figure 48).

Acetylcholine is more effective at contracting WT aortae in the presence of L-NAME than KO aortae from SM22α x fl CaSR mice.

The eNOS inhibitor L-NAME was used (100µM; Figure 48B) to determine whether nitric oxide signalling was altered in the relaxation or contraction of WT and KO aortae. L-NAME suppressed acetylcholine-induced relaxation and evoked contraction at concentrations greater than 1×10^{-7}M in both WT and KO aortae. It was seen that only in the presence of 100nM acetylcholine were differences in tone different between WT and KO aortae: 1×10^{-7}M was -17.44% (contracted) ± 4.02 (WT: N=4) compared with 10.90% (relaxed) ± 12.82 (KO: N=5). However, a two-way ANOVA of the WT and KO curves shows that there is a significant trend for WT aortae to contract more in the presence of L-NAME compared to KO aortae (P<0.001), indicating once again that KO aortae have reduced contractile tone. This trend was shown when the two-way ANOVA compared WT vs. KO aortae at all concentrations of acetylcholine tested. Contraction achieved by maximum concentrations of acetylcholine (3×10^{-5}M) was not significantly different. Percentage tone achieved at 3×10^{-5}M acetylcholine was: -56.56% (contracted) ± 5.451 (WT; N=4) vs. -31.93% (contracted) ± 6.44 (KO; N=5; Figure 48B).
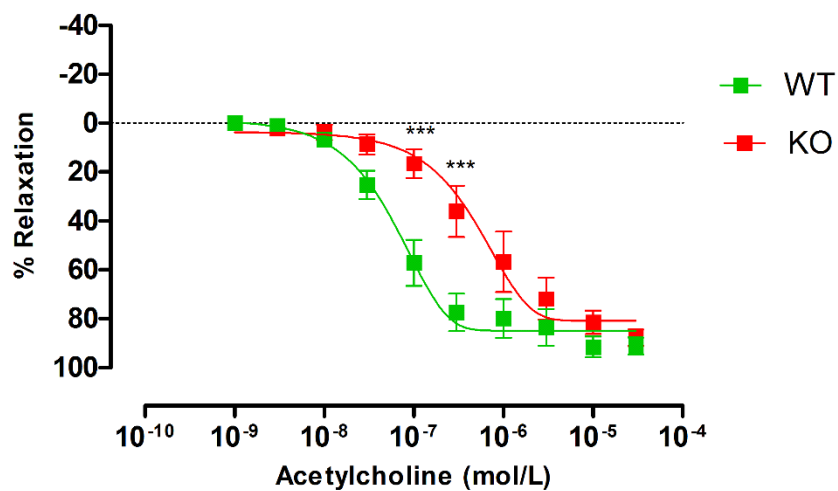
Figure 49. Selective CaSR ablation from mouse VSMCs significantly delays the acetylcholine-induced relaxation in mesenteric arteries. WT and KO mouse mesenteric arteries from 5-6 month old mice were mounted onto a wire myograph as described in methods. Once vessels were manually tensioned to 2mN, 70% of the maximum tone was applied. In all cases, this was 3μM phenylephrine. Once the tone had reached plateau, a concentration response of acetylcholine was performed (1×10^{-9}M to 3×10^{-5}M). Percentage relaxation from the phenylephrine pre-constricted aortic rings was calculated. (A): N=7 WT (EC_{50}= 7.50×10^{-8}M); N=5 KO (EC_{50}= 5.65×10^{-7}M). Sigmoidal lines of best fit are applied to data and data are expressed as mean ± SEM. Statistical analysis: two-way ANOVA. $P<0.001$=***. ns= not significant.

Mesenteric arteries in KO SM22α x fl CaSR mice exhibit an impaired response to acetylcholine compared to WT SM22α x fl CaSR mesenteric arteries.

Mesenteric arteries were pre-contracted with 300nM phenylephrine (to achieve ~70% tone) before an acetylcholine concentration response was performed in the same way as aortic rings. Once tone had stabilised, vessels were exposed to an acetylcholine concentration response with concentrations ranging from $1 \times 10^{-9}M - 3 \times 10^{-5}M$. Interestingly, significant differences were seen at the concentrations of $1 \times 10^{-7}M$ and $3 \times 10^{-7}M$ acetylcholine, where KO mesenteric arteries relax less than WT arteries. Relaxation at these concentrations were: 57.20% ± 9.40 (WT: N=7) vs. 16.60% ± 5.90 (KO: N=5) at $1 \times 10^{-7}M$ and; 77.5% ± 7.70 (WT: N=7) vs. 36.10% ± 10.50 (KO: N=5) at $3 \times 10^{-7}M$. For both of these concentrations, differences were significant using a two-way ANOVA test ($P < 0.001$; Figure 49). Despite these differences, when the maximum concentration of $3 \times 10^{-5}M$ acetylcholine was applied, both WT and KO mesenteric arteries reached the same amount of maximum relaxation compared to the initial 2mN tone. These values at $3 \times 10^{-5}M$ were: 91.20% ± 3.50 (WT: N=7) vs. 87.90% ± 3.40 (KO: N=5). Due to time constraints, the role of L-NAME on acetylcholine-induced relaxation in mesenteric arteries was not investigated.

CHAPTER 4: DISCUSSION

VSMC-CaSR ablation in SM22α x fl CaSR mice reduces blood vessel size in mice of 6 months.

CaSR ablation from VSMCs resulted in a reduction in the luminal diameter and circumference of aortae and mesenteric arteries (Figure 42). These data suggest that the VSMC-CaSR may play an important role in VSMC proliferation, vasculogenesis and vascular tone modulation. One can presume that differences observed in both conducting and resistant vessels could come from increases in VSMC numbers within the vascular wall, possibly brought about by increases in proliferation. Tunica media thickening by VSMC proliferation may cause minor occlusion of arteries. In fact, several studies have shown that specific activation of CaSR by calcimimetics is associated with a reduction in VSMC proliferation (Wada *et al.*, 1997b, Smajilovic *et al.*, 2006). If CaSR activation is associated with a reduction in VSMC proliferation, this would suggest that in the absence of a CaSR, VSMCs may proliferate at greater rates, unhindered by CaSR. If this is indeed the case, this hypothesis can be tested by isolating WT and KO VSMCs and determining proliferation rates *in vitro* (investigated in Chapter 6). Indeed, it has been well-documented that VSMC proliferation is associated with vascular disease where vascular damage, atherosclerosis, calcification and transdifferentiation can increase proliferation rates (Simionescu *et al.*, 2005). However, more importantly in context of the CaSR, other investigators have shown that the VSMC-CaSR is a critical modulator of proliferation, where activation by CaSR agonists can increase proliferation (Molostvov *et al.*, 2008). To investigate whether VMSC populations are greater in KO compared to WT mouse arteries further studies are required to determine their ability to proliferate *in vitro*, and to measure the media thickness of blood vessels in both WT and KO age-matched animals.

VSMC-CaSR ablation in SM22α x fl CaSR mice reduces contractile tone in the aorta but not in the mesenteric arteries.

Reduced vessel diameters seen in vessels from KO animals may be responsible for the reduced contractile force. It was shown in KO aortae that there was less contractile force in response to phenylephrine and KCl, only in the presence of NO (Figure 43, Figure 46). If the VSMC population of the tunica media is significantly different between WT and

KO animals, then this will presumably affect the contractile responses of these cells. Additionally, this may correlate with fewer features associated with normal vessel contraction. For example, a reduction in the total cell number would suggest less total myosin and α_1-adrenergic receptors for phenylephrine-induced contraction of the whole VSMC population in the tunica media. For this reason, it would perhaps not be so surprising that contractility was reduced significantly in KO mouse aortae. Contrary to this, L-NAME treated WT and KO vessels had the potential to contract to the same capacity in response to phenylephrine (Figure 43B). This would suggest that a factor may be at work which inhibits the full contraction in the absence of L-NAME. For this reason, one could speculate that KO vessels have increased NO activity, and so the relative VSMC number or potential differences in media thickness may not be such major contributors to reductions in vessel contractility. To test this hypothesis, future work is required to measure the transcriptional regulation of eNOS in KO mice, in addition to NO activity within vessels.

It is also important to remember that KO mice exhibit hypercalcaemia (Figure 36D, Figure 37D). Hypercalcaemia in patients with inactivating mutations of CaSR is often associated with hypertension (Frank-Raue *et al.*, 2011). Conversely, it is also reported that increases in dietary intake of Ca^{2+} induce a hypotensive effect in both humans and animals (Allender *et al.*, 1996, Buassi, 1998). However, since our SM22α x fl CaSR mouse is not a full inactivating mutant and has localised receptor ablation within the VSMCs, it is difficult to determine whether this hypercalcaemia evokes hyper- or hypotensive effects in these mice without having carried out blood pressure measurements. However, from the data in-hand, the reduced contractile tone in KO vessels would suggest a hypotensive phenotype of our KO animals.

In the experimental setup, the buffer that vessels were immersed in contained 1.0mM Ca^{2+}_o. Since we know from *in vivo* serum analysis that KO mice have hypercalcaemia, it would be interesting and informative to try and match the Ca^{2+}_o concentrations observed *in vivo* in the *ex vivo* setup. i.e. keep the base-line Ca^{2+}_o concentration for WT and KO vessels the same as observed *in vivo*. The fact that hypercalcaemia is present in KO mice

and that KO vessels contract less is somewhat more difficult to interpret. It is possible that elevated total serum $[Ca^{2+}]$ in KO mice promotes the NO pathway in endothelial cells leading to decreased contraction. Importantly, CaSR-KO VSMCs are acclimatised *in vivo* to higher total $[Ca^{2+}]$ (~3.0mM Ca^{2+}; Figure 36D, Figure 37D). It is crucial to note that this 3.0mM $[Ca^{2+}]$ represents both free ionized and bound Ca^{2+}. Free ionized Ca^{2+} should be half this value (~1.5mM). If this is true, placing them in the presence of 1.0mM Ca^{2+}_o in the experimental buffer would presumably impair the base-line contractile response observed *in vivo*. It would be beneficial to quantify the precise free-ionized Ca^{2+} concentration in WT vs. KO mice. It may also be the case that VSMCs in KO mice have adapted and remodelled significantly in response to life-long CaSR ablation in these cells in combination with hypercalcaemia.

Interestingly, significant reductions in tone were not observed in KO mesenteric arteries with phenylephrine (Figure 45) or KCl (Figure 47), even when KO mesenteric vessels were, overall, narrower than WT mesenteric vessels ($P<0.05$). Mesenteric arteries are much smaller and narrower than the aorta, and so contain less VSMCs in the tunica media (Miller *et al.*, 1987, Wagenseil and Mecham, 2009, Wagenseil *et al.*, 2009, Wagenseil *et al.*, 2010). For this reason, the EC:VSMC ratio is different to that of the aorta, although it should be noted that in both the aorta and mesenteric arteries there is one luminal monolayer of endothelial cells. Therefore, it may not be so surprising that differences observed in the WT and KO aorta were not also observed in mesenteric arteries. Additionally, it should be noted that both ECs and VSMCs express a CaSR which may play different and contrasting roles to one another (Weston, 2005, Alam *et al.*, 2008). Since there were no significant differences in contractile tone between WT and KO mesenteric arteries, it is plausible that the VSMC-CaSR plays a minimal role in tone modulation of resistance arteries which may or may not be detectable using wire myography. For this reason, we may need to measure such responses in these blood vessels using a different and more sensitive setup, possibly by employing electrophysiological techniques. By using such a setup, one could measure electrochemical currents in WT and KO VSMCs in response to vasoconstrictors, vasorelaxants and CaSR agonists.

VSMC-CaSR ablation in SM22α x fl CaSR mice does not significantly affect acetylcholine-induced relaxation but reduces contraction in the presence of L-NAME.

In WT and KO aortic rings exposed to an acetylcholine concentration-response in the absence of L-NAME, there was no significant difference (Figure 48A). This could be due to the relatively small numbers of animals. According to the power calculation, the sample size should be between 8 and 10 to indicate significance at P<0.05. Despite this, the EC_{50} values were different from one another (WT 6.93×10^{-8}M vs. KO 5.55×10^{-7}M) suggesting that acetylcholine is more potent in KO aortic rings. If this is indeed true, this would suggest that KO aortae may have greater NO activity in response to lower concentrations of acetylcholine. In the presence of L-NAME there was a significant difference in contractile ability between WT and KO aortae exposed to an acetylcholine concentration-response (P<0.001). Once again, less contractile tone was observed in the KO compared to WT aortae. Since this was seen in the presence of L-NAME, these differences should not be attributed to NO activity. It is therefore likely that there is either an upregulation of EDHFs in the aorta to prevent contraction, or that the decreased luminal diameter of KO aortae affects the contractile effects of acetylcholine in this way. It is also entirely possible that other endothelium-dependent dilation and relaxation pathways are different in KO arteries.

VSMC-CaSR ablation in SM22α x fl CaSR mice reduces the relaxation response of mesenteric arteries.

KO mesenteric arteries were shown to have a delayed concentration-dependent relaxation in response to acetylcholine when compared to WT mesenteric arteries. This meant that the cumulative response curve to acetylcholine was shifted to the right in KO arteries compared with WT arteries. Figure 49 shows that acetylcholine-induced relaxation in WT vessels started at approximately 3×10^{-9}M, while in KO vessels this started later at concentrations of 3×10^{-8}M. This result would suggest that acetylcholine is not as effective at producing a response in KO arteries compared to WT arteries. This may be due to a number of reasons. Firstly, acetylcholine binds to M3 GPCRs present on the endothelium. Since responses were shifted approximately 10-fold (EC_{50} values: 7.50

x 10^{-7}M WT vs. 5.65 x 10^{-7}M KO) stated, it may be that M3 receptors present in the endothelium of KO vessels are downregulated, therefore, relaxation following M3 receptor binding is less effective when compared to WT vessels. Conversely, upregulated M3 receptors may enhance the sensitivity of ECs to acetylcholine. Acetylcholine is associated with efflux of K^+ through SK_{Ca} and IK_{Ca} channels and it has been speculated that local K^+ clouds which form in myoendothelial environments can inhibit K^+-induced hyperpolarization and dilation of VSMCs by numerous groups (Busse *et al.*, 2002, Edwards and Weston, 2004). It has also been reported that NO, which plays a significant role in endothelium-dependent dilation and relaxation in larger vessels such as the aorta, plays less of a role in mesenteric arteries. These studies have shown that although NO is effective at inducing hyperpolarization in mesenteric arteries, this does not always result in relaxation (Garland and McPherson, 1992, Bolz *et al.*, 1999, Buus *et al.*, 2000). In relation to the previous hypothesis of NO upregulation in the aorta, is seems plausible that this may also be the case in mesenteric arteries, however, here it is not able to relax vessels as effectively.

Another important observation in these studies was that KO mesenteric arteries had a significantly narrower lumen compared to WT mesenteric arteries. This may also play an important role in inhibiting the relaxation response in numerous ways: (i) less endothelial cells due to a reduced luminal area that line these narrower vessels are present to respond to acetylcholine; (ii) vessel narrowing might be ascribed to thickening of the tunica media or a less developed tunica media; (iii) endothelium-dependent hyperpolarisation factor release may be suppressed in the mesenteric arteries from KO mice; and (iv) acetylcholine-dependent relaxation is partially impaired in KO mesenteric arteries. Each of these potential mechanisms would presumably alter the ability of VSMCs to co-ordinate vasocontractile or relaxation responses from adjacent ECs in mesenteric arteries.

CHAPTER 4: CONCLUSION

The VSMC-CaSR plays a significant role in the modulation of vascular tone in response to pharmacological agonists *ex vivo*.

Basic physiological responses from vasoconstrictors and vasorelaxants are very different across WT and KO aortae and mesenteric arteries. My results clearly demonstrate the important role of the VSMC-CaSR in vessel tone regulation as previous investigators have suggested (Ohanian *et al.*, 2005, Rybczyńska *et al.*, 2005, Weston, 2005, Smajilovic *et al.*, 2006, Smajilovic *et al.*, 2007). We have seen that, under the conditions tested, KO vessels generally exhibit less contractile tone, likely due to an increased basal level of NO compared to WT vessels. It is unclear whether this is the case *in vivo* and whether this may play a role in cardiovascular defects such as vascular calcification, atherosclerosis, or transdifferentiation of native VSMCs. The data suggest that the VSMC-CaSR is important in maintaining contractile response. When this is lost, contractile responses are reduced. My results suggest that VSMC-CaSR KO may reduce blood pressure, however, this remains to be investigated. If reductions in blood pressure are observed *in vivo*, it may be possible that the hypercalcaemia observed in KO mice contributes to this by promoting endothelium-dependent relaxation, or by switching the phenotypes of VSMCs to a less-contractile state.

CHAPTER 4: FUTURE WORK

My studies have shown that activation of adrenergic and muscarinic receptors in the VSMCs by their appropriate agonists has yielded different results when comparing WT and KO arteries. It would therefore be beneficial to test mRNA expression and protein levels of such receptors, in addition to other Ca^{2+}-channels such as Ca_V 1.2 which is highly expressed in VSMCs (Mangoni *et al.*, 2003, Rhee *et al.*, 2009). Additionally, eNOS expression and NO activity should be measured to confirm whether NO activity is significantly altered in KO vessels compared with WT vessels. Such experiments would be required in both aortae and mesenteric arteries in the presence and absence of L-NAME. If the observed hypotensive effects are true *in vivo*, this should be tested by carrying out blood pressure measurements on mice.

Also mentioned were the possible effects of differential baseline $[Ca^{2+}]_o$ used in myography experiments. If, indeed, the vasculature has acclimatised somehow to a hypercalcaemic environment *in vivo* then it is possible that numerous Ca^{2+}-related genes and proteins have been accordingly disturbed. Since WT VSMCs *in vivo* will be acclimatised to a total $[Ca^{2+}]$ of ~2.3mM (Figure 36D), and KO VSMCs *in vivo* will be acclimatised to a total $[Ca^{2+}]$ of ~3.0mM (Figure 36D), this hypercalcaemia seen in the KO would effectively act as the *in vivo* physiological base-line. After determining the $[Ca^{2+}]_o$ *in vivo* in both WT and KO mice, experiments should be repeated using these respective *in vivo* $[Ca^{2+}]_o$ as a baseline before application of contracting and dilatory and relaxation agents.

Chapter Acknowledgments

I would like to thank Dr. Polina Iarova for her help in these *ex vivo* studies. It was often a great deal of work to perform multiple dissections of numerous blood vessels in addition to the myography experiments that followed, and so her help with this is greatly appreciated.

CHAPTER 5:

EX-VIVO CHARACTERISATION OF THE SM22α X fl CaSR MOUSE MODEL: MODULATION OF TONE USING CaSR AGONISTS

CHAPTER 5: GENERAL INTRODUCTION

In order to determine the role of the CaSR in the modulation of vascular tone, it was crucial to conduct experiments where agonists of the receptor were used and to test the possibility that they might evoke differential responses in aortae and mesenteric arteries from WT and KO mice. In this chapter, the role of agonists of CaSR including Ca^{2+}_{o}, spermine and the calcimimetic R-568, will be investigated in the aorta and mesenteric artery using the *ex vivo* wire myography protocol. This way, consequences of activation at either the EC-CaSR or VSMC-CaSR can be determined in terms of vessel tone. In the aorta, the role of the VSMC-CaSR will also be investigated by excluding responses to NO using L-NAME.

CHAPTER 5: RESULTS
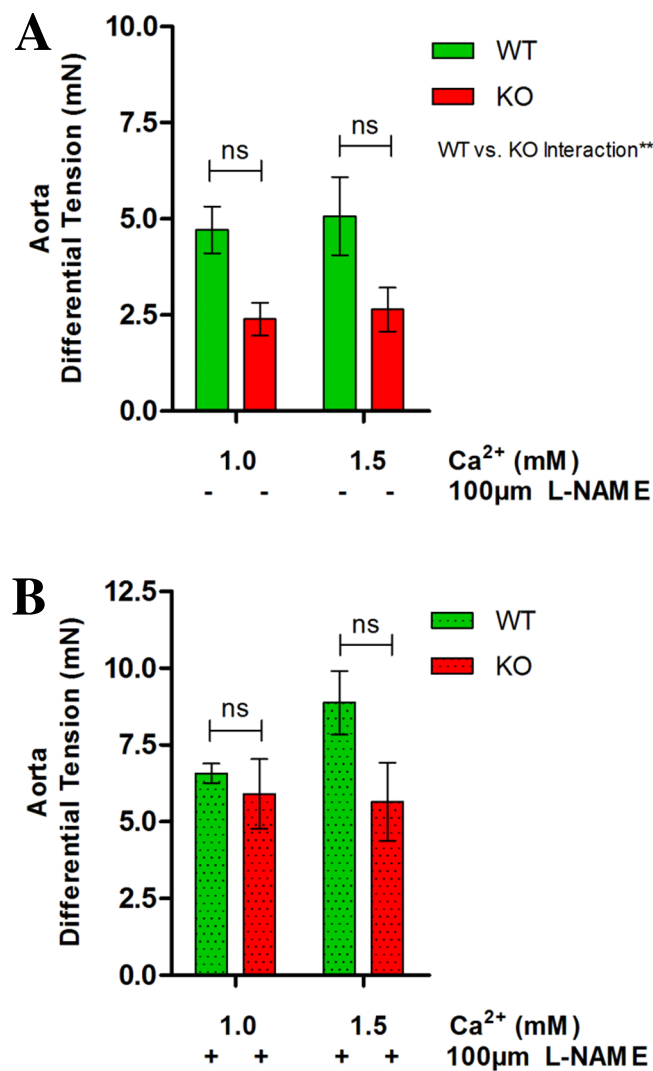
Figure 50. Selective CaSR ablation from mouse VSMCs reduces Ca^{2+}_o-induced vasoconstriction in the aorta. Mouse aortic rings were isolated as described and maintained in 1.0mM Ca^{2+}_o Krebs buffer. WT and KO aortic rings were incubated in the presence of 1.0mM Ca^{2+}_o or 1.5mM Ca^{2+}_o for 20 minutes before applying 300nM phenylephrine- which had previously been determined as the concentration required to achieve ~70% tone from a phenylephrine concentration response curve (Figure 43). Once tone had stabilised, differential tension was recorded for each vessel in the absence (A) or presence of L-NAME (100 μM) (A). WT N=4; KO N=4. (B) WT L-NAME N=3; KO L-NAME N=4. Data are expressed as mean ± SEM. Statistical analysis: two-way ANOVA with Bonferroni's post-test, P<0.01=**. ns= not significant.

Effects of Ca^{2+}_o on the modulation of phenylephrine-induced contraction.

It has previously been suggested that the CaSR might play a role in the modulation of vascular tone (Weston, 2005, Rybczynska *et al.*, 2006, Smajilovic *et al.*, 2006, Smajilovic and Tfelt-Hansen, 2008), In this set of experiments, the effects of $[Ca^{2+}]_o$ on the ability of aortae and mesenteric arteries from WT and KO animals to contact or relax was determined. For this purpose, 1.0mM Ca^{2+}_o (low activation of CaSR) and 1.5mM Ca^{2+}_o (high activation of CaSR) were used. Aortic rings were pre-incubated for 20 minutes with Krebs buffer containing either 1.0mM Ca^{2+}_o or 1.5mM Ca^{2+}_o then contracted using 300nM phenylephrine. After vessel tone had reached plateau (after approximately 3 minutes), the tension values before and after phenylephrine addition were recorded. For aortae in the absence of L–NAME, tension values were: 4.71mN ± 0.61 WT (N=4) vs. 2.39mN ± 0.42 KO (N=4, 1.0mM Ca^{2+}_o) and; 5.07mN ± 1.02 WT (N=4) vs. 2.64mN ± 0.57 KO (N=4, 1.5mM Ca^{2+}_o). In the presence of L-NAME tension values were: 6.57mN ± 0.32 WT (N=3) vs. 5.90mN ± 1.14 KO (N=4, 1.0mM Ca^{2+}_o) and; 8.87mN ± 1.03 WT (N=3) vs. 5.65mN ± 1.28 KO (N=4, 1.5mM Ca^{2+}_o). Although direct 1.0:1.5 mM Ca^{2+}_o comparisons in the absence of L-NAME were not significantly different, the ANOVA revealed that there was a significance difference (P<0.01) for WT:KO comparison for both Ca^{2+}_o concentrations, confirming observations in the previous chapter where WT aortic rings contract significantly more than KO aortic rings. Interestingly, in the presence of L-NAME a different set of observations was made. Firstly, it was consistently seen that all vessel rings contracted more with 100µM L-NAME (also seen in previous studies with phenylephrine concentration response curves) and secondly, although not significant, WT aortic rings contracted more in the presence of 1.5mM Ca^{2+}_o compared to 1.0mM Ca^{2+}_o. This trend was not observed in KO aortic rings.
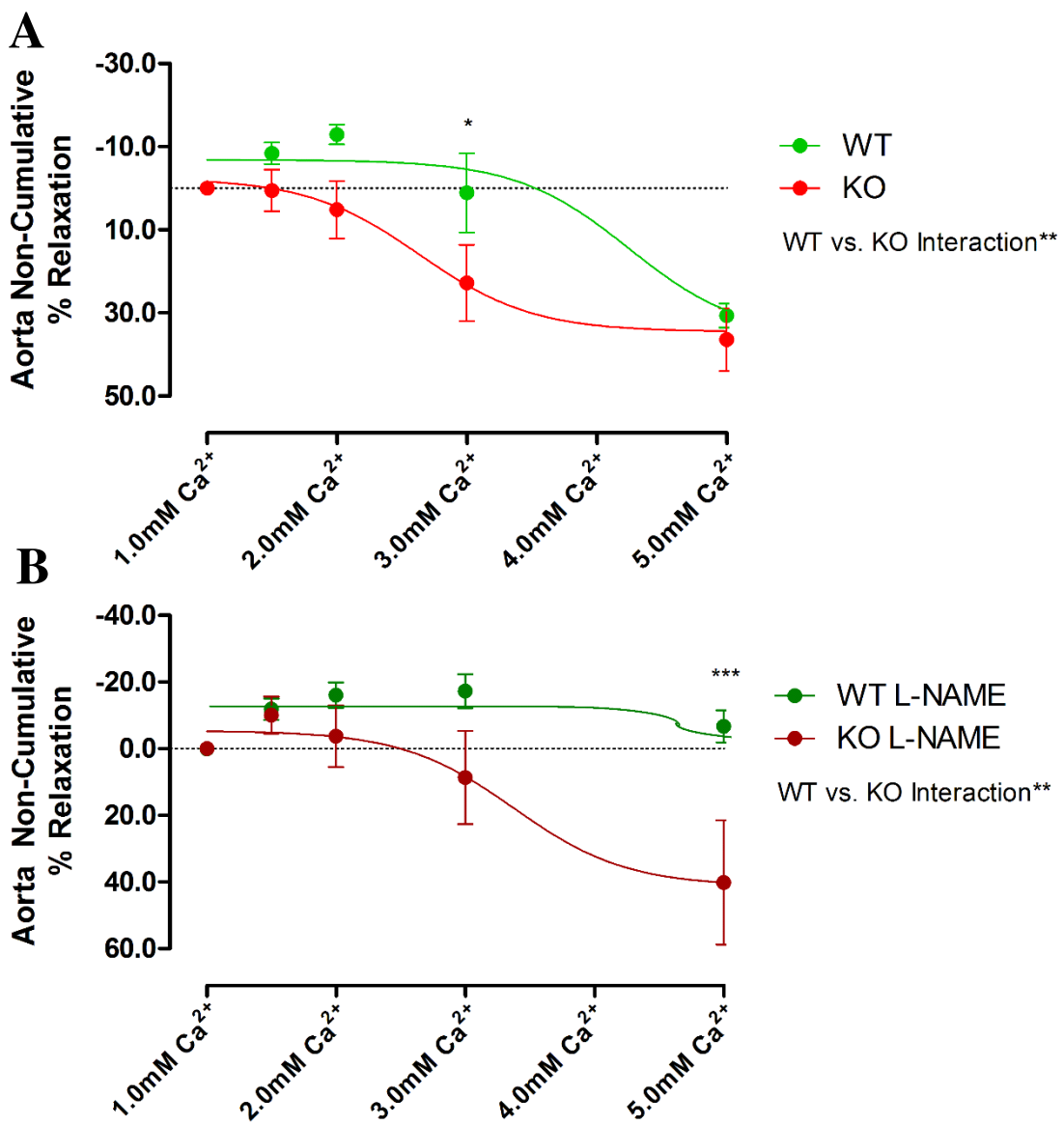
Figure 51. Selective CaSR ablation from mouse VSMCs prevents non-cumulative Ca^{2+}_o-induced vasocontraction. Aortic rings were isolated as previously described and incubated in Krebs buffer containing 1.0mM Ca^{2+}_o. Vessels were pre-constricted using 300nM phenylephrine to achieve 70% of maximum tone. After tone had reached a plateau, this point was considered the "0%" base-line. Ca^{2+}_o was then added to the solution to achieve concentrations of 1.5, 2.0, 3.0 and 5.0mM Ca^{2+}_o. After each addition, the response of the aortic rings was registered for 3 minutes. Time controls were also run in parallel where vessels did not have Ca^{2+}_o added with vehicle controls. These values were subtracted from each Ca^{2+}_o-supplemented well to remove normal tone drift responses. Once data had been recorded, wells were carefully washed with buffer and allowed to return to normal tone. Phenylephrine was applied freshly each time to perform a non-cumulative concentration response curve. (A) Ca^{2+}_o non-cumulative concentration response curve in the absence of L-NAME. (B) Ca^{2+}_o non-cumulative concentration response curve in the presence of 100µM L-NAME. (A) WT N=5 (EC_{50}= 3.53mM); KO N=5 (EC_{50}= 2.74mM). (B) WT L-NAME N=5 (EC_{50}= 3.75mM); KO L-NAME N=5 (EC_{50}= 3.41mM). Sigmoidal lines of best fit are applied to data and data are expressed as mean ± SEM. Statistical analysis: two-way ANOVA with Bonferroni's post-test. P<0.05=*. P<0.001=***. ns= not significant.

Ca^{2+}$_o$ induces vasoconstriction followed by vasorelaxation in aortic rings from WT mice, but only vasorelaxation in aortic rings from KO mice.

In order to investigate the role of Ca^{2+}$_o$ (the principal agonist of CaSR) on vascular tone, Ca^{2+}$_o$ concentration-response experiments were conducted. Two protocols were followed. Firstly, non-cumulative Ca^{2+}$_o$ concentration response curves to ascertain the significance of immediate application of a set concentration of Ca^{2+}$_o$ (Figure 51), and secondly; cumulative Ca^{2+}$_o$ concentration response experiments were carried out to determine the role of gradual Ca^{2+}$_o$ application over time. Ca^{2+}$_o$ is known to play different roles in tone modulation. It has been demonstrated that Ca^{2+}$_o$ induces vasoconstriction (Bohr, 1963, Crystal *et al.*, 1998, Wonneberger *et al.*, 2000) while others have reported it to induce relaxation (Bukoski *et al.*, 1997, Weston, 2005, Smajilovic *et al.*, 2006). In numerous studies, Ca^{2+}$_o$ is applied to vessels including the aorta where it induces relaxation, and it has since become widely accepted that Ca^{2+}$_o$ can induce endothelium-dependent relaxation of VSMCs (Bukoski *et al.*, 1997, Weston, 2005, Smajilovic *et al.*, 2006). However, some controversy remains as to the exact role of Ca^{2+}$_o$ in the cardiovascular system and its role in vascular tone.

Importantly, in these studies I used concentrations of Ca^{2+}$_o$ within the range of CaSR activation, and therefore within the sensitivity range of the CaSR (1.0-5.0mM Ca^{2+}$_o$). The purpose of these experiments was to unmask the role of the VSMC-CaSR in this process, determining any differences in conductance vs. resistance arteries. My observations show that in WT vessels, both Ca^{2+}-dependent contraction (negative values) and Ca^{2+}-dependent relaxation (positive values) were observed. In KO aortae, it appeared though only relaxation occurred, although on some occasions KO aortae contracted very slightly (~5%) in the presence of 1.5mM Ca^{2+}$_o$ while relaxing at all concentrations thereafter. In Figure 51, KO aortic ring responses from the 0% base-line were as follows: 1.5mM Ca^{2+}$_o$: -8.33% ± 2.60 WT (N=5) vs. 0.63% ± 5.00 KO (N=5); 2.0mM Ca^{2+}$_o$: -12.87% ± 2.38 WT (N=5) vs. 5.25% ± 6.94 KO (N=5); 3.0mM Ca^{2+}$_o$: -1.16% ± 9.53 (N=5) vs. 22.9% ± 9.17 KO (N=5) (P<0.05); 5.0mM Ca^{2+}$_o$: 30.72% ± 2.89 WT (N=5) vs. 36.49% ± 7.59 KO (N=4) (Figure 51A). These data suggest a biphasic response to Ca^{2+}$_o$ in aortae from WT mice and a monophasic (relaxation only) response to Ca^{2+}$_o$ in aortae from KO mice.

Ca^{2+}_o induces mild contraction and relaxation in aortic rings from KO mice in the presence of L-NAME, but only contraction in aortic rings from WT mice in the presence of L-NAME.

In contrast to the previous observations, treatment with L-NAME had quite opposite effects on aortae of both WT and KO mice. In WT aortae, the biphasic response was lost, and vessels only contracted in response to all concentrations of Ca^{2+}_o (1.5-5.0mM Ca^{2+}_o) with less contraction in the presence of 5.0mM Ca^{2+}_o. In KO aortae, small initial contractions were seen at 1.5 and 2.0mM Ca^{2+}_o. This was then followed by relaxation in all Ca^{2+}_o concentrations used thereafter. Therefore in the presence of L-NAME, KO aortae exhibited a biphasic response compared with the somewhat monophasic (contractile only) responses in WT aortae. For aortic rings in the presence of L-NAME, responses were as follows: 1.5mM Ca^{2+}_o -14.42% ± 2.15 WT (N=5) vs. -9.92% ± 5.54 KO (N=5); 2.0mM Ca^{2+}_o -19.55% ± 1.52 WT (N=5) vs. -3.69% ± 9.27 KO (N=5); 3.0mM Ca^{2+}_o -21.17% ± 3.90 WT (N=5) vs. 8.72% ± 13.98 KO (N=5); 5.0mM Ca^{2+}_o -8.99% ± 5.16 WT (N=5) vs. 40.24% ± 14.37 KO (N=4, P<0.001, Figure 51B).
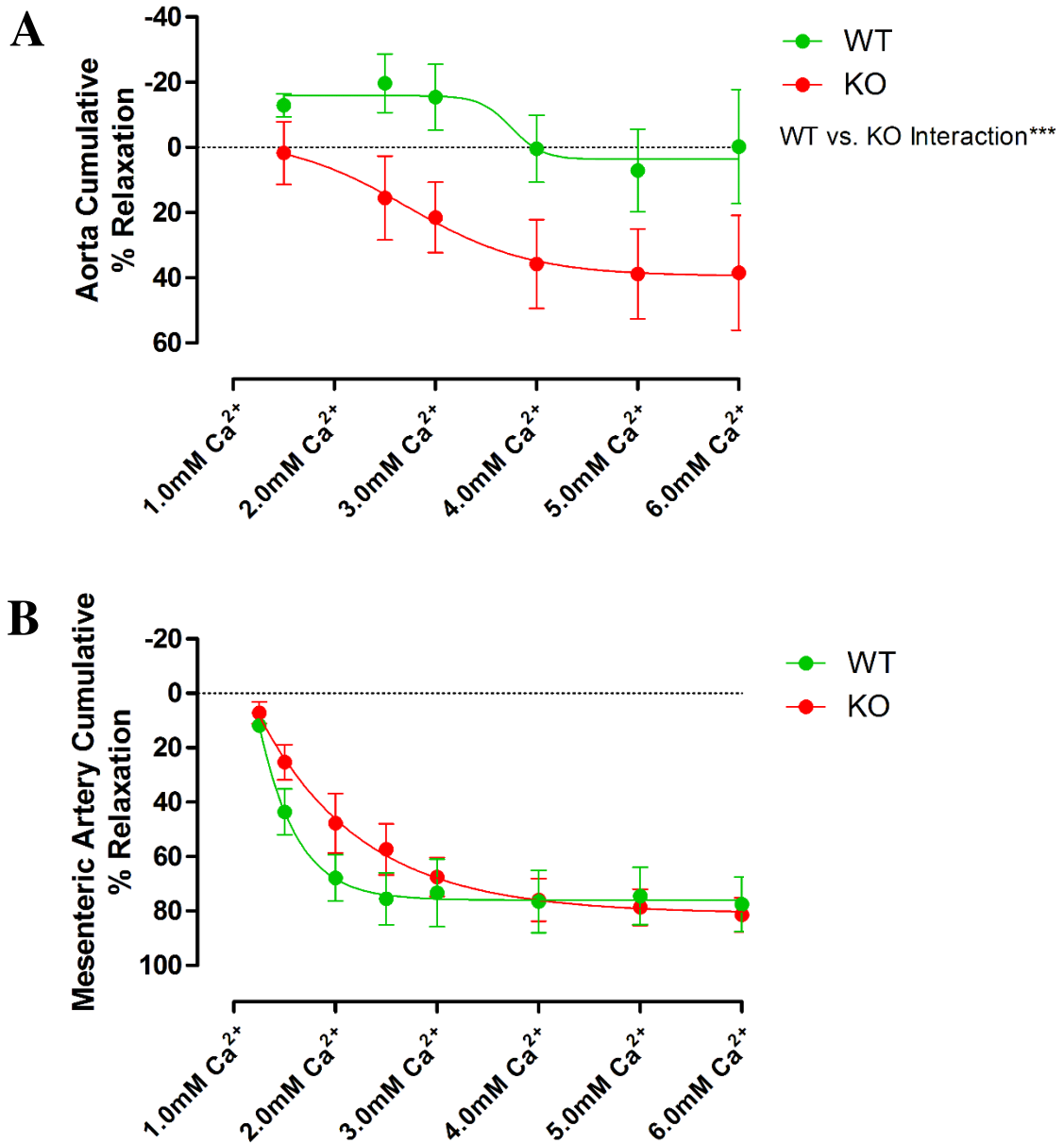
Figure 52. Effect of CaSR ablation on tone modulation by cumulative Ca^{2+}_o concentrations in aortae and mesenteric arteries. Aortic rings (A) and mesenteric arteries (B) were isolated as previously described and maintained in 1.0mM Ca^{2+}_o Krebs buffer. Experiments were carried out using the same concentrations of Ca^{2+}_o as in non-cumulative concentration response experiments in Figure 51, however, Ca^{2+}_o was instead applied cumulatively. Ca^{2+}_o was applied for ~3 minutes at each concentration before achieving a plateau and then applying the next concentration. (A) Cumulative Ca^{2+}_o concentration response curve in the aorta. (B) Cumulative Ca^{2+}_o concentration response curve in mesenteric arteries. (A) WT N=8 (EC_{50}= 3.84mM); KO N=5 (EC_{50}= 2.90mM). (B) WT N=8 (EC_{50}= 1.52mM); KO N=5 (EC_{50}= 1.92mM). Sigmoidal lines of best fit are applied to data and data are expressed as mean ± SEM. Statistical analysis: two-way ANOVA with Bonferroni's post-test. $P<0.001$=*** (WT vs. KO Interaction). ns = not significant.

CaSR ablation in mouse VSMCs does not affect Ca^{2+}_o-induced relaxation significantly in mesenteric arteries, but may play a role in aortic vascular tone.

In a similar manner to aortic rings exposed to non-cumulative Ca^{2+}_o application (Figure 51), cumulative Ca^{2+}_o application caused monophasic relaxation only in KO aortic rings (Figure 52). This finding was consistently observed at all concentrations tested (1.0-6.0mM Ca^{2+}_o). Thus, both data collected performing non-cumulative (Figure 51) and cumulative (Figure 52) Ca^{2+}_o concentration response curves were comparable. Additionally, consistent with my previous findings, WT aortic rings exhibited a biphasic response to Ca^{2+}_o. Although these data were not significantly different at each concentration, two-way ANOVA reveals that WT and KO responses are significantly different from one another across all concentrations (P<0.001). Furthermore, the profiles clearly match these that I observed previously in non-cumulative Ca^{2+}_o concentration response experiments whereby WT vessels initially contract and later relax (Figure 51). Genotype-dependent differences are particularly visible at concentrations of 2.0, 3.0 and 5.0mM Ca^{2+}_o with values as follows: 2.0mM Ca^{2+}_o: -10.40% ± 7.60 WT (N=8) vs. 7.70% ± 12.30 KO (N=5); 3.0mM Ca^{2+}_o: -15.30% ± 10.10 WT (N=8) vs. 21.60% ± 10.80 KO (N=5); 5.0mM Ca^{2+}_o: 7.20% ± 12.70 WT (N=8) vs. 38.90% ± 13.80 KO (N=5, Figure 52A).

It has been well-documented that Ca^{2+} can play opposing roles in conductance and resistance vessels, where conductance vessels contract to Ca^{2+} (Lee *et al.*, 2001, Guedes *et al.*, 2004) and resistance vessels relax in response to Ca^{2+} (Weston, 2005). This is also the case in our SM22α x fl CaSR mouse model where cumulative Ca^{2+}_o application induced relaxation in both WT and KO mesenteric arteries. These data were not significantly different. However, due to time constraints, only N=5 experiments were performed on KO mouse vessels. Using a power calculation, it is estimated that approximately 8-10 repeats will be required to achieve significance at P<0.05. Further repeats should be performed to fully assess whether Ca^{2+}_o plays a significant role in relaxation through the VSMC-CaSR in mesenteric arteries.
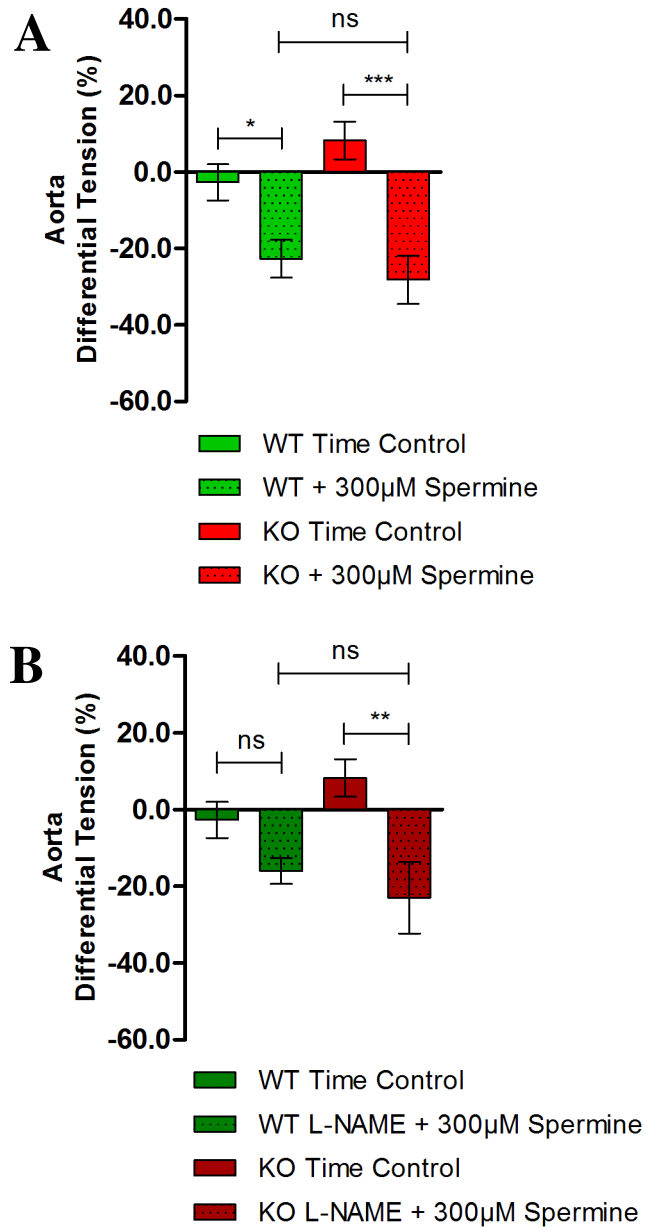
Figure 53. Selective CaSR ablation from mouse VSMCs increases spermine-induced relaxation in the aorta. Aortic rings were incubated in Krebs buffer as previously described and treated with 300nM phenylephrine to achieve 70% tone. Once tone had normalised, a measurement was taken at the plateau. This value was considered the 0% base-line. After this time, 300µM spermine was applied for 3 minutes. Time control experiments were also run to determine natural drift in each aorta. After 3 minutes, data were recorded and vessel rings were washed. (A) Spermine responses in WT and KO aortic rings in the absence of L-NAME. (B) Spermine responses in WT and KO aortic rings in the presence of 100µM L-NAME. (A) N=6 WT; N=7 KO. (B) N=4 WT; N=5 KO. Data are expressed as mean ± SEM. Statistical analysis: two-way ANOVA with Bonferroni's post-test. $P<0.05=$*. $P<0.01=$**. $P<0.001=$***. ns= not significant.

Spermine induces relaxation in KO and WT aortae in the absence of L-NAME, but only relaxes KO aortae in the presence of L-NAME.

Polyamines such as spermine are known CaSR activators (Quinn *et al.*, 1997, Canaff, 2000, Kelly *et al.*, 2011). For this reason, it was important to investigate whether spermine could affect vascular tone through the VSMC-CaSR. Spermine is positively charged at physiological pH, therefore having important implications on membrane potential as well as its ability to modulate the CaSR (Quinn *et al.*, 2004). Aortic rings were incubated in a physiological Krebs buffer containing 1.0mM Ca^{2+}_{o}; a concentration of Ca^{2+}_{o} which should cause minimal activation of CaSR. After phenylephrine pre-contraction, spermine was administered in a single application of 300μM. Once a plateau was reached as a consequence of application of 300nM phenylephrine, this point was considered as "0%" tone, and therefore, relaxation was measured as a percentage reduction from this value. To normalise for any drift in the tone of vessels over the course of spermine application (3 minutes), time controls were run in parallel and plotted (Figure 53). Upon spermine administration, relaxation was observed in both WT and KO aortae. In WT aorta relaxation was: 22.72% ± 4.95 WT (N=6) vs. -2.71% ± 4.74 WT time control (N=5, P<0.05). In KO aorta, relaxation was: 28.18% ± 6.30 KO (N=7) vs. 8.24% ± 4.88 KO time control (N=6, P<0.001, Figure 53). Spermine was significantly effective at relaxing both WT and KO aortae with greater relaxation in KO aortae compared to the time control. In the presence of L-NAME, relaxation was still observed. Values for WT aortae were: -16.02% ± 3.42 WT L-NAME (N=4) vs. -2.71% ± 4.74 WT time control (N=5) which was not significant. Values for KO aortae were: -22.97% ± 9.30 KO L-NAME (N=5) vs. 8.24% ± 4.88 KO time control (N=6, P<0.01). Although relaxation was maintained in the presence of L-NAME, it was reduced in both WT and KO aortae. This meant that WT aorta relaxation in the presence of L-NAME was no longer significantly different from the time control, while KO aorta relaxation in the presence of L-NAME was still present with a reduced P value (P<0.01, Figure 53B).
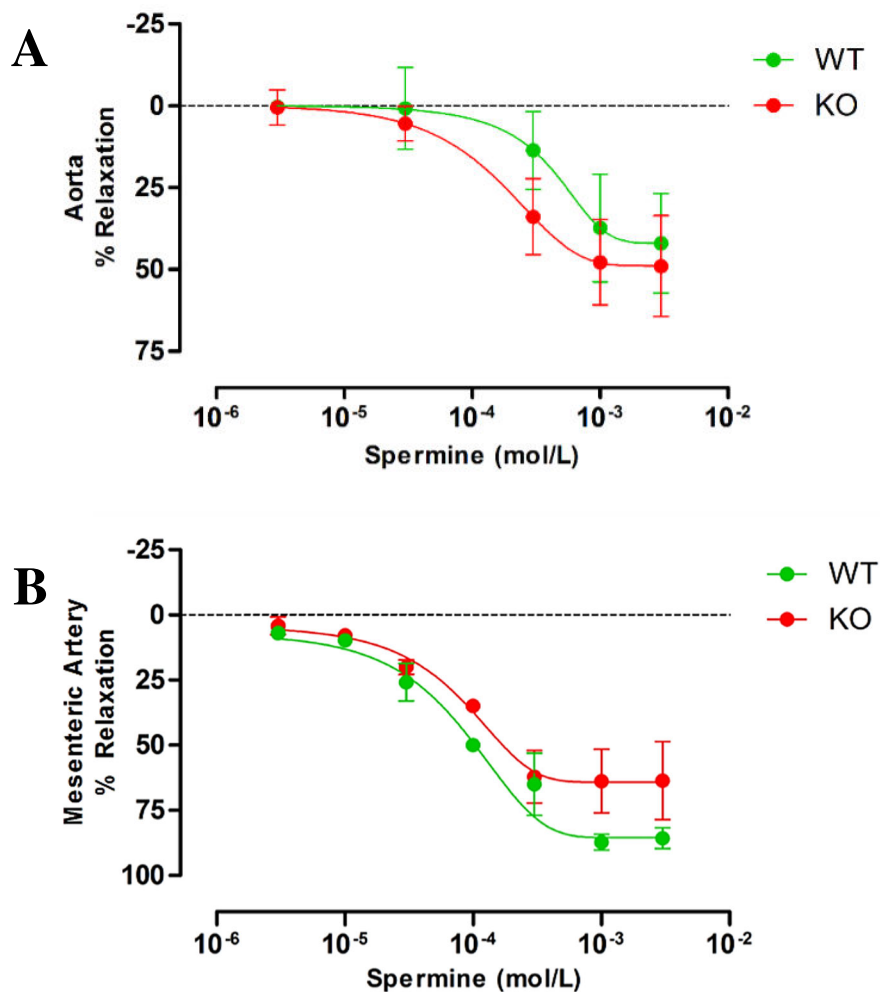
Figure 54. CaSR ablation in mouse VSMCs does not significantly affect spermine-induced relaxation of aortae and mesenteric arteries. Aortic (A) and mesenteric arteries (B) were incubated in Krebs buffer as previously described in the presence of 1.0mM Ca^{2+}_o. Vessels were pre-contracted using 300nM phenylephrine and tone was allowed to stabilise. A cumulative concentration-response curve for spermine was then carried out. Spermine was applied once tone achieved from the previous spermine application had stabilised. (A) WT N=6 (EC_{50}= 5.23 x 10^{-4}M); KO N=5 (EC_{50}= 2.13 x 10^{-4}M). (B) WT N=6 (EC_{50}= 1.76 x 10^{-4}M); KO N=5 (EC_{50}= 1.19 x 10^{-4}M). Sigmoidal lines of best fit are applied to data and data are expressed as mean ± SEM. Statistical analysis: two-way ANOVA with Bonferroni's post-test, ns= not significant.

Mouse VSMC CaSR ablation does not affect spermine-induced relaxation in WT and KO mesenteric arteries.

In addition to a single application of 300μM spermine (Figure 53), a concentration-response experiment of spermine on aortic rings and mesenteric arteries was also able to relax these vessels. However, results show that concentration-response experiments did not yield significant differences between WT and KO blood vessels (Figure 54). In the aorta, there were no significant differences in relaxation between WT and KO vessels in the presence of spermine (3×10^{-6}M - 3×10^{-3}M). There were also no significant differences in relaxation between WT and KO mesenteric arteries in the presence of spermine (3×10^{-6}M to 3×10^{-3}M).

A

Aorta Differential Tension (%)

20
15
10
5
0
-5
-10
-15
-20

** * ns

■ WT Time Control
▨ WT + 300nM R-568
■ KO Time Control
▨ KO + 300nM R-568

B

Aorta Differential Tension (%)

30
25
20
15
10
5
0
-5
-10

ns ns ns

■ WT Time Control
▨ WT L-NAME + 300nM R-568
■ KO Time Control
▨ KO L-NAME + 300nM R-568
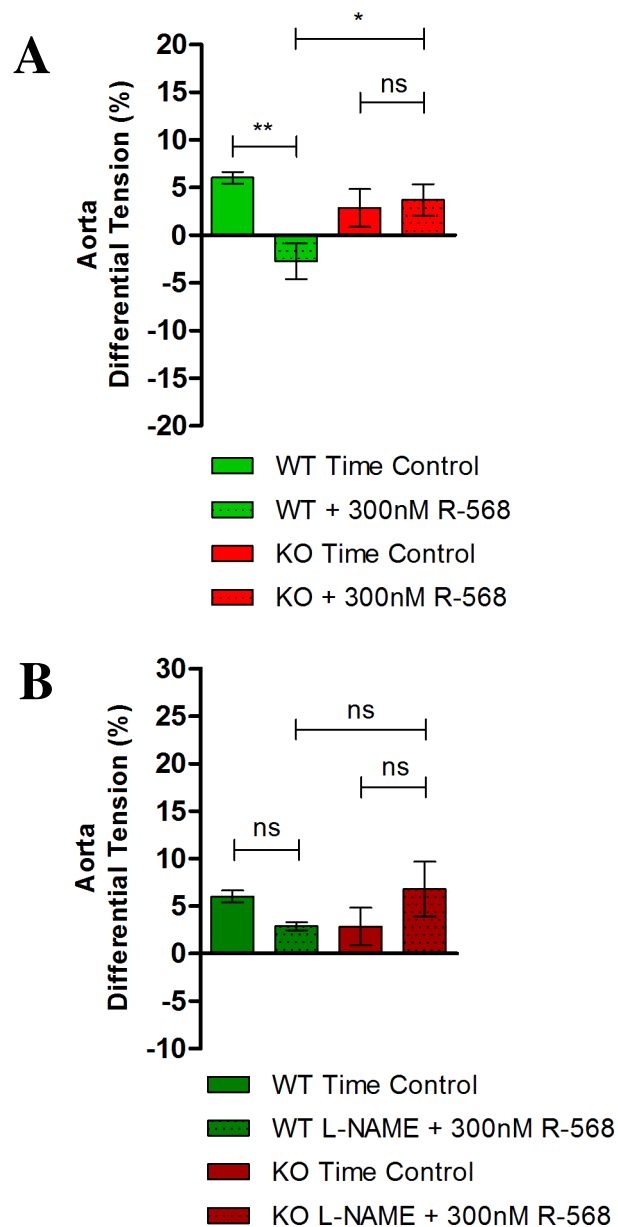
Figure 55. R-568 induces relaxation in WT aortic rings, but not in KO aortic rings. Aortic rings were incubated in Krebs buffer containing 1.5mM Ca^{2+}_o. Vessels were pre-constricted using 300nM phenylephrine and the tone allowed to plateau. After this, the plateau was regarded as 100% base-line tone before drug application. R-568 was applied at a concentration of 300nM and vessels were allowed to respond for 3 minutes. Negative time controls were also run to detect any natural drift in aortic rings over this time. (A) Effects of R-568 on aortic rings from WT and KO mice in the absence of L-NAME. (B) R-568 responses in WT and KO aortic rings in the presence of 100µM L-NAME. (A) WT N=6; KO N=7. (B) WT N=5; KO N=7. Data are expressed as mean ± SEM. Statistical analysis: two-way ANOVA with Bonferroni's post-test. P<0.05=*. P<0.01=**. ns= not significant.

R-568 (300nM) is effective at relaxing WT but not KO aortae.

In order to assess the ability of calcimimetics to modulate vascular tone, the effects of R-568 were tested in aorta rings. Calcimimetics have been used clinically to treat secondary hyperparathyroidism and reports indicate that calcimimetics are modulators of vascular tone and blood pressure (Ogata *et al.*, 2003, Rybczyńska *et al.*, 2005, Weston, 2005, Smajilovic *et al.*, 2007, Smajilovic and Tfelt-Hansen, 2008, Olgaard *et al.*, 2011). I tested the effects of both a single concentration of the calcimimetic R-568 (300nM) in the presence of 1.5mM Ca^{2+}_o on aortae pre-contracted with 300nM phenylephrine, and a concentration response of R-568 in the same conditions. 1.5mM Ca^{2+}_o and 300nM calcimimetic were selected since this has been shown in previous publications to be effective at relaxing blood vessels (Smajilovic *et al.*, 2007). In WT aortae, 300nM R-568 induced significant relaxation: -2.75% $\pm$ 1.88 WT (N=6) vs. 6.01% $\pm$ 0.62 WT time control (N=5, P<0.05). In KO aortae, 300nM R-568 did not induce affect vascular tone. KO values were: 3.68% $\pm$ 1.65 KO (N=7) vs. 2.85% $\pm$ 1.98 KO time control (N=7) which was not significant (Figure 55A). In the presence of 100μM L-NAME, R-568-induced relaxation in WT aortae was inhibited. Relaxation values were: 2.86% $\pm$ 0.44 WT (N=5) vs. 6.01% $\pm$ 0.62 WT time control (N=5), not significant. Values for KO relaxation were: 6.79% $\pm$ 2.88 KO (N=7) vs. 2.85% $\pm$ 1.98 KO time control (N=7), which was also not significant (Figure 55B).
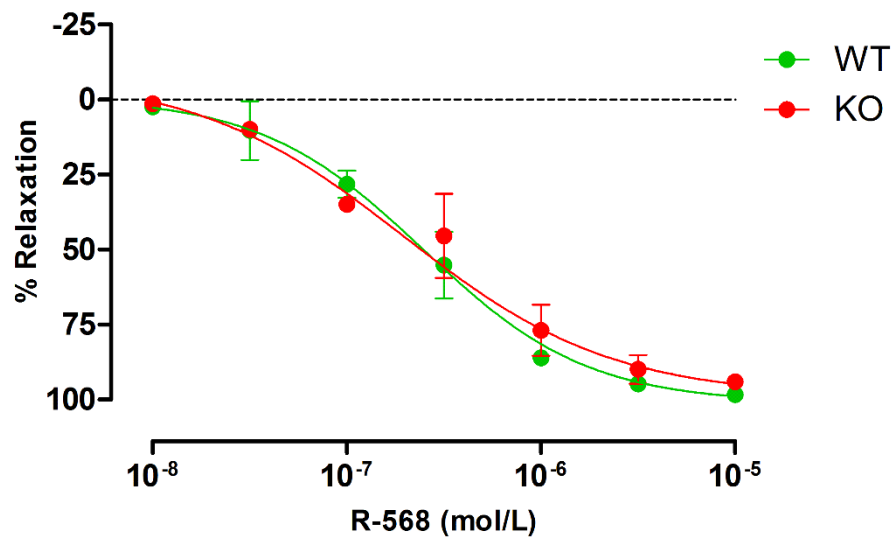
Figure 56. CaSR ablation in mouse VSMCs does not affect R-568-induced relaxation of mesenteric arteries. Mesenteric arteries were incubated in Krebs buffer as previously described in the presence of 1.5mM Ca^{2+}_o. After application of 300nM phenylephrine, tone was allowed to stabilise. After tone had reached a plateau, a cumulative concentration response of R-568 (1 x 10^{-8} to 1 x 10^{-5}M) was carried out. WT N=7 (EC_{50}= 2.57 x 10^{-7}M); KO N=5 (EC_{50}= 3.44 x 10^{-7}M). Sigmoidal lines of best fit are applied to data and data are expressed as mean ± SEM. Statistical analysis: two-way ANOVA with Bonferroni's post-test, ns= not significant.

R-568 is equally effective at relaxing mesenteric arteries from WT and KO SM22α x fl CaSR mice.

R-568 was applied to mesenteric arteries from both WT and KO mice from concentrations of 1 x 10^{-8}M to 1 x 10^{-5}M in the presence of Krebs buffer containing 1.5mM Ca^{2+}_o. Concentration response curves for WT and KO mesenteric arteries were super-imposable. There were no statistical difference at any concentration in responses to R-568, although it was seen in both WT and KO mesenteric vessels that R-568 induced relaxation in a concentration-dependent manner (Figure 56).

CHAPTER 5: DISCUSSION

The VSMC-CaSR mediates vasoconstriction and vasorelaxation in conductive and resistance vessels through $[Ca^{2+}]_o$.

Ca^{2+} has long been an implicated as an important player in the regulation of blood pressure, vascular tone and calcification of vessels (Eddington *et al.*, 2009, Giachelli, 2009, Rodriguez *et al.*, 2011). The role of Ca^{2+} in vessel tone, however, remains controversial since it has been reported that Ca^{2+}_o induces a biphasic response depending on vessel type and the concentrations used. In previously conducted studies which look at Ca^{2+}_o as a modulator of vascular tone, there appears to be little relevance to the role of the CaSR since buffers containing already maximally-activating concentrations of 2.5mM Ca^{2+}_o are employed as the baseline. At this concentration (and above), the role of CaSR becomes less important and the role of Ca^{2+}_o acting through Ca^{2+}-channels in vessel tone becomes predominant. Interestingly, the majority of relaxation observed in response to Ca^{2+}_o in larger vessels such as the aorta are observed beyond this range (>2.0 - 3.0mM Ca^{2+}_o) (Singer and Peach, 1982, Adegunloye and Sofola, 1998, Yildirim *et al.*, 1998), indicating CaSR-independent mechanisms of tone modulation. Conversely, small arteriole Ca^{2+}_o-dependent relaxation is observed from CaSR-sensitive levels of >0.5mM Ca^{2+}_o (Weston, 2005, Rybczynska *et al.*, 2006, Smajilovic *et al.*, 2006). For these reasons one can conclude that using a physiologically relevant *ex vivo* myography setup to determine the role of vascular CaSRs in tone modulation remains virtually unexplored. Only in recent years have investigators started to show the pivotal and biphasic role of Ca^{2+}_o in tone modulation at CaSR-sensitive concentrations (Ohanian *et al.*, 2005, Weston, 2005, Smajilovic *et al.*, 2007, Weston *et al.*, 2008).

In my study I showed that Ca^{2+}_o application in the aorta induced contraction, followed by relaxation at supraphysiological concentrations of Ca^{2+}_o at the CaSR (>2.0mM Ca^{2+}_o). This initial contraction was not present in KO aortae (Figure 51). This suggests that VSMC-CaSR activation by Ca^{2+}_o is responsible for vasoconstriction *ex vivo*, and therefore could relate to increases in blood pressure *in vivo*. In aortae treated with L-NAME, WT vessels incubated with 1.0-5.0mM Ca^{2+}_o showed no relaxation, only contraction. This once again illustrates the significance of the VSMC-CaSR in inducing contractions with Ca^{2+}_o (Figure 51). In KO vessels incubated with L-NAME, mild

contraction was seen which may be due to CaSR-unrelated mechanisms. Relaxation that consistently followed in KO aortae is, however, more difficult to define since the nitric oxide pathway was blocked by L-NAME (Figure 51B). This would indicate that relaxation of vessels can happen by two mechanisms. (i) Additional endothelium-derived hyperpolarization produced by factors other than NO may be upregulated in ECs as a consequence of VSMC-CaSR ablation; and (ii) VSMCs without a functional CaSR may have lower $[Ca^{2+}]_i$ or low Ca^{2+} in stores, leading to vessel dilation or relaxation by myosin inactivation.

In order to address the first point, it is important to remember crucial EDRFs involved in EC signalling. Although NO is largely considered as the major EDRF contributing to dilation and relaxation in vessels, some other hyperpolarizing factors have been described. These include ADP, ATP, bradykinin, thrombin, serotonin, histamine, acetylcholine, K^+, H_2O_2, epoxyeicosatrienoic acid (EET) and PGI_2. (Cherry *et al.*, 1982, Vanhoutte *et al.*, 1986, Palmer *et al.*, 1987, Vanhoutte, 1987, Furchgott and Vanhoutte, 1989, Bukoski *et al.*, 1997, Wang and Bukoski, 1998, Edwards *et al.*, 2008, Luksha *et al.*, 2009). It is possible that these factors may be Ca^{2+}-dependent and upregulated by endothelial cells in response to VSMC-CaSR ablation.

Already discussed in this thesis has been the *in vivo* hypercalcaemia resulting from VSMC-CaSR knockout. Hypercalcaemia *in vivo* often results from dysfunctional parathyroid gland signalling (Pearce *et al.*, 1995, Frank-Raue *et al.*, 2011). In this instance, the PTH/Ca^{2+} axis is affected and, presumably, hypercalcaemia is brought on by hyperparathyroidism which resorbs Ca^{2+} from bone. During this condition, systemic Ca^{2+}_o levels are inappropriately elevated (Pearce *et al.*, 1995, Frank-Raue *et al.*, 2011). However, in an *ex vivo* myography setup, the possibility of hormonal messengers such as PTH circulating in the blood is not possible, and therefore the effects seen cannot be attributed to systemic chances in plasma PTH. It has been shown that CaSR is linked to Ca^{2+}_o entry into VSMCs (Chow *et al.*, 2011), and it is therefore possible that in the absence a VSMC-CaSR, Ca^{2+}_o entry is reduced, preventing maximal contraction of KO aortae.

The potential effects of VSMC-CaSR ablation on Ca^{2+}-channels should also be addressed. It is largely known that CaSR activation can signal through the PLC pathway, activating IP_3Rs and inducing release of Ca^{2+} from internal stores (Brown *et al.*, 1993, Riccardi *et al.*, 1995). Consequently, this elevates $[Ca^{2+}]_i$ which in VSMCs would ordinarily lead to activation of myosin components and subsequent contraction (Wray *et al.*, 2005, House *et al.*, 2008). In physiological $[Ca^{2+}]_o$ (~1.05-1.2mM) (Brown, 1991, Kovacs and Kronenberg, 1997, Kovacs *et al.*, 1998, Finney *et al.*, 2008), the CaSR is activated in the PTGs. Presumably, if the VSMC-CaSR were to be similarly sensitive to this level of Ca^{2+}_o, one could also speculate that signalling through the VSMC-CaSR would occur, leading to elevated $[Ca^{2+}]_i$ levels and a more contractile state. This may have repercussions on the function of Ca^{2+}-channels expressed in the VSMC, namely, the VSMC voltage-gated Ca^{2+}-channel Ca_V 1.2 (Lipscombe, 2004, Rhee *et al.*, 2009). Ca_V 1.2 has been shown to be expressed in VSMCs, and knockdown of this is associated with reduced myogenic tone, reduced depolarisation and reduced VSMC contraction (Rhee *et al.*, 2009). On the other hand, hypertension in rodents has been associated with upregulation of Ca_V 1.2 at both the mRNA and protein level at the cell surface, indicating an important role in tone modulation (Ohya *et al.*, 1993, Pesic *et al.*, 2004). Whether the VSMC-CaSR and VSMC-Ca^{2+}-channels such as Ca_V 1.2 are functionally linked to one another remains to be investigated.

Although these hypotheses help illustrate the potential role of the VSMC-CaSR in the aorta, the role of Ca^{2+}_o in the aorta and mesenteric artery (Figure 52), and of acetylcholine in mesenteric arteries (Figure 49) appears less clear. Although there appear to be a trend for Ca^{2+}_o to relax these KO arteries less than WT mesenteric arteries, it is not significant. It is important to remember that in these mesenteric vessels, endothelial cells play a major role in tone modulation, exerting their effects on comparatively fewer adjacent VSMCs compared to large conductance vessels. It seems probable that Ca^{2+}_o in these two different vessel types preferentially acts on either ECs or VSMCs; depending on which cell type or response dominates the vessel. For example, in the aorta, rises in $[Ca^{2+}]_o$ (within the physiological range of 1.0-2.0mM Ca^{2+}_o) would presumably impact more on VSMCs which far outnumber ECs. In this instance Ca^{2+}_o-induced vasoconstriction may dominate over vasorelaxation which may be co-ordinated through EC and VSMC CaSRs. In fact,

we know these antagonistic responses to both be synergistically active since in the WT aorta we have seen that L-NAME incubation allows for contraction only, and no relaxation (up to 5.0mM Ca^{2+}_o, Figure 51B). In mesenteric vessels this may also be the case, however here, Ca^{2+}_o may impact the EC-CaSR more than VSMC-CaSR, and so relaxation responses through the NO pathway or other EDHs may dominate over contractile responses.

Importantly, it should also be remembered that acetylcholine-induced relaxation is delayed in KO mesenteric arteries compared to WT mesenteric arteries (Figure 49). Since we have also observed that Ca^{2+}_o may be less effective at relaxing KO mesenteric arteries (Figure 52), it seems likely that the physiological responses of GPCRs to their agonists in these arteries is somehow impaired. Again, it may be that the pattern of expression of Ca^{2+}-channels present in these vessels is slightly altered, or that alternative Ca^{2+}_o-sensing mechanisms are at work, I.e. GPRC6A which has been shown to be expressed in rat mesenteric arteries (Harno *et al.*, 2008). Due to time constraints NO/EDHF activity, Ca^{2+}-channel activity/expression and GPRC6A activity/expression were not investigated. However, it is likely that looking at these factors in addition to the role of the EC-CaSR in the future will shed more light on the role of Ca^{2+}_o in arteriolar tone modulation. For this reason, it would be extremely beneficial to develop an EC x fl CaSR mouse. Such endothelial cell-specific models have been developed using the *Tie2* promoter which is expressed specifically in ECs (Kisanuki *et al.*, 2001). Using this mouse model alone or in combination with the VSMC CaSR-KO mouse, a more intelligible role of Ca^{2+}_o and CaSR activation in the cardiovascular system could be understood. Furthermore, a double-knockout of CaSR in both ECs and VSMCs would provide greater insight into Ca^{2+} signalling in the vessel wall.

Spermine-induced relaxation in the aorta may be mediated by the VSMC-CaSR.

Spermine, an activator of the CaSR, is a positively charged polyamine and perhaps it is not so striking that this is able to activate CaSR, a sensor of cations (Brown, 1991, Riccardi *et al.*, 1995). Studies in HEK293 cells overexpressing a human CaSR have

shown spermine to be effective in increasing intracellular Ca^{2+} through IP_3 receptor activation at the ER/SR (Quinn *et al.*, 1997, Canaff, 2000, Conigrave and Quinn, 2000, Conigrave *et al.*, 2002, Kelly *et al.*, 2011). For the characterisation of the SM22α x fl CaSR mouse model, I used spermine as a CaSR agonist to determine its effects on vascular tone. In the aorta, 300µM (3 x 10^{-4}M) was sufficient to induce relaxation in both WT and KO aortic rings. Interestingly, cumulative experiments in the aorta (Figure 54) suggest that spermine could be acting through the EC-CaSR to relax VSMCs, or somehow hyperpolarize KO VSMCs to a greater degree than WT VSMCs. Spermine binds to the CaSR to increase $[Ca^{2+}]_i$ which in VSMCs would be expected to lead to contraction (Quinn *et al.*, 1997). Conversely, in ECs, $[Ca^{2+}]_i$ increases can induce dilation and relaxation through NO (Kerr *et al.*, 2012, Tran *et al.*, 2012). Interestingly, relaxation was still seen in L-NAME treated vessels, albeit, significantly reduced. For this reason, relaxation here cannot be attributed to NO effects, therefore alternative mechanisms of actions need to be tested. Numerous investigators have reported that (i) spermine exists as a cation at physiological pH of 7.4, and; (ii) spermine can enter endothelial cells through a carrier protein (Bogle *et al.*, 1994, Seiler *et al.*, 1996). Although there are currently no studies stating that VSMCs can take up spermine, this also seems possible, particularly since almost all cells synthesize their own polyamines (Pajula *et al.*, 1979, Heby and Persson, 1990). If indeed the case, uptake of this polyamine cation in VSMCs by a its' respective carrier protein may or may not be mediated by the VSMC CaSR. Effects within the cell that lead to vasodilation and vasorelaxation remain unclear. It may be possible that elevations in this cationic polyamine inside the cell promote release of Ca^{2+} from internal stores, or hyperpolarization by K^+ efflux.

In terms of responses observed in the presence of L-NAME, it seems likely that additional EDHs induced by, for example, PGI_2 could be responsible for these effects in the presence of L-NAME (Triggle *et al.*, 2012). The fact that relaxation was observed in the presence of L-NAME suggests that the relaxation observed is at least in some part independent of NO. The important role of PGI_2 as a hyperpolarising and relaxation factor has become more recognised in recent years. Furthermore, it has been reported in a double knockout model for eNOS and COX-1 that relaxation still occurs by additional (so far unknown) hyperpolarising factors (Scotland *et al.*, 2005). From my data, there

appear to be some CaSR-dependent and CaSR-independent actions of spermine in WT and KO vessels which remain to be clarified (Figure 53).

There were no significant differences in contractile tone when comparing WT and KO mesenteric arteries (Figure 54B), indicating that: (i) any visible trends require more repeats for clarification, or (ii) selective CaSR ablation in VSMCs does not affect the relaxation responses to spermine in mesenteric arteries.

R-568 modulated aortic tone through the VSMC-CaSR.

R-568 is a calcimimetic currently used to treat secondary hyperparathyroidism in patients suffering from CKD (Francis *et al.*, 2008). A number of studies have demonstrated the ability of calcimimetics in modulating vascular tone, in addition to reducing vascular calcification (Ogata *et al.*, 2003, Rybczyńska *et al.*, 2005, Weston, 2005, Lopez, 2006, Smajilovic *et al.*, 2007, Alam *et al.*, 2008, Kawata *et al.*, 2008, Piecha *et al.*, 2008, Ivanovski *et al.*, 2009, Koleganova *et al.*, 2009). Conversely, a number of studies have shown that calcimimetics have no beneficial effects on cardiovascular outcome (Chertow *et al.*, 2012a). For this reason it was important to investigate the effect of calcimimetics using the *ex vivo* myography setup. Calcimimetics require the presence of submaximal concentrations of $[Ca^{2+}]_o$ and for this reason I used Ca^{2+}_o at a concentration which has previously been shown to be the EC_{50} in VSMCs (Smajilovic *et al.*, 2006, Smajilovic *et al.*, 2007). R-568 has been shown to left-shift the concentration response curve for Ca^{2+}_o by increasing the Ca^{2+}_o-dependent responses (Nemeth *et al.*, 1998, Hebert, 2006), so this concentration was selected for all experiments.

My experiments show that a single application of 300nM R-568 to WT aortic rings induced significant relaxation compared to WT time controls (P<0.01) over the course of 3 minutes. This was also significantly different to KO aortic rings in which 300nM R-568 did not relax these vessels (P<0.05, Figure 55A). These observations would suggest (as others have shown) that R-568 can play a role in relaxing the vessel. Interestingly,

these observations suggest that the effects of R-568 appear to be endothelium-specific since addition of L–NAME inhibited this relaxation (Figure 55B). Furthermore, they would suggest that R-568 activation of CaSR is somehow linked to NO synthesis. Although relaxation in WT aortae in response to 300nM R-568 was small (-2.75% ± 1.88 WT (N=6) vs. 6.01% ± 0.62 WT time control), these results are in agreement with the literature where calcimimetics have been shown to induce a hypotensive effect (Rybczyńska *et al.*, 2005, Smajilovic *et al.*, 2007). However, when looking at the myography trace the relaxation was small (2.75%). Further experiments with the drug at different concentrations in the presence of 1.0-1.5mM Ca^{2+}_o may lead to greater responses. Also, pre-treatment with the drug could be used to prime the CaSR, which might lead to increased responses. In addition, the effects of calcimimetics on isolated VSMCs and ECs should be tested in future experiments to determine the sensitivity to R-568 in these two cell types. However, since R-568 has been shown to act on Ca^{2+}-channels at concentrations of >1µM, only concentrations of <1µM should be used.

My observations show that KO vessels did not respond to R-568 (Figure 55). Since KO ECs should still contain a functional CaSR, and since R-568 appears to be acting through the EC-CaSR, this outcome was slightly unexpected. However, as KO aortae already have a reduced contractile tone, perhaps R-568 was not able to evoke further relaxation. Determining whether R-568 at different concentrations can induce similar hypotensive effects in the aorta remains to be investigated.

Also investigated was a concentration response of R-568 in mesenteric arteries from WT and KO animals (Figure 56). It was seen that R-568 induced relaxation in both WT and KO arteries at a concentration range of 1 x 10^{-8} to 1 x 10^{-5}M. Interestingly, mesenteric arteries contain far fewer VSMCs (Wagenseil and Mecham, 2009, Wagenseil *et al.*, 2009, Wagenseil *et al.*, 2010), therefore any mesenteric artery VSMC-CaSR KO phenotype would presumably be different compared to arteries with significantly more CaSR-KO VSMCs, I.e. the aorta. At the concentrations of R-568 used for my experiments (up to 1µM), R-568 acts selectively on the CaSR and induced relaxation in both WT and KO mesenteric arteries. My results suggest that relaxation at concentrations of R-568 of

<1µM in both WT and KO aortae should be mediated through the EC-CaSR. However, above this concentration range, R-568 (a phenylalkylamine) may act non-specifically on Ca^{2+}-channels (Tuckwell, 2012). Indeed, high concentrations of calcimimetics (>1µM) induce dilation and relaxation by blockage of Ca^{2+}-channels (Thakore and Ho, 2011). These data suggest that R-568 may be effective in dilating and relaxing mesenteric arteries by the EC-CaSR, but not the VSMC-CaSR.

CHAPTER 5: CONCLUSION

The VSMC-CaSR is a modulator of vascular tone in both conductance and resistance vessels.

CaSR is expressed in both ECs and VSMCs (Weston, 2005, Smajilovic *et al.*, 2006, Smajilovic *et al.*, 2007, Alam *et al.*, 2008). From my data, it is clear that the VSMC-CaSR plays an important role in tone modulation. In its' absence, responses from agonists such as Ca^{2+}_{o}, spermine and R-568 are significantly altered in the aorta. Ca^{2+}_{o}, spermine and R-568 appear to induce greater relaxation, suggesting that the EC-CaSR may promote relaxation, while the VSMC-CaSR may promote contraction. This suggests that our KO mice would be expected to exhibit a hypotensive phenotype, which is consistent from observations seen in Chapter 4, where aortae exhibit reduced contractile tone. To test this hypothesis, blood pressure measurements should be taken in both WT and KO mice.

The role of R-568 in these studies remains unclear. Although it appears to induce relaxation in WT aortae only, it is not fully clear why this was not also observed in KO aortae. It seems likely that, in the experimental conditions I have used, R-568 does not play a major role in blood vessel tone by acting through the VSMC-CaSR. Any effects that are mediated through blood vessel CaSRs seems likely to be due to the EC-CaSR.

Chapter Acknowledgments

Once again I would like to thank Dr. Polina Iarova for her help with dissections and myography experiments.

CHAPTER 5: FUTURE WORK

Future work crucial to this project would include using such pharmacological agents as (i) S-568: to determine any stereoselective effects of the R/S-568 compounds, and; (ii) calcilytics to determine any effects of CaSR inhibition in WT and KO vessels. Furthermore, these responses should be tested in both the aorta and mesenteric arteries in the presence and absence of L-NAME. Due to time constraints and limited tissue availability, L-NAME was not investigated in mesenteric arteries during these studies.

An additional benefit this project would gain would be to further investigate the role of the vascular CaSR in both ECs and VSMCs and consequences of their inactivation. For this, it would be crucial to develop a Tie2-driven CaSR knockout which would knock the receptor out specifically in the endothelium. Additionally, it would be interesting to characterise a SM22α-driven and Tie2-driven double CaSR knockout. Further repeats in mesenteric arteries would also be beneficial in determining whether the trends and changes observed in response to Ca^{2+}_{o} and spermine are indeed real. Additionally, myography may not be sensitive enough to determine levels of $[Ca^{2+}]_i$ in whole vessels in response to these agonists. Therefore measurements of $[Ca^{2+}]_i$ using imaging techniques may be required to test the effects of calcimimetics on the VSMC and EC CaSR, and the ability of calcilytics to prevent agonist-induced, CaSR-mediated increases in $[Ca^{2+}]_i$ in these cells.

CHAPTER 6:

IN VITRO CHARACTERISATION OF THE SM22α X fl CaSR MOUSE MODEL WITH SELECTIVE ABLATION OF CaSR IN VASCULAR SMOOTH MUSCLE CELLS

CHAPTER 6: GENERAL INTRODUCTION

Vascular smooth muscle cells from aortic explants are widely used in investigations of vascular calcification (Smajilovic *et al.*, 2006, Kircelli *et al.*, 2012). Chapters 3-5 have shown clearly that targeted CaSR ablation from VSMCs leads to altered serum biochemistry, increased heart weight, reductions in bone mineral density and impaired contractile response. To characterise further the phenotype of the VSMC-CaSR KO, and to test the hypothesis that loss of CaSR increases vascular calcification, an *in vitro* approach is required. In this way, the VSMC-CaSR KO phenotype at the cellular level can be investigated.

CHAPTER 6: RESULTS
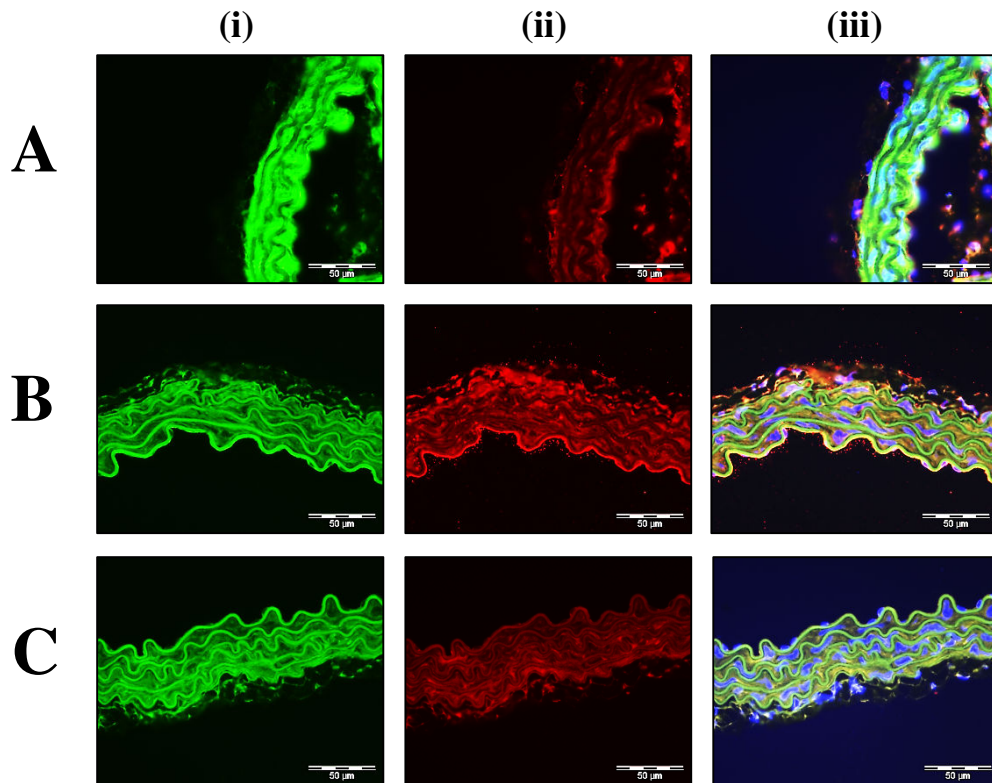
Figure 57. Mouse aortic endothelial cells and vascular smooth muscle cells express the CaSR. Mouse thoracic aortae were obtained from C57BL/6 WT animals of approximately 3 months of age, washed in 1X PBS then fixed in 4% PFA for 60 minutes. Organs were washed in 1X PBS, then placed in OCT cryostat mounting medium and allowed to freeze at -80ºC. After freezing, aortae were cut into 6µm sections and mounted on microscope slides. Sections were stained using antibodies for (Ai) anti-SM22α;green and (Aii) anti-CaSR;red (Aiii composite) or (Bi) anti-PECAM-1;green and (Bii) anti-CaSR;red (Biii composite). Negative controls for both goat antibodies (SM22α and PECAM-1) are shown in Ci. Rabbit IgG negative control is shown in Cii and a composite of negative control auto-fluorescence in Ciii. Nuclear staining (blue) was performed using Hoescht. Images are representative of 3 separate aortic isolations with similar immunofluorescent results.

Mouse endothelial and vascular smooth muscle cells both express a CaSR.

To confirm the presence of the CaSR protein in the vasculature, WT C57BL/6 aortae of 3 month old male mice were prepared and stained using antibodies to anti-SM22a, anti-PECAM-1 and an N-terminal antibody to anti-CaSR. Figure 57Aii shows that VSMCs express a CaSR. Figure 57Bii shows intense red staining in the endothelial cell layer indicating the presence of CaSR in the tunica intima. Although CaSR immunoreactivity is faint in the VSMC layer (Figure 57 Aii), this staining is more prominent than the negative rabbit IgG control in Figure 57Cii. In contrast, EC-CaSR immunoreactivity is high.
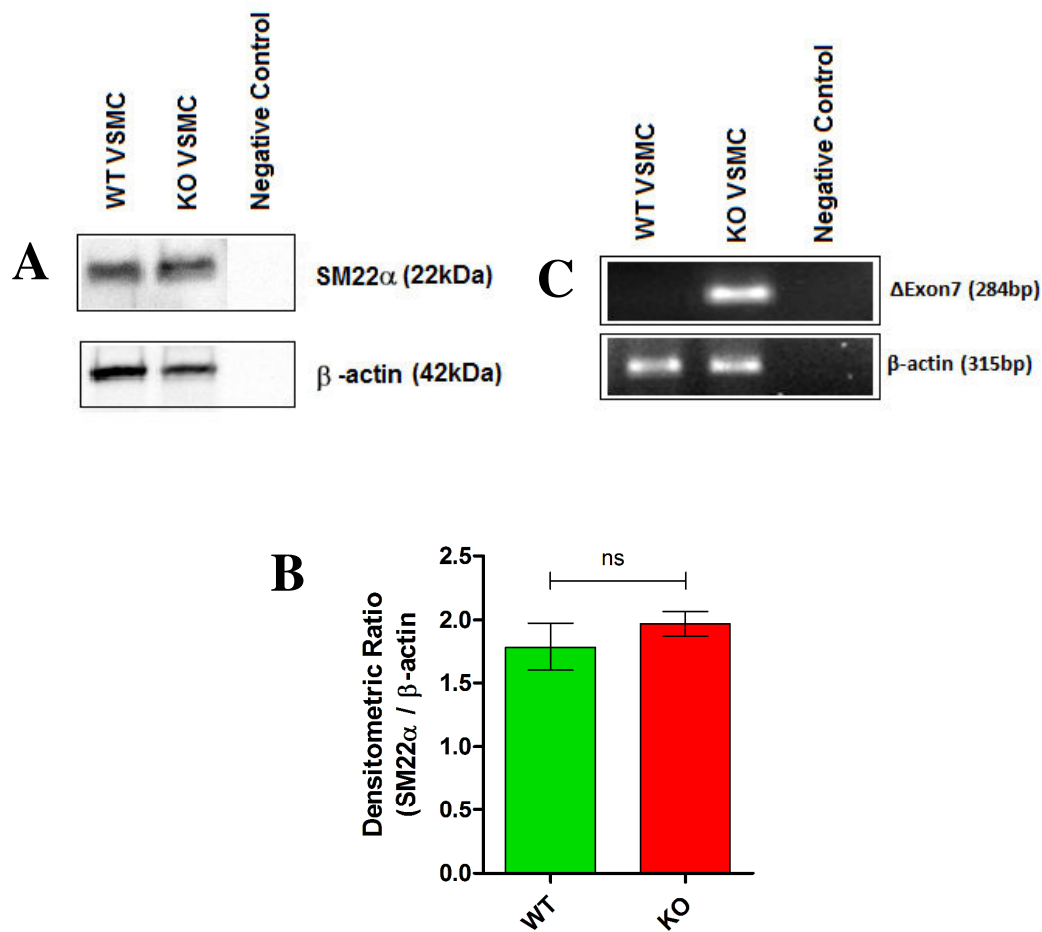
Figure 58. WT and KO vascular smooth muscle cells from mouse aortic explant cultures express the VSMC marker: SM22α. Mice of 3 months of age were humanely culled by cervical dislocation and descending thoracic aortae were isolated. VSMCs were isolated by the explant method as described in Methods (2.11 Isolation of mouse primary vascular smooth muscle cells VSMCs). After the first passage to passage 1, cells were plated in 24-well plated and allowed to reach confluence. (A) Protein isolated was quantified using the BCA method and SM22α expression is confirmed by western blot. Primary antibodies for SM22α and β-actin; 1:1,000. Secondary HRP-conjugated antibody; 1:10,000. (B) SM22α levels were calculated semi-quantitatively using densitometry (N=3). (C) Genomic DNA isolated from confluent VSMCs was used as a template for the amplification of CaSR exon 7. The truncated Δexon 7 amplicon produced in SM22α x fl CaSR KO mice is shown as a 284bp product (absent in all WT VSMC preparations). Cell genotyping was repeated for 3 independent WT and KO VSMC isolations with the same results. Data expressed as mean ± SEM. Statistical analysis: unpaired two-tailed t-test. ns= not significant.

WT and KO mouse VSMCs express the marker SM22α.

In order to determine whether CaSR ablation affected the expression of SM22α, protein lysates were isolated from confluent WT and KO VSMCs. Figure 58A shows that SM22α protein of the predicted 22kDa size is detected in both WT and KO VSMC preparations. SM22α expression was comparable as shown in Figure 58B.

KO mouse genomic DNA in VSMCs has specific deletion of exon 7 in the CaSR gene.

To determine whether mouse genotyping had been performed correctly and that only CaSR-KO products could be detected in KO preparations, gDNA was isolated from confluent cells and the ΔExon 7 KO product was amplified from these preparations. Figure 58C shows that all WT preparations (3 separate batches tested) showed no detectable truncated knocked out CaSR. Conversely, all KO batches (3 separate batches tested) all confirmed the absence of exon 7 in the CaSR genomic DNA.
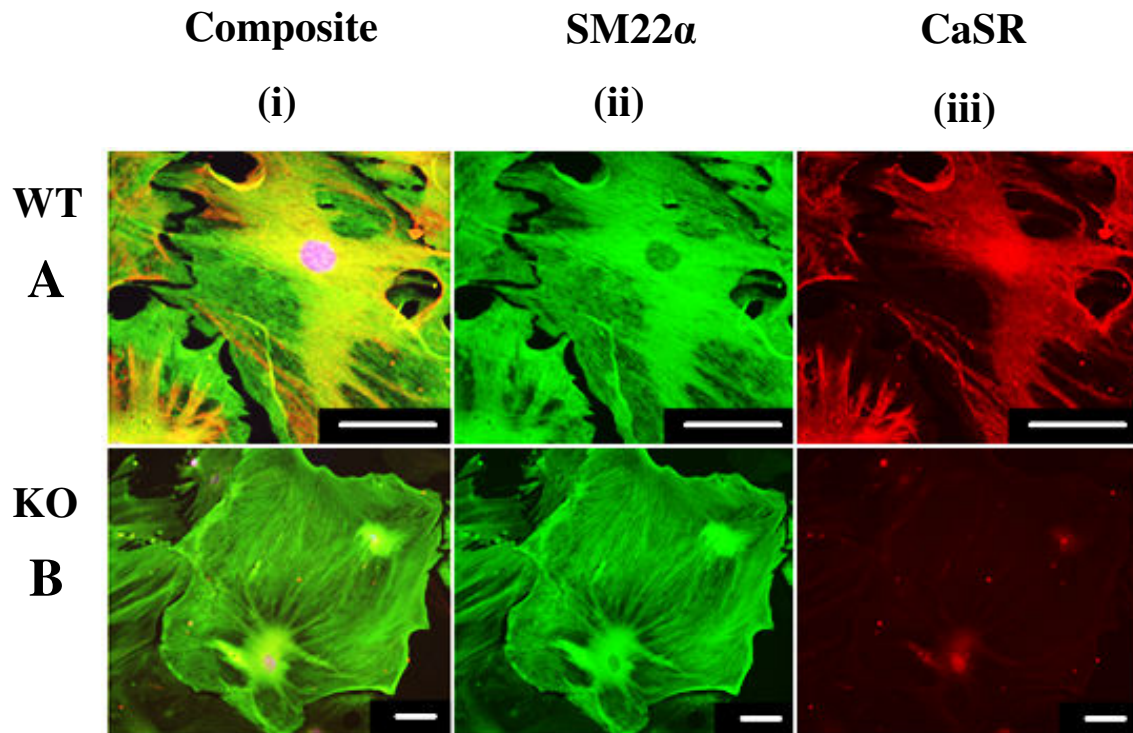
Figure 59. WT- and KO-CaSR mouse VSMCs express an N-terminal CaSR protein product. Primary mouse VSMCs were isolated from the thoracic aorta of WT and KO mice. Passage 1 VSMCs were cultured in the presence of 1.2mM Ca^{2+}_o and 10% FBS in DMEM. Cells were seeded at 10,000 cells per coverslip in 4-well plates and left in culture medium for 5 days. At this time, medium was removed and cells were washed with 1 X PBS and fixed in 4% PFA for 10 minutes. Immunofluorescent staining was then carried out as described in methods. Pictures show VSMCs in a typical synthetic, non-contractile proliferative phenotype. Row A: WT-CaSR VSMC staining, and Row B: KO-CaSR VSMC staining. (Ai) Composite anti-SM22a (green)/anti-CaSR (red). (Aii) anti-SM22a. (Aiii) anti-CaSR. (Bi) Composite anti-SM22a (green)/ anti-CaSR (red). (Bii) anti-SM22a. (Biii) anti-CaSR. Anti-CaSR antibody binds to the N-terminal CaSR product expressed as a full-length CaSR in WT-CaSR VSMCs, and a truncated protein in KO-CaSR VSMCs. Primary antibody dilutions= 1:100. Secondary antibody dilutions= 1:500. Scale bar: 100µm. Image kindly provided by Martin Schepelmann.
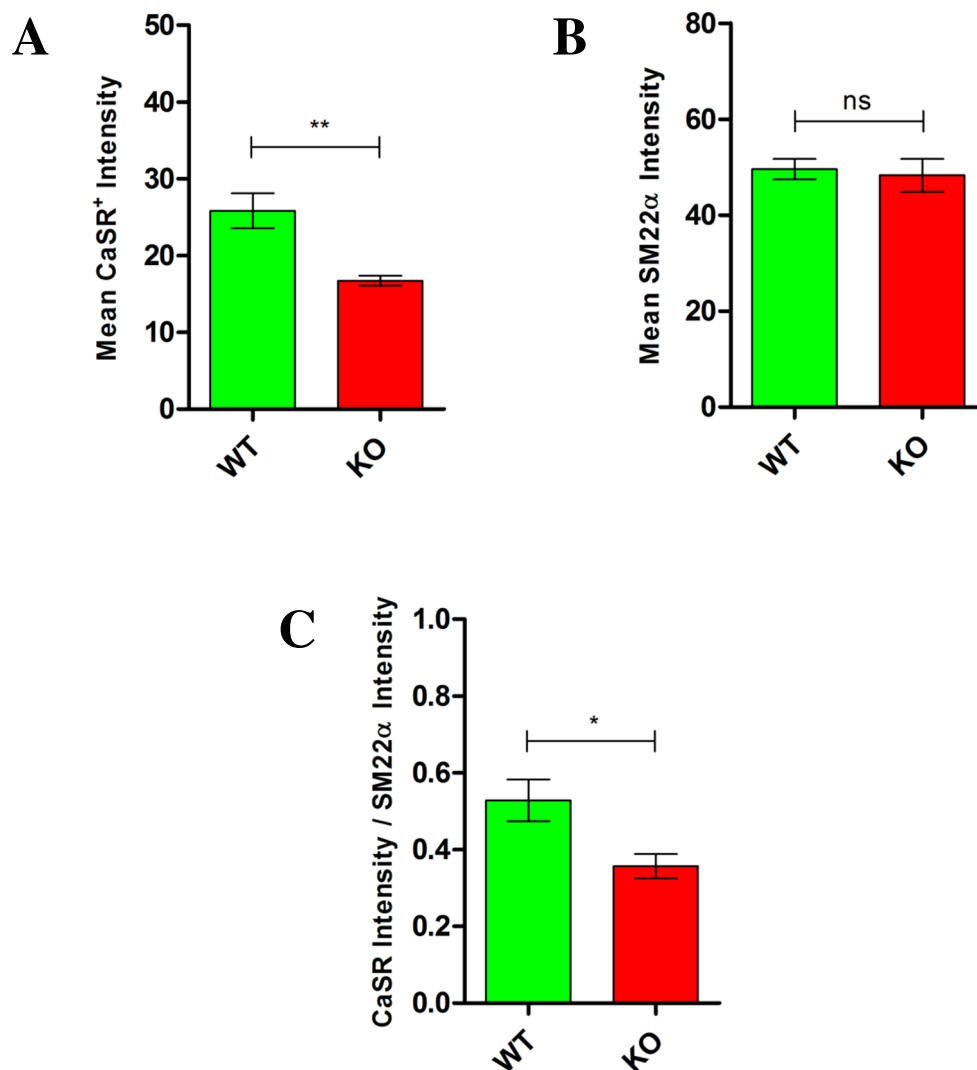
Figure 60. KO mouse VSMCs express less CaSR immunoreactivity compared to WT mouse VSMCs. A population of passage 1 explanted WT and KO mouse VSMCs (10,000) were plated onto glass coverslips and immunofluorescence was performed using an anti-SM22a antibody (1:250) and an anti-N-terminal CaSR antibody (1:100). Cells were fixed after staining and semi-quantitative analysis was carried out using Tissue Quest^{TM} software and epi-fluorescent microscopes. The system calculated average intensity values within a radius of 8.28µm of VSMC nuclei (blue Hoechst-stained). Intensity values for SM22α-positive cells (VSMCs) and CaSR-positive cells were calculated by exposing fixed VSMCs to 488nm (green) filters and 594nm (red) filters respectively. Manual calibration was carried out by Martin Schepelmann to confirm which cells were to be considered positive or negative for SM22α or CaSR stains. (A) CaSR-positive cells within a WT and KO VSMC population. (B) SM22α-positive cells within a WT and KO VSMC population. (C) CaSR-positive cells within the SM22α-positive VSMC population. Statistical analysis: two-way ANOVA with Bonferroni's post-test. Data expressed as mean ± SEM. $P<0.05$=*. $P<0.01$=**. ns= not significant.

WT and KO mouse SM22α x fl CaSR VSMCs express an N-terminal CaSR protein product with significantly reduced amounts in KO mouse VSMCs.

With reliable antibodies which detect the carboxy terminal domain of the CaSR being very limited, I was limited to just one amino terminus antibody which worked well in the mouse. Unfortunately, this antibody cannot distinguish between WT and KO CaSR proteins. The N-terminal domain of CaSR is encoded by exons 2-6. Since only Exon 7 is knocked out in our mouse model, KO VSMCs are still able to produce a truncated exon 2-6 product, which our N-terminal antibody was able to detect. Numerous other antibodies were used but showed non-specific nuclear staining in all VSMCs tested. As a consequence, immunostaining WT and KO VSMCs both yielded positive results (Figure 59). However, automated semi-quantification of CaSR immunofluorescence performed by Martin Schepelmann using a TissueFAX system and TissueQuest^{TM} software showed firstly that in the whole population of cells on each slide, CaSR immunoreactivity was less intense in KO VSMCs compared to WT VSMCs (Figure 60A). Fluorescent arbitrary values were: 25.84 ± 2.27 WT (N=3/n=6) vs. 16.73 ± 0.66 KO (N=3/n=6). This difference was significant at $P<0.01$ using an unpaired two-tailed t-test, and demonstrated 35.26% less protein in KO VSMCs compared to WT VSMCs. Secondly, analysis of SM22α content of the VSMC populations of each genotype was carried out (Figure 60B). The results revealed that there was no significant difference in SM22α immunostaining intensity, as also shown previously from whole protein isolation, between WT and KO VSMCs (Figure 58). Lastly, when CaSR immunostaining was normalised relative to VSMC markers within the population (by SM22α staining) in VSMCs at passage 1, KO VSMCs expressed significantly less CaSR when compared with WT VSMCs ($P<0.05$; Figure 60C). Data for CaSR/SM22α, in fluorescent units were: 0.53 ± 0.05 WT (N=3/n=6) vs. 0.36 ± 0.03 KO (N=3/n=6).
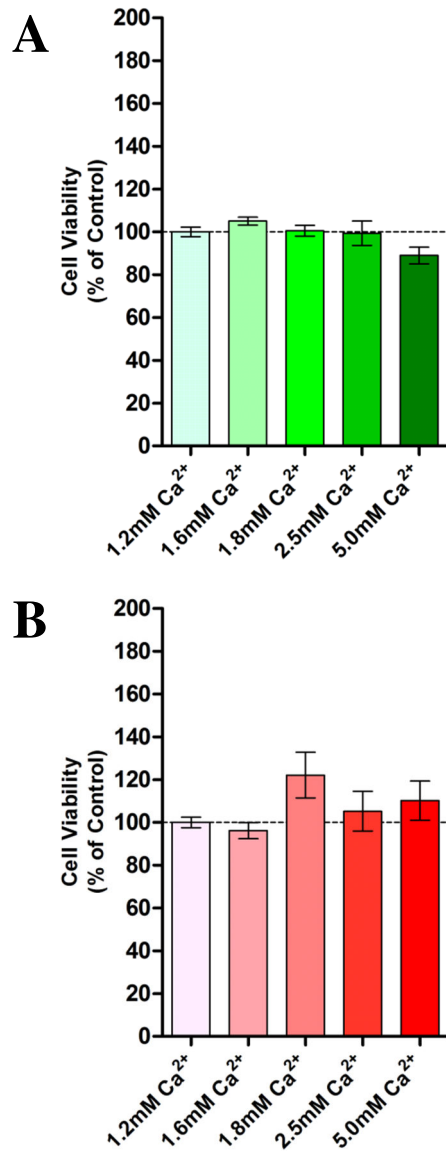
Figure 61. Ca^{2+}_o does not significantly affect the viability of mouse primary WT and KO VSMCs.
(A) WT and (B) KO VSMCs were seeded at 2,000 cells per 96-well in DMEM containing 10% FBS and 1.2mM Ca^{2+}_o. After 24h, cells were quiesced for 24h in DMEM containing 1% FBS and 1.2mM Ca^{2+}_o and 1.0mM Pi. After 24h quiescing, medium was changed to contain different Ca^{2+}_o concentrations (supplemented with $CaCl_2$) which marked day 0. Media were changed every 2-3 days. At the end-point (7 days), cells were incubated with 0.5mg/mL MTT for 2 hours at 37ºC. MTT crystals (a product of mitochondrial reductase activity) were solubilised in DMSO. Solubilised crystals were quantified in an Optima plate-reader; absorbance was measured at 570nm wavelength (N=3/n=9 WT; N=2/n=6 KO). Data are expressed as average ± SEM. Statistical analysis: one-way ANOVA.
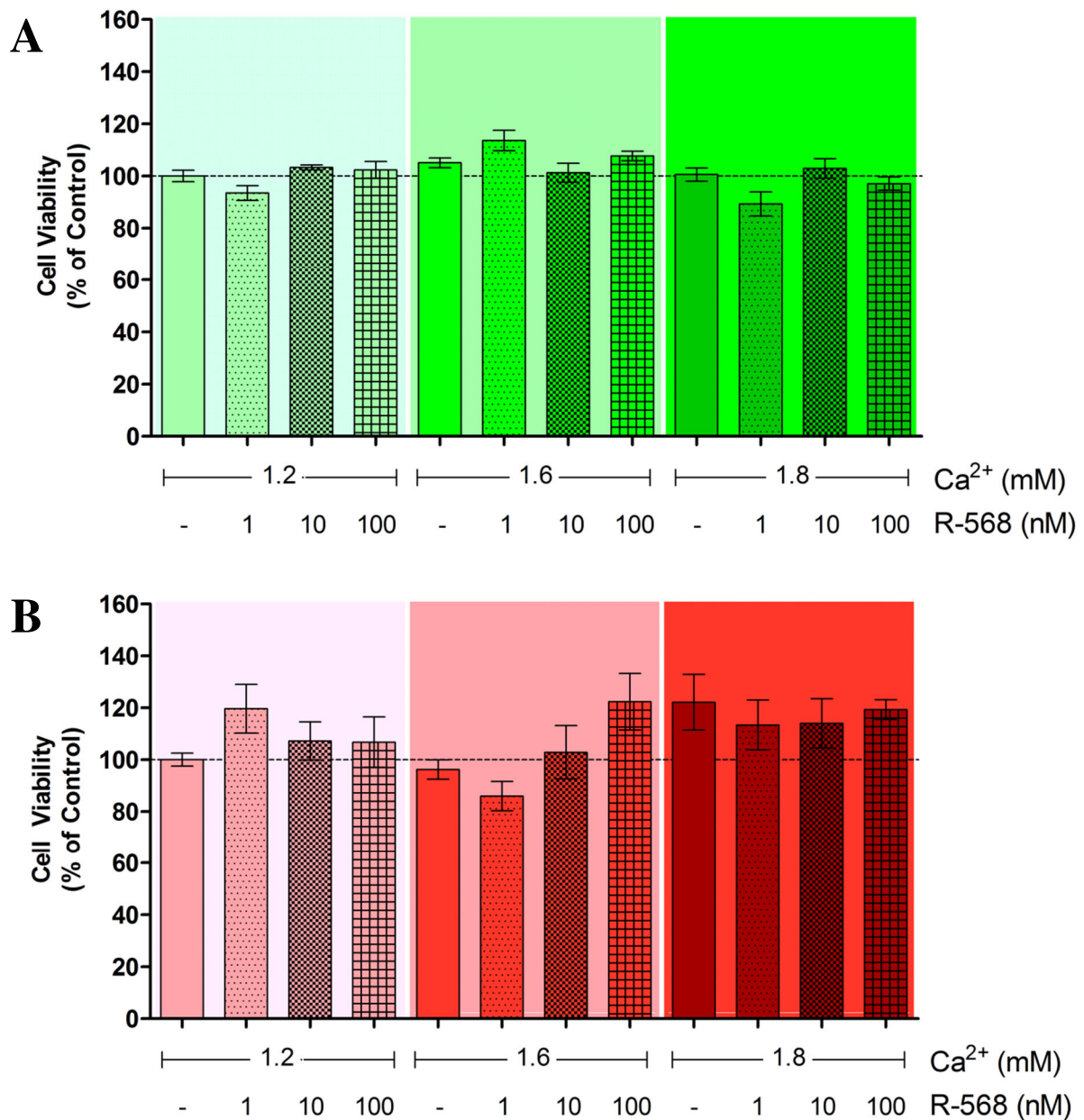
Figure 62. The calcimimetic R-568 does not significantly affect the viability of mouse primary WT and KO VSMCs. (A) WT and (B) KO VSMCs were seeded at 2,000 cells per 96-well in DMEM containing 10% FBS and 1.2mM Ca^{2+}_o. After 24h, cells were quiesced for 24h in DMEM containing 1% FBS and 1.2mM Ca^{2+}_o and 1.0mM Pi. After 24h quiescing, medium was changed to contain different Ca^{2+}_o concentrations (supplemented with $CaCl_2$) which marked day 0. VSMCs were incubated with calcimimetic or vehicle control (0.01% DMSO). Media were changed every 2-3 days. At the end-point (7 days), cells were incubated with 0.5mg/mL MTT for 2 hours at 37ºC. MTT crystals (a product of mitochondrial reductase activity) were solubilised in DMSO. Solubilised crystals were quantified in an Optima plate-reader; absorbance was measured at 570nm wavelength (N=3/n=9 WT; N=2/n=6 KO). Data are expressed as average ± SEM. Statistical analysis: two-way ANOVA.

Ca^{2+}_o and the calcimimetic R-568 do not affect the viability of VSMC from WT and KO aortae.

Using 3-(4,5-dimethylthiazol-2-yl)-2,5-diphenyltetrazolium bromide (MTT), cell viability in the presence of different concentrations of Ca^{2+}_o and the calcimimetic R-568 (1-100nM) was tested. MTT is a substrate for mitochondrial reductase enzymes. In healthy metabolising and proliferating cells, these enzymes are active in the mitochondria. When cell viability is impeded, enzyme function is reduced. Similarly, when cells proliferate actively, mitochondrial reductase activity is increased (Mosmann, 1983). Figure 61A shows that in the presence of Ca^{2+}_o (1.6-5.0mM), there is no significant difference in cell viability compared to the 1.2mM Ca^{2+}_o control in WT and KO VSMCs. Figure 62 also shows that R-568 (1-100nM) in the presence of Ca^{2+}_o (1.2-1.8mM) had no significant effects on WT and KO VSMC viability when compared to untreated controls.
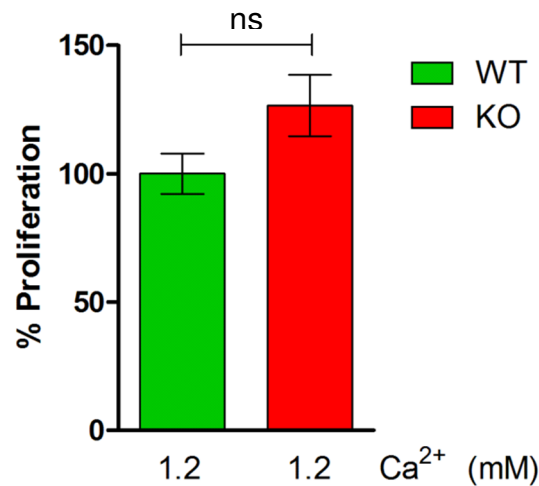
Figure 63. Proliferation rates of WT- and KO-CaSR VSMCs *in vitro*. VSMCs were seeded at 10,000 cells per 12-well plate and allowed to adhere for 24h in DMEM containing 10% FBS and 1.2mM Ca^{2+}_o. After 24h, medium was changed to contain 1.2mM Ca^{2+}_o and 1% FBS. After a further 24h, medium was changed to contain 1.2mM Ca^{2+}_o and 10% FBS. Cells were left for 10 days with medium changing every 3 days. At day 10, cells were trypsinised in 0.05% trypsin EDTA and manually counted using a haemocytometer. To normalise data, WT VSMC numbers were averaged. Counts for KO VSMCs were then normalised to these data to express them as fold changes compared to WT VSMCs. WT N=4/n=8. KO N=4/n=8. Data are expressed as average ± SEM. Statistical analysis: unpaired two-tailed t-test. ns= not significant.

KO-CaSR VSMCs exhibit comparable proliferation rates to WT-CaSR VSMCS at physiological Ca$^{2+}_o$ *in vitro*.

When culturing WT-CaSR and KO-CaSR VSMCs *in-vitro* it was often seen that KO VSMCs proliferated at faster rates than WT VSMCs. Therefore, it was important to determine whether this observation was statistically significant under standard conditions of culture (DMEM containing 10% FBS and 1.2mM Ca$^{2+}_o$). Cell counts were performed after 10 days in culture in these conditions. The previous observation that KO VSMCs proliferate faster than WT VSMCs was seen in data presented in Figure 63, however, this was not significant. It is therefore likely that more repeats are required to obtain significance (P value 0.08, Figure 63).
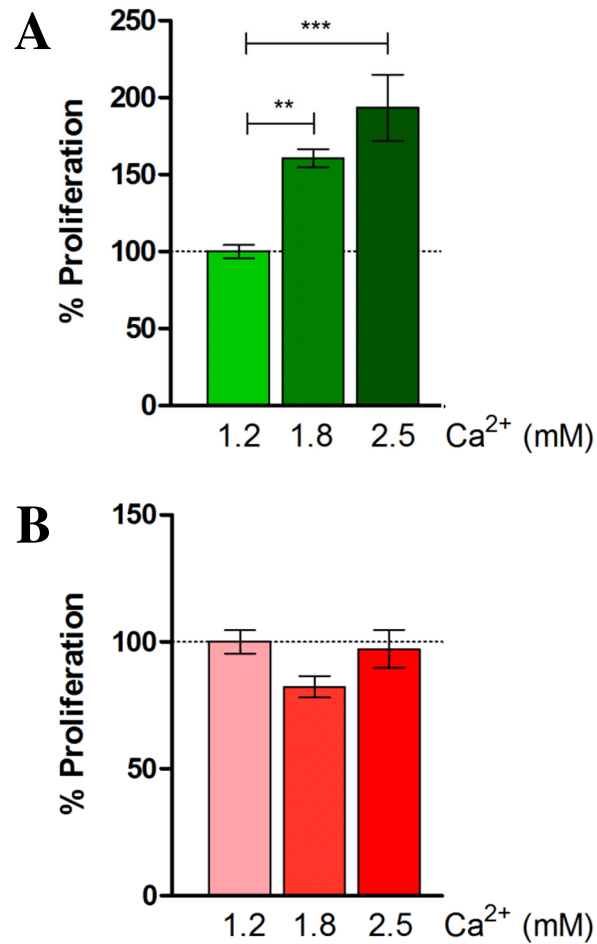
Figure 64. Ca^{2+}_o increases VSMC proliferation in a concentration-dependent manner in WT, but not in KO VSMCs. (A) WT-CaSR VSMC proliferation. (B) KO-CaSR VSMC proliferation. VSMCs were seeded at 10,000 cells per 12-well plate and allowed to adhere for 24h in DMEM containing 10% FBS and 1.2mM Ca^{2+}_o. After 24h, medium was changed to contain 1.2mM Ca^{2+}_o and 1% FBS. After a further 24h, medium was changed to contain 1.2, 1.8 or 2.5mM Ca^{2+}_o in the presence of a 0.001% DMSO vehicle control. Cells were left for 10 days with medium changing every 3 days. At day 10, cells were trypsinised in 0.05% trypsin EDTA and manually counted using a haemocytometer. Data were normalised to each respective batch of cells to the 1.2mM Ca^{2+}_o control. This approach was taken to minimise cell batch variability. (A) N=4/n=8. (B) N=4/n=8. Data are expressed as average ± SEM. Statistical analysis: one-way ANOVA. P<0.01=**. P<0.001=***.
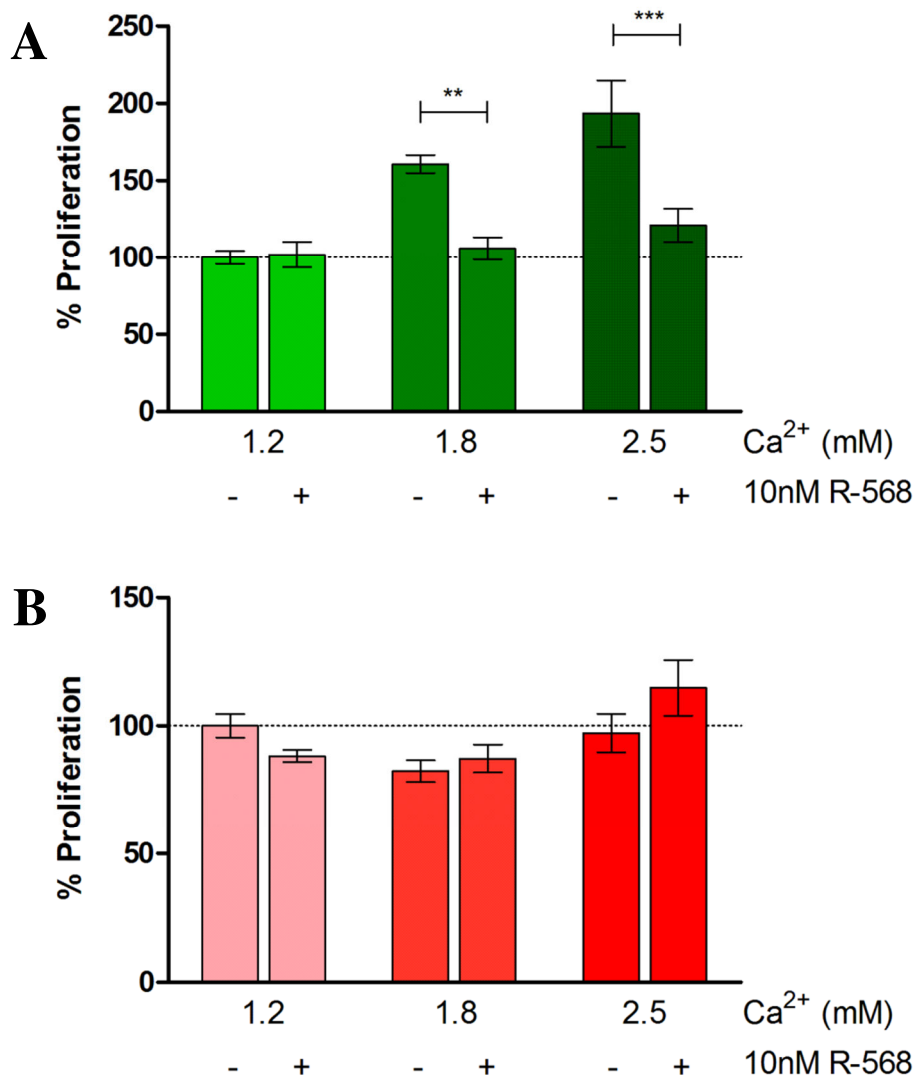
Figure 65. Calcimimetics reduce Ca^{2+}_o-induced proliferation in WT-CaSR VSMCs, but not in KO-CaSR VSMCs. (A) WT-CaSR VSMC proliferation. (B) KO-CaSR VSMC proliferation. VSMCs were seeded at 10,000 cells per 12-well plate and allowed to adhere for 24h in DMEM containing 10% FBS and 1.2mM Ca^{2+}_o. After 24h, medium was changed to contain 1.2mM Ca^{2+}_o and 1% FBS. After a further 24h, medium was changed to contain 1.2, 1.8 or 2.5mM Ca^{2+}_o in the presence of 10nM R-568 or a 0.001% DMSO vehicle control. Cells were left for 10 days with medium changing every 3 days. At day 10, cells were trypsinised in 0.05% trypsin EDTA and manually counted using a haemocytometer. Data were normalised to each respective batch of cells to the 1.2mM vehicle-treated Ca^{2+}_o control. This approach was taken to minimise cell batch variability (A) N=4/n=8. (B) N=4/n=8. Data are expressed as average ± SEM. Statistical analysis: one-way ANOVA. $P<0.01$=**. $P<0.001$=***.

Ca^{2+}_o increases proliferation in WT-CaSR VSMCs in a concentration dependent manner, but not in KO-CaSR VSMCs.

WT-CaSR VSMCs that were cultured in the presence of >1.2mM Ca^{2+}_o had significant increases in proliferation. Cell counts were normalised to the baseline 1.2mM Ca^{2+}_o culture conditions in each batch of cells. Although un-normalised data showed the same trend, data became more reliable during normalisation due to cell batch variability. For this reason baseline proliferation rates in both WT and KO VSMCs (in the presence of 1.2mM Ca^{2+}_o) averaged 100%. Proliferation values for WT VSMCs were as follows: For 1.2mM Ca^{2+}_o 100% ± 4.31 (N=4/n=8); for 1.8mM Ca^{2+}_o 160.78% ± 5.80 (N=4/n=8, P<0.01 vs. 1.2mM Ca^{2+}_o); for 2.5mM Ca^{2+}_o 193.37% ± 21.54 (N=4/n=8, P<0.001 vs. 1.2mM Ca^{2+}_o). Conversely, KO-CaSR VSMCs showed no significant changes in proliferation in response to Ca^{2+}_o when compared to the KO control VSMCs cultured in the presence of 1.2mM Ca^{2+}_o. Proliferation values for KO-CaSR VSMCs were as follows: For 1.2mM Ca^{2+}_o 100% ± 4.59 (N=4/n=8); for 1.8mM Ca^{2+}_o 82.33% ± 4.22 (N=4/n=8); for 2.5mM Ca^{2+}_o 97.15% ± 7.49 (N=4/n=8). Comparisons between KO-CaSR VSMCs across all Ca^{2+}_o concentrations showed no significant differences by two-way ANOVA with Bonferroni's post-test (Figure 64).

Calcimimetics reduce Ca^{2+}_o-dependent proliferation *in vitro* in WT-CaSR VSMCs, but not in KO-CaSR VSMCs.

The role of R-568 was also investigated in the proliferation of WT- and KO-CaSR VSMCs. VSMCs cultured in different Ca^{2+}_o concentrations (Figure 64) were also cultured in the presence of 10nM R-568 for 10 days (Figure 65). For all experiments, N=4; n=8. It was shown that in WT-CaSR VSMCs, R-568 reduced Ca^{2+}_o-dependent proliferation in the presence of 1.8mM Ca^{2+}_o and 2.5mM Ca^{2+}_o. Proliferation values for WT VSMCs in the presence of 10nM R-568 vs. vehicle control were as follows: For 1.2mM Ca^{2+}_o 101.95% ± 8.38 vs. 100% ± 4.31- not significant. For 1.8mM Ca^{2+}_o 105.88% ± 7.24 vs. 160.78% ± 5.80 (P<0.01). For 2.5mM Ca^{2+}_o 120.96% ± 10.83 vs. 193.37% ± 21.54 (P<0.001). Effects of R-568 on Ca^{2+}_o-dependent proliferation were not seen in KO-CaSR VSMCs. Proliferation values for KO VSMCs in the presence of 10nM R-568 vs. vehicle control were as follows: For 1.2mM Ca^{2+}_o 85.38% ± 3.51 vs. 100% ±

4.59- not significant. For 1.8mM Ca^{2+}_o 87.21% ± 5.41 vs. 82.33% ± 4.22- not significant. For 2.5mM Ca^{2+}_o 114.82% ± 10.83 vs. 97.15% ± 7.49- not significant.
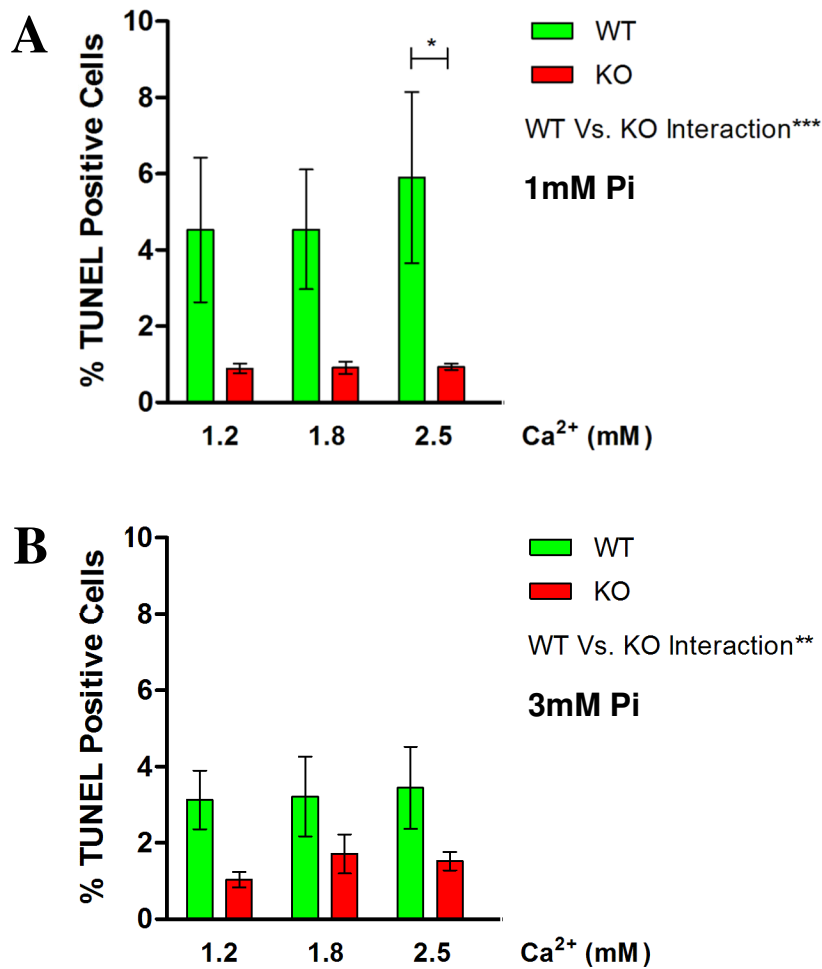
Figure 66. CaSR ablation from VSMCs significantly reduces Ca^{2+}_o-induced apoptosis. WT or KO VSMCs were seeded at 25,000 cells per 24-well plate onto glass coverslips. VSMCs were left for 24h to adhere in DMEM containing 10% FBS, 0.001% DMSO and 1.2mM Ca^{2+}_o. After this time, medium was changed to contain just 1% FBS for 24h. After 24h, medium was switched to contain 1.0 or 3mM Pi in the presence of 1.2, 1.8 or 2.5mM Ca^{2+}_o. VSMCs were left in this medium for 48h before fixing in 4% PFA for 10 minutes. Cells were then stained for TUNEL as described in methods. TUNEL-positive nuclei were then counted using a TissueFAX system by Martin Schepelmann. (A) WT (N=3/n=6) vs. KO (N=4/n=8) VSMCs in the presence of 1mM Pi. (B) WT vs. KO VSMCs in the presence of 3mM Pi. Data are expressed as mean ± SEM. Statistical analysis: two-way ANOVA with Bonferroni's post-test. $P<0.05=*$. $P<0.01=**$. $P<0.001=***$.
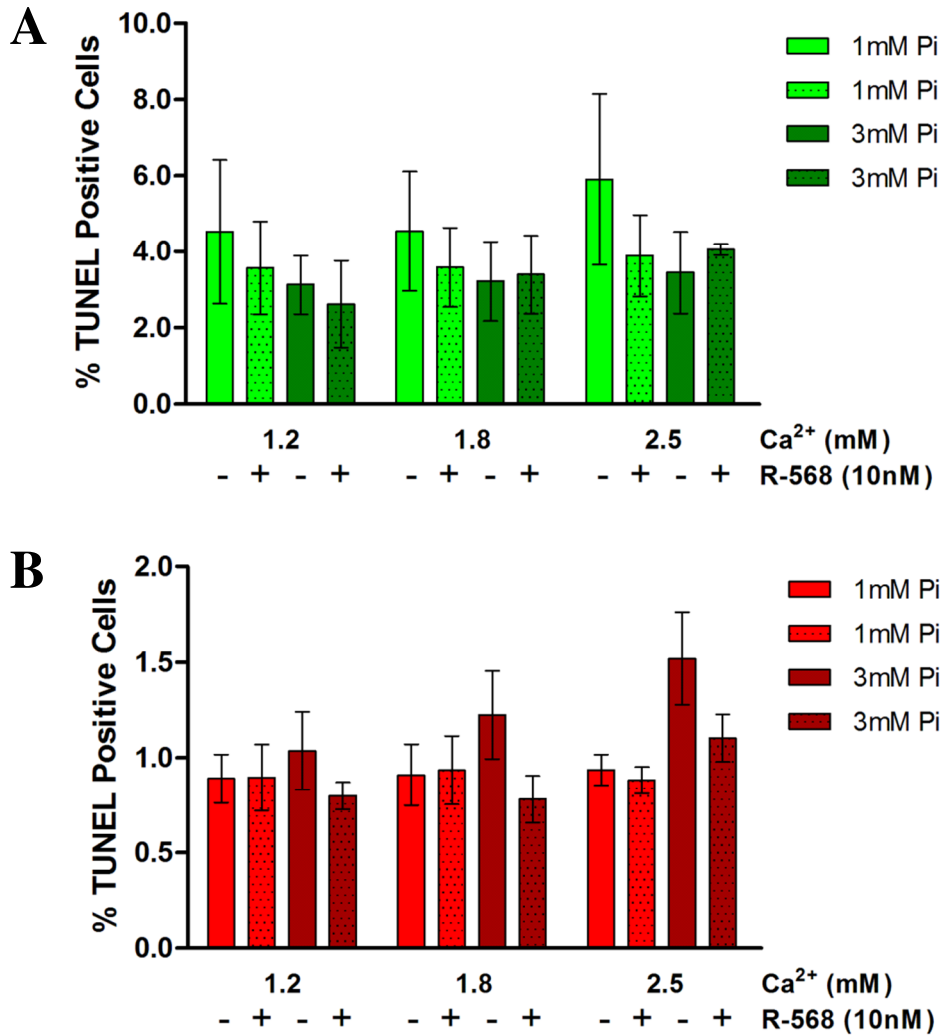
Figure 67. R-568 does not affect apoptosis either in CaSR-WT or in CaSR-KO VSMCs. WT or KO VSMCs were seeded at 25,000 cells per 24-well plate onto glass coverslips. VSMCs were left for 24h to adhere in DMEM containing 10% FBS, 0.001% DMSO and 1.2mM Ca^{2+}_o. After this time, medium was changed to contain 1% FBS for 24h. After 24h, medium was switched to contain 1.0 or 3mM Pi in the presence of 1.2, 1.8 or 2.5mM Ca^{2+}_o. Cells were also treated with 10nM R-568 or a 0.001% DMSO vehicle. VSMCs were left in this medium for 48h before fixing in 4% PFA for 10 minutes. Cells were then stained for TUNEL as described in methods. TUNEL-positive nuclei were then counted using a TissueFAX system by Martin Schepelmann. (A) WT (N=3/n=6) vs. KO (N=4/n=8) VSMCs in the presence of 1mM Pi. (B) WT vs. KO VSMCs in the presence of 3mM Pi. Data are expressed as mean ± SEM. Statistical analysis: two-way ANOVA with Bonferroni's post-test.

CaSR ablation in VSMCs reduces Ca^{2+}_o-induced apoptosis *in vitro*.

To assess the role of the VSMC-CaSR in VSMC apoptosis, TUNEL analysis was carried out to determine DNA fragmentation in response to different culture conditions. Figure 66 shows that there was a significant decrease in the rate of Ca^{2+}_o-induced apoptosis in KO-CaSR VSMCs compared to WT-CaSR VSMCs in the presence of 2.5mM Ca^{2+}_o and 1mM Pi. Data values were: 5.90% ± 1.59 WT (N=3/n=6) vs. 0.94% ± 0.06 KO (N=4/n=8; P<0.05). There was also a very significant decrease in the rates of apoptosis in KO VSMCs compared to WT VSMCs at all Ca^{2+}_o concentrations tested overall (Figure 66A, P<0.001). In experiments using mineralising conditions (I.e. 3mM Pi) DNA fragmentation was reduced at all Ca^{2+}_o concentrations tested in WT VSMCs compared to that seen in the presence of 1mM Pi. Values for WT VSMCs were: 4.53% ± 1.34 (1.2mM Ca^{2+}_o/1mM) vs. 3.13% ± 0.54 (1.2 Ca^{2+}_o/3mM Pi); 4.54% ± 1.11 (1.8 Ca^{2+}_o/1mM Pi) vs. 3.22% ± 0.74 (1.8 Ca^{2+}_o/3mM Pi); 5.90% ± 1.59 (2.5 Ca^{2+}_o/1mM Pi) vs. 3.44 ± 0.76 (2.5 Ca^{2+}_o/3mM Pi).

R-568 (10nM) does not significantly affect apoptosis in WT-CaSR or KO-CaSR VSMCs.

To assess the role of calcimimetics in VSMC apoptosis, 10nM R-568 was used to treat both WT and KO VSMCs in the presence of medium containing either 1mM or 3mM Pi and different concentrations of Ca^{2+}_o (1.2-2.5mM). Although it was observed that R-568 reduced apoptosis in KO VSMCs in the presence of 3mM Pi and either 1.8 or 2.5mM Ca^{2+}_o, this was not significant. There were also no significant effects of R-568 on apoptosis in WT VSMCs.

| 0.8mM Ca^{2+}_o | 1.2mM Ca^{2+}_o | 1.2mM Ca^{2+}_o R-568 |
| 1.8mM Ca^{2+}_o | 1.8mM Ca^{2+}_o R-568 | 2.5mM Ca^{2+}_o |
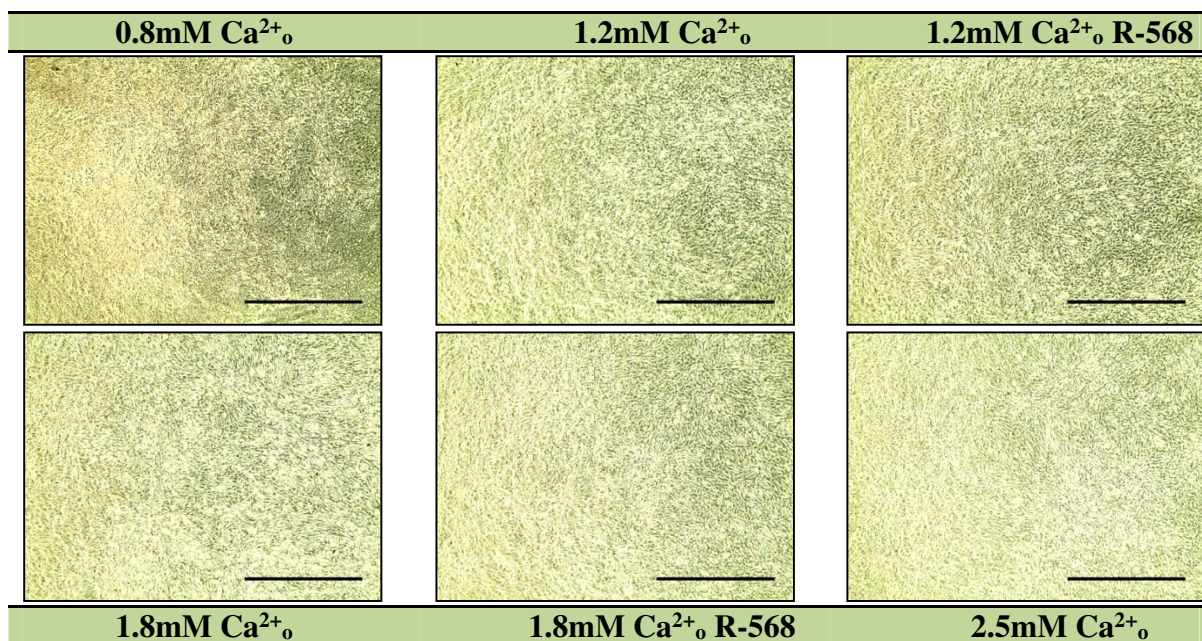
Figure 68. Mineralisation cultures of 3 month old mouse primary WT VSMCs at passage 6 exposed to medium containing different [Ca^{2+}]$_o$ in the presence of 1.4mM Pi ± R-568. Cells were plated in 24-well plates at a density of 40,000 cells per well and left for approximately 1 week until confluent in standard DMEM with 1.2mM Ca^{2+}_o and 10% FBS. Confluency was achieved at approximately 1 week and media were switched to mineralising medium which contained DMEM with 10% FBS, supplemented with $CaCl_2$ with or without the calcimimetic R-568 at 10nM (or 0.001% DMSO control). These media were also supplemented with 0.4mM Pi giving a total Pi of 1.4mM. Cells were cultured for 10 days with media changing every 2-3 days. At day 10, cells were washed in 1X PBS and fixed in 4% PFA and stained with Alizarin Red S for 5 minutes. Cells were washed in dH_2O and photographed at 4 magnification (Scale bar=1,000µm). Experiments were performed in quadruplicate for each condition yielding consistent results (n=4), with 3 separate batches of cells (N=3).

0.8mM Ca²⁺ₒ	1.2mM Ca²⁺ₒ	1.2mM Ca²⁺ₒ R-568
1.8mM Ca²⁺ₒ	1.8mM Ca²⁺ₒ R-568	2.5mM Ca²⁺ₒ

Figure 69. Mineralisation cultures of 3 month old mouse primary WT VSMCs at passage 6 exposed to medium containing different [Ca²⁺]ₒ in the presence of 3.0mM Pi ± R-568. Cells were plated in 24-well plates at a density of 40,000 cells per well and left for approximately 1 week until confluent in standard DMEM with 1.2mM Ca²⁺ₒ and 10% FBS. Confluency was achieved at approximately 1 week and media were switched to mineralising medium which contained DMEM with 10% FBS, supplemented with $CaCl_2$ with or without the calcimimetic R-568 at 10nM (or 0.001% DMSO control). These media were also supplemented with 2.0mM Pi giving a total Pi of 3.0mM. Cells were cultured for 10 days with media changing every 2-3 days. At day 10, cells were washed in 1X PBS and fixed in 4% PFA and stained with Alizarin Red S for 5 minutes. Cells were washed in dH_2O and photographed at 4 magnification (Scale bar=1,000µm). Experiments were performed in quadruplicate for each condition yielding consistent results (n=4), with 6 separate batches of cells (N=6).

0.8mM Ca^{2+}_o	1.2mM Ca^{2+}_o	1.2mM Ca^{2+}_o R-568
1.8mM Ca^{2+}_o	1.8mM Ca^{2+}_o R-568	2.5mM Ca^{2+}_o
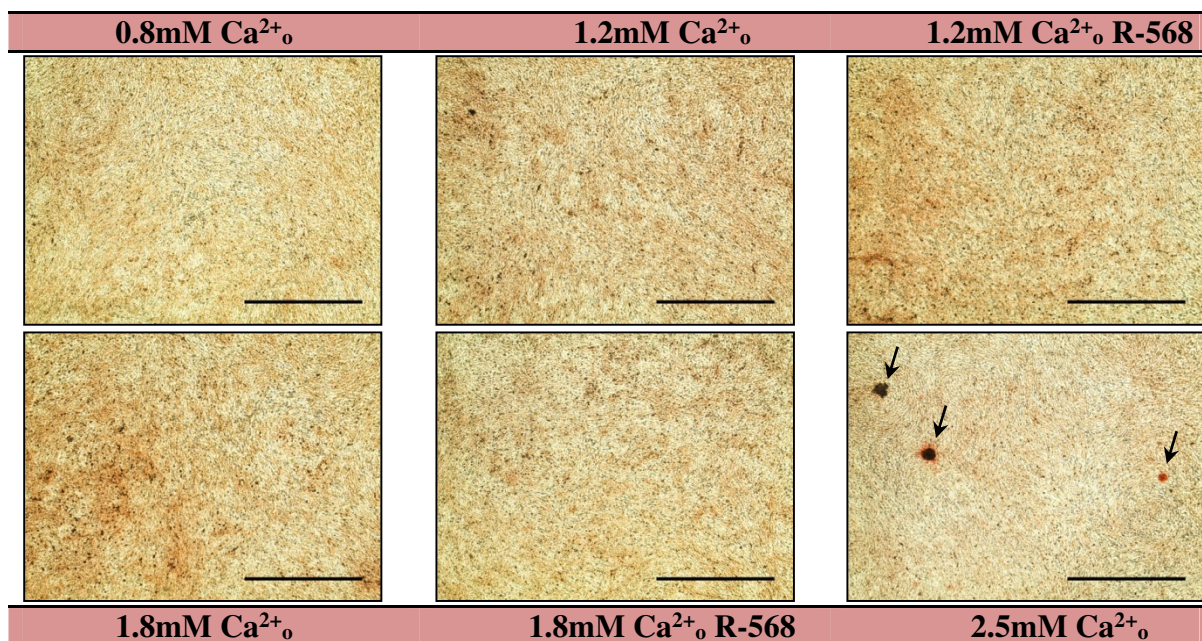
Figure 70. Mineralisation cultures of 3 month old mouse primary KO VSMCs at passage 6 exposed to medium containing different $[Ca^{2+}]_o$ in the presence of 1.4mM Pi ± R-568. Cells were plated in 24-well plates at a density of 40,000 cells per well and left for approximately 1 week until confluent in standard DMEM with 1.2mM Ca^{2+}_o and 10% FBS. Confluency was achieved at approximately 1 week and media were switched to mineralising medium which contained DMEM with 10% FBS, supplemented with $CaCl_2$ with or without the calcimimetic R-568 at 10nM (or 0.001% DMSO control). These media were also supplemented with 0.4mM Pi giving a total Pi of 1.4mM. Cells were cultured for 10 days with media changing every 2-3 days. At day 10, cells were washed in 1X PBS and fixed in 4% PFA and stained with Alizarin Red S for 5 minutes. Cells were washed in dH_2O and photographed at 4 magnification (Scale bar=1,000µm). Experiments were performed in quadruplicate for each condition yielding consistent results (n=4), with 3 separate batches of cells (N=3).

0.8mM Ca^{2+}_o	1.2mM Ca^{2+}_o	1.2mM Ca^{2+}_o R-568
1.8mM Ca^{2+}_o	1.8mM Ca^{2+}_o R-568	2.5mM Ca^{2+}_o

Figure 71. Mineralisation cultures of 3 month old mouse primary KO VSMCs at passage 6 exposed to medium containing different $[Ca^{2+}]_o$ in the presence of 3.0mM Pi ± R-568. Cells were plated in 24-well plates at a density of 40,000 cells per well and left for approximately 1 week until confluent in standard DMEM with 1.2mM Ca^{2+}_o and 10% FBS. Confluency was achieved at approximately 1 week and media were switched to mineralising medium which contained DMEM with 10% FBS, supplemented with $CaCl_2$ with or without the calcimimetic R-568 at 10nM (or 0.001% DMSO control). These media were also supplemented with 2.0mM Pi giving a total Pi of 3.0mM. Cells were cultured for 10 days with media changing every 2-3 days. At day 10, cells were washed in 1X PBS and fixed in 4% PFA and stained with Alizarin Red S for 5 minutes. Cells were washed in dH_2O and photographed at 4 magnification (Scale bar=1,000µm). Experiments were performed in quadruplicate for each condition yielding consistent results (n=4), with 5 separate batches of cells (N=5).
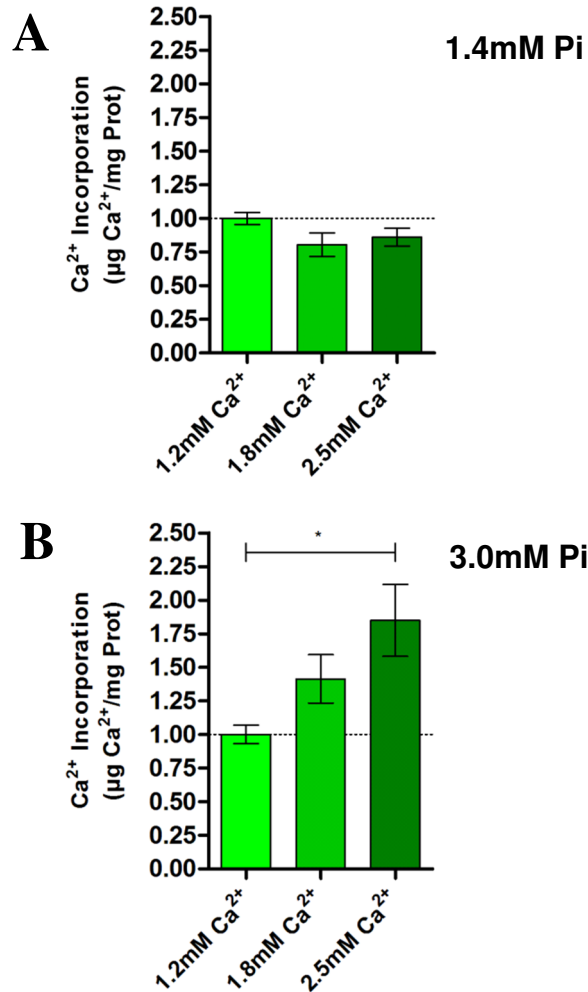
Figure 72. Ca^{2+} incorporation in mineralised cultures of 3 month old mouse primary WT VSMCs cells. WT VSMCs were plated and mineralised as described in Figures 68 and 69 in medium containing different $[Ca^{2+}]_o$ in the presence of either 1.4 or 3.0mM Pi. At day 10, cells were washed in 1X PBS and Ca^{2+} was eluted and quantified as described in the methods using the O-cresolphthalein complexone method. Protein was also quantified using the BCA assay as described. Units are in µg Ca^{2+}/mg protein, and expressed as fold-changes compared to Ca^{2+} incorporation within each batch of VSMCs in the presence of the 1.2mM Ca$^{2+}_o$ for each Pi concentration. (A) VSMCs mineralised in 1.4mM Pi (N=3/n=12). (B) VSMCs mineralised in 3.0mM Pi (N=5/n=20). Data are expressed as mean ± SEM. Statistical analysis: one-way ANOVA. P<0.05=*.
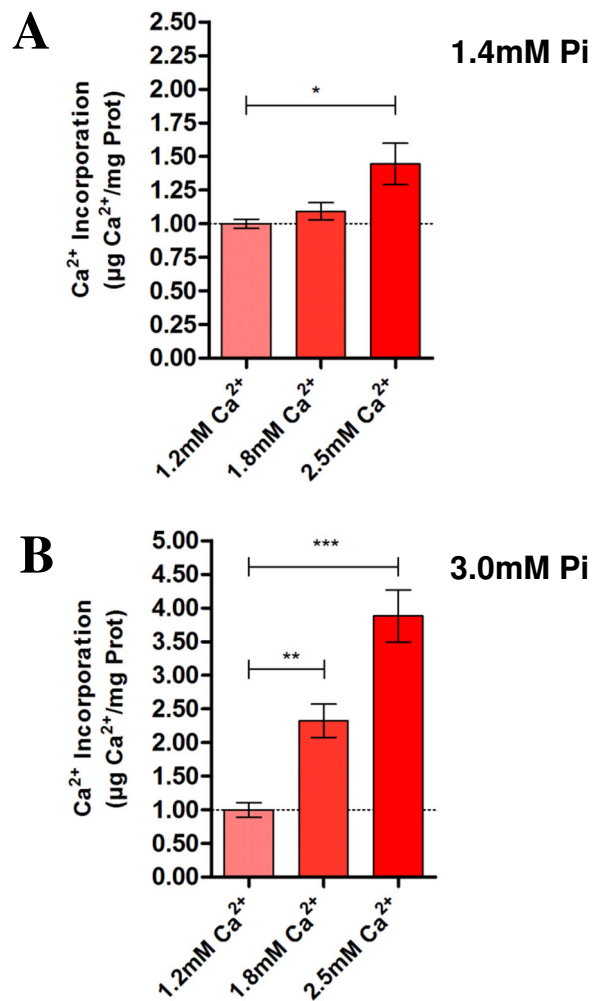
Figure 73. Ca²⁺ incorporation in mineralised cultures of 3 month old mouse primary KO VSMCs cells. KO VSMCs were plated and mineralised as described in Figures 70 and 71 in medium containing different $[Ca^{2+}]_o$ in the presence of either 1.4 or 3.0mM Pi. At day 10, cells were washed in 1X PBS and Ca^{2+} was eluted and quantified as described in the methods using the O-cresolphthalein complexone method. Protein was also quantified using the BCA assay as described. Units are in µg Ca^{2+}/mg protein, and expressed as fold-changes compared to Ca^{2+} incorporation within each batch of VSMCs in the presence of the 1.2mM Ca^{2+}_o for each Pi concentration. (A) VSMCs mineralised in 1.4mM Pi (N=2/n=8). (B) VSMCs mineralised in 3.0mM Pi (N=5/n=20). Data are expressed as mean ± SEM. Statistical analysis: one-way ANOVA. P<0.05=*. P<0.01=**. P<0.001=***.
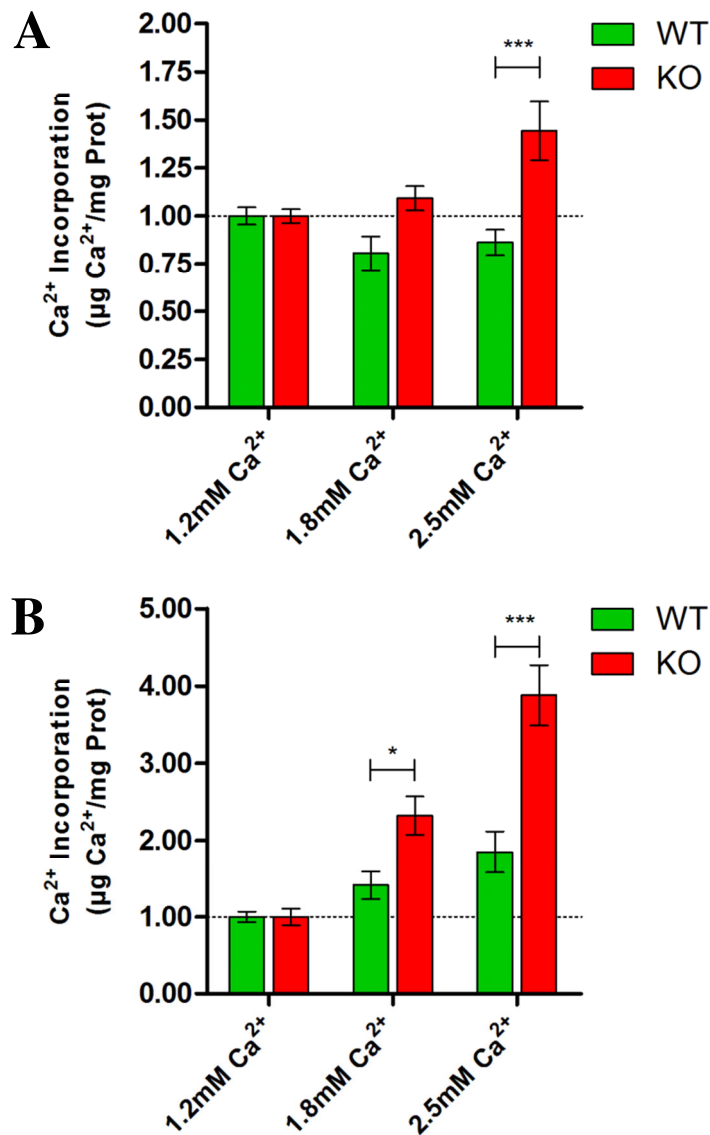
Figure 74. CaSR-KO VSMCs incorporate more Ca²⁺ mineral than CaSR-WT VSMCs in both mineralising and non-mineralising conditions. WT and KO VSMCs were mineralised as described in Figures 72 and 73). Data from Figures 73 and 74 are compiled here for statistical analyses against one another to demonstrate differences in mineralisation of these WT and KO VSMCs. (A) WT vs. KO VSMCs cultured in the presence of 1.4mM Pi. (B) WT vs. KO VSMCs cultures in the presence of 3.0mM Pi. Data are expressed as mean ± SEM. Statistical analysis: two-way ANOVA with Bonferroni's post-test. $P<0.05=*$. $P<0.001=***$.

KO VSMCs mineralise more readily in the presence of high phosphate (Pi) than WT VSMCs.

In the presence of 1.4mM Pi, Ca^{2+}_o at all concentrations tested (1.2-2.5mM) did not increase calcification in WT VSMCs (Figure 72A). However, in KO VSMCs, 2.5mM Ca^{2+}_o was sufficient to increase Ca^{2+} incorporation significantly from the 1.2mM Ca^{2+}_o control (Figure 73A). Values in the presence of 2.5mM Ca^{2+}_o were: 1.44 ± 0.15 (N=3/n=12) vs. 1.00 ± 0.04 (N=3/n=12) in the 1.2mM Ca^{2+}_o control (P<0.05). In the presence of 3.0mM Pi (mineralising conditions), calcification was only significantly increased in WT VSMC mineralised cultures in the presence of 2.5mM Ca^{2+}_o (Figure 72B). Values were: 1.85 ± 0.27 (N=5/n=20) vs. 1.00 ± 0.07 (N=5/n=20) in the 1.2mM Ca^{2+}_o control (P<0.05). Conversely, in KO VSMCs cultured in the presence of 3.0mM Pi, calcification was significantly increased in the presence of both 1.8 and 2.5mM Ca^{2+}_o (Figure 73B). Values for 1.8mM Ca^{2+}_o were 2.42 ± 0.24 (N=5/n=20) vs. 1.00 ± 0.11 (N=5/n=20, P<0.01). Values for 2.5mM Ca^{2+}_o were 3.88 ± 0.44 (N=5/n=20) vs. 1.00 ± 0.11 (N=5/n=20, P<0.001).

In Figures 72 and 73 it was shown that within each genotype in the presence of 3.0mM Pi, Ca^{2+}_o induced significantly more calcification than 1.2mM Ca^{2+}_o in a concentration dependent manner. Figure 74 demonstrates that KO VSMCs mineralise more than WT VSMCs relative to their 1.2mM Ca^{2+}_o controls in both the presence of 1.4mM Pi and 3.0mM Pi. In the presence of 1.4mM Pi and 2.5mM Ca^{2+}_o, KO VSMCs had significantly more Ca^{2+} incorporation compared to WT VSMCs. Fold changes at 2.5mM Ca^{2+}_o were as follows: 0.86 ± 0.07 (N=3/n=12) WT vs. 1.44 ± 0.15 (N=3/n=12, P<0.001). Increases in Ca^{2+} incorporation were more observable in the presence of 3.0mM Pi. There were no significant differences at 1.2mM Ca^{2+}_o since these were the normalised values however, Ca^{2+}_o incorporation values at 1.8mM Ca^{2+}_o were as follows: 1.41 ± 0.18 (N=5/n=20) WT vs. 2.32 ± 0.25 (N=5/n=20, KO, P<0.05). Ca^{2+}_o incorporation values at 2.5mM Ca^{2+}_o were 1.85 ± 0.27 (N=5/n=20, WT) vs. 3.88 ± 0.44 (N=5/n=20, KO, P<0.001).
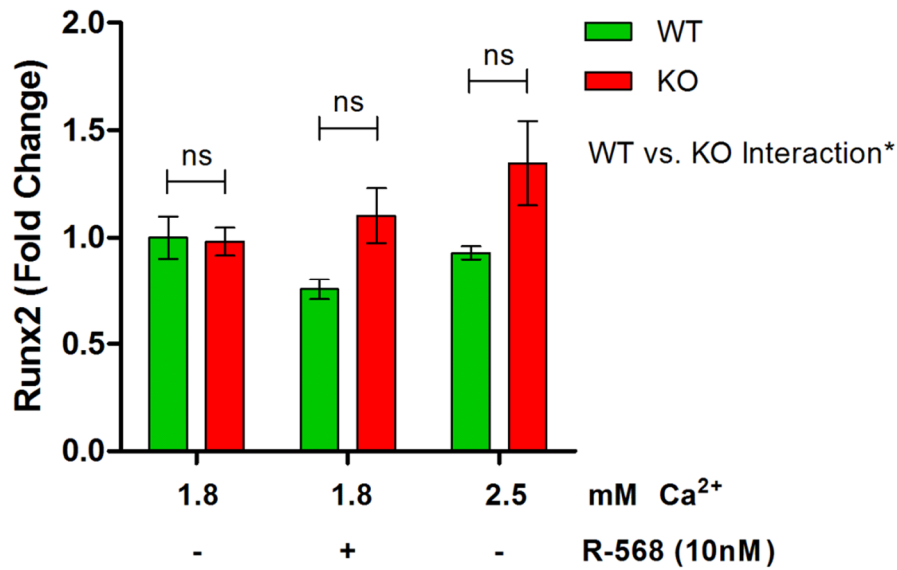
Figure 75. Selective ablation of CaSR in VSMCs promotes osteogenic transdifferentiation by upregulating Runx2. WT and KO VSMCs were plated and mineralised as described in Figures 68 and 71 in medium containing different $[Ca^{2+}]_o$ in the presence of 3.0mM Pi. At day 5, cells were washed in 1X PBS and TRIzol® reagent was added to cell monolayers. RNA was obtained and converted to cDNA as described in methods. 50ng of cDNA was used in each qPCR reaction with GAPDH and Runx2 primer sets as described in methods. Plasmid clones containing either GAPDH or Runx2 amplicons were also run alongside experimental cDNA to confirm efficient amplification. Runx2 Ct values were normalised to GAPDH Ct levels present in each sample. All data were then normalised to Runx2 ΔCt values from cDNA of WT VSMCs cultures in the presence of 1.8mM Ca^{2+}_o and 3.0mM Pi sample averages. This was considered the baseline level of Runx2 expression. WT: N=2/n=4, KO: N=4/n=8. Data are expressed as mean ± SEM. Statistical analysis: one-way ANOVA. P<0.05=*.

Selective ablation of CaSR in VSMCs promotes osteogenic transdifferentiation by upregulation of Runx2.

To investigate whether mineralising conditions of culture (3.0mM Pi and 1.8mM or 2.5mM Ca^{2+}_o) were sufficient to promote osteogenic transdifferentiation in mouse VSMCs, qPCR was performed to amplify Runx2 mRNA. Runx2 is considered as an early master osteoblastic transcription factor upregulated in VSMCs in pro-mineralising conditions (Sun *et al.*, 2010). Demer *et* al first described the process of calcification as a cell-mediated process associated with abnormal upregulation of osteogenic markers in calcified arteries (Demer and Watson, 1994). To test whether mineral deposition in mouse VSMCs cultured *in vitro* involved upregulation of osteoblast gene expression, the expression of Runx2 mRNA, not normally expressed in non-mineralising conditions, was analysed. WT and KO cells were mineralised in the presence of 3.0mM Pi and 1.8mM $Ca^{2+}_o \pm$ R-568, or 2.5mM Ca^{2+}_o in the absence of R-568. Runx2 primer sets were used in qPCR reactions with cDNA from mineralised WT and KO VSMCs. GAPDH primer sets were also used for normalisation to a house-keeping gene. Data show that, when cells were cultured in the presence of 1.8mM and 2.5mM Ca^{2+}_o, Runx2 mRNA expression was not significantly different in WT mineralised VSMCs compared to KO mineralised VSMCs. Additionally, there was no significant difference in levels of Runx2 mRNA cells cultured in the presence of 1.8mM Ca^{2+}_o added with 10nM R-568. However, there was an overall significant increase in Runx2 expression in mineralised KO VSMCs compared to mineralised WT VSMCs at all concentrations tested (P<0.05, Figure 75).
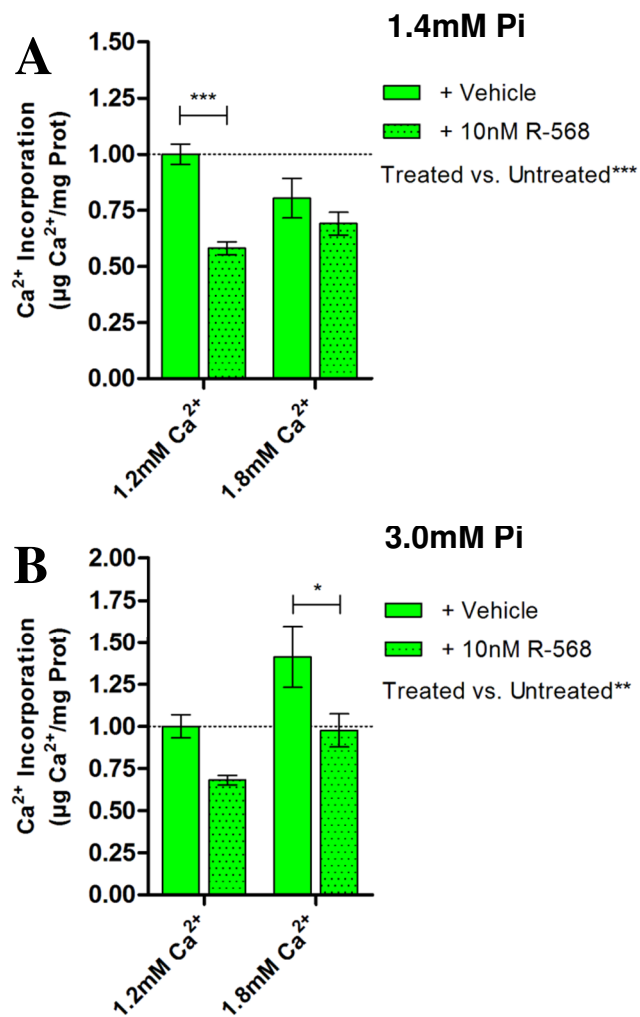
Figure 76. R-568 reduces Ca^{2+}_o-dependent mineralisation of 3 month old mouse primary WT VSMCs. WT VSMCs were prepared and mineralised in the same way as Figure 68 and 69 in medium containing either 1.4 or 3.0mM Pi in the presence of 1.2mM or 1.8mM Ca^{2+}_o, with either 10nM R-568 or a 0.001% DMSO vehicle. Mineralisation was performed using the same method. (A) VSMC mineralisation in the presence of 1.4mM Pi (N=3/n=12). (B) VSMC mineralisation in the presence of 3.0mM Pi. (N=5/n=20). Data are expressed as mean ± SEM. Statistical analysis: one-way ANOVA. P<0.05=*. P<0.01=**. P<0.001=***.
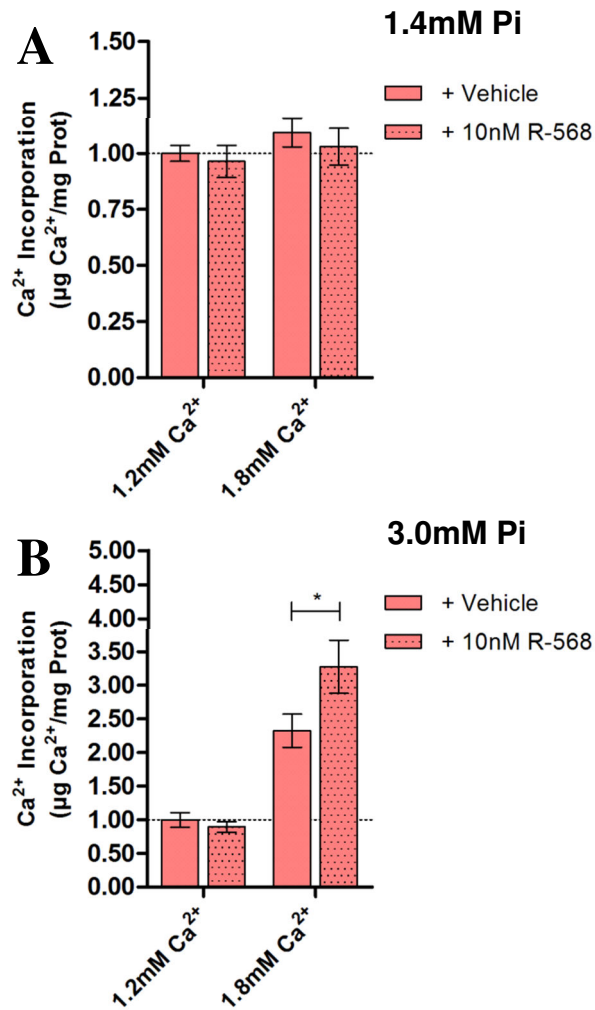
Figure 77. R-568 did not effect Ca$^{2+}_o$-dependent mineralisation of 3 month old mouse primary KO VSMCs. KO VSMCs were prepared and mineralised in the same way as Figure 70 and 71 in medium containing either 1.4 or 3.0mM Pi in the presence of 1.2mM or 1.8mM Ca$^{2+}_o$, with either 10nM R-568 or a 0.001% DMSO vehicle. Mineralisation was performed using the same method. (A) VSMC mineralisation in the presence of 1.4mM Pi (N=3/n=12). (B) VSMC mineralisation in the presence of 3.0mM Pi. (N=5/n=20). Data are expressed as mean ± SEM. Statistical analysis: one-way ANOVA. P<0.05=*.

The calcimimetic R-568 reduces Ca^{2+} incorporation and mineralisation in WT mouse VSMCs but not in KO mouse VSMCs.

As described previously, cells were mineralised in the presence of 1.4mM and 3.0mM Pi with different Ca^{2+}_o concentrations. 10nM R-568 was also used in the presence of either 1.2mM Ca^{2+}_o or 1.8mM Ca^{2+}_o to determine any effect through the VSMC-CaSR. WT and KO VSMCs were mineralised as described in the presence of 10nM R-568 or a vehicle of 0.001% DMSO for 10 days. At day 10, WT VSMCs cultured in medium containing 1.4mM Pi exhibited significantly reduced Ca^{2+} incorporation. Ca^{2+} incorporation in the presence of 1.2mM Ca^{2+}_o was: 0.58 ± 0.03 treated vs. 1.00 ± 0.04 untreated (N=3/n=12, P<0.001, Figure 76A). Although differences in the presence of 1.8mM Ca^{2+}_o were not significant, it was shown that the overall relationship between treated and untreated WT VSMCs was significant (P<0.001; Figure 76A). In the presence of 3.0mM Pi, R-568 also reduced calcification in the presence of 1.8mM Ca^{2+}_o. R-568 decreased calcification from 1.41 ± 0.18 (vehicle) to 0.98 ± 0.09 (treated) (N=5/n=20, P<0.05). Although R-568 treatment in the presence of 1.2mM Ca^{2+}_o was not significant, there was a significant effect of R-568 treatment vs. no treatment overall (P<0.01; Figure 76B). R-568 did not reduce mineralisation in KO VSMC cultures in the presence of 1.4mM Pi and either 1.2 or 1.8mM Ca^{2+}_o (Figure 77A). Interestingly, in the presence of 3.0mM Pi and 1.8mM Ca^{2+}_o, R-568 actually increased calcification from 2.32 ± 0.25 (vehicle) to 3.28 ± 0.40 (treated, N=5/n=20, P<0.05, Figure 77B).

CHAPTER 6: DISCUSSION

CaSR is expressed in mouse vascular smooth muscle cells and mouse endothelial cells.

It has previously been demonstrated that, endothelial cells express the CaSR where the receptor plays a crucial role in blood vessel tone modulation (Weston, 2005). My findings show that mouse aortae also express very intense CaSR immunoreactivity in the endothelium. Whether this CaSR protein is localised to the plasma membrane or not has not yet been determined, although it is likely since CaSR is functionally active in endothelial cells. Comparatively, CaSR immunostaining in VSMCs in the tunica media appears to be less intense and more diffuse throughout the cytosol as shown by immunofluorescent imaging. Albeit fainter than in ECs, VSMC CaSR staining is above that seen in the negative controls. Whether VSMC-CaSR protein is at the plasma membrane or not has also yet to be determined.

Ablation of CaSR in VSMCs reduces total CaSR protein as determined by semi-quantitative immunofluorescent imaging.

Studies from several laboratories indicate that CaSR is a poorly expressed protein, particularly outside of the parathyroid glands. Indeed, many groups have failed to detect it at the mRNA level and/or the protein level. For this reason it has been difficult to amplify CaSR transcripts by qPCR which are lowly expressed. Semi-quantitative immunofluorescent imaging offers some benefits here in determining the expression levels of the protein by using an N-terminal antibody to CaSR. As one of the few antibodies that shows specificity and cross-reactivity in mouse tissue and cells, this N-terminal antibody (AnaSpec) has been used for my protein expression studies. By using the Tissue Quest^{TM} software on slides stained at the same time using the same protocol, we were able to quantify the relative brightness of the CaSR signal in these immunofluorescently-labelled VSMCs. Data showed a 35.26% reduction in the intensity of CaSR-positive cells, when comparing WT to KO VSMCs under cultured under physiological conditions (Figure 60). Although only semi-quantitative, these data suggest that the CaSR expression is downregulated in KO VSMCs. Importantly, it should also be noted that although CaSR protein remains in KO VSMCs (~35.26%), this is a truncated form that encodes the N-terminus of the CaSR unable to bind agonists as shown by the

Chang group (Chang *et al.*, 2008). The development of novel antibody directed against the carboxy terminus of the CaSR, to distinguish between WT and KO CaSR proteins, will provide a significant advantage for studies which use the exon 7 CaSR deletion mouse model.

Ca^{2+}_o (1.2-1.8mM) and R-568 (1-100nM) do not affect cell viability in WT and KO VSMCs.

In order to determine whether Ca^{2+}_o and R-568 effected cell viability in the exon 7 CaSR deletion mouse model, an MTT assay was performed. This study was important since a variety of *in vitro* conditions were to be tested in both WT and KO-CaSR VSMCs. My studies revealed that at 7 days in culture in the conditions tested (1.2-5.0mM Ca^{2+}_o and 1.2-1.6mM $Ca^{2+}_o \pm$ 1-100nM R-568) there was no significant effect of Ca^{2+}_o or R-568 on cell viability of WT and KO VSMCs compared to the 1.2mM Ca^{2+}_o/1mM Pi control culture conditions. In the case of R-568, there was no difference in all treatments (1-100nM) vs. untreated VSMCs in the presence of 1.2-1.6mM Ca^{2+}_o. Due to time constraints the role of Pi in VSMC cell viability was not investigated. However, it would be beneficial to investigate the role of Pi in VSMC viability since hyperphosphataemia is correlated with calcification an apoptosis. One might presume that VSMC viability would be affected in mineralising conditions, particularly in the presence of R-568.

KO-VSMC and WT-VSMC proliferation rates are not different in standard conditions of VSMC culture.

During my experiments, I observed that KO-VSMCs appear to proliferate faster than WT VSMCs and therefore I tested this possibility *in vitro*. My data reflect that this is indeed the case, however, this was not significant using a two-tailed t-test with a P value of 0.08. It is therefore likely that more repeats (n=8 as determined using the power calculation) will need to be carried out to obtain significance. It has been reported previously that activation of CaSR by calcimimetics suppress parathyroid cell proliferation both *in vivo* and *in vitro* (Wada *et al.*, 1997a, Wada *et al.*, 2000, Roussanne *et al.*, 2001, Colloton *et al.*, 2005). In our KO VSMCs where there is no functional CaSR, this would suggest that

under normal conditions of 1.2mM Ca^{2+}_o and 1.0mM Pi in culture, activation of CaSR is not possible and therefore, CaSR-dependent inhibition of proliferation could not occur resulting in faster proliferation rates.

Ca^{2+}_o induces proliferation in a concentration-dependent manner in WT VSMCs, but not in KO VSMCs.

The role of Ca^{2+}_o in proliferation of VSMCs was investigated (Figure 64). My results show that WT VSMC proliferation rates greatly increased in response to increasing $[Ca^{2+}]_o$. We have previously shown in bovine VSMCs that culturing cells in the presence of Ca^{2+}_o higher than 1.2mM leads to downregulation of CaSR protein by, so far, unknown mechanisms (Alam *et al.*, 2008). Therefore, this increase in proliferation may be a consequence of downregulation of CaSR in the presence of 1.8 and 2.5mM Ca^{2+}_o. Furthermore, activation of CaSR by agonists such as calcimimetics has been shown to suppress proliferation both *in vivo* and *in vitro* (Wada *et al.*, 1997a, Wada *et al.*, 2000, Roussanne *et al.*, 2001, Colloton *et al.*, 2005), possibly by upregulating membrane CaSR (Mizobuchi *et al.*, 2004). If this is true, then the anti-proliferative properties of CaSR diminish in the presence of increasing concentrations of Ca^{2+}_o. This may perhaps be the reason why Ca^{2+}_o induces proliferation in a concentration dependent manner in WT VSMCs only.

My observations also show that KO VSMC proliferation rates in the presence of 1.2, 1.8 and 2.5mM Ca^{2+}_o were not different from one another. This would illustrate that KO-CaSR VSMCs are unable to 'sense' Ca^{2+}_o through the CaSR and respond accordingly to alterations in VSMC proliferation as WT-CaSR VSMCs have. What remains unclear is a reason for WT VSMC proliferation in the presence of 1.8 and 2.5mM Ca^{2+}_o to be higher than KO VSMC proliferation under these same conditions. Since the CaSR has previously been linked to regulation of the cell cycle protein Ki 67 in parathyroid glands (Roussanne *et al.*, 2001), I hypothesize that CaSR ablation in VSMCs has phenotypically altered these cells and so limited their maximal proliferation rates.

R-568 (10nM) reduces Ca^{2+}_o-induced proliferation in WT VSMCs, but not in KO VSMCs.

It was also shown that R-568 reduced Ca^{2+}_o-induced proliferation in WT VSMCs but not in KO VSMCs. R-568 did not significantly affect KO VSMC proliferation. This is in agreement with previous observations that calcimimetics reduce proliferation in parathyroid cells (Wada *et al.*, 1997a, Wada *et al.*, 2000, Roussanne *et al.*, 2001, Colloton *et al.*, 2005). This suggests that both the PTG-CaSR and VSMC-CaSR share some similar function, particularly in their reduced proliferation rates in response to calcimimetics. Calcimimetics have been shown to increase $[Ca^{2+}]_i$ in cells, and it can therefore be speculated that increases in $[Ca^{2+}]_i$ through this pathway are associated with reductions in proliferation. If this is the case, this would suggest that KO VSMCs have reduced $[Ca^{2+}]_i$ as suggested in previous chapters where CaSR ablation in VSMCs is associated with reductions in contractile tone. However, this remains to be investigated using, for example, calcium imaging experiments.

KO VSMCs have reduced apoptosis compared to WT VSMCs.

Increased apoptosis is correlated with increased vascular calcification *in vivo* and *in vitro* (Proudfoot *et al.*, 2000, Clarke *et al.*, 2008). For this reason it was important to investigate apoptosis rates of both WT and KO VSMCs in physiological and pathophysiological conditions. Figures 66 and 67 show that there was no significant effect of a range of $[Ca^{2+}]_o$ on apoptosis. Interestingly, I have consistently shown that KO VSMCs had decreased levels of apoptosis at all concentrations compared to WT VSMCs overall in the presence of both 1mM and 3mM Pi (P<0.001 and P<0.01 respectively). These results were surprising since this suggests that CaSR expression and activation promotes apoptosis, which is in stark contrast to what previous investigators have shown. One study by Molostov and colleagues showed that CaSR activation by neomycin can reduce apoptosis in VSMCs, and that disrupting neomycin signalling through ERK inhibition increases apoptotic rates (Molostvov *et al.*, 2008). It has also been shown that activation of CaSR by Mg^{2+} and La^{3+} significantly reduces apoptosis and calcification (Shi *et al.*, 2009, Kircelli *et al.*, 2012). Additionally, in a mouse model of selective ablation of CaSR in osteoblasts, developed by Dr. Chang, the group report that apoptosis is increased

(Chang *et al.*, 2008). This further supports the idea that CaSR protects against apoptosis. It is therefore possible that during apoptosis experiments of KO VSMCs, cells detach from coverslips. In this way, only apoptotic cells which still remain adhered to coverslips are detectable by immunostaining. To test this hypothesis, supernatants from cells in mineralising medium should be taken in the future to test for the presence of apoptotic or dead cells. The role of R-568 was also investigated to determine whether pharmacological allosteric activation of the VSMC CaSR had an effect on apoptosis. My observations show that there are no significant effects of Ca^{2+}_o (1.2-2.5mM), Pi (1.0 and 3.0mM) and R-568 (10nM) at all concentrations tested. Furthermore, when group comparisons were made to compare all conditions within each Pi group or within each genotype, there was also no significant effect. This was not so surprising since apoptosis is considered quite a rare event with rates normally at <5%. It is likely that by using different conditions, I.e. concentrations of 100nM R-568, the role of R-568, if any, on the VSMC CaSR may become clear.

CaSR protects against calcification *in vitro* in mouse VSMCs.

The rate of mineralisation was significantly augmented by selective ablation of CaSR from VSMCs. As previously demonstrated in bovine VSMCs, loss of expression of CaSR is associated with increased mineralisation of VSMCs (Alam *et al.*, 2008). Here, I provide conclusive evidence that this is indeed the case using the SM22α x fl CaSR mouse model.

We have seen in previous chapters that VSMC-KO of the CaSR induces (i) hypercalcaemia, (ii) heavier hearts, (iii) reduced contractile tone, and (iv) monophasic vasorelaxation of the aorta/aortic VSMCs. In particular, the lack of contractile tone suggests that VSMCs cannot regulate Ca^{2+}_o levels effectively through activation of the CaSR. This could either be by preventing Ca^{2+}_o release from internal stores or by preventing Ca^{2+}_o uptake from extracellular environments. CaSR is linked to the expression of Ca^{2+}_o-binding proteins such as MGP (Mendoza *et al.*, 2010) and there is evidence for an upregulation of MGP mRNA during R-568 treatment and

hypercalcaemia. Given this evidence, it is difficult to determine expression levels of MGP in KO VSMCs without yet performing qPCR experiments. On one hand, WT VSMCs containing a functional CaSR may upregulate MGP expression. Conversely, KO VSMCs that are associated with a hypercalcaemic environment *in vivo* are also likely to upregulate MGP expression in a compensatory manner. It is therefore difficult to speculate whether MGP levels will be up- or downregulated in KO VSMCs, or whether there will be no difference compared to WT MGP levels.

Selective ablation of CaSR in VSMCs promotes osteogenic transdifferentiation.

Runx2 is a master regulator of osteoblastic differentiation (Sun *et al.*, 2010). My observations show that there is an increase in Runx2 mRNA expression in KO VSMCs compared to WT VSMCs in the presence of mineralising conditions (Figure 75). Although the individual inter-sample comparisons were not statistically different, the fact that there are only 2 WT VSMC isolations run in duplicate (n=4) is likely to account for the lack of inter-sample significance. However, these preliminary observations support the well-established fact that increased calcification is associated with Runx2 upregulation. Although the mechanisms by which CaSR achieves this effect are unknown, previous studies have suggested the possibility that it is likely due to a lack of expression of protective factors such as MGP, which have also been shown to be linked to CaSR expression and activation (Mendoza *et al.*, 2010). Due to time constraints, I was unable to perform qPCRs for other important genes involved in the calcification process such as SM22α, BMPs and MGP. This remains an important area for future investigation.

R-568 significantly reduces mineralisation in mouse WT VSMCs but not in KO VSMCs *in vitro*.

Our group has previously reported that R-568 attenuates calcification *in vitro* at concentrations as low as 1nM (Alam *et al.*, 2008). For this study we assessed the ability of R-568 to activate the VSMC CaSR. In this study I showed that R-568 in the presence of mineralising conditions (3.0mM Pi) significantly reduced calcification in WT-CaSR mouse VSMCs *in vitro*. It has been shown that when R-568 binds to the CaSR, this leads

to an increase in the phosphorylation of ERK, as well as increases in $[Ca^{2+}]_i$ mediated by IP$_3$Rs (Brown *et al.*, 1993). This may possibly be a pathway activated to reduce calcification and will be tested in the future.

There is now also growing evidence that calcimimetics can up-regulate CaSR mRNA and CaSR protein at the plasma membrane by a pharmacochaperone mechanism (Mizobuchi *et al.*, 2004, Mendoza *et al.*, 2009). In these studies, uremic rats were treated with a vehicle or calcimimetics (R-568/AMG 641). Rats exhibited significantly elevated CaSR mRNA expression and CaSR protein in response to R-568 treatment. In this regard, our initial hypothesis of the CaSR being protective against vascular calcification appears very relevant, particularly since we have demonstrated that R-568 treatment decreases calcification. If CaSR mRNA and protein are indeed upregulated in response to R-568, then the anti-calcifying effects of CaSR may be accentuated in such a scenario. Interestingly, I have shown that R-568 had no significant effect on KO VSMCs in the presence of 1.4mM Pi, however, in the presence of 3.0mM Pi, there was an unexpectedly significant effect of R-568 increasing calcification (P<0.05). Whether R-568 enhances calcification through alternative mechanisms in the absence of a CaSR remains to be investigated. It is possible that these effects are modulated through an additional GPCR with similar sequence homology. One such candidate is GPRC6A which has been shown to be expressed in rat mesenteric arteries (Harno *et al.*, 2008). Since GPRC6A is also a Ca^{2+}_o sensor (Pi *et al.*, 2008), it may be possible that this is upregulated in response to the loss of CaSR expression. GPRC6A can respond to Ca^{2+}_o at a much greater range of concentrations compared to CaSR (1-60mM). It is also upregulated in response to the Ca^{2+}_o-binding protein osteocalcin, and for this reason GPRC6A is often termed a bone Ca^{2+}_o-sensor (Pi *et al.*, 2005). GPRC6A has been shown to be upregulated in areas where Pi handling is common such as bone and the kidney (Pi *et al.*, 2005, Pi *et al.*, 2008). The role of R-568 in GPRC6A activation remains controversial since the only evidence that it does so comes from experiments by Pi *et al* where concentrations between 500nM and 5µM have been used on HEK293 cells over expressing GPRC6A (Pi *et al.*, 2005). It is speculated that at 500nM, R-568 may act specifically through CaSR (Nemeth *et al.*, 1998) or GPRC6A, however, whether the is enhanced calcification observed in

mineralised KO VSMCs is due to GPRC6A activation seems unlikely since only 10nM R-568 was been used .

Although the role of GPRC6A has not been investigated in these studies, it seems likely that GPRC6A may be upregulated in KO CaSR VSMCs as an alternative Ca^{2+}_{o}-sensing mechanism. If so, Pi and Ca^{2+} may be handled in a similar manner to bone, promoting mineralisation and a less contractile SMC-like phenotype. To investigate this hypothesis further, gene expression studies and immunohistochemical analysis of isolated arteries should be performed.

CHAPTER 6: CONCLUSION

CaSR is protective against vascular calcification *in vitro*.

Taken together, my data confirm that CaSR plays a significant role in proliferation, apoptosis and mineralisation *in vitro*. The previously hypothesized protective role of CaSR in bovine VSMC mineralisation has now been confirmed in our model of targeted deletion of CaSR in VSMCs. Furthermore, R-568 appears to be specific to the VSMC CaSR by significantly reducing both proliferation and mineralisation *in vitro*. In the context of cardiovascular disease and calcification, the existence of proliferation and apoptosis *in vivo* in VSMCs are key features of vessel damage or calcification. For these reasons, there is now strong evidence that calcimimetics such as R-568 may be effective at reducing vascular calcification *in vivo*.

CHAPTER 6: FUTURE WORK

From these studies it is clear that calcimimetics, at the concentrations tested (1-100nM), act on the CaSR, and appear to be specific to this receptor in physiological conditions. However, in light of mineralisation data in VSMCs from KO mice, it appears as though R-568 is having additional effects in mineralising conditions. For this reason, it is likely that under these pathophysiological conditions, R-568 may be carrying out additional roles by so far unknown mechanisms. This is crucially important from a clinical perspective since patients with calcified vessels may have diminished CaSR expression. *In vitro* data suggest that R-568 treatment in such pathological conditions may enhance calcification. It is therefore important to perform additional experiments to determine the mechanism of action of R-568 in KO VSMCs in these mineralising conditions. It would be interesting to investigate the role of calcilytics in proliferation, apoptosis and mineralisation *in vitro* in both WT and KO VSMC.

To determine whether unexpected responses in mineralisation experiments are the result of expression of the GPRC6A receptor, the presence of GPRC6A in both normal and mineralising culture conditions should firstly be investigated. It would be interesting to analyse mRNA expression patterns in these conditions in addition to immunohistochemical analysis. Furthermore, however unlikely it may be that R-568 is producing these unexpected effects through Ca^{2+}-channels, this should still be investigated by using S-568, a stereoisomer of R-568.

Due to time constraints, extensive gene expression analyses were not yet carried out to determine the role of protective factors against vascular calcification in WT and KO VSMCs. It was shown that Runx2 was significantly upregulated in KO VSMC mineralisation cultures, however the exact mechanism of action of this remains unclear. Future studies should include a more extensive analysis of the expression of vascular smooth muscle cell markers, osteoblast markers and protective factors such as MGP to draw more complete conclusions to the exact actions of R-568 in VSMCs. Furthermore, the role of apoptosis on mineralisation should also be investigated by analysing the

medium supernatants of mineralising VSMC cultures. Here, apoptotic cells and markers of cell death such as caspases could be investigated.

CHAPTER 7:

THESIS DISCUSSION & FINAL CONCLUSIONS

The aims of my investigation were to characterise the cardiovascular role of the CaSR in physiology, in the control of vessel tone, and in vascular calcification. This task was to be performed using a new transgenic mouse model with selective ablation of CaSR in VSMCs; the SM22α x fl CaSR mouse model. Summarised overleaf are the key findings discovered within each experimental chapter of this thesis:

A

Chapter 3 (*in vivo*)	Key findings
	VSMC-CaSR KO mice exhibit hypercalcaemia throughout adulthood
	VSMC-CaSR KO mice exhibit mild hyperkalaemia at 3 months of age
	VSMC-CaSR KO mice exhibit reduced bone integrity
	VSMC-CaSR KO mice exhibit increased FGF23 levels throughout adulthood
	VSMC-CaSR KO mice exhibit increased heart weights at 18 months of age

B

Chapter 4 (*ex vivo*)	Key findings
	VSMC-CaSR KO mice exhibit reduced luminal diameters of the aorta and mesenteric arteries
	VSMC-CaSR KO mice exhibit reduced contractile tone of the aorta
	VSMC-CaSR KO mice exhibit reduced acetylcholine-dependent contraction in the presence of L-NAME
	VSMC-CaSR KO mice exhibit reduced acetylcholine-dependent relaxation in mesenteric arteries

C

Chapter 5 (*ex vivo*)	Key findings
	VSMC-CaSR KO mice exhibit loss of Ca^{2+}_o-dependent contraction in the aorta
	VSMC-CaSR KO mice exhibit Ca^{2+}_o-dependent relaxation in the aorta in the presence of L-NAME
	VSMC-CaSR KO mice exhibit greater relaxation in response to spermine in the aorta
	VSMC-CaSR KO mice exhibit loss of R-568-induced relaxation in the aorta

D

Chapter 6 (*in vitro*)	Key findings
	KO-CaSR VSMC cultures show that the CaSR gene is knocked down
	KO-CaSR VSMC cultures show reduced CaSR protein
	WT-CaSR VSMCs proliferate in response to Ca^{2+}_o, KO-CaSR VSMCs do not
	KO-CaSR VSMCs have reduced apoptosis compared to WT-CaSR VSMCs
	KO-CaSR VSMCs mineralise more and faster than WT-CaSR VSMCs.
	R-568 reduces proliferation and mineralisation in WT-CaSR VSMCs but not in KO-CaSR VSMCs

Table 7. Holistic characterisation of the SM22a x fl CaSR mouse model. *In vivo*, *ex vivo* and *in vitro* phenotypes demonstrated experimentally in each chapter are described in these tables. (A) Chapter 3 *in vivo*. (B) Chapter 4 *ex vivo*. (C) Chapter 5 *ex vivo*. (D) Chapter 6 *in vitro*.

The SM22α fl CaSR Mouse Model

↑ Serum Ca^{2+}

HYPERPARATHYROIDISM?

(i) Heavier Hearts
**HYPERTROPHY/
CARDIAC
REMODELLING?**

Narrower blood vessels

↑ Serum Ca^{2+}
↑ Serum K^+
Reduced Contractile tone
HYPOTENSION?

↑FGF23
Pi retention?

HYPERPHOSPHATAEMIA?

Elevated 1,25-$(OH)_2D_3$?
↑ Serum K^+
↓Angiotensin? **(ii)**

Aortic VSMC
↑ Proliferation
↓ Apoptosis
↑ Mineralisation

Reduced mineral
↑FGF23
(iii)
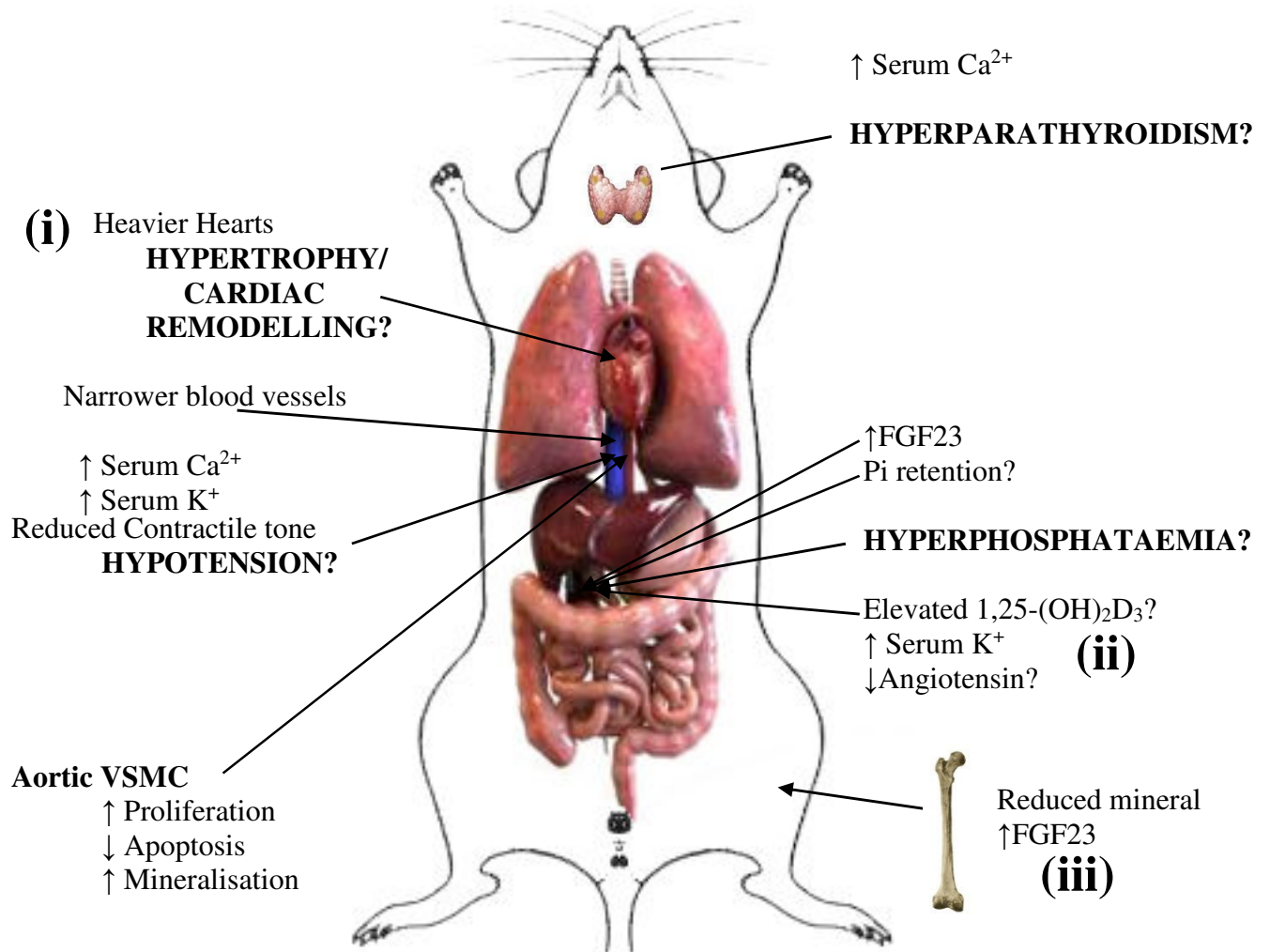
Figure 78. Key features of the SM22a x fl CaSR mouse model. (i) KO Mice exhibit elevated serum Ca^{2+} and K^+. Elevated serum Ca^{2+} most likely comes from increases in circulating PTH (not yet tested). Increases in PTH secretion also occur in response to elevated Pi (not yet tested). PTH could act on intestines, kidney and bone to increase overall $[Ca^{2+}]_o$. (ii) Elevated K^+ suggests renal insufficiency, specifically inhibition of aldosterone and a reduction in K^+ excretion. Inactivation of the RAAS would result in a hypotensive phenotype which has been observed. 1,25-$(OH)_2D_3$ activity may also be increased in the kidney in response to PTH secretion to increase Ca^{2+} retention. (iii) Possible elevations in Pi are implicated by increases in FGF23 levels which promote Pi excretion. Elevations in Pi could come from bone which appears less dense.

When investigating the role of CaSR in any tissue or cell type, particularly through transgenic mouse models, one has to consider the more widespread implications of overexpression or in this case, tissue-specific gene knockout. This is particularly the case in my studies, where CaSR ablation in VSMCs could affect many organs. At the initial outlook, one might presume that any gene knockout in one cell type may produce a very localised and specific phenotype. However this is seldom the case, particularly in the case of CaSR which is a crucial regulator of Ca^{2+}_o homeostasis in the parathyroid glands, bone, kidney and intestines. In the last 20 years, we have learned that CaSR is expressed widely (Riccardi *et al.*, 1995, Kifor *et al.*, 1997, Kovacs and Kronenberg, 1997, Cheng *et al.*, 1999, Shozo *et al.*, 2004, Busque *et al.*, 2005, Dufner *et al.*, 2005, Weston, 2005, Levin *et al.*, 2006, Smajilovic *et al.*, 2006, Smajilovic *et al.*, 2007, Alam *et al.*, 2008, Finney *et al.*, 2008, Vizard *et al.*, 2008, Weston *et al.*, 2008, Caudrillier *et al.*, 2010, Christian *et al.*, 2010) and that it plays a major role in the Ca^{2+}_o/Pi/Vitamin D/PTH/FGF23 axis (Shanahan *et al.*, 2011). For this reason, knockout of CaSR in VSMCs has expectedly demonstrated more systemic effects on organs typically associated with Ca^{2+}_o homeostasis such as the kidneys, bone and parathyroid. The *in vivo* data presented in this thesis have confirmed that this is indeed the case with elevated FGF23 levels, reduced bone content, hypercalcaemia and mild hyperkalaemia in younger mice. The challenging part of these concluding remarks comes when attempting to determine the sequence in which such events would occur, and ultimately, which is the main driver of each of these deviations from normal physiology. Presented overleaf is my interpretation of the data currently available and how the observed phenotype in VSMC-CaSR KO mice may arise.
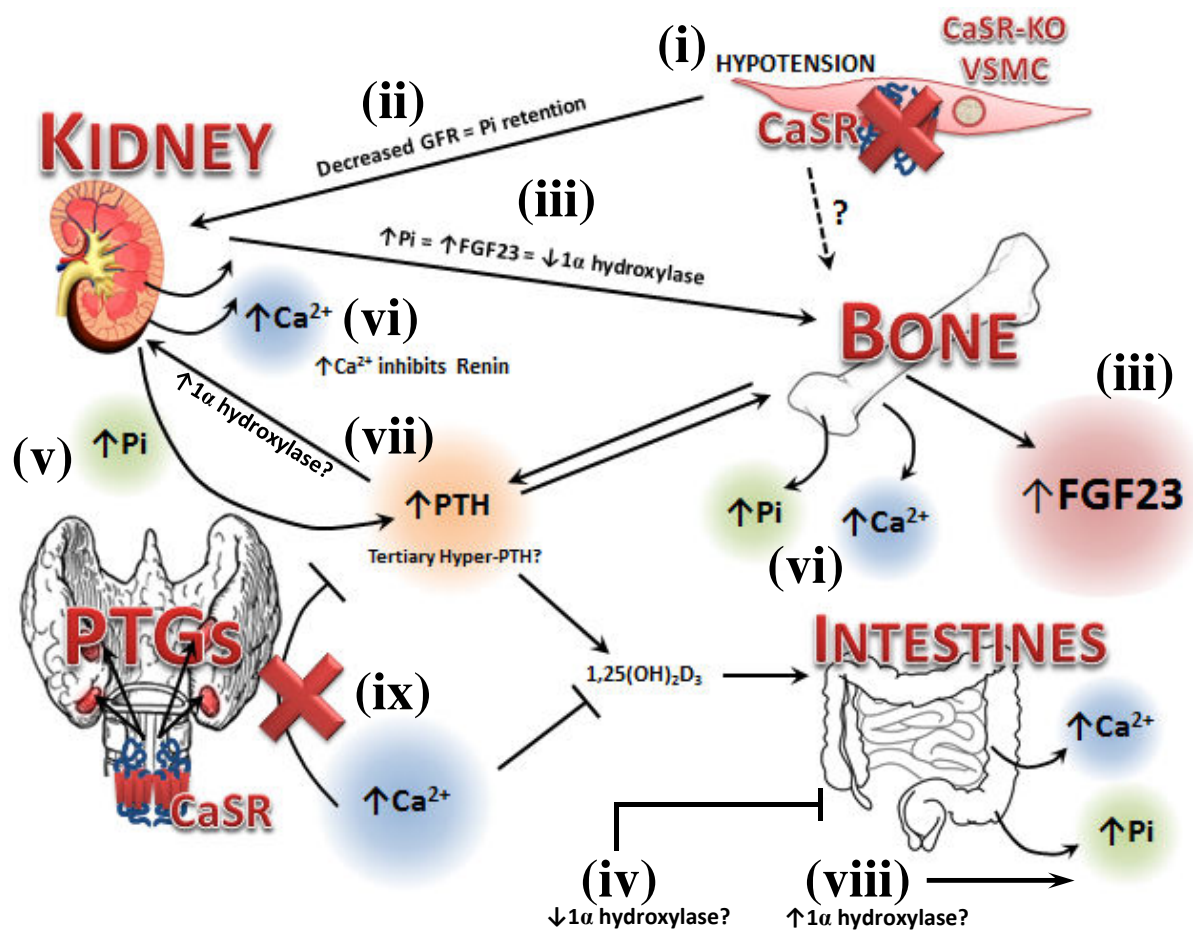
Figure 79. Physiology of the SM22α x fl CaSR KO mouse model. The phenotype observed appears to come from VSMC-KO of CaSR. (i) CaSR-KO in VSMCs results in a systemic hypotensive phenotype. (ii) Glomerular filtration rate (GFR) could be compromised and a reduction in vascular pressure within the kidney reduces excretion of Pi through the glomerulus. (iii) Sustained elevated serum Pi induces FGF23 formation and secretion by osteocytes of bone. (iv) FGF23 also inhibits 1α-hydroxylase activity in the kidney, reducing the uptake of Ca^{2+} from the intestines. (v) Elevations in serum Pi are sufficient to drive PTH secretion from the PTGs. (vi) PTH can act on kidney to reabsorb Ca^{2+}, bone to reabsorb Ca^{2+} and Pi (vi), and may play a role in the rescue of downregulated kidney 1α-hydroxylase (vii). (viii) 1α-hydroxylase may cause increases in $1,25(OH)_2D_3$, thereby increasing Ca^{2+} and Pi absorption in the intestine. (vi) Hypercalcaemia can also inhibit renin secretion and reduce the RAAS system, inducing hyperkalaemia by inhibiting downstream the actions of angiotensin II. (ix) Finally, chronic and sustained hypercalcaemia is sufficient to downregulate the parathyroid CaSR to the PTH-inhibiting effects of Ca^{2+}_o. This results in tertiary hyperparathyroidism as seen in patients with CKD. To combat hypotension, hearts of ageing mice are remodelled and may become heavier (hypertrophic). Abbreviations= CKD: Chronic kidney disease; PTH: Parathyroid hormone; PTG: Parathyroid glands; RAAS: Renin-angiotensin-aldosterone system.

Figure 79 illustrates the proposed pathway in which VSMC-CaSR KO leads to the hypotensive and hypercalcaemic phenotype present in our mice. Through a so far unknown mechanism, we know that VSMC-CaSR KO reduces contractile tone generating a hypotensive phenotype. Principles of renal physiology dictate that blood pressure in the kidney is crucially important for glomerular filtration rate (GFR) (Seifter *et al.*, 2005, Rhoades and Bell, 2012). When blood pressure in the afferent arteriole is low, this reduces the GFR. Consequently, solutes and small molecules are retained. GFR can be calculated using the Starling-Landis equation:

$$\frac{\mathrm{d}Q}{\mathrm{d}T} = \mathrm{K}_f \times (\mathrm{P}_G - \mathrm{P}_B - \mathrm{II}_G + \mathrm{II}_B)$$

$\dfrac{\mathrm{d}Q}{\mathrm{d}T}$ = Glomerular filtration rate (GFR)

K_f = Filtration constant
P_G = Hydrostatic pressure within the glomerular capillaries
P_B = Hydrostatic pressure within the Bowman's capsule
II_G = Colloid osmotic pressure within the glomerular capillaries
II_B = Colloid osmotic pressure within the Bowman's capsule

Using the Starling-Landis equation for the calculation of GFR, one can see the effects of arterial pressure on GFR (Seifter *et al.*, 2005, Rhoades and Bell, 2012). P_G and P_B represent the arterial blood pressure and Bowman's capsule respectively. Normally, P_G is greater than P_B, increasing the glomerular hydrostatic pressure, therefore increasing the GFR. During poor blood flow, often a consequence of atherosclerosis or hypotension, P_G is decreased. P_G can be restored by an increase in efferent arteriolar pressure brought about by increases in angiotensin II; a vasoconstrictor (Seifter *et al.*, 2005). In our SM22α x fl CaSR KO mouse model we have evidence to suggest that RAAS is impaired since mice exhibit hyperkalaemia. This would also suggest that overall kidney function is also impaired. Consequently, the rescue of renal hypotension and low GFR may not occur by the actions of angiotensin II, or this pathway is at least significantly reduced.

From my data and the hypothesis described in Figure 79, it appears that the hypotensive phenotype of CaSR-KO VSMCs is the cause of the systemic phenotype observed in

SM22α x fl CaSR KO mice. Figure 79 describes how impaired renal function, resulting in Pi retention (yet to be measured) could lead to FGF23 elevation and likely hyperparathyroidism (since serum $[Ca^{2+}]$ is significantly elevated in KO mice) in a sustained manner. Furthermore, it has been shown that Ca^{2+}_o, PTH and the CaSR are negative regulators of renin secretion (Atchison *et al.*, 2011). Increased $[Ca^{2+}]_o$ has been shown to activate the CaSR on juxtaglomerular cells in the kidney. This is associated with downstream activation of the ryanodine receptor which releases Ca^{2+} from internal stores. These increases in $[Ca^{2+}]_i$, in combination with decreases in cAMP inhibit renin secretion (Ortiz-Capisano *et al.*, 2013). When components of RAAS such as renin are impaired, this can have knock-down effects on vasoconstrictors such as aldosterone. In addition to reductions in blood pressure, consequences of RAAS impairment are an increase in K^+ retention- which we have observed in our KO mice (Atchison *et al.*, 2011). Although serum Pi and PTH remain to be tested, we have observed the consequences resulting from elevated levels of these which have been incorporated into the hypothetical pathway in Figure 79. To more fully understand the role of Pi and PTH in the SM22α x fl CaSR KO phenotype, serum Pi and PTH will require measurement in both WT and KO mice in the future.

A possible mechanism for CaSR-KO VSMC hypotension

Despite the emerging evidence of the CaSR-KO VSMC exhibiting a hypotensive phenotype, the mechanism of this hypotension remains to be elucidated. It is likely that future Ca^{2+}-imaging experiments and patch clamp electrophysiology are required to confidently describe Ca^{2+} handling mechanisms within the CaSR-KO VSMC. Figure 80 below describes the *in vitro* phenotype observed at the cellular level and how this may contribute to the hypotensive and hypercalcaemic phenotype we have measured.
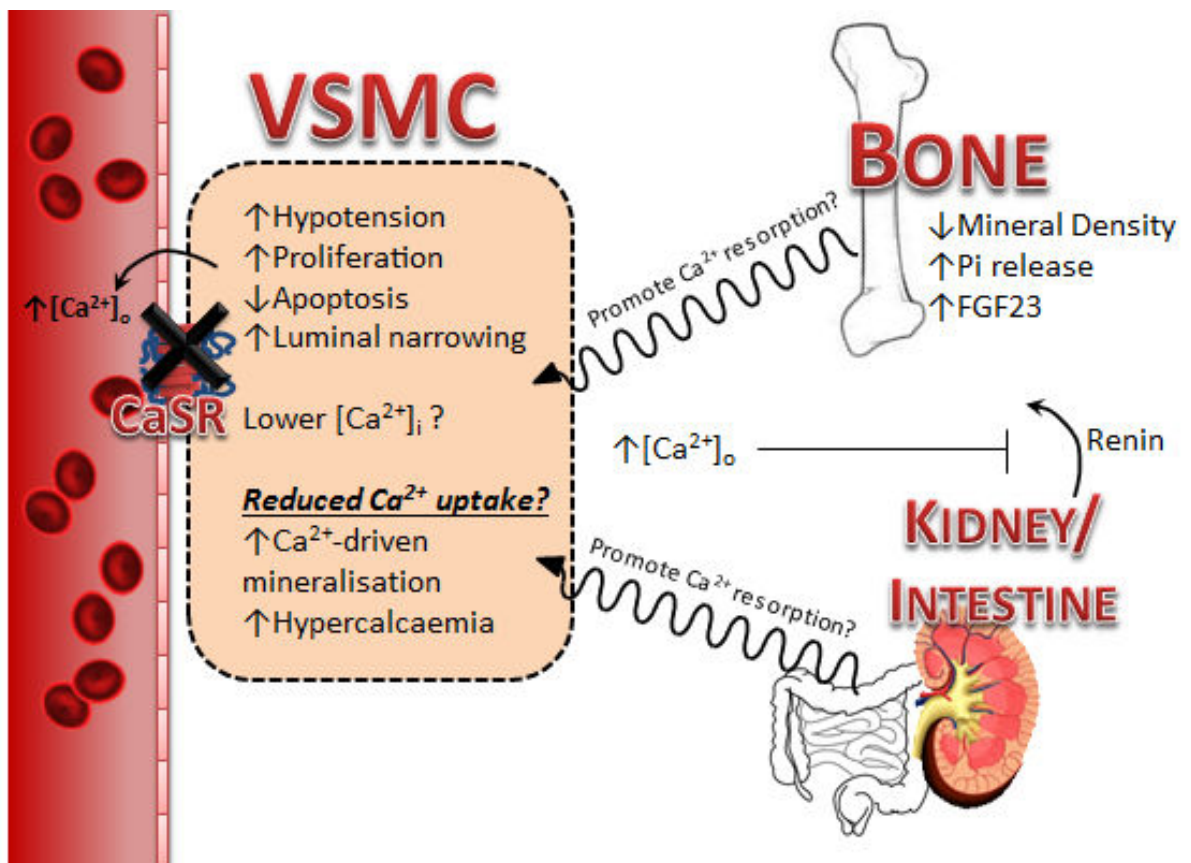
Figure 80. Possible consequences of VSMC-CaSR knockout. SM22α x fl CaSR demonstrate decreased VSMC apoptosis, increased hypotension, increased luminal narrowing, increased VSMC mineralisation and possibly increased proliferation *in vitro*. Activation of the CaSR increases $[Ca^{2+}]_i$ from internal stores and knockout of CaSR in VSMCs may prevents uptake of extracellular $Ca^{2+}{}_o$. Increased Ca^{2+} resorption from bone may also liberate Pi, resulting in increased FGF23 (observed *in vivo*) and reduced mineral density (observed *in vivo*).

SM22α x fl CaSR KO mouse model validation

Importantly, with the demonstrated phenotype affecting bone, kidneys and presumably the parathyroid gland from hyperparathyroidism, one should consider whether there is any knockout of CaSR in these tissues associated with Ca^{2+}_o homeostasis. Since blood vessels permeate all organs and are extremely widespread, this makes isolating tissues in the absence of blood vessels almost impossible. However, we do know from transgenic studies that knockout of CaSR in both the parathyroid and in bone results in severe skeletal retardation (Chang *et al.*, 2008), and from a group investigating the role of the CaSR in the kidney by a similar knockout strategy only a hypercalciuric phenotype was observed (Toka *et al.*, 2012). Since impaired growth and severe skeletal retardation are not observed in our mouse, we can presume that CaSR is not knocked out in the parathyroid, bone or kidney. Additionally, when considering the specificity of the ΔSM22α promoter, the tool by which we have driven VSMC-specific knockout, we know this to be localised specifically to VSMCs in all arteries through embryogenesis up to at least 1 month post-natally (Li *et al.*, 1996a, Li *et al.*, 1996b). Of course, we cannot rule out a partial leakage of the cre recombinase promoter.

Collectively, the evidence supports that we have a VSMC-CaSR knockout which is responsible for the phenotype observed. However, the question still remains as to how VSMC-CaSR KO leads to this hypotensive phenotype. Figure 80 sheds some light on processes involving the VSMC-CaSR, and the SM22α x fl CaSR phenotype at the cellular level: (i) KO VSMCs exhibit a hypotensive phenotype and CaSR agonist binding causes increases in $[Ca^{2+}]_i$ (Ward, 2004). In the absence of a CaSR, increases in $[Ca^{2+}]_i$ are not possible through CaSR. Indeed, it has also been shown that CaSR activation is linked to Ca^{2+}_o uptake through Ca^{2+}-channels, particularly in VSMCs (McGehee *et al.*, 1997, Chow *et al.*, 2011). If KO VSMCs also have reduced uptake of Ca^{2+}_o, this Ca^{2+}_o may be available to act on endothelial cells to promote NO release, reducing the Ca^{2+}_o-dependent contraction of VSMCs, potentiating hypotensive effects. (ii) KO VSMCs may have increased proliferation. It has been shown that increased VSMC proliferation is associated with downregulation of both RyR and SERCA (Lompré, 1999, Vallot *et al.*, 2000). Again, in the absence of a CaSR, CaSR agonists are not able activate the receptor

and increase $[Ca^{2+}]_i$. (iii) KO VSMCS exhibit reduced apoptosis compared to WT VSMCs. Though in stark contrast to what has been previously published, it is likely apoptotic cells are detached from the coverslip. Whether this is true remains to be investigated in future studies. (iv) KO VSMCs exhibit increased calcification. Once again, it is likely that in the absence of the CaSR, Ca^{2+}_o uptake is reduced. It is likely that this may then be available for mineralisation in extracellular environments. Of course, it is also likely that, since CaSR has been shown to be linked to upregulation of MGP, protective Ca^{2+}_o-binding proteins also play a prominent role in this process.

Validation of R-568 specificity on the VSMC-CaSR

At a concentration of <1µM, R-568 has been shown to act specifically at the CaSR (Nemeth *et al.*, 1998). Despite this, it has been reported that R-568 at concentrations of >500nM and in the presence of physiological Ca^{2+}_o (2-3mM) can also activate GPRC6A (Pi *et al.*, 2005). ERK phosphorylation in response to 500nM R-568 was observed in HEK293 cells overexpressing GPRC6A, however, the group did also use concentrations >1µM which may activate Ca^{2+}-channels (Nemeth *et al.*, 1998). Furthermore, it has been shown that GPRC6A is functionally expressed in rat mesenteric arteries and can respond to calcimimetics (Harno *et al.*, 2008). This activity is now widely believed to be because GPRC6A and CaSR share identical calcimimetics binding sites at the protein level (Faure *et al.*, 2009). However, the role of R-568 in GPRC6A signalling has not been investigated in-depth. Although the literature does support that R-568 is a CaSR-specific allosteric modulator, the possibility that R-568 may also be activating an additional Ca^{2+}_o-sensor, GPRC6A, also requires investigation. Data from R-568 experiments are summarised overleaf:

Ex vivo myography:

     (i)   300nM R-568 relax aortae from WT mice, but not aortae from KO mice.

     (ii)   300nM R-568 does not relax aortae from WT and KO mice in the presence of L-NAME.

     (iii)   R-568 (10^{-8}-10^{-5}M) relaxes mesenteric arteries from both WT and KO mice.

In vitro cell studies:

     (i)   10nM R-568 reduces proliferation in WT VSMCs but not KO VSMCs.

     (ii)   10nM R-568 reduces calcification in WT VSMCs, but not in KO VSMCs.

     (iii)   10nM R-568 enhances calcification in KO VSMCs in the presence of 2.5mM Ca^{2+}_o and 3mM Pi.

Given the specificity of R-568 for CaSR, the results obtained from KO VSMC mineralisation experiments are somewhat surprising, especially since the only effect I have observed in these experiments is increased calcification in response to R-568. Until this study, the role of R-568 has not been investigated in mouse VSMCs. The fact that this agonist gives unexpected results raises the possibility that GPRC6A may be expressed or upregulated in KO VSMCs. The possibility that R-568 may act on this receptor should be tested in future experiments.

R-568 Conclusions

Although it is highly likely that R-568 is acting through the CaSR (which is supported by a plethora of studies in the literature) R-568 may also be acting through GPRC6A. It would be interesting to see whether these effects would still be present in CaSR-KO VSMCs which also have GPRC6A-KO in these cells. Furthermore, the possibility of GPCR heterodimerisation between, for example, CaSR and GPRC6A should be investigated.

FUTURE WORK

From the data obtained within this thesis, I can only speculate on the highly suggestive roles of hormones, proteins and enzymes that we have not yet quantified. Future work to further confirm the roles of the VSMC-CaSR would firstly involve characterising these from mouse serum. For this reason, future work will entail characterising the role of the following components:

COMPONENT/TEST	HYPOTHESIZED OBSERVATION?
Blood pressure	Decreased
Nitric Oxide	Increased
Renin	Decreased
Aldosterone	Decreased
Angiotensin-converting enzyme	Decreased
$1,25(OH_2)D_3$	Increased/Decreased
Serum Pi	Increased
Serum MGP	Decreased
PTH	Increased

Table 8. Speculative roles of components so far not measured in SM22α x fl CaSR KO mice. Tests that have not yet been performed are required in the future to determine whether the hypotheses suggested are correct.

REFERENCES

AARONSON, P. 2012. Does TRPC3 macrodominate the myoendothelial gap junction microdomain? *Cardiovascular Research*, 95, 399-400.

ABEDIN, M., TINTUT, Y., DEMER, L. 2004. Vascular Calcification: Mechanisms and Clinical Ramifications. *Arteriosclerosis, Thrombosis, and Vascular Biology,* 24, 1161-1170.

ABEDIN, M., LIM J., TANG, T., PARK, D., DEMER, L., TINTUT, Y. 2006. N-3 Fatty Acids Inhibit Vascular Calcification Via the p38-Mitogen-Activated Protein Kinase and Peroxisome Proliferator-Activated Receptor- Pathways. *Circulation Research,* 98, 727-9.

ABRAMOWITZ, M., MUNTNER, P., COCO, M., SOUTHERN, W., LOTWIN, I., HOSTETTER, T. & MELAMED, M. 2010. Serum alkaline phosphatase and phosphate and risk of mortality and hospitalization. *Clinical journal of the American Society of Nephrology : CJASN,* 5**,** 1064-1135.

ADAMS, D., BARAKEH, J., LASKEY, R. & VAN BREEMEN, C. 1989. Ion channels and regulation of intracellular calcium in vascular endothelial cells. *FASEB journal : official publication of the Federation of American Societies for Experimental Biology,* 3**,** 2389-2789.

ADEGUNLOYE, B. & SOFOLA, O. 1998. Relaxation responses of aortic rings from salt-loaded high calcium fed rats to potassium chloride, calcium chloride and magnesium sulphate. *Pathophysiology,* 4**,** 275-280.

AGUIRRE, A., GONZÁLEZ, A., PLANELL, J. A. & ENGEL, E. 2010. Extracellular calcium modulates in vitro bone marrow-derived Flk-1+ CD34+ progenitor cell chemotaxis and differentiation through a calcium-sensing receptor. *Biochemical and Biophysical Research Communications,* 393, 156-61.

AHMED, S., O'NEILL, K., HOOD, A., EVAN, A. & MOE, S. 2001. Calciphylaxis is associated with hyperphosphatemia and increased osteopontin expression by vascular smooth muscle cells. *American journal of kidney diseases : the official journal of the National Kidney Foundation,* 37**,** 1267-1343.

AIDA, K., KOISHI, S., TAWATA, M. & ONAYA, T. 1995. Molecular cloning of a putative Ca(2+)-sensing receptor cDNA from human kidney. *Biochemical and Biophysical Research Communications,* 214**,** 524-533.

AKINTONWA, A., AUDITORE, J. & GREEN, L. 1979. The toxicological effects of pure dietary adenine base in the rat. *Toxicology and applied pharmacology,* 47**,** 229-264.

AL-BAAJ, F., SPEAKE, M. & HUTCHISON, A. 2005. Control of serum phosphate by oral lanthanum carbonate in patients undergoing haemodialysis and continuous ambulatory peritoneal dialysis in a short-term, placebo-controlled study. *Nephrology, dialysis,*

transplantation : official publication of the European Dialysis and Transplant Association - European Renal Association, 20**,** 775-857.

ALAM, M.-U., KIRTON, J. P., WILKINSON, F. L., TOWERS, E., SINHA, S., ROUHI, M., VIZARD, T. N., SAGE, A. P., MARTIN, D., WARD, D. T., ALEXANDER, M. Y., RICCARDI, D. & CANFIELD, A. E. 2008. Calcification is associated with loss of functional calcium-sensing receptor in vascular smooth muscle cells. *Cardiovascular Research,* 81, 260-268.

ALBAAJ, F. & HUTCHISON, A. 2005. Lanthanum carbonate for the treatment of hyperphosphataemia in renal failure and dialysis patients. *Expert opinion on pharmacotherapy,* 6**,** 319-347.

ALLENDER, P., CUTLER, J., FOLLMANN, D., CAPPUCCIO, F., PRYER, J. & ELLIOTT, P. 1996. Dietary calcium and blood pressure: a meta-analysis of randomized clinical trials. *Annals of internal medicine,* 124**,** 825-831.

ALLISON, M. A. 2004. Patterns and Risk Factors for Systemic Calcified Atherosclerosis. *Arteriosclerosis, Thrombosis, and Vascular Biology,* 24, 331-336.

AMENTO, E. P., EHSANI, N., PALMER, H. & LIBBY, P. 1991. Cytokines And Growth Factors Positively And Negatively Regulate Interstitial Collagen Gene Expression In Human Vascular Smooth Muscle Cells. *Arteriosclerosis, Thrombosis, And Vascular Biology***,** 1223-1230.

ANDERSON, H., GARIMELLA, R. & TAGUE, S. 2005. The role of matrix vesicles in growth plate development and biomineralization. *Frontiers in bioscience : a journal and virtual library,* 10**,** 822-859.

ANDERSON, H. C. 2003. Matrix Vesicles And Calcification. *Current Rheumatology Reports,* 5**,** 222-226.

ANDERSSON, K. E. 2002. Potential benefits of muscarinic M3 receptor selectivity. *European Urology Supplements,* 1**,** 23-51.

ARMBRECHT, H., HODAM, T., BOLTZ, M., PARTRIDGE, N., BROWN, A. & KUMAR, V. 1998. Induction of the vitamin D 24-hydroxylase (CYP24) by 1,25-dihydroxyvitamin D3 is regulated by parathyroid hormone in UMR106 osteoblastic cells. *Endocrinology,* 139**,** 3375-3456.

ATCHISON, D. K., HARDING, P. & BEIERWALTES, W. H. 2011. Hypercalcemia Reduces Plasma Renin via Parathyroid Hormone, Renal Interstitial Calcium, and the Calcium-Sensing Receptor. *Hypertension,* 58, 604-10.

BA, J. & FRIEDMAN, P. 2004. Calcium-sensing receptor regulation of renal mineral ion transport. *Cell calcium,* 35**,** 229-237.

BAI, M. & TRIVEDI, S. 1998. Dimerization of the extracellular calcium-sensing receptor (CaR) on the cell surface of CaR-transfected HEK293 cells. *Journal of Biological Chemistry*, 164, 884–893.

BAI, M., TRIVEDI, S., KIFOR, O., QUINN, S. & BROWN, E. 1999. Intermolecular interactions between dimeric calcium-sensing receptor monomers are important for its normal function. *Proceedings of the National Academy of Sciences of the United States of America,* 96**,** 2834-2843.

BÁRÁNY, M. 1967. ATPase activity of myosin correlated with speed of muscle shortening. *The Journal of general physiology,* 50**,** 218.

BEAZLEY, K., DEASEY, S., LIMA, F. & NURMINSKAYA, M. 2012. Transglutaminase 2-mediated activation of β-catenin signaling has a critical role in warfarin-induced vascular calcification. *Arteriosclerosis, Thrombosis, and Vascular Biology,* 32**,** 123-153.

BELLASI, A., KOOIENGA, L., BLOCK, G., VELEDAR, E., SPIEGEL, D. & RAGGI, P. 2009. How long is the warranty period for nil or low coronary artery calcium in patients new to hemodialysis? *Journal of nephrology,* 22**,** 255-262.

BENDECK, M. P., KEELEY, F. W. & LANGILLE, B. L. 1994. Perinatal Accumulation Of Arterial Wall Constituents: Relation To Hemodynamic Changes At Birth. *American Journal Of Physiology- Heart And Circulatory Physiology,* 267**,** H2268-H2279.

BENHAM, C., HESS, P. & TSIEN, R. 1987. Two types of calcium channels in single smooth muscle cells from rabbit ear artery studied with whole-cell and single-channel recordings. *Circulation Research,* 61**,** 6.

BERGWITZ, C. & JÜPPNER, H. 2010. Regulation of phosphate homeostasis by PTH, vitamin D, and FGF23. *Annual review of medicine,* 61**,** 91-195.

BERRIDGE, M. 1984. Inositol trisphosphate and diacylglycerol as second messengers. *The Biochemical journal,* 220**,** 345-405.

BERRIDGE, M. 1993. Cell signalling. A tale of two messengers. *Nature,* 365**,** 388-397.

BERRIDGE, M. & IRVINE, R. 1984. Inositol trisphosphate, a novel second messenger in cellular signal transduction. *Nature,* 312**,** 315-336.

BETTLER, B., KAUPMANN, K., MOSBACHER, J. & GASSMANN, M. 2004. Molecular structure and physiological functions of GABA(B) receptors. *Physiological Reviews,* 84**,** 835-902.

BINDER, C. J., HARTVIGSEN, K., CHANG, M.K., MILLER, M., BROIDE, D., PALINSKI, W., CURTISS, L.K., CORR, M., WITZTUM, J.L. 2004. IL-5 links adaptive and natural immunity specific for epitopes of oxidized LDL and protects from atherosclerosis. *Journal of Clinical Investigation,* 114, 427-437.

BLANKENSHIP, K., WILLIAMS, J., LAWRENCE, M., MCLEISH, K., DEAN, W. & ARTHUR, J. 2001. The calcium-sensing receptor regulates calcium absorption in MDCK cells by inhibition of PMCA. *American journal of physiology. Renal physiology,* 280**,** 22.

BLOCK, G., HULBERT-SHEARON, T., LEVIN, N. & PORT, F. 1998. Association of serum phosphorus and calcium x phosphate product with mortality risk in chronic hemodialysis patients: a national study. *American journal of kidney diseases : the official journal of the National Kidney Foundation,* 31**,** 607-624.

BOGLE, R., MANN, G., PEARSON, J. & MORGAN, D. 1994. Endothelial polyamine uptake: selective stimulation by L-arginine deprivation or polyamine depletion. *The American journal of physiology,* 266**,** 83.

BOHR, D. 1963. Vascular Smooth Muscle: Dual Effect of Calcium. *Science (New York, N.Y.),* 139**,** 597-599.

BOLOTINA, V., NAJIBI, S., PALACINO, J., PAGANO, P. & COHEN, R. 1994. Nitric oxide directly activates calcium-dependent potassium channels in vascular smooth muscle. *Nature,* 368**,** 850-853.

BOLZ, S., DE WIT, C. & POHL, U. 1999. Endothelium-derived hyperpolarizing factor but not NO reduces smooth muscle Ca2+ during acetylcholine-induced dilation of microvessels. *British Journal of Pharmacology,* 128**,** 124-134.

BORLE, A. 1974. Calcium and phosphate metabolism. *Annual Review of Physiology*, 36, 361-390.

BOSTRÖM, K., TSAO, D., SHEN, S., WANG, Y. & DEMER, L. L. 2001. Matrix Gla Protein Modulates Differentiation Induced By Bone Morphogenetic Protein-2 In C3H10T1/2 Cells. *The Journal Of Biological Chemistry,* 276**,** 14044-14052.

BOSTRÖM, K., WATSON, K. & HORN, S. 1993. Bone morphogenetic protein expression in human atherosclerotic lesions. *Journal of Clinical Investigation*, 91, 1800-1809.

BOULANGER, C., MORRISON, K. & VANHOUTTE, P. 1994. Mediation by M3-muscarinic receptors of both endothelium-dependent contraction and relaxation to acetylcholine in the aorta of the spontaneously hypertensive rat. *British Journal of Pharmacology,* 112**,** 519-543.

BRÄUNER-OSBORNE, H., JENSEN, A., SHEPPARD, P., O'HARA, P. & KROGSGAARD-LARSEN, P. 1999. The agonist-binding domain of the calcium-sensing receptor is located at the amino-terminal domain. *The Journal of biological chemistry,* 274**,** 18382-18388.

BRÄUNER-OSBORNE, H., WELLENDORPH, P. & JENSEN, A. 2007. Structure, pharmacology and therapeutic prospects of family C G-protein coupled receptors. *Current drug targets,* 8**,** 169-253.

BREDT, D. & SNYDER, S. 1990. Isolation of nitric oxide synthetase, a calmodulin-requiring enzyme. *Proceedings of the National Academy of Sciences of the United States of America,* 87**,** 682-687.

BREITWIESER, G. 2012. Minireview: The Intimate Link Between Calcium Sensing Receptor Trafficking and Signaling: Implications for Disorders of Calcium Homeostasis. *Molecular endocrinology (Baltimore, Md.)*, 26, 1482-1495.

BRENZA, H., KIMMEL-JEHAN, C., JEHAN, F., SHINKI, T., WAKINO, S., ANAZAWA, H., SUDA, T. & DELUCA, H. 1998. Parathyroid hormone activation of the 25-hydroxyvitamin D3-1alpha-hydroxylase gene promoter. *Proceedings of the National Academy of Sciences of the United States of America, 95***,** 1387-1478.

BRO, S., BENTZON, J., FALK, E., ANDERSEN, C., OLGAARD, K. & NIELSEN, L. 2003. Chronic renal failure accelerates atherogenesis in apolipoprotein E-deficient mice. *Journal of the American Society of Nephrology : JASN,* 14**,** 2466-2540.

BROWN, E. 1991. Extracellular Ca2+ sensing, regulation of parathyroid cell function, and role of Ca2+ and other ions as extracellular (first) messengers. *Physiological Reviews,* 71**,** 371-782.

BROWN, E. 1999. Physiology and pathophysiology of the extracellular calcium-sensing receptor. *The American Journal of Medicine,* 106**,** 238-291.

BROWN, E., GAMBA, G., RICCARDI, D., LOMBARDI, M., BUTTERS, R., KIFOR, O., SUN, A., HEDIGER, M., LYTTON, J. & HEBERT, S. 1993. Cloning and characterization of an extracellular Ca(2+)-sensing receptor from bovine parathyroid. *Nature,* 366**,** 575-655.

BROWN, E. & MACLEOD, R. 2001. Extracellular calcium sensing and extracellular calcium signaling. *Physiological reviews,* 81, 239-297.

BRUNET, P., GONDOUIN, B., DUVAL-SABATIER, A., DOU, L., CERINI, C., DIGNAT-GEORGE, F., JOURDE-CHICHE, N., ARGILES, A. & BURTEY, S. 2011. Does uremia cause vascular dysfunction? *Kidney & blood pressure research,* 34**,** 284-290.

BUASSI, N. 1998. High dietary calcium decreases blood pressure in normotensive rats. *Brazilian journal of medical and biological research = Revista brasileira de pesquisas médicas e biológicas / Sociedade Brasileira de Biofísica ... [et al.],* 31**,** 1099-1101.

BUCAY, N., SAROSI, I., DUNSTAN, C., MORONY, S., TARPLEY, J., CAPPARELLI, C., SCULLY, S., TAN, H., XU, W., LACEY, D., BOYLE, W. & SIMONET, W. 1998. Osteoprotegerin-deficient mice develop early onset osteoporosis and arterial calcification. *Genes & development,* 12, 1260-1268.

BUCHAN, A., SQUIRES, P., RING, M. & MELOCHE, R. 2001. Mechanism of action of the calcium-sensing receptor in human antral gastrin cells. *Gastroenterology,* 120, 1128-1167.

BUDOFF, M. J. & GUL, K. M. 2008. Expert Review On Coronary Calcium. *Vascular Health And Risk Management,* 4**,** 315-324.

BUKOSKI, R., BIAN, K., WANG, Y. & MUPANOMUNDA, M. 1997. Perivascular sensory nerve Ca2+ receptor and Ca2+-induced relaxation of isolated arteries. *Hypertension,* 30**,** 1431-1440.

BURTON, A. 1954. Relation of structure to function of the tissues of the wall of blood vessels. *Physiological reviews,* 34**,** 619-661.

BURTON, D., GILES, P., SHEERIN, A., SMITH, S., LAWTON, J., OSTLER, E., RHYS-WILLIAMS, W., KIPLING, D. & FARAGHER, R. 2009. Microarray analysis of senescent vascular smooth muscle cells: A link to atherosclerosis and vascular calcification. *Experimental Gerontology,* 44**,** 659-724.

BURTON, D. G. A., MATSUBARA, H. & IKEDA, K. 2010. Pathophysiology of vascular calcification: Pivotal role of cellular senescence in vascular smooth muscle cells. *Experimental Gerontology,* 45, 819–824.

BUSQUE, S., KERSTETTER, J., GEIBEL, J. & INSOGNA, K. 2005. L-type amino acids stimulate gastric acid secretion by activation of the calcium-sensing receptor in parietal cells. *American journal of physiology. Gastrointestinal and liver physiology,* 289**,** 9.

BUSSE, R., EDWARDS, G., FÉLÉTOU, M., FLEMING, I., VANHOUTTE, P. & WESTON, A. 2002. EDHF: bringing the concepts together. *Trends in pharmacological sciences,* 23**,** 374-380.

BUUS, N., SIMONSEN, U., PILEGAARD, H. & MULVANY, M. 2000. Nitric oxide, prostanoid and non-NO, non-prostanoid involvement in acetylcholine relaxation of isolated human small arteries. *British Journal of Pharmacology,* 129**,** 184-192.

CANAFF, L. 2000. Extracellular Calcium-sensing Receptor Is Expressed in Rat Hepatocytes. COUPLING TO INTRACELLULAR CALCIUM MOBILIZATION AND STIMULATION OF BILE FLOW. *Journal of Biological Chemistry,* 276, 4070-4079.

CANAFF, L. 2002. Human Calcium-sensing Receptor Gene. VITAMIN D RESPONSE ELEMENTS IN PROMOTERS P1 AND P2 CONFER TRANSCRIPTIONAL RESPONSIVENESS TO 1,25-DIHYDROXYVITAMIN D. *Journal of Biological Chemistry,* 277, 30337-30350.

CAO, Y., OH, B. & STRYER, L. 1998. Cloning and localization of two multigene receptor families in goldfish olfactory epithelium. *Proceedings of the National Academy of Sciences of the United States of America,* 95**,** 11987-12079.

CARAFOLI, E. 1987. Intracellular calcium homeostasis. *Annual review of biochemistry*, 56, 395-433.

CARAFOLI, E. 2002. Calcium signaling: A tale for all seasons. *Proceedings of the National Academy of Sciences,* 99, 1115–1122.

CARDIOSMART 2012. Coronary Heart Disease (CAD), A more detailed explanation. *CardioSmart American College of Cardiology.*

CASTRO, M., DICKER, F., VILARDAGA, J.-P., KRASEL, C., BERNHARDT, M. & LOHSE, M. 2002. Dual regulation of the parathyroid hormone (PTH)/PTH-related peptide receptor signaling by protein kinase C and beta-arrestins. *Endocrinology,* 143**,** 3854-3919.

CATTERALL, W., PEREZ-REYES, E., SNUTCH, T. & STRIESSNIG, J. 2005. International Union of Pharmacology. XLVIII. Nomenclature and structure-function relationships of voltage-gated calcium channels. *Pharmacological reviews,* 57**,** 411-436.

CAUDRILLIER, A., MENTAVERRI, R., BRAZIER, M., KAMEL, S. & MASSY, Z. 2010. Calcium-sensing receptor as a potential modulator of vascular calcification in chronic kidney disease. *Journal of nephrology,* 23**,** 17-39.

CHADHA, P., LIU, L., RIKARD-BELL, M., SENADHEERA, S., HOWITT, L., BERTRAND, R., GRAYSON, T., MURPHY, T. & SANDOW, S. 2011. Endothelium-dependent vasodilation in human mesenteric artery is primarily mediated by myoendothelial gap junctions intermediate conductance calcium-activated K+ channel and nitric oxide. *The Journal of pharmacology and experimental therapeutics,* 336**,** 701-708.

CHAMLEY-CAMPBELL, J. & CAMPBELL, G. 1981. What controls smooth muscle phenotype? *Atherosclerosis,* 40**,** 347-404.

CHANG, W., PRATT, S., CHEN, T., NEMETH, E., HUANG, Z. & SHOBACK, D. 1998. Coupling of calcium receptors to inositol phosphate and cyclic AMP generation in mammalian cells and Xenopus laevis oocytes and immunodetection of receptor protein by region-specific antipeptide antisera. *Journal of bone and mineral research : the official journal of the American Society for Bone and Mineral Research,* 13**,** 570-650.

CHANG, W. & SHOBACK, D. 2004. Extracellular Ca2+-sensing receptors--an overview. *Cell Calcium,* 35**,** 183-196.

CHANG, W., TU, C., CHEN, T. H., BIKLE, D. & SHOBACK, D. 2008. The Extracellular Calcium-Sensing Receptor (CaSR) Is a Critical Modulator of Skeletal Development. *Science Signaling,* 1.

CHATTOPADHYAY, N., CHENG, I., ROGERS, K., RICCARDI, D., HALL, A., DIAZ, R., HEBERT, S., SOYBEL, D. & BROWN, E. 1998. Identification and localization of extracellular Ca(2+)-sensing receptor in rat intestine. *The American journal of physiology,* 274**,** 30.

CHAYTOR, A., EVANS, W. & GRIFFITH, T. 1998. Central role of heterocellular gap junctional communication in endothelium-dependent relaxations of rabbit arteries. *The Journal of Physiology,* 508 (Pt 2)**,** 561-573.

CHEN, H., HU, B., ALLEGRETTO, E. & ADAMS, J. 2000. The vitamin D response element-binding protein. A novel dominant-negative regulator of vitamin D-directed transactivation. *The Journal of biological chemistry,* 275**,** 35557-35621.

CHEN, N., KIRCELLI, F., O'NEILL, K., CHEN, X. & MOE, S. 2010a. Verapamil inhibits calcification and matrix vesicle activity of bovine vascular smooth muscle cells. *Kidney International,* 77**,** 436-478.

CHEN, N., MOE, S., EGGLESTON-GULYAS, T., CHEN, X., HOFFMEYER, W., BACALLAO, R., HERBERT, B. & GATTONE, V. 2011. Calcimimetics inhibit renal pathology in rodent nephronophthisis. *Kidney international,* 80**,** 612-621.

CHEN, N. X., CHEN, X., NEILL, K. D. O., ATKINSON, S. J. & MOE, S. M. 2010b. RhoA/Rho kinase (ROCK) alters fetuin-A uptake and regulates calcification in bovine vascular smooth muscle cells (BVSMC). *AJP: Renal Physiology,* 299.

CHENG, I., QURESHI, I., CHATTOPADHYAY, N. & QURESHI, A. 1999. Expression of an extracellular calcium-sensing receptor in rat stomach. *Gastroenterology*.

CHENG, Z., TU, C., RODRIGUEZ, L., CHEN, T.-H., DVORAK, M., MARGETA, M., GASSMANN, M., BETTLER, B., SHOBACK, D. & CHANG, W. 2007. Type B gamma-aminobutyric acid receptors modulate the function of the extracellular Ca2+-sensing receptor and cell differentiation in murine growth plate chondrocytes. *Endocrinology,* 148**,** 4984-5076.

CHERRY, P., FURCHGOTT, R., ZAWADZKI, J. & JOTHIANANDAN, D. 1982. Role of endothelial cells in relaxation of isolated arteries by bradykinin. *Proceedings of the National Academy of Sciences of the United States of America,* 79**,** 2106-2116.

CHERTOW, G., BLOCK, G., CORREA-ROTTER, R., DRÜEKE, T., FLOEGE, J., GOODMAN, W., HERZOG, C., KUBO, Y., LONDON, G., MAHAFFEY, K., MIX, T., MOE, S., TROTMAN, M.-L., WHEELER, D. & PARFREY, P. 2012a. Effect of cinacalcet on cardiovascular disease in patients undergoing dialysis. *The New England journal of medicine,* 367**,** 2482-2494.

CHERTOW, G., CORREA-ROTTER, R., BLOCK, G., DRUEKE, T., FLOEGE, J., GOODMAN, W., HERZOG, C., KUBO, Y., LONDON, G., MAHAFFEY, K., MIX, T.-C., MOE, S., WHEELER, D. & PARFREY, P. 2012b. Baseline characteristics of subjects enrolled in the Evaluation of Cinacalcet HCl Therapy to Lower Cardiovascular Events (EVOLVE) trial. *Nephrology, dialysis, transplantation : official publication of the European Dialysis and Transplant Association - European Renal Association,* 27**,** 2872-2881.

CHO, H., KOZASA, T., BONDJERS, C., BETSHOLTZ, C. & KEHRL, J. 2003. Pericyte-specific expression of Rgs5: implications for PDGF and EDG receptor signaling during vascular maturation. *FASEB journal : official publication of the Federation of American Societies for Experimental Biology,* 17**,** 440-442.

CHOW, J., ESTREMA, C., ORNELES, T., DONG, X., BARRETT, K. & DONG, H. 2011. Calcium-sensing receptor modulates extracellular Ca(2+) entry via TRPC-encoded receptor-operated channels in human aortic smooth muscle cells. *American journal of physiology. Cell physiology,* 301**,** 8.

CHRISTIAN, R., RUJUAN, H., RANA, S., ISABEL, B., DENGSHUN, M., EDWARD, M. B., GEOFFREY, N. H. & DAVID, G. 2010. The calcium-sensing receptor and 25-hydroxyvitamin D-1α-hydroxylase interact to modulate skeletal growth and bone turnover. *Journal of Bone and Mineral Research,* 25.

CICERI, P., VOLPI, E., BRENNA, I., ARNABOLDI, L., NERI, L., BRANCACCIO, D. & COZZOLINO, M. 2011. Combined effects of ascorbic acid and phosphate on rat VSMC osteoblastic differentiation. *Nephrology Dialysis Transplantation.*

CICERI, P., VOLPI, E., BRENNA, I., ELLI, F., BORGHI, E., BRANCACCIO, D. & COZZOLINO, M. 2012. The combination of lanthanum chloride and the calcimimetic calindol delays the progression of vascular smooth muscle cells calcification. *Biochemical and Biophysical Research Communications,* 418**,** 770-773.

CLARKE, M., LITTLEWOOD, T., FIGG, N., MAGUIRE, J., DAVENPORT, A., GODDARD, M. & BENNETT, M. 2008. Chronic apoptosis of vascular smooth muscle cells accelerates atherosclerosis and promotes calcification and medial degeneration. *Circulation Research,* 102**,** 1529-1538.

CLARKE, M. C. H., FIGG, N., MAGUIRE, J. J., DAVENPORT, A. P., GODDARD, M., LITTLEWOOD, T. D. & BENNETT, M. R. 2006. Apoptosis Of Vascular Smooth Muscle Cells Induces Features Of Plaque Vulnerability In Atherosclerosis. *Nature Medicine,* 12**,** 1075-1080.

COLLETT, G. D. M. & CANFIELD, A. 2005. Angiogenesis and Pericytes in the Initiation of Ectopic Calcification. *Circulation Research,* 96, 930-938.

COLLOTON, M., SHATZEN, E., MILLER, G., STEHMAN-BREEN, C., WADA, M., LACEY, D. & MARTIN, D. 2005. Cinacalcet HCl attenuates parathyroid hyperplasia in a rat model of secondary hyperparathyroidism. *Kidney International,* 67**,** 467-476.

CONIGRAVE, A. & BROWN, E. 2006. Taste receptors in the gastrointestinal tract. II. L-amino acid sensing by calcium-sensing receptors: implications for GI physiology. *American journal of physiology. Gastrointestinal and liver physiology,* 291**,** 61.

CONIGRAVE, A., FRANKS, A., BROWN, E. & QUINN, S. 2002. L-amino acid sensing by the calcium-sensing receptor: a general mechanism for coupling protein and calcium metabolism? *European journal of clinical nutrition,* 56**,** 1072-1152.

CONIGRAVE, A., MUN, H.-C. & LOK, H.-C. 2007. Aromatic L-amino acids activate the calcium-sensing receptor. *The Journal of nutrition,* 137.

CONIGRAVE, A., QUINN, S. & BROWN, E. 2000. L-amino acid sensing by the extracellular Ca2+-sensing receptor. *Proceedings of the National Academy of Sciences of the United States of America,* 97**,** 4814-4819.

CONWAY, E., COLLEN, D. & CARMELIET, P. 2001. Molecular mechanisms of blood vessel growth. *Cardiovascular research,* 49**,** 507-528.

COTTLER-FOX, M., LAPIDOT, T., PETIT, I., KOLLET, O., DIPERSIO, J., LINK, D. & DEVINE, S. 2003. Stem cell mobilization. *Hematology / the Education Program of the American Society of Hematology. American Society of Hematology. Education Program,* 419-437.

CRYSTAL, G., ZHOU, X. & SALEM, M. 1998. Is calcium a coronary vasoconstrictor in vivo? *Anesthesiology,* 88**,** 735-743.

D'SOUZA-LI, L. 2006. The calcium-sensing receptor and related diseases. *Arquivos brasileiros de endocrinologia e metabologia,* 50**,** 628-667.

DAUGHERTY, A., PURÉ, E. & DELFEL-BUTTEIGER, D. 1997. The effects of total lymphocyte deficiency on the extent of atherosclerosis in apolipoprotein E-/-mice. *Journal of Clinical ...*

DAVIES, M. & HRUSKA, K. 2001. Pathophysiological mechanisms of vascular calcification in end-stage renal disease. *Kidney international,* 60**,** 472-481.

DAVIES, M. R. 2003. BMP-7 Is an Efficacious Treatment of Vascular Calcification in a Murine Model of Atherosclerosis and Chronic Renal Failure. *Journal of the American Society of Nephrology,* 14.

DELMEZ, J., KELBER, J., NORWORD, K., GILES, K. & SLATOPOLSKY, E. 1996. Magnesium carbonate as a phosphorus binder: a prospective, controlled, crossover study. *Kidney International,* 49**,** 163-170.

DELSING, D., OFFERMAN, E., VAN DUYVENVOORDE, W., VAN DER BOOM, H., DE WIT, E., GIJBELS, M., VAN DER LAARSE, A., JUKEMA, J., HAVEKES, L. & PRINCEN, H. 2001. Acyl-CoA:cholesterol acyltransferase inhibitor avasimibe reduces atherosclerosis in addition to its cholesterol-lowering effect in ApoE*3-Leiden mice. *Circulation,* 103**,** 1778-1864.

DEMER, L. 2001. Cholesterol in vascular and valvular calcification. *Circulation,* 104**,** 1881-1884.

DEMER, L. & WATSON, K. 1994. Mechanism of calcification in atherosclerosis. *Trends in cardiovascular medicine*.

DEMER, L. L. & TINTUT, Y. 2008. Vascular Calcification: Pathobiology of a Multifaceted Disease. *Circulation,* 117.

DHORE, C., CLEUTJENS, J., LUTGENS, E., CLEUTJENS, K., GEUSENS, P., KITSLAAR, P., TORDOIR, J., SPRONK, H., VERMEER, C. & DAEMEN, M. 2001. Differential expression of bone matrix regulatory proteins in human atherosclerotic plaques. *Arteriosclerosis, Thrombosis, and Vascular Biology,* 21**,** 1998-4001.

DILLON, P., AKSOY, M., DRISKA, S. & MURPHY, R. 1981. Myosin phosphorylation and the cross-bridge cycle in arterial smooth muscle. *Science (New York, N.Y.),* 211**,** 495-502.

DORA, K. A. 2010. Coordination of Vasomotor Responses by the Endothelium. *Circulation Journal,* 74.

DORAI, H., VUKICEVIC, S. & SAMPATH, T. 2000. Bone morphogenetic protein-7 (osteogenic protein-1) inhibits smooth muscle cell proliferation and stimulates the expression of markers that are characteristic of SMC phenotype in vitro. *Journal of cellular physiology,* 184**,** 37-82.

DRÜEKE, T. B. & MASSY, Z. A. 2011. Chronic kidney disease: Medial or intimal calcification in CKD—does it matter? *Nature Reviews Nephrology,* 7.

DUFNER, M., KIRCHHOFF, P., REMY, C., HAFNER, P., MÜLLER, M., CHENG, S., TANG, L.-Q., HEBERT, S., GEIBEL, J. & WAGNER, C. 2005. The calcium-sensing receptor acts as a modulator of gastric acid secretion in freshly isolated human gastric glands. *American journal of physiology. Gastrointestinal and liver physiology,* 289**,** 90.

DUHN, V., D'ORSI, E., JOHNSON, S., D'ORSI, C., ADAMS, A. & O'NEILL, W. 2011. Breast arterial calcification: a marker of medial vascular calcification in chronic kidney disease. *Clinical journal of the American Society of Nephrology : CJASN,* 6**,** 377-459.

DUSSO, A., GONZÁLEZ, E. & MARTIN, K. 2011. Vitamin D in chronic kidney disease. *Best practice & research. Clinical endocrinology & metabolism,* 25**,** 647-702.

DWIVEDI, P., HII, C., FERRANTE, A., TAN, J., DER, C., OMDAHL, J., MORRIS, H. & MAY, B. 2002. Role of MAP kinases in the 1,25-dihydroxyvitamin D3-induced transactivation of the rat cytochrome P450C24 (CYP24) promoter. Specific functions for ERK1/ERK2 and ERK5. *The Journal of biological chemistry,* 277**,** 29643-29696.

EDDINGTON, H., SINHA, S. & KALRA, P. 2009. Vascular calcification in chronic kidney disease: a clinical review. *Journal of renal care,* 35 Suppl 1**,** 45-95.

EDWARDS, D., LI, Y. & GRIFFITH, T. 2008. Hydrogen peroxide potentiates the EDHF phenomenon by promoting endothelial Ca2+ mobilization. *Arteriosclerosis, Thrombosis, and Vascular Biology,* 28**,** 1774-1781.

EDWARDS, G. & WESTON, A. 2004. Potassium and potassium clouds in endothelium-dependent hyperpolarizations. *Pharmacological research : the official journal of the Italian Pharmacological Society,* 49**,** 535-541.

EIPERS, P., KALE, S., TAICHMAN, R., PIPIA, G., SWORDS, N., MANN, K. & LONG, M. 2000. Bone marrow accessory cells regulate human bone precursor cell development. *Experimental hematology,* 28**,** 815-840.

EL-ABBADI, M., PAI, A., LEAF, E., YANG, H.-Y., BARTLEY, B., QUAN, K., INGALLS, C., LIAO, H. & GIACHELLI, C. 2009. Phosphate feeding induces arterial medial calcification in uremic mice: role of serum phosphorus, fibroblast growth factor-23, and osteopontin. *Kidney International,* 75**,** 1297-1604.

ELDEIRY, L., RUAN, D., BROWN, E., GAGLIA, J. & GARBER, J. 2012. Primary Hyperparathyroidism and FHH: Relationships and Clinical Implications. *Endocrine*

practice : official journal of the American College of Endocrinology and the American Association of Clinical Endocrinologists, 1-20.

FARZANEH-FAR, A., PROUDFOOT, D., WEISSBERG, P. & SHANAHAN, C. 2000. Matrix gla protein is regulated by a mechanism functionally related to the calcium-sensing receptor. *Biochemical and biophysical research communications,* 277**,** 736-776.

FAURE, H., GOROJANKINA, T., RICE, N., DAUBAN, P., DODD, R., BRÄUNER-OSBORNE, H., ROGNAN, D. & RUAT, M. 2009. Molecular determinants of non-competitive antagonist binding to the mouse GPRC6A receptor. *Cell Calcium,* 46**,** 323-332.

FAVERMAN, L., MIKHAYLOVA, L., MALMQUIST, J. & NURMINSKAYA, M. 2008. Extracellular transglutaminase 2 activates beta-catenin signaling in calcifying vascular smooth muscle cells. *FEBS Letters,* 582**,** 1552-1559.

FAYAD, Z. A. & FUSTER, V. 2001. Clinical Imaging of the High-Risk or Vulnerable Atherosclerotic Plaque. *Circulation Research,* 89.

FELDER, C. 1995. Muscarinic acetylcholine receptors: signal transduction through multiple effectors. *The FASEB journal : official publication of the Federation of American Societies for Experimental Biology,* 9**,** 619-644.

FINNEY, B., DEL MORAL, P., WILKINSON, W., CAYZAC, S., COLE, M., WARBURTON, D., KEMP, P. & RICCARDI, D. 2008. Regulation of mouse lung development by the extracellular calcium-sensing receptor, CaR. *The Journal of physiology,* 586**,** 6007-6026.

FLOEGE, J. & KETTELER, M. 2004. Vascular calcification in patients with end-stage renal disease. *Nephrology, dialysis, transplantation : official publication of the European Dialysis and Transplant Association - European Renal Association,* 19 Suppl 5**,** 66.

FOLEY, T., HARRISON, H. & ARNAUD, C. 1972. Familial benign hypercalcemia. *The Journal of pediatrics,* 81**,** 1060-1067.

FRANCIS, J., SIMON, D. B., JEURGENSEN, P. & FINKELSTEIN, F. O. 2008. Calcimimetics for the treatment of secondary hyperparathyroidism in peritoneal dialysis patients. *Peritoneal Dialysis International,* 28.

FRANCIS, M., RUSSELL, R. & FLEISCH, H. 1969. Diphosphonates inhibit formation of calcium phosphate crystals in vitro and pathological calcification in vivo. *Science (New York, N.Y.),* 165**,** 1264-1270.

FRANK-RAUE, K., LEIDIG-BRUCKNER, G., HAAG, C., SCHULZE, E., LORENZ, A., SCHMITZ-WINNENTHAL, H. & RAUE, F. 2011. Inactivating calcium-sensing receptor mutations in patients with primary hyperparathyroidism. *Clinical Endocrinology*.

FRAZÃO, J. & ADRAGÃO, T. 2012. Non-calcium-containing phosphate binders: comparing efficacy, safety, and other clinical effects. *Nephron. Clinical practice,* 120**,** 19.

FREEMAN, R. & OTTO, C. 2005. Spectrum of calcific aortic valve disease: pathogenesis, disease progression, and treatment strategies. *Circulation,* 111**,** 3316-3342.

FRYER, R., SEGRETI, J., WIDOMSKI, D., FRANKLIN, P., BANFOR, P., KOCH, K., NAKANE, M., WU-WONG, J., COX, B. & REINHART, G. 2007. Systemic activation of the calcium sensing receptor produces acute effects on vascular tone and circulatory function in uremic and normal rats: focus on central versus peripheral control of vascular tone and blood pressure by cinacalcet. *The Journal of pharmacology and experimental therapeutics,* 323**,** 217-243.

FU, Y., LIU, H., FORSYTHE, S., KOGUT, P., MCCONVILLE, J., HALAYKO, A., CAMORETTI-MERCADO, B. & SOLWAY, J. 2000. Mutagenesis analysis of human SM22: characterization of actin binding. *Journal of applied physiology (Bethesda, Md. : 1985),* 89**,** 1985-2075.

FUJITA, T., MEGURO, T., FUKUYAMA, R., NAKAMUTA, H. & KOIDA, M. 2002. New signaling pathway for parathyroid hormone and cyclic AMP action on extracellular-regulated kinase and cell proliferation in bone cells. Checkpoint of modulation by cyclic AMP. *The Journal of biological chemistry,* 277**,** 22191-22391.

FURCHGOTT, R. 1984. The role of endothelium in the responses of vascular smooth muscle to drugs. *Annual review of pharmacology and toxicology,* 24**,** 175-272.

FURCHGOTT, R., CHERRY, P., ZAWADZKI, J. & JOTHIANANDAN, D. 1984. Endothelial cells as mediators of vasodilation of arteries. *Journal of cardiovascular pharmacology,* 6 Suppl 2**,** 43.

FURCHGOTT, R. & VANHOUTTE, P. 1989. Endothelium-derived relaxing and contracting factors. *The FASEB journal : official publication of the Federation of American Societies for Experimental Biology,* 3**,** 2007-2025.

FURIE, B. 1990. Molecular basis of vitamin K-dependent gamma-carboxylation. *Blood,* 75**,** 1753-1815.

GALVEZ, T., URWYLER, S., PRÉZEAU, L., MOSBACHER, J., JOLY, C., MALITSCHEK, B., HEID, J., BRABET, I., FROESTL, W., BETTLER, B., KAUPMANN, K. & PIN, J. 2000. Ca(2+) requirement for high-affinity gamma-aminobutyric acid (GABA) binding at GABA(B) receptors: involvement of serine 269 of the GABA(B)R1 subunit. *Molecular Pharmacology,* 57**,** 419-445.

GAMA, L. 2001. Heterodimerization of Calcium Sensing Receptors with Metabotropic Glutamate Receptors in Neurons. *Journal of Biological Chemistry,* 276.

GAMA, L., BAXENDALE-COX, L. & BREITWIESER, G. 1997. Ca2+-sensing receptors in intestinal epithelium. *The American journal of physiology,* 273**,** 75.

GARLAND, C. & WESTON, A. 2011. The vascular endothelium: still amazing us 30 years on. *British journal of pharmacology,* 164**,** 837-845.

GARLAND, J. & MCPHERSON, G. 1992. Evidence that nitric oxide does not mediate the hyperpolarization and relaxation to acetylcholine in the rat small mesenteric artery. *British Journal of Pharmacology,* 105**,** 429-435.

GEIBEL, J., WAGNER, C., CAROPPO, R., QURESHI, I., GLOECKNER, J., MANUELIDIS, L., KIRCHHOFF, P. & RADEBOLD, K. 2001. The stomach divalent ion-sensing receptor scar is a modulator of gastric acid secretion. *The Journal of biological chemistry,* 276**,** 39549-39601.

GENGE, B. R., WU, L. N. Y. & WUTHIER, R. E. 2008. Mineralization of Annexin-5-containing Lipid-Calcium-Phosphate Complexes: MODULATION BY VARYING LIPID COMPOSITION AND INCUBATION WITH CARTILAGE COLLAGENS. *Journal of Biological Chemistry,* 283.

GERRITY, R. G. & CLIFF, W. J. 1972. The Aortic Tunica Intima In Young And Aging Rats. *Experimental And Molecular Pathology***,** 382-402.

GHISELLI, G., SCHAEFER, E., GASCON, P. & BRESER, H. 1981. Type III hyperlipoproteinemia associated with apolipoprotein E deficiency. *Science (New York, N.Y.),* 214**,** 1239-1280.

GIACHELLI, C. M. 1999. Ectopic Calcification: *Gathering Hard Facts About Soft Tissue Mineralization. The American Journal Of Pathology,* 154**,** 671-675.

GIACHELLI, C. M. 2004. Vascular Calcification Mechanisms. *Journal of the American Society of Nephrology,* 15, 2959-2964.

GIACHELLI, C. M. 2009. The emerging role of phosphate in vascular calcification. *Kidney International,* 75, 890–897.

GLASS, C. & WITZTUM, J. 2001. Atherosclerosis. the road ahead. *Cell,* 104**,** 503-519.

GO, G.-W. & MANI, A. 2012. Low-density lipoprotein receptor (LDLR) family orchestrates cholesterol homeostasis. *The Yale journal of biology and medicine,* 85**,** 19-47.

GOODMAN, W., GOLDIN, J., KUIZON, B., YOON, C., GALES, B., SIDER, D., WANG, Y., CHUNG, J., EMERICK, A., GREASER, L., ELASHOFF, R. & SALUSKY, I. 2000. Coronary-artery calcification in young adults with end-stage renal disease who are undergoing dialysis. *The New England journal of medicine,* 342**,** 1478-1561.

GOSAU, N., FAHIMI-VAHID, M., MICHALEK, C., SCHMIDT, M. & WIELAND, T. 2002. Signalling components involved in the coupling of alpha 1-adrenoceptors to phospholipase D in neonatal rat cardiac myocytes. *Naunyn-Schmiedeberg's archives of pharmacology,* 365**,** 468-544.

GRANT, M., STEPANCHICK, A., CAVANAUGH, A. & BREITWIESER, G. 2011. Agonist-driven maturation and plasma membrane insertion of calcium-sensing receptors dynamically control signal amplitude. *Science signaling,* 4.

GUANG-WEI, L., QIU-SHI, W., JING-HUI, H., WEN-JING, X., JIN, G., HONG-ZHU, L., SHU-ZHI, B., HONG-XIA, L., WEI-HUA, Z., BAO-FENG, Y., GUANG-DONG, Y., LING-YUN, W., RUI, W. & CHANG-QING, X. 2011. The functional expression of extracellular calcium-sensing receptor in rat pulmonary artery smooth muscle cells. *Journal of Biomedical Science,* 18.

GUEDES, D., SILVA, D., BARBOSA-FILHO, J. & MEDEIROS, I. 2004. Calcium antagonism and the vasorelaxation of the rat aorta induced by rotundifolone. *Brazilian journal of medical and biological research = Revista brasileira de pesquisas médicas e biológicas / Sociedade Brasileira de Biofísica ... [et al.],* 37**,** 1881-1887.

GUÉRIN, A., LONDON, G., MARCHAIS, S. & METIVIER, F. 2000. Arterial stiffening and vascular calcifications in end-stage renal disease. *Nephrology, dialysis, transplantation : official publication of the European Dialysis and Transplant Association - European Renal Association,* 15**,** 1014-1035.

GUTIÉRREZ, O., JANUZZI, J., ISAKOVA, T., LALIBERTE, K., SMITH, K., COLLERONE, G., SARWAR, A., HOFFMANN, U., COGLIANESE, E., CHRISTENSON, R., WANG, T., DEFILIPPI, C. & WOLF, M. 2009. Fibroblast growth factor 23 and left ventricular hypertrophy in chronic kidney disease. *Circulation,* 119**,** 2545-2552.

GUTTERMAN, D. 1999. Adventitia-dependent influences on vascular function. *American Journal of Physiology-Heart and ...*

HAAS, T. & DULING, B. 1997. Morphology favors an endothelial cell pathway for longitudinal conduction within arterioles. *Microvascular research,* 53**,** 113-133.

HACKETT, B., MCALEER, M., SHEEHAN, G., POWELL, F. & O'DONNELL, B. 2009. Calciphylaxis in a patient with normal renal function: response to treatment with sodium thiosulfate. *Clinical and experimental dermatology,* 34**,** 39-81.

HAGSTRÖM, E., HELLMAN, P., LARSSON, T., INGELSSON, E., BERGLUND, L., SUNDSTRÖM, J., MELHUS, H., HELD, C., LIND, L., MICHAËLSSON, K. & ARNLÖV, J. 2009. Plasma parathyroid hormone and the risk of cardiovascular mortality in the community. *Circulation,* 119**,** 2765-2836.

HAI, C. & MURPHY, R. 1989. Ca2+, crossbridge phosphorylation, and contraction. *Annual Review of Physiology,* 51**,** 285-383.

HAN, M., DONG, L.-H., ZHENG, B., SHI, J.-H., WEN, J.-K. & CHENG, Y. 2009. Smooth muscle 22 alpha maintains the differentiated phenotype of vascular smooth muscle cells by inducing filamentous actin bundling. *Life Sciences,* 84**,** 394-795.

HARNO, E., EDWARDS, G., GERAGHTY, A., WARD, D., DODD, R., DAUBAN, P., FAURE, H., RUAT, M. & WESTON, A. 2008. Evidence for the presence of GPRC6A receptors in rat mesenteric arteries. *Cell Calcium,* 44**,** 210-219.

HAYDEN, M. & GOLDSMITH, D. 2010. Sodium thiosulfate: new hope for the treatment of calciphylaxis. *Seminars in Dialysis,* 23**,** 258-320.

HEBERLEIN, K., STRAUB, A. & ISAKSON, B. 2009. The myoendothelial junction: breaking through the matrix? *Microcirculation (New York, N.Y. : 1994),* 16**,** 307-329.

HEBERT, S. 2006. Therapeutic use of calcimimetics. *Annual Review of Medicine,* 57**,** 349-413.

HEBY, O. & PERSSON, L. 1990. Molecular genetics of polyamine synthesis in eukaryotic cells. *Trends in biochemical sciences,* 15**,** 153-158.

HENDY, G., D'SOUZA-LI, L., YANG, B., CANAFF, L. & COLE, D. 2000. Mutations of the calcium-sensing receptor (CASR) in familial hypocalciuric hypercalcemia, neonatal severe hyperparathyroidism, and autosomal dominant hypocalcemia. *Human mutation,* 16**,** 281-377.

HERDEWIJN, P. & MARLIÈRE, P. 2012. Redesigning the leaving group in nucleic acid polymerization. *FEBS Letters,* 586**,** 2049-2105.

HERMANS, E. & CHALLISS, R. 2001. Structural, signalling and regulatory properties of the group I metabotropic glutamate receptors: prototypic family C G-protein-coupled receptors. *The Biochemical journal,* 359**,** 465-549.

HERRADA, G. & DULAC, C. 1997. A novel family of putative pheromone receptors in mammals with a topographically organized and sexually dimorphic distribution. *Cell,* 90**,** 763-836.

HEUSCH, G. 2011. The paradox of α-adrenergic coronary vasoconstriction revisited. *Journal of molecular and cellular cardiology,* 51**,** 16-39.

HOFFMAN, B. & LEFKOWITZ, R. 1982. Adrenergic receptors in the heart. *Annual review of physiology,* 44**,** 475-559.

HOFMANN, C., BRONCKERS, A. & SOHOCKI, M. 1995. BMP-7 is an inducer of nephrogenesis, and is also required for eye development and skeletal patterning. ... *& development.*

HOON, M., ADLER, E., LINDEMEIER, J., BATTEY, J., RYBA, N. & ZUKER, C. 1999. Putative mammalian taste receptors: a class of taste-specific GPCRs with distinct topographic selectivity. *Cell,* 96**,** 541-592.

HOUSE, M., KOHLMEIER, L., CHATTOPADHYAY, N., KIFOR, O., YAMAGUCHI, T., LEBOFF, M., GLOWACKI, J. & BROWN, E. 1997. Expression of an extracellular calcium-sensing receptor in human and mouse bone marrow cells. *Journal of bone and*

mineral research : the official journal of the American Society for Bone and Mineral Research, 12**,** 1959-2029.

HOUSE, S., POTIER, M., BISAILLON, J., SINGER, H. & TREBAK, M. 2008. The non-excitable smooth muscle: calcium signaling and phenotypic switching during vascular disease. *Pflügers Archiv : European journal of physiology,* 456**,** 769-854.

HOWARD, G., WAGENKNECHT, L., BURKE, G., DIEZ-ROUX, A., EVANS, G., MCGOVERN, P., NIETO, F. & TELL, G. 1998. Cigarette smoking and progression of atherosclerosis: The Atherosclerosis Risk in Communities (ARIC) Study. *JAMA : the journal of the American Medical Association,* 279**,** 119-143.

HRUSKA, K. A. 2005. Bone Morphogenetic Proteins in Vascular Calcification. *Circulation Research,* 97.

HRUSKA, K. A. 2009. Vascular Smooth Muscle Cells in the Pathogenesis of Vascular Calcification. *Circulation Research,* 104.

HU, J. & SPIEGEL, A. 2003. Naturally occurring mutations of the extracellular Ca2+-sensing receptor: implications for its structure and function. *Trends in endocrinology and metabolism: TEM,* 14**,** 282-288.

HU, P., XUAN, Q., HU, B., LU, L., WANG, J. & QIN, Y. 2012. Fibroblast growth factor-23 helps explain the biphasic cardiovascular effects of vitamin D in chronic kidney disease. *International journal of biological sciences,* 8**,** 663-734.

HUANG, C., HANDLOGTEN, M. & MILLER, R. 2002. Parallel activation of phosphatidylinositol 4-kinase and phospholipase C by the extracellular calcium-sensing receptor. *The Journal of biological chemistry,* 277**,** 20293-20593.

HUJAIRI, N., AFZALI, B. & GOLDSMITH, D. 2004. Cardiac calcification in renal patients: what we do and don't know. *American journal of kidney diseases : the official journal of the National Kidney Foundation,* 43**,** 234-277.

HUTCHISON, A., LAVILLE, M. & GROUP, S. P. D. L. S. 2008. Switching to lanthanum carbonate monotherapy provides effective phosphate control with a low tablet burden. *Nephrology, dialysis, transplantation : official publication of the European Dialysis and Transplant Association - European Renal Association,* 23**,** 3677-3761.

IDDO, Z. B.-D., HILLEL, G., VARDIT, L.-M., REGINA, G., MAKOTO, K.-O., MOOSA, M., ROY, S., TALLY, N.-M. & JUSTIN, S. 2007. The parathyroid is a target organ for FGF23 in rats. *Journal of Clinical Investigation.*

ISHIBASHI, S., BROWN, M., GOLDSTEIN, J., GERARD, R., HAMMER, R. & HERZ, J. 1993. Hypercholesterolemia in low density lipoprotein receptor knockout mice and its reversal by adenovirus-mediated gene delivery. *The Journal of clinical investigation,* 92**,** 883-893.

ISHIMURA, E., OKUNO, S., YAMAKAWA, T., INABA, M. & NISHIZAWA, Y. 2007. Serum magnesium concentration is a significant predictor of mortality in maintenance

hemodialysis patients. *Magnesium research : official organ of the International Society for the Development of Research on Magnesium,* 20**,** 237-281.

ITO, K., IKEMOTO, T. & TAKAKURA, S. 1991. Involvement of Ca2+ influx-induced Ca2+ release in contractions of intact vascular smooth muscles. *The American journal of physiology,* 261**,** 70.

ITOH, T., IKEBE, M., KARGACIN, G., HARTSHORNE, D., KEMP, B. & FAY, F. 1989. Effects of modulators of myosin light-chain kinase activity in single smooth muscle cells. *Nature,* 338**,** 164-171.

IVANOVSKI, O., NIKOLOV, I. G., JOKI, N., CAUDRILLIER, A., PHAN, O., MENTAVERRI, R., MAIZEL, J., HAMADA, Y., NGUYEN-KHOA, T., FUKAGAWA, M., KAMEL, S., LACOUR, B., DRÜEKE, T. B. & MASSY, Z. A. 2009. The calcimimetic R-568 retards uremia-enhanced vascular calcification and atherosclerosis in apolipoprotein E deficient (apoE−/−) mice. *Atherosclerosis,* 205.

JAFFE, I. Z., TINTUT, Y., NEWFELL, B. G., DEMER, L. L. & MENDELSOHN, M. E. 2007. Mineralocorticoid Receptor Activation Promotes Vascular Cell Calcification. *Arteriosclerosis, Thrombosis, and Vascular Biology,* 27**,** 799-805.

JAGGAR, J., WELLMAN, G., HEPPNER, T., PORTER, V., PEREZ, G., GOLLASCH, M., KLEPPISCH, T., RUBART, M., STEVENSON, A., LEDERER, W., KNOT, H., BONEV, A. & NELSON, M. 1998. Ca2+ channels, ryanodine receptors and Ca(2+)-activated K+ channels: a functional unit for regulating arterial tone. *Acta physiologica Scandinavica,* 164**,** 577-664.

JAHNEN-DECHENT, W., HEISS, A., SCHAFER, C. & KETTELER, M. 2011. Fetuin-A Regulation of Calcified Matrix Metabolism. *Circulation Research,* 108.

JAIN, R. 2003. Molecular regulation of vessel maturation. *Nature Medicine,* 9**,** 685-778.

JINGAMI, H., NAKANISHI, S. & MORIKAWA, K. 2003. Structure of the metabotropic glutamate receptor. *Current opinion in neurobiology,* 13**,** 271-279.

JOHNSON, K. 2005. Chondrogenesis Mediated by PPi Depletion Promotes Spontaneous Aortic Calcification in NPP1-/- Mice. *Arteriosclerosis, Thrombosis, and Vascular Biology,* 25.

JOHNSON, R. C., LEOPOLD, J. A. & LOSCALZO, J. 2006. Vascular Calcification: Pathobiological Mechanisms and Clinical Implications. *Circulation Research,* 99.

JONGSTRA-BILEN, J., HAIDARI, M., ZHU, S.-N., CHEN, M., GUHA, D. & CYBULSKY, M. 2006. Low-grade chronic inflammation in regions of the normal mouse arterial intima predisposed to atherosclerosis. *The Journal of experimental medicine,* 203**,** 2073-2156.

JONO, S., MCKEE, M., MURRY, C., SHIOI, A., NISHIZAWA, Y., MORI, K., MORII, H. & GIACHELLI, C. 2000. Phosphate regulation of vascular smooth muscle cell calcification. *Circulation research,* 87**,** 7.

KALAJZIC, Z., LI, H., WANG, L.-P., JIANG, X., LAMOTHE, K., ADAMS, D., AGUILA, H., ROWE, D. & KALAJZIC, I. 2008. Use of an alpha-smooth muscle actin GFP reporter to identify an osteoprogenitor population. *Bone,* 43**,** 501-511.

KAPUSTIN, A. & SHANAHAN, C. 2009. Targeting vascular calcification: softening-up a hard target. *Current opinion in pharmacology,* 9**,** 84-93.

KAPUSTIN, A. N., DAVIES, J. D., REYNOLDS, J. L., MCNAIR, R., JONES, G. T., SIDIBE, A., SCHURGERS, L. J., SKEPPER, J. N., PROUDFOOT, D., MAYR, M. & SHANAHAN, C. M. 2011. Calcium Regulates Key Components of Vascular Smooth Muscle Cell-Derived Matrix Vesicles to Enhance Mineralization. *Circulation Research,* 109.

KAWATA, T., NAGANO, N., OBI, M., MIYATA, S., KOYAMA, C., KOBAYASHI, N., WAKITA, S. & WADA, M. 2008. Cinacalcet suppresses calcification of the aorta and heart in uremic rats. *Kidney International,* 74**,** 1270-1277.

KELLY, J., LUNGCHUKIET, P. & MACLEOD, R. 2011. Extracellular Calcium-Sensing Receptor Inhibition of Intestinal EpithelialTNF Signaling Requires CaSR-Mediated Wnt5a/Ror2 Interaction. *Frontiers in Physiology,* 2**,** 17.

KENDRICK, J. & CHONCHOL, M. 2011. The Role of Phosphorus in the Development and Progression of Vascular Calcification. *American Journal of Kidney Diseases,* 58.

KERR, P., TAM, R., ONDRUSOVA, K., MITTAL, R., NARANG, D., TRAN, C., WELSH, D. & PLANE, F. 2012. Endothelial feedback and the myoendothelial projection. *Microcirculation (New York, N.Y. : 1994),* 19**,** 416-438.

KHOSHNIAT, S., BOURGINE, A., JULIEN, M., PETIT, M., PILET, P., ROUILLON, T., MASSON, M., GATIUS, M., WEISS, P., GUICHEUX, J. & BECK, L. 2011. Phosphate-dependent stimulation of MGP and OPN expression in osteoblasts via the ERK1/2 pathway is modulated by calcium. *Bone,* 48.

KIFOR, O., DIAZ, R., BUTTERS, R. & BROWN, E. 1997. The Ca2+-sensing receptor (CaR) activates phospholipases C, A2, and D in bovine parathyroid and CaR-transfected, human embryonic kidney (HEK293) cells. *Journal of bone and mineral research : the official journal of the American Society for Bone and Mineral Research,* 12**,** 715-740.

KIFOR, O., MACLEOD, R., DIAZ, R., BAI, M., YAMAGUCHI, T., YAO, T., KIFOR, I. & BROWN, E. 2001. Regulation of MAP kinase by calcium-sensing receptor in bovine parathyroid and CaR-transfected HEK293 cells. *American journal of physiology. Renal physiology,* 280**,** 302.

KIP, S. & STREHLER, E. 2003. Characterization of PMCA isoforms and their contribution to transcellular Ca2+ flux in MDCK cells. *American journal of physiology. Renal physiology,* 284**,** 32.

KIRCELLI, F., PETER, M. E., OK, E. S., CELENK, F. G., YILMAZ, M., STEPPAN, S., ASCI, G., OK, E. & PASSLICK-DEETJEN, J. 2012. Magnesium reduces calcification

in bovine vascular smooth muscle cells in a dose-dependent manner. *Nephrology Dialysis Transplantation.*

KISANUKI, Y., HAMMER, R., MIYAZAKI, J., WILLIAMS, S., RICHARDSON, J. & YANAGISAWA, M. 2001. Tie2-Cre transgenic mice: a new model for endothelial cell-lineage analysis in vivo. *Developmental Biology,* 230**,** 230-242.

KITAZAWA, T., SEMBA, S., HUH, Y., KITAZAWA, K. & ETO, M. 2009. Nitric oxide-induced biphasic mechanism of vascular relaxation via dephosphorylation of CPI-17 and MYPT1. *The Journal of Physiology,* 587**,** 3587-4190.

KNOWLES, R. & MONCADA, S. 1994. Nitric oxide synthases in mammals. *The Biochemical journal,* 298 (Pt 2)**,** 249-307.

KOBAYASHI, R., KUBOTA, T. & HIDAKA, H. 1994. Purification, characterization, and partial sequence analysis of a new 25-kDa actin-binding protein from bovine aorta: a SM22 homolog. *Biochemical and Biophysical Research Communications,* 198**,** 1275-1355.

KOBILKA, B. 2000. Allosteric activation of the CaR by L-amino acids. *Proceedings of the National Academy of Sciences of the United States of America,* 97**,** 4419-4439.

KOLEGANOVA, N., PIECHA, G., RITZ, E., SCHMITT, C. P. & GROSS, M.-L. 2009. A calcimimetic (R-568), but not calcitriol, prevents vascular remodeling in uremia. *Kidney International,* 75**,** 60-71.

KOVACS, C., HO-PAO, C., HUNZELMAN, J., LANSKE, B., FOX, J., SEIDMAN, J., SEIDMAN, C. & KRONENBERG, H. 1998. Regulation of murine fetal-placental calcium metabolism by the calcium-sensing receptor. *The Journal of clinical investigation,* 101**,** 2812-2820.

KOVACS, C. & KRONENBERG, H. 1997. Maternal-fetal calcium and bone metabolism during pregnancy, puerperium, and lactation. *Endocrine Reviews,* 18**,** 832-904.

KUNISHIMA, N., SHIMADA, Y., TSUJI, Y., SATO, T., YAMAMOTO, M., KUMASAKA, T., NAKANISHI, S., JINGAMI, H. & MORIKAWA, K. 2000. Structural basis of glutamate recognition by a dimeric metabotropic glutamate receptor. *Nature,* 407**,** 971-978.

KUNKEL, M. & PERALTA, E. 1993. Charged amino acids required for signal transduction by the m3 muscarinic acetylcholine receptor. *The EMBO journal,* 12**,** 3809-3824.

KURO-O, M., MATSUMURA, Y., AIZAWA, H., KAWAGUCHI, H., SUGA, T., UTSUGI, T., OHYAMA, Y., KURABAYASHI, M., KANAME, T., KUME, E., IWASAKI, H., IIDA, A., SHIRAKI-IIDA, T., NISHIKAWA, S., NAGAI, R. & NABESHIMA, Y. 1997. Mutation of the mouse klotho gene leads to a syndrome resembling ageing. *Nature,* 390**,** 45-51.

LAU, W. L., FESTING, M. H. & GIACHELLI, C. M. 2010. Phosphate and vascular calcification: Emerging role of the sodium-dependent phosphate co-transporter PiT-1. *Thrombosis and Haemostasis,* 104.

LEDOUX, J. 2006. Calcium-Activated Potassium Channels and the Regulation of Vascular Tone. *Physiology,* 21.

LEE, C., WONG, K., LIU, J., CHEN, Y., CHENG, J. & CHAN, P. 2001. Inhibitory effect of stevioside on calcium influx to produce antihypertension. *Planta medica,* 67**,** 796-799.

LEE, M., KWON, T., PARK, H. & WOZNEY, J. 2003. BMP-2-induced Osterix expression is mediated by Dlx5 but is independent of Runx2. *... and biophysical research ...*

LEE, W. J. & KIM, H. J. 2007. Inhibition Of DNA Methylation Is Involved In Transdifferentiation Of Myoblasts Into Smooth Muscle Cells. *Molecules And Cells,* 24**,** 441-444.

LEVIN, A., BAKRIS, G. L., MOLITCH, M., SMULDERS, M., TIAN, J., WILLIAMS, L. A. & ANDRESS, D. L. 2006. Prevalence of abnormal serum vitamin D, PTH, calcium, and phosphorus in patients with chronic kidney disease: Results of the study to evaluate early kidney disease. *Kidney International,* 71.

LEW, M., RIVERS, R. & DULING, B. 1989. Arteriolar smooth muscle responses are modulated by an intramural diffusion barrier. *The American journal of physiology,* 257**,** 6.

LI, L., MIANO, J., CSERJESI, P. & OLSON, E. 1996a. SM22 alpha, a marker of adult smooth muscle, is expressed in multiple myogenic lineages during embryogenesis. *Circulation Research,* 78**,** 188-195.

LI, L., MIANO, J., MERCER, B. & OLSON, E. 1996b. Expression of the SM22alpha promoter in transgenic mice provides evidence for distinct transcriptional regulatory programs in vascular and visceral smooth muscle cells. *The Journal of cell biology,* 132**,** 849-908.

LI, X., YANG, H.-Y. & GIACHELLI, C. 2006. Role of the Sodium-Dependent Phosphate Cotransporter, Pit-1, in Vascular Smooth Muscle Cell Calcification. *Circulation Research,* 98.

LI, Y., SONG, Y., RAIS, N., CONNOR, E., SCHATZ, D., MUIR, A. & MACLAREN, N. 1996c. Autoantibodies to the extracellular domain of the calcium sensing receptor in patients with acquired hypoparathyroidism. *The Journal of clinical investigation,* 97**,** 910-914.

LIBBY, P. 2002. Inflammation in atherosclerosis. *Nature,* 420**,** 868-942.

LIBBY, P. & AIKAWA, M. 2002. Stabilization Of Atherosclerotic Plaques: New Mechanisms And Clinical Targets. *Nature Medicine,* 8**,** 1257-1262.

LINDROOS, M., KUPARI, M., HEIKKILÄ, J. & TILVIS, R. 1993. Prevalence of aortic valve abnormalities in the elderly: an echocardiographic study of a random population sample. *Journal of the American College of Cardiology,* 21**,** 1220-1225.

LIPS, P. 2006. Vitamin D physiology. *Progress in Biophysics and Molecular Biology,* 92.

LIPSCOMBE, D. 2004. L-Type Calcium Channels: The Low Down. *Journal of Neurophysiology,* 92.

LIU, D., ZHANG, J., WANG, G., LIU, X., WANG, S. & YANG, M. 2012. The Dual-Effects of LaCl(3) on the Proliferation, Osteogenic Differentiation, and Mineralization of MC3T3-E1 Cells. *Biological trace element research.*

LLOYD-JONES, D., ADAMS, R., BROWN, T., CARNETHON, M., DAI, S., DE SIMONE, G., FERGUSON, T., FORD, E., FURIE, K., GILLESPIE, C., GO, A., GREENLUND, K., HAASE, N., HAILPERN, S., HO, P., HOWARD, V., KISSELA, B., KITTNER, S., LACKLAND, D., LISABETH, L., MARELLI, A., MCDERMOTT, M., MEIGS, J., MOZAFFARIAN, D., MUSSOLINO, M., NICHOL, G., ROGER, V., ROSAMOND, W., SACCO, R., SORLIE, P., STAFFORD, R., THOM, T., WASSERTHIEL-SMOLLER, S., WONG, N., WYLIE-ROSETT, J., AMERICAN HEART ASSOCIATION STATISTICS, C. & STROKE STATISTICS, S. 2010a. Executive summary: heart disease and stroke statistics--2010 update: a report from the American Heart Association. *Circulation,* 121**,** 948-1002.

LLOYD-JONES, D., ADAMS, R., BROWN, T., CARNETHON, M., DAI, S., DE SIMONE, G., FERGUSON, T., FORD, E., FURIE, K., GILLESPIE, C., GO, A., GREENLUND, K., HAASE, N., HAILPERN, S., HO, P., HOWARD, V., KISSELA, B., KITTNER, S., LACKLAND, D., LISABETH, L., MARELLI, A., MCDERMOTT, M., MEIGS, J., MOZAFFARIAN, D., MUSSOLINO, M., NICHOL, G., ROGER, V., ROSAMOND, W., SACCO, R., SORLIE, P., STAFFORD, R., THOM, T., WASSERTHIEL-SMOLLER, S., WONG, N., WYLIE-ROSETT, J., AMERICAN HEART ASSOCIATION STATISTICS, C. & STROKE STATISTICS, S. 2010b. Heart disease and stroke statistics--2010 update: a report from the American Heart Association. *Circulation,* 121.

LLOYD-JONES, D., ADAMS, R., CARNETHON, M., DE SIMONE, G., FERGUSON, T., FLEGAL, K., FORD, E., FURIE, K., GO, A., GREENLUND, K., HAASE, N., HAILPERN, S., HO, M., HOWARD, V., KISSELA, B., KITTNER, S., LACKLAND, D., LISABETH, L., MARELLI, A., MCDERMOTT, M., MEIGS, J., MOZAFFARIAN, D., NICHOL, G., O'DONNELL, C., ROGER, V., ROSAMOND, W., SACCO, R., SORLIE, P., STAFFORD, R., STEINBERGER, J., THOM, T., WASSERTHIEL-SMOLLER, S., WONG, N., WYLIE-ROSETT, J., HONG, Y., AMERICAN HEART ASSOCIATION STATISTICS, C. & STROKE STATISTICS, S. 2009. Heart disease and stroke statistics--2009 update: a report from the American Heart Association Statistics Committee and Stroke Statistics Subcommittee. *Circulation,* 119**,** 480-486.

LLOYD-JONES, D., ADAMS, R., CARNETHON, M., SIMONE, G. D., FERGUSON, T. B., FLEGAL, K., FORD, E., FURIE, K., GO, A., GREENLUND, K., HAASE, N., HAILPERN, S., HO, M., HOWARD, V., KISSELA, B., KITTNER, S., LACKLAND,

D., LISABETH, L., MARELLI, A., MCDERMOTT, M., MEIGS, J., MOZAFFARIAN, D., NICHOL, G., DONNELL, C. O., ROGER, V., ROSAMOND, W., SACCO, R., SORLIE, P., STAFFORD, R., STEINBERGER, J., THOM, T., WASSERTHIEL-SMOLLER, S., WONG, N., WYLIE-ROSETT, J. & HONG, Y. 2008. Heart Disease and Stroke Statistics--2009 Update: A Report From the American Heart Association Statistics Committee and Stroke Statistics Subcommittee. *Circulation,* 119.

LOMPRÉ, A. 1999. Sarcoplasmic reticulum in vascular cells in hypertension and during proliferation. *Clinical and experimental pharmacology & physiology,* 26**,** 553-557.

LONDON, G. 2003. Cardiovascular disease in chronic renal failure: pathophysiologic aspects. *Seminars in dialysis,* 16**,** 85-179.

LONDON, G. 2011. Soft bone - hard arteries: a link? *Kidney & blood pressure research,* 34**,** 203-211.

LOPEZ-JARAMILLO, P., GONZALEZ, M., PALMER, R. & MONCADA, S. 1990. The crucial role of physiological Ca2+ concentrations in the production of endothelial nitric oxide and the control of vascular tone. *British Journal of Pharmacology,* 101**,** 489-493.

LOPEZ, I. 2006. Calcimimetic R-568 Decreases Extraosseous Calcifications in Uremic Rats Treated with Calcitriol. *Journal of the American Society of Nephrology,* 17.

LORETZ, C. 2008. Extracellular calcium-sensing receptors in fishes. *Comparative biochemistry and physiology. Part A, Molecular & integrative physiology,* 149**,** 225-270.

LUKSHA, L., AGEWALL, S. & KUBLICKIENE, K. 2009. Endothelium-derived hyperpolarizing factor in vascular physiology and cardiovascular disease. *Atherosclerosis,* 202**,** 330-374.

LUO, G., DUCY, P., MCKEE, M., PINERO, G., LOYER, E., BEHRINGER, R. & KARSENTY, G. 1997. Spontaneous calcification of arteries and cartilage in mice lacking matrix GLA protein. *Nature,* 386**,** 78-159.

LÜSCHER, T. & VANHOUTTE, P. 1986. Endothelium-dependent contractions to acetylcholine in the aorta of the spontaneously hypertensive rat. *Hypertension,* 8**,** 344-348.

MALIK, T. H., CORTINI, A., CARASSITI, D., BOYLE, J. J., HASKARD, D. O. & BOTTO, M. 2010. The Alternative Pathway Is Critical for Pathogenic Complement Activation in Endotoxin- and Diet-Induced Atherosclerosis in Low-Density Lipoprotein Receptor-Deficient Mice. *Circulation,* 122.

MAMILLAPALLI, R., VANHOUTEN, J., ZAWALICH, W. & WYSOLMERSKI, J. 2008. Switching of G-protein usage by the calcium-sensing receptor reverses its effect on parathyroid hormone-related protein secretion in normal versus malignant breast cells. *The Journal of biological chemistry,* 283**,** 24435-24482.

MAMILLAPALLI, R. & WYSOLMERSKI, J. 2010. The calcium-sensing receptor couples to Galpha(s) and regulates PTHrP and ACTH secretion in pituitary cells. *The Journal of endocrinology,* 204**,** 287-384.

MANGONI, M., COUETTE, B., BOURINET, E., PLATZER, J., REIMER, D., STRIESSNIG, J. & NARGEOT, J. 2003. Functional role of L-type Cav1.3 Ca2+ channels in cardiac pacemaker activity. *Proceedings of the National Academy of Sciences of the United States of America,* 100**,** 5543-5548.

MARIANO, R., ESCOLÁSTICO, A.-T., MENDOZA, F. J., FÁTIMA, G. & IGNACIO, L. 2008. Effects of calcimimetics on extraskeletal calcifications in chronic kidney disease. *Kidney International,* 74.

MASAKI, T. 1995. Possible role of endothelin in endothelial regulation of vascular tone. *Annual review of pharmacology and toxicology,* 35**,** 235-290.

MASSBERG, S., SAUSBIER, M., KLATT, P., BAUER, M., PFEIFER, A., SIESS, W., FÄSSLER, R., RUTH, P., KROMBACH, F. & HOFMANN, F. 1999. Increased adhesion and aggregation of platelets lacking cyclic guanosine 3',5'-monophosphate kinase I. *The Journal of experimental medicine,* 189**,** 1255-1319.

MASSY, Z. A., IVANOVSKI, O., NGUYEN-KHOA, T., ANGULO, J., SZUMILAK, D., MOTHU, N., PHAN, O., DAUDON, M., LACOUR, B., DRUEKE, T. B. & MUNTZEL, M. S. 2005. Uremia Accelerates both Atherosclerosis and Arterial Calcification in Apolipoprotein E Knockout Mice. *Journal of the American Society of Nephrology,* 16**,** 109-116.

MATHEW, S., LUND, R., CHAUDHARY, L., GEURS, T. & HRUSKA, K. 2008. Vitamin D Receptor Activators Can Protect against Vascular Calcification. *Journal of the American Society of Nephrology,* 19, 1509–1519.

MATSUNAMI, H. & BUCK, L. 1997. A multigene family encoding a diverse array of putative pheromone receptors in mammals. *Cell,* 90**,** 775-859.

MCGEHEE, D., ALDERSBERG, M., LIU, K., HSUING, S., HEATH, M. & TAMIR, H. 1997. Mechanism of extracellular Ca2+ receptor-stimulated hormone release from sheep thyroid parafollicular cells. *The Journal of Physiology,* 502 (Pt 1)**,** 31-44.

MCLARNON, S., HOLDEN, D., WARD, D., JONES, M., ELLIOTT, A. & RICCARDI, D. 2002. Aminoglycoside antibiotics induce pH-sensitive activation of the calcium-sensing receptor. *Biochemical and Biophysical Research Communications,* 297**,** 71-78.

MEI, B. 2004. Structure–function relationship of the extracellular calcium-sensing receptor. *Cell Calcium,* 35, 197-207.

MENDOZA, F., LOPEZ, I., CANALEJO, R., ALMADEN, Y., MARTIN, D., AGUILERA-TEJERO, E. & RODRIGUEZ, M. 2009. Direct upregulation of parathyroid calcium-sensing receptor and vitamin D receptor by calcimimetics in uremic rats. *American journal of physiology. Renal physiology,* 296**,** 13.

MENDOZA, F. J., MARTINEZ-MORENO, J., ALMADEN, Y., RODRIGUEZ-ORTIZ, M. E., LOPEZ, I., ESTEPA, J. C., HENLEY, C., RODRIGUEZ, M. & AGUILERA-TEJERO, E. 2010. Effect of Calcium and the Calcimimetic AMG 641 on Matrix-Gla Protein in Vascular Smooth Muscle Cells. *Calcified Tissue International,* 88.

MERX, M., SCHÄFER, C., WESTENFELD, R., BRANDENBURG, V., HIDAJAT, S., WEBER, C., KETTELER, M. & JAHNEN-DECHENT, W. 2005. Myocardial stiffness, cardiac remodeling, and diastolic dysfunction in calcification-prone fetuin-A-deficient mice. *Journal of the American Society of Nephrology : JASN,* 16**,** 3357-3421.

MICHEL, R., HU, F. & MEYRICK, B. 1995. Myoendothelial junctional complexes in postobstructive pulmonary vasculopathy: a quantitative electron microscopic study. *Experimental lung research,* 21**,** 437-489.

MICHELETTI, R. G., FISHBEIN, G. A., CURRIER, J. S. & FISHBEIN, M. C. 2008. Monckeberg Sclerosis Revisited: A Clarification Of The Histologic Definition Of Mönckeberg Sclerosis. *Archives Of Pathology & Laboratory Medicine***,** 43-47.

MIEDLICH, S., GAMA, L., SEUWEN, K., WOLF, R. & BREITWIESER, G. 2004. Homology modeling of the transmembrane domain of the human calcium sensing receptor and localization of an allosteric binding site. *The Journal of biological chemistry,* 279**,** 7254-7317.

MIKHAYLOVA, L., MALMQUIST, J. & NURMINSKAYA, M. 2007. Regulation of in vitro vascular calcification by BMP4, VEGF and Wnt3a. *Calcified Tissue International,* 81**,** 372-453.

MILLER, B., CONNORS, B., BOHLEN, H. & EVAN, A. 1987. Cell and wall morphology of intestinal arterioles from 4- to 6- and 17- to 19-week-old Wistar-Kyoto and spontaneously hypertensive rats. *Hypertension,* 9**,** 59-127.

MINNEMAN, K. 1988. Alpha 1-adrenergic receptor subtypes, inositol phosphates, and sources of cell Ca2+. *Pharmacological reviews,* 40**,** 87-206.

MIZOBUCHI, M., HATAMURA, I., OGATA, H., SAJI, F., UDA, S., SHIIZAKI, K., SAKAGUCHI, T., NEGI, S., KINUGASA, E., KOSHIKAWA, S. & AKIZAWA, T. 2004. Calcimimetic compound upregulates decreased calcium-sensing receptor expression level in parathyroid glands of rats with chronic renal insufficiency. *Journal of the American Society of Nephrology : JASN,* 15**,** 2579-2587.

MIZOBUCHI, M., TOWLER, D. & SLATOPOLSKY, E. 2009. Vascular calcification: the killer of patients with chronic kidney disease. *Journal of the American Society of Nephrology : JASN,* 20**,** 1453-1517.

MOE, S. M. 2004. Pathophysiology of Vascular Calcification in Chronic Kidney Disease. *Circulation Research,* 95, 560-567.

MOLOSTVOV, G., FLETCHER, S. & BLAND, R. 2008. Extracellular calcium-sensing receptor mediated signalling is involved in human vascular smooth muscle cell proliferation and apoptosis. *Cellular Physiology and Biochemistry,* 22, 413-22.

MOLOSTVOV, G., JAMES, S., FLETCHER, S., BENNETT, J., LEHNERT, H., BLAND, R. & ZEHNDER, D. 2007. Extracellular calcium-sensing receptor is functionally expressed in human artery. *AJP: Renal Physiology,* 293, F946-55.

MÖNCKEBERG, J. G. 1903. Ueber Die Reine Mediaverkalkung Der Extremitaetenarterien Und Ihr Verhalten Zur Arteriosklerose. *Virchows Archiv - A: Pathological Anatomy,* 1903**,** 141-167.

MOORE, D. & RUSKA, H. 1957. The fine structure of capillaries and small arteries. *The Journal of biophysical and biochemical cytology,* 3**,** 457-519.

MORGAN, J. & MORGAN, K. 1984a. Calcium and cardiovascular function. Intracellular calcium levels during contraction and relaxation of mammalian cardiac and vascular smooth muscle as detected with aequorin. *The American journal of medicine,* 77**,** 33-79.

MORGAN, J. & MORGAN, K. 1984b. Stimulus-specific patterns of intracellular calcium levels in smooth muscle of ferret portal vein. *The Journal of Physiology,* 351**,** 155-222.

MORONY, S., TINTUT, Y., ZHANG, Z., CATTLEY, R. C., VAN, G., DWYER, D., STOLINA, M., KOSTENUIK, P. J. & DEMER, L. L. 2008. Osteoprotegerin Inhibits Vascular Calcification Without Affecting Atherosclerosis in ldlr(/) Mice. *Circulation,* 117.

MORRIS, S. & BILLIAR, T. 1994. New insights into the regulation of inducible nitric oxide synthesis. *The American journal of physiology,* 266**,** 39.

MOSMANN, T. 1983. Rapid colorimetric assay for cellular growth and survival: application to proliferation and cytotoxicity assays. *Journal of immunological methods,* 65**,** 55-63.

MULVANY, M. & AALKJAER, C. 1990. Structure and function of small arteries. *Physiological Reviews,* 70**,** 921-982.

MULVANY, M. & NYBORG, N. 1980. An increased calcium sensitivity of mesenteric resistance vessels in young and adult spontaneously hypertensive rats. *British Journal of Pharmacology,* 71**,** 585.

MUN, H.-C., CULVERSTON, E., FRANKS, A., COLLYER, C., CLIFTON-BLIGH, R. & CONIGRAVE, A. 2005. A double mutation in the extracellular Ca2+-sensing receptor's venus flytrap domain that selectively disables L-amino acid sensing. *The Journal of biological chemistry,* 280**,** 29067-29139.

MUN, H.-C., FRANKS, A., CULVERSTON, E., KRAPCHO, K., NEMETH, E. & CONIGRAVE, A. 2004. The Venus Fly Trap domain of the extracellular Ca2+ -sensing receptor is required for L-amino acid sensing. *The Journal of biological chemistry,* 279**,** 51739-51783.

MURAYAMA, A., TAKEYAMA, K., KITANAKA, S., KODERA, Y., KAWAGUCHI, Y., HOSOYA, T. & KATO, S. 1999. Positive and negative regulations of the renal 25-

hydroxyvitamin D3 1alpha-hydroxylase gene by parathyroid hormone, calcitonin, and 1alpha,25(OH)2D3 in intact animals. *Endocrinology,* 140**,** 2224-2255.

MURPHY, W., NEDDEN DZ, D. Z., GOSTNER, P., KNAPP, R., RECHEIS, W. & SEIDLER, H. 2003. The iceman: discovery and imaging. *Radiology,* 226**,** 614-643.

NAGPAL, S., NA, S. & RATHNACHALAM, R. 2005. Noncalcemic actions of vitamin D receptor ligands. *Endocrine Reviews,* 26**,** 662-749.

NAKAGAWA, K., PAREKH, N., KOLEGANOVA, N., RITZ, E., SCHAEFER, F. & SCHMITT, C. 2009. Acute cardiovascular effects of the calcimimetic R-568 and its enantiomer S-568 in rats. *Pediatric nephrology (Berlin, Germany),* 24**,** 1385-1389.

NAKANISHI, S. 1992. Molecular diversity of glutamate receptors and implications for brain function. *Science (New York, N.Y.),* 258**,** 597-1200.

NAKANO-KURIMOTO, R., KOJI-IKEDA, URAOKA, M., NAKAGAWA, Y., YUTAKA, K., KOIDE, M., TAKAHASHI, T., MATOBA, S., YAMADA, H., OKIGAJI, M. & MATSUBARA, J. 2009. Replicative Senescence Of Vascular Smooth Muscle Cells Enhances The Calcification Through Initiating The Osteoblastic Transition. *American Journal Of Physiology- Heart And Circulatory Physiology,* 297**,** H1673-H1684.

NELSON, G., CHANDRASHEKAR, J., HOON, M., FENG, L., ZHAO, G., RYBA, N. & ZUKER, C. 2002. An amino-acid taste receptor. *Nature,* 416**,** 199-401.

NEMETH, E. 2002. The search for calcium receptor antagonists (calcilytics). *Journal of molecular endocrinology,* 29**,** 15-36.

NEMETH, E., DELMAR, E., HEATON, W., MILLER, M., LAMBERT, L., CONKLIN, R., GOWEN, M., GLEASON, J., BHATNAGAR, P. & FOX, J. 2001. Calcilytic compounds: potent and selective Ca2+ receptor antagonists that stimulate secretion of parathyroid hormone. *The Journal of pharmacology and experimental therapeutics,* 299**,** 323-354.

NEMETH, E., STEFFEY, M., HAMMERLAND, L., HUNG, B., VAN WAGENEN, B., DELMAR, E. & BALANDRIN, M. 1998. Calcimimetics with potent and selective activity on the parathyroid calcium receptor. *Proceedings of the National Academy of Sciences of the United States of America,* 95**,** 4040-4045.

NEVEN, E., PERSY, V., DAUWE, S., SCHUTTER, T. D., BROE, M. E. D. & HAESE, P. C. D. 2010. Chondrocyte Rather Than Osteoblast Conversion of Vascular Cells Underlies Medial Calcification in Uremic Rats. *Arteriosclerosis, Thrombosis, and Vascular Biology,* 30.

NICHOLS, M., TOWNSEND, N., LUENGO-FERNANDEZ, R., LEAL, J., GREY, A., SCARBOROUGH, P. & RAYNER, M. 2012. European Cardiovascular Disease Statistics 2012. *European Heart Network, Brussels, European Society of Cardiology, Sophia Antipolis,* http://www.ehnheart.org/.

NICHOLSON, S. & BRUZZONE, R. 1997. Gap junctions: getting the message through. *Current biology : CB,* 7**,** 4.

NIGAM, V. & SRIVASTAVA, D. 2009. Notch1 represses osteogenic pathways in aortic valve cells. *Journal of Molecular and Cellular Cardiology,* 47**,** 828-862.

NITTA, K. 2011. Vascular calcification in patients with chronic kidney disease. *Therapeutic apheresis and dialysis : official peer-reviewed journal of the International Society for Apheresis, the Japanese Society for Apheresis, the Japanese Society for Dialysis Therapy,* 15**,** 513-534.

NITTA, K., AKIBA, T., UCHIDA, K., OTSUBO, S., OTSUBO, Y., TAKEI, T., OGAWA, T., YUMURA, W., KABAYA, T. & NIHEI, H. 2004. Left ventricular hypertrophy is associated with arterial stiffness and vascular calcification in hemodialysis patients. *Hypertension research : official journal of the Japanese Society of Hypertension,* 27**,** 47-99.

O'CONNELL, M., MURTHY, S., PHAN, S., XU, C., BUCHANAN, J., SPILKER, R., DALMAN, R., ZARINS, C., DENK, W. & TAYLOR, C. 2008. The three-dimensional micro- and nanostructure of the aortic medial lamellar unit measured using 3D confocal and electron microscopy imaging. *Matrix biology : journal of the International Society for Matrix Biology,* 27**,** 171-252.

O'DONOVAN, R., BALDWIN, D., HAMMER, M., MONIZ, C. & PARSONS, V. 1986. Substitution of aluminium salts by magnesium salts in control of dialysis hyperphosphataemia. *Lancet,* 1**,** 880-882.

O'NEILL, W. C. 2008. Treatment of vascular calcification. *Kidney International,* 74, 1376-1378.

O'NEILL, W. C. & KOBA, A. L. 2010. Recent progress in the treatment of vascular calcification. *Kidney International,* 78, 1232-1239.

OGATA, H., RITZ, E., ODONI, G., AMANN, K. & ORTH, S. 2003. Beneficial effects of calcimimetics on progression of renal failure and cardiovascular risk factors. *Journal of the American Society of Nephrology : JASN,* 14**,** 959-967.

OHANIAN, J., GATFIELD, K., WARD, D. & OHANIAN, V. 2005. Evidence for a functional calcium-sensing receptor that modulates myogenic tone in rat subcutaneous small arteries. *American journal of physiology. Heart and circulatory physiology,* 288**,** 62.

OHYA, Y., ABE, I., FUJII, K., TAKATA, Y. & FUJISHIMA, M. 1993. Voltage-dependent $Ca2+$ channels in resistance arteries from spontaneously hypertensive rats. *Circulation Research,* 73**,** 1090-1099.

OLESEN, P., NGUYEN, K., WOGENSEN, L., LEDET, T. & RASMUSSEN, L. M. 2006. Calcification of human vascular smooth muscle cells: associations with osteoprotegerin expression and acceleration by high-dose insulin. *AJP: Heart and Circulatory Physiology,* 292.

OLGAARD, K., LEWIN, E. & SILVER, J. 2011. Calcimimetics, vitamin D and ADVANCE in the management of CKD-MBD. *Nephrology Dialysis Transplantation,* 26.

ORTIZ-CAPISANO, M., REDDY, M., MENDEZ, M., GARVIN, J. & BEIERWALTES, W. 2013. Juxtaglomerular cell CaSR stimulation decreases renin release via activation of the PLC/IP3 pathway and the ryanodine receptor. *American journal of physiology. Renal physiology,* 304**,** 56.

PAI, A., LEAF, E., EL-ABBADI, M. & GIACHELLI, C. 2011. Elastin degradation and vascular smooth muscle cell phenotype change precede cell loss and arterial medial calcification in a uremic mouse model of chronic kidney disease. *The American journal of pathology,* 178**,** 764-837.

PAJULA, R., RAINA, A. & ELORANTA, T. 1979. Polyamine synthesis in mammalian tissues. Isolation and characterization of spermine synthase from bovine brain. *European journal of biochemistry / FEBS,* 101**,** 619-626.

PAL, S. & GOLLEDGE, J. 2011. Osteo-progenitors in vascular calcification: a circulating cell theory. *Journal of atherosclerosis and thrombosis,* 18**,** 551-560.

PALLAIS, J., KIFOR, O., CHEN, Y.-B., SLOVIK, D. & BROWN, E. 2004. Acquired hypocalciuric hypercalcemia due to autoantibodies against the calcium-sensing receptor. *The New England journal of medicine,* 351**,** 362-371.

PALMER, R., ASHTON, D. & MONCADA, S. 1988. Vascular endothelial cells synthesize nitric oxide from L-arginine. *Nature,* 333**,** 664-670.

PALMER, R., FERRIGE, A. & MONCADA, S. 1987. Nitric oxide release accounts for the biological activity of endothelium-derived relaxing factor. *Nature,* 327**,** 524-530.

PANIZO, S., CARDUS, A., ENCINAS, M., PARISI, E., VALCHEVA, P., LOPEZ-ONGIL, S., COLL, B., FERNANDEZ, E. & VALDIVIELSO, J. M. 2009. RANKL Increases Vascular Smooth Muscle Cell Calcification Through a RANK-BMP4-Dependent Pathway. *Circulation Research,* 104.

PASCH, A., SCHAFFNER, T., HUYNH-DO, U., FREY, B., FREY, F. & FARESE, S. 2008. Sodium thiosulfate prevents vascular calcifications in uremic rats. *Kidney International,* 74**,** 1444-1497.

PEARCE, S., TRUMP, D., WOODING, C., BESSER, G., CHEW, S., GRANT, D., HEATH, D., HUGHES, I., PATERSON, C., WHYTE, M. 1995. Calcium-sensing receptor mutations in familial benign hypercalcemia and neonatal hyperparathyroidism. *Journal of Clinical Investigation,* 96, 2683-2692.

PEIRIS, D., PACHECO, I., SPENCER, C. & MACLEOD, R. J. 2006. The extracellular calcium-sensing receptor reciprocally regulates the secretion of BMP-2 and the BMP antagonist Noggin in colonic myofibroblasts. *AJP: Gastrointestinal and Liver Physiology,* 292.

PESIC, A., MADDEN, J., PESIC, M. & RUSCH, N. 2004. High blood pressure upregulates arterial L-type Ca2+ channels: is membrane depolarization the signal? *Circulation Research,* 94**,** 104.

PETREL, C., KESSLER, A., DAUBAN, P., DODD, R., ROGNAN, D. & RUAT, M. 2004. Positive and negative allosteric modulators of the Ca2+-sensing receptor interact within overlapping but not identical binding sites in the transmembrane domain. *The Journal of biological chemistry,* 279**,** 18990-18997.

PETREL, C., KESSLER, A., MASLAH, F., DAUBAN, P., DODD, R., ROGNAN, D. & RUAT, M. 2003. Modeling and mutagenesis of the binding site of Calhex 231, a novel negative allosteric modulator of the extracellular Ca(2+)-sensing receptor. *The Journal of biological chemistry,* 278**,** 49487-49581.

PI, M., CHEN, L., HUANG, M.-Z., ZHU, W., RINGHOFER, B., LUO, J., CHRISTENSON, L., LI, B., ZHANG, J., JACKSON, P., FABER, P., BRUNDEN, K., HARRINGTON, J. & QUARLES, L. 2008. GPRC6A null mice exhibit osteopenia, feminization and metabolic syndrome. *PLoS ONE,* 3.

PI, M., FABER, P., EKEMA, G., JACKSON, P., TING, A., WANG, N., FONTILLA-POOLE, M., MAYS, R., BRUNDEN, K., HARRINGTON, J. & QUARLES, L. 2005. Identification of a novel extracellular cation-sensing G-protein-coupled receptor. *The Journal of biological chemistry,* 280**,** 40201-40209.

PI, M., GARNER, S., FLANNERY, P., SPURNEY, R. & QUARLES, L. 2000. Sensing of extracellular cations in CasR-deficient osteoblasts. Evidence for a novel cation-sensing mechanism. *The Journal of biological chemistry,* 275**,** 3256-3319.

PIECHA, G., KOKENY, G., NAKAGAWA, K., KOLEGANOVA, N., GELDYYEV, A., BERGER, I., RITZ, E., SCHMITT, C. & GROSS, M.-L. 2008. Calcimimetic R-568 or calcitriol: equally beneficial on progression of renal damage in subtotally nephrectomized rats. *American journal of physiology. Renal physiology,* 294**,** 57.

PISTILLI, M., PETRIK, J., HOLLOWAY, A. & CRANKSHAW, D. 2012. Immunohistochemical and functional studies on calcium-sensing receptors in rat uterine smooth muscle. *Clinical and experimental pharmacology & physiology,* 39**,** 37-79.

PLAGEMANN, T., PRENZLER, A. & MITTENDORF, T. 2011. Considerations about the effectiveness and cost effectiveness of therapies in the treatment of hyperphosphataemia. *Health economics review,* 1**,** 1.

PRICE, P., FAUS, S. & WILLIAMSON, M. 1998. Warfarin causes rapid calcification of the elastic lamellae in rat arteries and heart valves. *Arteriosclerosis, Thrombosis, and Vascular Biology,* 18**,** 1400-1407.

PRICE, P., FAUS, S. & WILLIAMSON, M. 2000. Warfarin-induced artery calcification is accelerated by growth and vitamin D. *Arteriosclerosis, Thrombosis, and Vascular Biology,* 20**,** 317-344.

PRICE, P., ROUBLICK, A. & WILLIAMSON, M. 2006. Artery calcification in uremic rats is increased by a low protein diet and prevented by treatment with ibandronate. *Kidney International,* 70**,** 1577-1660.

PRICE, P. & WILLIAMSON, M. 1985. Primary structure of bovine matrix Gla protein, a new vitamin K-dependent bone protein. *The Journal of biological chemistry,* 260**,** 14971-14976.

PROSDOCIMO, D. A., WYLER, S. C., ROMANI, A. M., NEILL, W. C. O. & DUBYAK, G. R. 2010. Regulation of vascular smooth muscle cell calcification by extracellular pyrophosphate homeostasis: synergistic modulation by cyclic AMP and hyperphosphatemia. *AJP: Cell Physiology,* 298.

PROUDFOOT, D. & SHANAHAN, C. 2006. Molecular mechanisms mediating vascular calcification: role of matrix Gla protein. *Nephrology (Carlton, Vic.),* 11**,** 455-516.

PROUDFOOT, D., SKEPPER, J., HEGYI, L., BENNETT, M., SHANAHAN, C. & WEISSBERG, P. 2000. Apoptosis regulates human vascular calcification in vitro: evidence for initiation of vascular calcification by apoptotic bodies. *Circulation research,* 87**,** 1055-1117.

PROUDFOOT, D., SKEPPER, J., SHANAHAN, C. & WEISSBERG, P. 1998. Calcification of human vascular cells in vitro is correlated with high levels of matrix Gla protein and low levels of osteopontin expression. *Arteriosclerosis, Thrombosis, and Vascular Biology,* 18**,** 379-467.

QUINN, S., BAI, M. & BROWN, E. 2004. pH Sensing by the calcium-sensing receptor. *The Journal of biological chemistry,* 279**,** 37241-37250.

QUINN, S., KIFOR, O., TRIVEDI, S. & DIAZ, R. 1998. Sodium and ionic strength sensing by the calcium receptor. *Journal of Biological Chemistry,* 273, 19579-89.

QUINN, S., YE, C., DIAZ, R. & KIFOR, O. 1997. The Ca2+-sensing receptor: a target for polyamines. *American Journal of Physiology,* 273, C1315-C1323.

RADCLIFF, K. 2005. Insulin-Like Growth Factor-I Regulates Proliferation and Osteoblastic Differentiation of Calcifying Vascular Cells via Extracellular Signal-Regulated Protein Kinase And Phosphatidylinositol 3-Kinase Pathways. *Circulation Research,* 96.

RADER, J., BAYLINK, D., HUGHES, M., SAFILIAN, E. & HAUSSLER, M. 1979. Calcium and phosphorus deficiency in rats: effects on PTH and 1,25-dihydroxyvitamin D3. *The American journal of physiology,* 236**,** 22.

RAGGI, P., CHERTOW, G., TORRES, P., CSIKY, B., NASO, A., NOSSULI, K., MOUSTAFA, M., GOODMAN, W., LOPEZ, N., DOWNEY, G., DEHMEL, B., FLOEGE, J. & GROUP, A. S. 2011. The ADVANCE study: a randomized study to evaluate the effects of cinacalcet plus low-dose vitamin D on vascular calcification in patients on hemodialysis. *Nephrology, dialysis, transplantation : official publication of the European Dialysis and Transplant Association - European Renal Association,* 26**,** 1327-1366.

RAJASREE, S., RAJPAL, K., KARTHA, C., SARMA, P., KUTTY, V., IYER, C. & GIRIJA, G. 2001. Serum 25-hydroxyvitamin D3 levels are elevated in South Indian patients with ischemic heart disease. *European journal of epidemiology,* 17**,** 567-638.

RAUE, F., PICHL, J., DÖRR, H.-G., SCHNABEL, D., HEIDEMANN, P., HAMMERSEN, G., JAURSCH-HANCKE, C., SANTEN, R., SCHÖFL, C., WABITSCH, M., HAAG, C., SCHULZE, E. & FRANK-RAUE, K. 2011. Activating mutations in the calcium-sensing receptor: genetic and clinical spectrum in 25 patients with autosomal dominant hypocalcaemia - a German survey. *Clinical Endocrinology,* 75**,** 760-765.

RAY, K., HAUSCHILD, B., STEINBACH, P., GOLDSMITH, P., HAUACHE, O. & SPIEGEL, A. 1999. Identification of the cysteine residues in the amino-terminal extracellular domain of the human Ca(2+) receptor critical for dimerization. Implications for function of monomeric Ca(2+) receptor. *The Journal of biological chemistry,* 274**,** 27642-27650.

RENKEMA, K., ALEXANDER, R., BINDELS, R. & HOENDEROP, J. 2008. Calcium and phosphate homeostasis: concerted interplay of new regulators. *Annals of medicine,* 40**,** 82-173.

REYNOLDS, J. L. 2004. Human Vascular Smooth Muscle Cells Undergo Vesicle-Mediated Calcification in Response to Changes in Extracellular Calcium and Phosphate Concentrations: A Potential Mechanism for Accelerated Vascular Calcification in ESRD. *Journal of the American Society of Nephrology,* 15.

REYNOLDS, J. L. 2005. Multifunctional Roles for Serum Protein Fetuin-A in Inhibition of Human Vascular Smooth Muscle Cell Calcification. *Journal of the American Society of Nephrology,* 16.

RHEE, S., STIMERS, J., WANG, W. & PANG, L. 2009. Vascular smooth muscle-specific knockdown of the noncardiac form of the L-type calcium channel by microRNA-based short hairpin RNA as a potential antihypertensive therapy. *The Journal of pharmacology and experimental therapeutics,* 329**,** 775-782.

RHOADES, R. & BELL, D. 2012. Medical Physiology: Principles for Clinical Medicine (Fourth Edition). Lippincott Williams & Wilkins.

RICCARDI, D. & BROWN, E. M. 2009. Physiology and pathophysiology of the calcium-sensing receptor in the kidney. *AJP: Renal Physiology,* 298.

RICCARDI, D., HALL, A., CHATTOPADHYAY, N., XU, J., BROWN, E. & HEBERT, S. 1998. Localization of the extracellular Ca2+/polyvalent cation-sensing protein in rat kidney. *The American journal of physiology,* 274**,** 22.

RICCARDI, D., PARK, J. & LEE, W. 1995. Cloning and functional expression of a rat kidney extracellular calcium/polyvalent cation-sensing receptor. *Proceedings of the ...*

RINGER, S. 1882a. Concerning the Influence exerted by each of the Constituents of the Blood on the Contraction of the Ventricle. *The Journal of physiology,* 3**,** 380-473.

RINGER, S. 1882b. Regarding the Action of Hydrate of Soda, Hydrate of Ammonia, and Hydrate of Potash on the Ventricle of the Frog's Heart. *The Journal of physiology,* 3**,** 195-397.

RINGER, S. 1883. A further Contribution regarding the influence of the different Constituents of the Blood on the Contraction of the Heart. *The Journal of physiology,* 4**,** 29-71.

RODRIGUES, L., CÁU, A., BUSSMANN, L., BASTIDA, G., BRUNETTO, O., CORRÊA, P. & MARTIN, R. 2011. New mutation in the CASR gene in a family with familial hypocalciuric hypercalcemia (FHH) and neonatal severe hyperparathyroidism (NSHPT). *Arquivos brasileiros de endocrinologia e metabologia,* 55**,** 67-138.

RODRIGUEZ, M., MARTINEZ-MORENO, J., RODRÍGUEZ-ORTIZ, M., MUÑOZ-CASTAÑEDA, J. & ALMADEN, Y. 2011. Vitamin D and vascular calcification in chronic kidney disease. *Kidney & blood pressure research,* 34**,** 261-269.

ROGER, V., GO, A., LLOYD-JONES, D., ADAMS, R., BERRY, J., BROWN, T., CARNETHON, M., DAI, S., DE SIMONE, G., FORD, E., FOX, C., FULLERTON, H., GILLESPIE, C., GREENLUND, K., HAILPERN, S., HEIT, J., HO, P., HOWARD, V., KISSELA, B., KITTNER, S., LACKLAND, D., LICHTMAN, J., LISABETH, L., MAKUC, D., MARCUS, G., MARELLI, A., MATCHAR, D., MCDERMOTT, M., MEIGS, J., MOY, C., MOZAFFARIAN, D., MUSSOLINO, M., NICHOL, G., PAYNTER, N., ROSAMOND, W., SORLIE, P., STAFFORD, R., TURAN, T., TURNER, M., WONG, N. & WYLIE-ROSETT, J. 2011. Heart disease and stroke statistics--2011 update: a report from the American Heart Association. *Circulation,* 123.

ROGER, V., GO, A., LLOYD-JONES, D., BENJAMIN, E., BERRY, J., BORDEN, W., BRAVATA, D., DAI, S., FORD, E., FOX, C., FULLERTON, H., GILLESPIE, C., HAILPERN, S., HEIT, J., HOWARD, V., KISSELA, B., KITTNER, S., LACKLAND, D., LICHTMAN, J., LISABETH, L., MAKUC, D., MARCUS, G., MARELLI, A., MATCHAR, D., MOY, C., MOZAFFARIAN, D., MUSSOLINO, M., NICHOL, G., PAYNTER, N., SOLIMAN, E., SORLIE, P., SOTOODEHNIA, N., TURAN, T., VIRANI, S., WONG, N., WOO, D. & TURNER, M. 2012. Executive Summary: Heart Disease and Stroke Statistics--2012 Update: A Report From the American Heart Association. *Circulation,* 125.

ROGERS, N., TEUBNER, D. & COATES, P. 2007. Calcific uremic arteriolopathy: advances in pathogenesis and treatment. *Seminars in Dialysis,* 20**,** 150-157.

ROSAMOND, W., FLEGAL, K., FRIDAY, G., FURIE, K., GO, A., GREENLUND, K., HAASE, N., HO, M., HOWARD, V., KISSELA, B., KISSELA, B., KITTNER, S., LLOYD-JONES, D., MCDERMOTT, M., MEIGS, J., MOY, C., NICHOL, G., O'DONNELL, C., ROGER, V., RUMSFELD, J., SORLIE, P., STEINBERGER, J., THOM, T., WASSERTHIEL-SMOLLER, S., HONG, Y., AMERICAN HEART ASSOCIATION STATISTICS, C. & STROKE STATISTICS, S. 2007. Heart disease and stroke statistics--2007 update: a report from the American Heart Association Statistics Committee and Stroke Statistics Subcommittee. *Circulation,* 115**,** 171.

ROSAMOND, W., FLEGAL, K., FURIE, K., GO, A., GREENLUND, K., HAASE, N., HAILPERN, S., HO, M., HOWARD, V., KISSELA, B., KISSELA, B., KITTNER, S., LLOYD-JONES, D., MCDERMOTT, M., MEIGS, J., MOY, C., NICHOL, G., O'DONNELL, C., ROGER, V., SORLIE, P., STEINBERGER, J., THOM, T., WILSON, M., HONG, Y., AMERICAN HEART ASSOCIATION STATISTICS, C. & STROKE STATISTICS, S. 2008. Heart disease and stroke statistics--2008 update: a report from the American Heart Association Statistics Committee and Stroke Statistics Subcommittee. *Circulation,* 117**,** 146.

ROSS, R. 1993. The pathogenesis of atherosclerosis: a perspective for the 1990s. *Nature,* 362**,** 801-810.

ROSS, R. 1999. Atherosclerosis is an inflammatory disease. *American heart journal,* 138**,** 20.

ROTHE, H. M., LIANGOS, O., BIGGAR, P., PETERMANN, A. & KETTELER, M. 2011. Cinacalcet Treatment of Primary Hyperparathyroidism. *International Journal of Endocrinology,* 2011.

ROUSSANNE, M., LIEBERHERR, M., SOUBERBIELLE, J., SARFATI, E., DRÜEKE, T. & BOURDEAU, A. 2001. Human parathyroid cell proliferation in response to calcium, NPS R-467, calcitriol and phosphate. *European Journal of Clinical Investigation,* 31**,** 610-616.

RUAT, M. & MOLLIVER, M. 1995. Calcium sensing receptor: molecular cloning in rat and localization to nerve terminals. *Proceedings of the National Academy of Sciences of the United States of America*, 92, 3161–3165.

RUTSCH, F., RUF, N., VAINGANKAR, S., TOLIAT, M., SUK, A., HÖHNE, W., SCHAUER, G., LEHMANN, M., ROSCIOLI, T., SCHNABEL, D., EPPLEN, J., KNISELY, A., SUPERTI-FURGA, A., MCGILL, J., FILIPPONE, M., SINAIKO, A., VALLANCE, H., HINRICHS, B., SMITH, W., FERRE, M., TERKELTAUB, R. & NÜRNBERG, P. 2003. Mutations in ENPP1 are associated with 'idiopathic' infantile arterial calcification. *Nature genetics,* 34**,** 379-460.

RUTSCH, F., VAINGANKAR, S. & JOHNSON, K. 2001. PC-1 nucleoside triphosphate pyrophosphohydrolase deficiency in idiopathic infantile arterial calcification. *The American journal ...*

RYBCZYŃSKA, A., BOBLEWSKI, K., LEHMANN, A., ORLEWSKA, C. & FOKS, H. 2006. Pharmacological activity of calcimimetic NPS R-568 administered intravenously in rats: dose dependency. *Pharmacological reports : PR,* 58**,** 533-539.

RYBCZYŃSKA, A., BOBLEWSKI, K., LEHMANN, A., ORLEWSKA, C., FOKS, H., DREWNOWSKA, K. & HOPPE, A. 2005. Calcimimetic NPS R-568 induces hypotensive effect in spontaneously hypertensive rats. *American journal of hypertension,* 18**,** 364-371.

RYBCZYŃSKA, A., JURSKA-JASKO, A., BOBLEWSKI, K., LEHMANN, A. & ORLEWSKA, C. 2010. Blockade of calcium channels and AT1 receptor prevents the

hypertensive effect of calcilytic NPS 2143 in rats. *Journal of physiology and pharmacology : an official journal of the Polish Physiological Society,* 61**,** 163-233.

RYBCZYNSKA, A., LEHMANN, A., JURSKA-JASKO, A., BOBLEWSKI, K., ORLEWSKA, C., FOKS, H. & DREWNOWSKA, K. 2006. Hypertensive effect of calcilytic NPS 2143 administration in rats. *The Journal of endocrinology,* 191**,** 189-195.

SAGE, A., LU, J., TINTUT, Y. & DEMER, L. 2011. Hyperphosphatemia-induced nanocrystals upregulate the expression of bone morphogenetic protein-2 and osteopontin genes in mouse smooth muscle cells in vitro. *Kidney International,* 79**,** 414-436.

SAGE, A., TINTUT, Y., GARFINKEL, A. & DEMER, L. 2009. Systems biology of vascular calcification. *Trends in cardiovascular medicine,* 19**,** 118-141.

SANDERS, J., CHATTOPADHYAY, N., KIFOR, O., YAMAGUCHI, T. & BROWN, E. 2000. Extracellular calcium-sensing receptor (CaR) expression and its potential role in parathyroid hormone-related peptide (PTHrP) secretion in the H-500 rat Leydig cell model of humoral hypercalcemia of malignancy. *Biochemical and Biophysical Research Communications,* 269**,** 427-459.

SANDOW, S., HADDOCK, R., HILL, C., CHADHA, P., KERR, P., WELSH, D. & PLANE, F. 2009. What's where and why at a vascular myoendothelial microdomain signalling complex. *Clinical and experimental pharmacology & physiology,* 36**,** 67-76.

SCHMIEDER, R., HILGERS, K., SCHLAICH, M. & SCHMIDT, B. 2007. Renin-angiotensin system and cardiovascular risk. *Lancet,* 369**,** 1208-1219.

SCHOPPET, M. & SHANAHAN, C. M. 2008. Role for alkaline phosphatase as an inducer of vascular calcification in renal failure? *Kidney International,* 73.

SCHURGERS, L., SPRONK, H., SOUTE, B., SCHIFFERS, P., DEMEY, J. & VERMEER, C. 2007. Regression of warfarin-induced medial elastocalcinosis by high intake of vitamin K in rats. *Blood,* 109**,** 2823-2854.

SCOTLAND, R., MADHANI, M., CHAUHAN, S., MONCADA, S., ANDRESEN, J., NILSSON, H., HOBBS, A. & AHLUWALIA, A. 2005. Investigation of vascular responses in endothelial nitric oxide synthase/cyclooxygenase-1 double-knockout mice: key role for endothelium-derived hyperpolarizing factor in the regulation of blood pressure in vivo. *Circulation,* 111**,** 796-803.

SEIFTER, J., SLOANE, D. & RATNER, A. 2005. *Concepts In Medical Physiology*, Lippincott Williams & Wilkins.

SEILER, N., DELCROS, J. & MOULINOUX, J. 1996. Polyamine transport in mammalian cells. An update. *The International Journal of Biochemistry & Cell Biology,* 28**,** 843-861.

SERRA, A., BRAUN, S., STARKE, A., SAVOCA, R., HERSBERGER, M., RUSSMANN, S., CORTI, N. & WÜTHRICH, R. 2008. Pharmacokinetics and pharmacodynamics of cinacalcet in patients with hyperparathyroidism after renal transplantation. *American journal of transplantation : official journal of the American Society of Transplantation and the American Society of Transplant Surgeons,* 8**,** 803-813.

SEVÁ PESSÔA, B., VAN DER LUBBE, N., VERDONK, K., ROKS, A., HOORN, E. & DANSER, A. 2012. Key developments in renin-angiotensin-aldosterone system inhibition. *Nature reviews. Nephrology,* 9**,** 26-36.

SHALHOUB, V., SHATZEN, E., HENLEY, C., BOEDIGHEIMER, M., MCNINCH, J., MANOUKIAN, R., DAMORE, M., FITZPATRICK, D., HAAS, K., TWOMEY, B., KIAEI, P., WARD, S., LACEY, D. L. & MARTIN, D. 2006. Calcification Inhibitors and Wnt Signaling Proteins Are Implicated in Bovine Artery Smooth Muscle Cell Calcification in the Presence of Phosphate and Vitamin D Sterols. *Calcified Tissue International,* 79.

SHALHOUB, V., SHATZEN, E. M., WARD, S. C., YOUNG, J. I., BOEDIGHEIMER, M., TWEHUES, L., MCNINCH, J., SCULLY, S., TWOMEY, B., BAKER, D., KIAEI, P., DAMORE, M. A., PAN, Z., HAAS, K. & MARTIN, D. 2010. Chondro/osteoblastic and cardiovascular gene modulation in human artery smooth muscle cells that calcify in the presence of phosphate and calcitriol or paricalcitol. *Journal of Cellular Biochemistry,* 111.

SHANAHAN, C., CROUTHAMEL, M., KAPUSTIN, A. & GIACHELLI, C. 2011. Arterial calcification in chronic kidney disease: key roles for calcium and phosphate. *Circulation research,* 109**,** 697-1408.

SHAO, J.-S., CHENG, S.-L., PINGSTERHAUS, J., CHARLTON-KACHIGIAN, N., LOEWY, A. & TOWLER, D. 2005. Msx2 promotes cardiovascular calcification by activating paracrine Wnt signals. *The Journal of clinical investigation,* 115**,** 1210-1230.

SHAO, J. S. 2006. Molecular Mechanisms of Vascular Calcification: Lessons Learned From The Aorta. *Arteriosclerosis, Thrombosis, and Vascular Biology,* 26.

SHEN, J., YANG, M. & JIANG, H. 2011. Arterial injury promotes medial chondrogenesis in Sm22 knockout mice. *Cardiovascular ...*

SHI, Y.-L., WANG, L.-W., HUANG, J., GOU, B.-D., ZHANG, T.-L. & WANG, K. 2009. Lanthanum suppresses osteoblastic differentiation via pertussis toxin-sensitive G protein signaling in rat vascular smooth muscle cells. *Journal of Cellular Biochemistry,* 108**,** 1184-1275.

SHIGEMATSU, T., NAKASHIMA, Y., OHYA, M., TATSUTA, K., KOREEDA, D., YOSHIMOTO, W., YAMANAKA, S., SAKAGUCHI, T., HANBA, Y., MIMA, T. & NEGI, S. 2012. The management of hyperphosphatemia by lanthanum carbonate in chronic kidney disease patients. *International journal of nephrology and renovascular disease,* 5**,** 81-90.

SHIMADA, T., HASEGAWA, H., YAMAZAKI, Y., MUTO, T., HINO, R., TAKEUCHI, Y., FUJITA, T., NAKAHARA, K., FUKUMOTO, S. & YAMASHITA, T. 2004. FGF-23 is a potent regulator of vitamin D metabolism and phosphate homeostasis. *Journal of bone and mineral research : the official journal of the American Society for Bone and Mineral Research,* 19**,** 429-435.

SHIOI, A., NISHIZAWA, Y., JONO, S., KOYAMA, H., HOSOI, M. & MORII, H. 1995. Beta-glycerophosphate accelerates calcification in cultured bovine vascular smooth muscle cells. *Arteriosclerosis, thrombosis, and vascular biology,* 15**,** 2003-2012.

SHOBEIRI, N., ADAMS, M. & HOLDEN, R. 2010. Vascular calcification in animal models of CKD: A review. *American Journal of Nephrology,* 31**,** 471-552.

SHOZO, Y., EDWARD, M. B. & NAIBEDYA, C. 2004. Calcium-sensing receptor in the brain. *Cell Calcium,* 35, E1206-E1213.

SHROFF, R., MCNAIR, R. & SKEPPER, J. 2010. Chronic mineral dysregulation promotes vascular smooth muscle cell adaptation and extracellular matrix calcification. *Journal of the American Society of Nephrology,* 21, 103–112.

SHROFF, R. & SHANAHAN, C. 2007. The vascular biology of calcification. *Seminars in dialysis,* 20**,** 103-112.

SHU, L., JI, J., ZHU, Q., CAO, G., KARAPLIS, A., POLLAK, M., BROWN, E., GOLTZMAN, D. & MIAO, D. 2010. The calcium sensing receptor mediates bone turnover induced by dietary calcium and parathyroid hormone in neonates. *Journal of bone and mineral research : the official journal of the American Society for Bone and Mineral Research.*

SIMIONESCU, A., PHILIPS, K. & VYVAHARE, N. 2005. Elastin-derived peptides and TGF-beta1 induce osteogenic responses in smooth muscle cells. *Biochemical and Biophysical Research Communications,* 334**,** 524-532.

SIMMERMAN, H. & JONES, L. 1998. Phospholamban: protein structure, mechanism of action, and role in cardiac function. *Physiological Reviews,* 78**,** 921-968.

SIMON, A. M. & MCWHORTER, A. R. 2002. Vascular Abnormalities in Mice Lacking the Endothelial Gap Junction Proteins connexin37 and connexin40. *Developmental Biology,* 251.

SINGER, H. & PEACH, M. 1982. Calcium- and endothelial-mediated vascular smooth muscle relaxation in rabbit aorta. *Hypertension,* 4**,** 19-25.

SLATOPOLSKY, E., CAGLAR, S., GRADOWSKA, L., CANTERBURY, J., REISS, E. & BRICKER, N. 1972. On the prevention of secondary hyperparathyroidism in experimental chronic renal disease using "proportional reduction" of dietary phosphorus intake. *Kidney International,* 2**,** 147-151.

SLATOPOLSKY, E., WEERTS, C., THIELAN, J., HORST, R., HARTER, H. & MARTIN, K. 1984. Marked suppression of secondary hyperparathyroidism by intravenous

administration of 1,25-dihydroxy-cholecalciferol in uremic patients. *The Journal of clinical investigation,* 74**,** 2136-2143.

SMAJILOVIC, S., HANSEN, J. L., CHRISTOFFERSEN, T. E. H., LEWIN, E., SHEIKH, S. P., TERWILLIGER, E. F., BROWN, E. M., STIG, H. & TFELT-HANSEN, J. 2006. Extracellular calcium sensing in rat aortic vascular smooth muscle cells. *Biochemical and Biophysical Research Communications,* 348.

SMAJILOVIC, S., SHEYKHZADE, M., HOLMEGARD, H., HAUNSO, S. & TFELT-HANSEN, J. 2007. Calcimimetic, AMG 073, induces relaxation on isolated rat aorta. *Vascular pharmacology,* 47**,** 222-230.

SMAJILOVIC, S. & TFELT-HANSEN, J. 2007. Calcium acts as a first messenger through the calcium-sensing receptor in the cardiovascular system. *Cardiovascular Research,* 75**,** 457-467.

SMAJILOVIC, S. & TFELT-HANSEN, J. 2008. Novel Role of the Calcium-Sensing Receptor in Blood Pressure Modulation. *Hypertension,* 52.

SMAJILOVIC, S., YANO, S., JABBARI, R. & TFELT-HANSEN, J. 2011. The calcium-sensing receptor and calcimimetics in blood pressure modulation. *British Journal of Pharmacology,* 164**,** 884-893.

SMIRNOV, S. & AARONSON, P. 1992. Ca2+ currents in single myocytes from human mesenteric arteries: evidence for a physiological role of L-type channels. *The Journal of Physiology,* 457**,** 455-530.

SOVERSHAEV, M. A., EGORINA, E. M., BOGDANOV, V. Y., SEREDKINA, N., FALLON, J. T., VALKOV, A. Y., ØSTERUD, B. & HANSEN, J. B. 2010. Bone morphogenetic protein -7 increases thrombogenicity of lipid-rich atherosclerotic plaques via activation of tissue factor. *Thrombosis Research,* 126.

SPEER, M., YANG, H.-Y., BRABB, T., LEAF, E., LOOK, A., LIN, W.-L., FRUTKIN, A., DICHEK, D. & GIACHELLI, C. 2009. Smooth muscle cells give rise to osteochondrogenic precursors and chondrocytes in calcifying arteries. *Circulation Research,* 104**,** 733-774.

SPRAGUE, S., LLACH, F., AMDAHL, M., TACCETTA, C. & BATLLE, D. 2003. Paricalcitol versus calcitriol in the treatment of secondary hyperparathyroidism. *Kidney international,* 63**,** 1483-1573.

STENMARK, K. R. 2006. Role of the Adventitia in Pulmonary Vascular Remodeling. *Physiology,* 21.

STEWART, K., CHARONKO, J., NIEBEL, C., LITTLE, W. & VLACHOS, P. 2012. Left ventricle filling vortex formation is unaffected by diastolic impairment. *American journal of physiology. Heart and circulatory physiology.*

STUBBS, J., LIU, S., TANG, W., ZHOU, J., WANG, Y., YAO, X. & QUARLES, L. 2007. Role of hyperphosphatemia and 1,25-dihydroxyvitamin D in vascular calcification and

mortality in fibroblastic growth factor 23 null mice. *Journal of the American Society of Nephrology : JASN,* 18**,** 2116-2140.

SUN, W., LIU, J., ZHOU, X., XIAO, Y., KARAPLIS, A., POLLAK, M. R., BROWN, E., GOLTZMAN, D. & MIAO, D. 2010. Alterations in phosphorus, calcium and PTHrP contribute to defects in dental and dental alveolar bone formation in calcium-sensing receptor-deficient mice. *Development,* 137.

TAKEDA, M., YAMASHITA, T., SASAKI, N., NAKAJIMA, K., KITA, T., SHINOHARA, M., ISHIDA, T. & HIRATA, K.-I. 2010. Oral administration of an active form of vitamin D3 (calcitriol) decreases atherosclerosis in mice by inducing regulatory T cells and immature dendritic cells with tolerogenic functions. *Arteriosclerosis, Thrombosis, and Vascular Biology,* 30**,** 2495-2998.

TAMAGAKI, K., YUAN, Q., OHKAWA, H., IMAZEKI, I., MORIGUCHI, Y., IMAI, N., SASAKI, S., TAKEDA, K. & FUKAGAWA, M. 2006. Severe hyperparathyroidism with bone abnormalities and metastatic calcification in rats with adenine-induced uraemia. *Nephrology, dialysis, transplantation : official publication of the European Dialysis and Transplant Association - European Renal Association,* 21**,** 651-660.

TAN, Y., CARDINAL, J., FRANKS, A., MUN, H. C., LEWIS, N., HARRIS, L., PRINS, J. & CONIGRAVE, A. 2003. Autosomal dominant hypocalcemia: a novel activating mutation (E604K) in the cysteine-rich domain of the calcium-sensing receptor. *The Journal of clinical endocrinology and metabolism,* 88**,** 605-615.

TEITELBAUM, A., SILVE, C., NYIREDY, K. & ARNAUD, C. 1986. Down-regulation of parathyroid hormone (PTH) receptors in cultured bone cells is associated with agonist-specific intracellular processing of PTH-receptor complexes. *Endocrinology,* 118**,** 595-1197.

TENG, M., WOLF, M., OFSTHUN, M., LAZARUS, J., HERNÁN, M., CAMARGO, C. & THADHANI, R. 2005. Activated injectable vitamin D and hemodialysis survival: a historical cohort study. *Journal of the American Society of Nephrology : JASN,* 16**,** 1115-1140.

TFELT-HANSEN, J., SCHWARZ, P., BROWN, E. & CHATTOPADHYAY, N. 2003. The calcium-sensing receptor in human disease. *Frontiers in bioscience : a journal and virtual library,* 8**,** 90.

THAKORE, P. & HO, W. S. V. 2011. Vascular actions of calcimimetics: role of Ca²(+) -sensing receptors versus Ca²(+) influx through L-type Ca²(+) channels. *British Journal of Pharmacology,* 162**,** 749-762.

THOM, T., HAASE, N., ROSAMOND, W., HOWARD, V., RUMSFELD, J., MANOLIO, T., ZHENG, Z.-J., FLEGAL, K., O'DONNELL, C., KITTNER, S., LLOYD-JONES, D., GOFF, D., HONG, Y., ADAMS, R., FRIDAY, G., FURIE, K., GORELICK, P., KISSELA, B., MARLER, J., MEIGS, J., ROGER, V., SIDNEY, S., SORLIE, P., STEINBERGER, J., WASSERTHIEL-SMOLLER, S., WILSON, M., WOLF, P., AMERICAN HEART ASSOCIATION STATISTICS, C. & STROKE STATISTICS, S. 2006. Heart disease and stroke statistics--2006 update: a report from the American

Heart Association Statistics Committee and Stroke Statistics Subcommittee. *Circulation,* 113**,** 151.

THOMSEN, A., HVIDTFELDT, M. & BRÄUNER-OSBORNE, H. 2012. Biased agonism of the calcium-sensing receptor. *Cell Calcium.*

THYBERG, J., BLOMGREN, K., HEDIN, U. & DRYJSKI, M. 1995. Phenotypic modulation of smooth muscle cells during the formation of neointimal thickenings in the rat carotid artery after balloon injury: an electron-microscopic and stereological study. *Cell and Tissue Research,* 281**,** 421-454.

TING, T., MIYAZAKI-ANZAI, S., MASUDA, M., LEVI, M., DEMER, L., TINTUT, Y. & MIYAZAKI, M. 2011. Increased lipogenesis and stearate accelerate vascular calcification in calcifying vascular cells. *The Journal of biological chemistry,* 286**,** 23938-23987.

TOKA, H., AL-ROMAIH, K., KOSHY, J., DIBARTOLO, S., KOS, C., QUINN, S., CURHAN, G., MOUNT, D., BROWN, E. & POLLAK, M. 2012. Deficiency of the calcium-sensing receptor in the kidney causes parathyroid hormone-independent hypocalciuria. *Journal of the American Society of Nephrology : JASN,* 23**,** 1879-1890.

TORRES, P. & DE BROE, M. 2012. Calcium-sensing receptor, calcimimetics, and cardiovascular calcifications in chronic kidney disease. *Kidney International,* 82**,** 19-25.

TRAN, C., TAYLOR, M., PLANE, F., NAGARAJA, S., TSOUKIAS, N., SOLODUSHKO, V., VIGMOND, E., FURSTENHAUPT, T., BRIGDAN, M. & WELSH, D. 2012. Endothelial Ca2+ wavelets and the induction of myoendothelial feedback. *American journal of physiology. Cell physiology,* 302**,** 42.

TRIGGLE, C., SAMUEL, S., RAVISHANKAR, S., MAREI, I., ARUNACHALAM, G. & DING, H. 2012. The endothelium: influencing vascular smooth muscle in many ways. *Canadian journal of physiology and pharmacology,* 90**,** 713-738.

TUCKWELL, H. 2012. Quantitative aspects of L-type Ca2+ currents. *Progress in Neurobiology,* 96**,** 1-31.

TURGUT, F., KANBAY, M., METIN, M., UZ, E., AKCAY, A. & COVIC, A. 2008. Magnesium supplementation helps to improve carotid intima media thickness in patients on hemodialysis. *International urology and nephrology,* 40**,** 1075-1157.

TZANAKIS, I., PRAS, A., KOUNALI, D., MAMALI, V., KARTSONAKIS, V., MAYOPOULOU-SYMVOULIDOU, D. & KALLIVRETAKIS, N. 1997. Mitral annular calcifications in haemodialysis patients: a possible protective role of magnesium. *Nephrology, dialysis, transplantation : official publication of the European Dialysis and Transplant Association - European Renal Association,* 12**,** 2036-2037.

USUI, E., NOSHIRO, M. & OKUDA, K. 1990. Molecular cloning of cDNA for vitamin D3 25-hydroxylase from rat liver mitochondria. *FEBS Letters,* 262**,** 135-143.

VALLOT, O., COMBETTES, L., JOURDON, P., INAMO, J., MARTY, I., CLARET, M. & LOMPRÉ, A. 2000. Intracellular Ca(2+) handling in vascular smooth muscle cells is affected by proliferation. *Arteriosclerosis, Thrombosis, and Vascular Biology,* 20**,** 1225-1235.

VANHOUTTE, P. 1987. Endothelium and the control of vascular tissue. *Physiology,* 2**,** 18-40.

VANHOUTTE, P., FELETOU, M. & TADDEI, S. 2005. Endothelium-dependent contractions in hypertension. *British Journal of Pharmacology,* 144**,** 449-458.

VANHOUTTE, P., RUBANYI, G., MILLER, V. & HOUSTON, D. 1986. Modulation of vascular smooth muscle contraction by the endothelium. *Annual Review of Physiology,* 48**,** 307-327.

VARGAS-POUSSOU, R., HUANG, C., HULIN, P., HOUILLIER, P., JEUNEMAÎTRE, X., PAILLARD, M., PLANELLES, G., DÉCHAUX, M., MILLER, R. & ANTIGNAC, C. 2002. Functional characterization of a calcium-sensing receptor mutation in severe autosomal dominant hypocalcemia with a Bartter-like syndrome. *Journal of the American Society of Nephrology : JASN,* 13**,** 2259-2325.

VATTIKUTI, R. & TOWLER, D. A. 2004. Osteogenic Regulation Of Vascular Calcification: An Early Perspective. *The American Physiological Society,* 286**,** E686-E696.

VILLA-BELLOSTA, R., WANG, X., MILLAN, J. L., DUBYAK, G. R. & NEILL, W. C. O. 2011. Extracellular pyrophosphate metabolism and calcification in vascular smooth muscle. *AJP: Heart and Circulatory Physiology,* 301.

VIZARD, T., O'KEEFFE, G., GUTIERREZ, H., KOS, C., RICCARDI, D. & DAVIES, A. 2008. Regulation of axonal and dendritic growth by the extracellular calcium-sensing receptor. *Nature Neuroscience,* 11**,** 285-376.

WADA, M., FURUYA, Y., SAKIYAMA, J., KOBAYASHI, N., MIYATA, S., ISHII, H. & NAGANO, N. 1997a. The calcimimetic compound NPS R-568 suppresses parathyroid cell proliferation in rats with renal insufficiency. Control of parathyroid cell growth via a calcium receptor. *The Journal of clinical investigation,* 100**,** 2977-2983.

WADA, M., FURUYA, Y., SAKIYAMA, J., KOBAYASHI, N., MIYATA, S., ISHII, H. & NAGANO, N. 1997b. The calcimimetic compound NPS R-568 suppresses parathyroid cell proliferation in rats with renal insufficiency. Control of parathyroid cell growth via a calcium receptor. *The Journal of clinical investigation,* 100**,** 2977-3060.

WADA, M., NAGANO, N., FURUYA, Y., CHIN, J., NEMETH, E. & FOX, J. 2000. Calcimimetic NPS R-568 prevents parathyroid hyperplasia in rats with severe secondary hyperparathyroidism. *Kidney International,* 57**,** 50-58.

WAGENSEIL, J. & MECHAM, R. 2009. Vascular extracellular matrix and arterial mechanics. *Physiological Reviews,* 89**,** 957-1046.

WAGENSEIL, J. E., CILIBERTO, C. H., KNUTSEN, R. H., LEVY, M. A., KOVACS, A. & MECHAM, R. P. 2009. Reduced Vessel Elasticity Alters Cardiovascular Structure and Function in Newborn Mice. *Circulation Research,* 104.

WAGENSEIL, J. E., CILIBERTO, C. H., KNUTSEN, R. H., LEVY, M. A., KOVACS, A. & MECHAM, R. P. 2010. The importance of elastin to aortic development in mice. *AJP: Heart and Circulatory Physiology,* 299.

WALFORD, G. & LOSCALZO, J. 2003. Nitric oxide in vascular biology. *Journal of thrombosis and haemostasis : JTH,* 1**,** 2112-2120.

WALLIN, R. & HUTSON, S. 2004. Warfarin and the vitamin K-dependent gamma-carboxylation system. *Trends in molecular medicine,* 10**,** 299-601.

WALLIN, R., HUTSON, S., CAIN, D., SWEATT, A. & SANE, D. 2001. A molecular mechanism for genetic warfarin resistance in the rat. *FASEB journal : official publication of the Federation of American Societies for Experimental Biology,* 15**,** 2542-2546.

WANG, R., XU, C., ZHAO, W., ZHANG, J., CAO, K., YANG, B. & WU, L. 2003. Calcium and polyamine regulated calcium-sensing receptors in cardiac tissues. *European journal of biochemistry / FEBS,* 270**,** 2680-2688.

WANG, Y. & BUKOSKI, R. 1998. Distribution of the perivascular nerve Ca2+ receptor in rat arteries. *British Journal of Pharmacology,* 125**,** 1397-1801.

WARD, D. 2004. Calcium receptor-mediated intracellular signalling. *Cell Calcium,* 35**,** 217-245.

WARD, D. 2011. New Concepts In Calcium-Sensing Receptor Pharmacology And Signalling. *British Journal of Pharmacology.*

WATANABE, S., FUKUMOTO, S., CHANG, H., TAKEUCHI, Y., HASEGAWA, Y., OKAZAKI, R., CHIKATSU, N. & FUJITA, T. 2002. Association between activating mutations of calcium-sensing receptor and Bartter's syndrome. *Lancet,* 360**,** 692-696.

WEISS, S. & PUTNEY, J. 1978. Does calcium mediate the increase in potassium permeability due to phenylephrine or angiotensin II in the liver? *The Journal of pharmacology and experimental therapeutics,* 207**,** 669-745.

WEN, C., LEIYANG, Z., FEI, D., YIFAN, Z., XIAO, R., LI, L., LIANG, Z., GANGGANG, M., ZIRUN, L. & XIN, C. 2012. Decreased and inactivated nuclear factor kappa B 1 (p50) in human degenerative calcified aortic valve. *Cardiovascular pathology : the official journal of the Society for Cardiovascular Pathology.*

WESTON, A. H. 2005. Evidence in Favor of a Calcium-Sensing Receptor in Arterial Endothelial Cells: Studies With Calindol and Calhex 231. *Circulation Research,* 97.

WESTON, A. H., ABSI, M., HARNO, E., GERAGHTY, A. R., WARD, D. T., RUAT, M., DODD, R. H., DAUBAN, P. & EDWARDS, G. 2008. The expression and function of

Ca 2+ -sensing receptors in rat mesenteric artery; comparative studies using a model of type II diabetes. *British Journal of Pharmacology,* 154.

WILLIAMS, H., PEASE, R., NEWELL, L., CORDELL, P., GRAHAM, R., KEARNEY, M., JACKSON, C. & GRANT, P. 2010. Effect of transglutaminase 2 (TG2) deficiency on atherosclerotic plaque stability in the apolipoprotein E deficient mouse. *Atherosclerosis,* 210**,** 94-103.

WILMER, W. & MAGRO, C. 2002. Calciphylaxis: emerging concepts in prevention, diagnosis, and treatment. *Seminars in Dialysis,* 15**,** 172-258.

WITTEMAN, J., GROBBEE, D., VALKENBURG, H., VAN HEMERT, A., STIJNEN, T. & HOFMAN, A. 1993. Cigarette smoking and the development and progression of aortic atherosclerosis. A 9-year population-based follow-up study in women. *Circulation,* 88**,** 2156-2218.

WITTEMAN, J., KOK, F., VAN SAASE, J. & VALKENBURG, H. 1986. Aortic calcification as a predictor of cardiovascular mortality. *Lancet,* 2**,** 1120-1122.

WONNEBERGER, K., SCOFIELD, M. & WANGEMANN, P. 2000. Evidence for a calcium-sensing receptor in the vascular smooth muscle cells of the spiral modiolar artery. *The Journal of membrane biology,* 175**,** 203-215.

WRAY, S., BURDYGA, T. & NOBLE, K. 2005. Calcium signalling in smooth muscle. *Cell Calcium,* 38**,** 397-407.

WU, C. & BOHR, D. 1991. Mechanisms of calcium relaxation of vascular smooth muscle. *The American journal of physiology,* 261**,** 6.

YAMAZAKI, M., OZONO, K., OKADA, T., TACHIKAWA, K., KONDOU, H., OHATA, Y. & MICHIGAMI, T. 2010. Both FGF23 and extracellular phosphate activate Raf/MEK/ERK pathway via FGF receptors in HEK293 cells. *Journal of Cellular Biochemistry,* 111**,** 1210-1231.

YAO, Y., BENNETT, B., WANG, X., ROSENFELD, M., GIACHELLI, C., LUSIS, A. & BOSTRÖM, K. 2010. Inhibition of bone morphogenetic proteins protects against atherosclerosis and vascular calcification. *Circulation Research,* 107**,** 485-579.

YATZIDIS, H. & AGROYANNIS, B. 1987. Sodium thiosulfate treatment of soft-tissue calcifications in patients with end-stage renal disease. *Peritoneal Dialysis International,* 7**,** 250-502.

YILDIRIM, S., KAMOY, H. & DEMIREL-YILMAZ, E. 1998. Possible mechanism of high calcium-induced relaxation of rabbit thoracic aorta. *General pharmacology,* 30**,** 347-350.

YOSHIDA, T., AZUMA, H., AIHARA, K.-I., FUJIMURA, M., AKAIKE, M., MITSUI, T. & MATSUMOTO, T. 2005. Vascular smooth muscle cell proliferation is dependent upon upregulation of mitochondrial transcription factor A (mtTFA) expression in injured rat carotid artery. *Atherosclerosis,* 178**,** 39-86.

ZEBBOUDJ, A., IMURA, M. & BOSTRÖM, K. 2002. Matrix GLA protein, a regulatory protein for bone morphogenetic protein-2. *The Journal of biological chemistry,* 277**,** 4388-4482.

ZEBBOUDJ, A., SHIN, V. & BOSTRÖM, K. 2003. Matrix GLA protein and BMP-2 regulate osteoinduction in calcifying vascular cells. *Journal of Cellular Biochemistry,* 90**,** 756-821.

ZHANG, S., REDDICK, R., PIEDRAHITA, J. & MAEDA, N. 1992. Spontaneous hypercholesterolemia and arterial lesions in mice lacking apolipoprotein E. *Science (New York, N.Y.),* 258**,** 468-471.

ZHANG, Z., QIU, W., QUINN, S., CONIGRAVE, A., BROWN, E. & BAI, M. 2002. Three adjacent serines in the extracellular domains of the CaR are required for L-amino acid-mediated potentiation of receptor function. *The Journal of biological chemistry,* 277**,** 33727-33762.

ZHANG, Z., SUN, S., QUINN, S., BROWN, E. & BAI, M. 2001. The extracellular calcium-sensing receptor dimerizes through multiple types of intermolecular interactions. *The Journal of biological chemistry,* 276**,** 5316-5338.

ZHAO, W.-H., GOU, B.-D., ZHANG, T.-L. & WANG, K. 2011. Lanthanum chloride bidirectionally influences calcification in bovine vascular muscle smooth cells. *Journal of Cellular Biochemistry*.